Measurement and Assessment of Passenger Vehicle Compatibility in Front and Side Collisions

A thesis submitted in fulfilment of the requirements for the degree of Doctor of Philosophy

Sean O'Brien

Bachelor of Engineering (Aerospace), RMIT University, 2003
Bachelor of Business (Business Administration), RMIT University, 2004

School of Aerospace, Mechanical and Manufacturing Engineering
Faculty of Engineering
RMIT University

February 2010

The results, opinions and conclusions expressed in this thesis are not necessarily those of Volkswagen AG.

Declaration

I certify that except where due acknowledgement has been made, the work is that of the author alone; the work has not been submitted previously, in whole or in part, to qualify for any other academic award; the content of the thesis is the result of work which has been carried out since the official commencement date of the approved research program; and, any editorial work, paid or unpaid, carried out by a third party is acknowledged.

Sean O'Brien
Melbourne, 23.02.2010

Acknowledgements

I would sincerely like to thank Professor Sylvester Abanteriba for his vision and perseverance in developing and continuing to organise the RMIT International Industry Experience and Research Program. His tireless support of this program is truly commendable. I would also like to thank him for providing the University supervision of the thesis.

I would like to thank Dr. Robert Zobel for his support, supervision, and tutorship over the course of my work within the Volkswagen Group Accident Research and also for his ongoing guidance in all matters of vehicle crash compatibility. Many thanks are owed to Dr. Zobel and Professor Abanteriba for the collaboration that resulted in me being offered the opportunity to write my thesis in Germany at Volkswagen.

I would like to thank Mr. Michael Stanzel and Dr. Mirko Junge for their encouragement and friendship over the course of my thesis. Furthermore, their knowledge of all matters in relation to accident statistics was quite invaluable, and their general feedback on my research was much appreciated. I would also like to Mr. Jens Weber for his patience and assistance in getting me started in the world of collision simulations.

My research on crash compatibility at Volkswagen was preceded by the theses of Dr. Thomas Schwarz and Dr. Gareth Thomas. I sincerely thank them both for their support and feedback during my research.

The ideas and results in this thesis have benefited from numerous debates and discussions that I have had with various other researchers, experts, and

managers over the course of the last five years. I would therefore like to extend my thanks to my many other friends and colleagues at Volkswagen and in the various working groups and research projects that I have been involved in during that time.

My friends, both new and old, deserve more of an apology than an acknowledgement. They have admirably put up with ever decreasing communication from myself but continued to provide support and encouragement. Thanks guys, and sorry. I promise to keep in touch a bit better now.

I have a loving and caring family that has supported me throughout my life. Writing a PhD thesis whilst separated from them by 16,000 km was a challenge for all of us, but I will always be grateful for the strength and encouragement that they provided. Despite the distance, they were always able to generate a warmth in my heart that spurred me on and kept me striving to achieve my goals. A great credit is also due to the Link family, who have taken me in as one of their own and given me the kind of support that is really only possible when you live a little closer.

Finally, I cannot thank Anika enough for everything that she has done and put up with over the last four and a half years. I would not be the same person without her. Many people would think that she is crazy for sticking with me through all of this, but I love her so I'm truly grateful that her perseverance and hard work have finally paid off.

Nomenclature

$ADOD$	Average Depth Of Deformation, Assessment Metric
$AHOD$	Average Height Of Deformation, Assessment Metric
$AHOF$	Average Height Of Force, Assessment Metric
C_R	Coefficient of Restitution
Δv	Change in Velocity
$E\Delta v$	Equivalent Change in Velocity
HC	Homogeneity Criteria, Assessment Metric
HIC	Head Injury Criterion
HSI	Horizontal Structural Interaction, Assessment Metric
$K_{W_{400}}$	Work Stiffness, Assessment Metric
R^2	Coefficient of Variance
VSI	Vertical Structural Interaction, Assessment Metric

List of Acronyms

ADR	Australian Design Rule
AE-MDB	Advanced European Mobile Deformable Barrier
AIS	Abbreviated Injury Scale
AIT	International Touring Alliance (*Alliance Internationale de Tourisme*)
ANCAP	Australasian New Car Assessment Program
APROSYS	Advanced Protection Systems Project
ATD	Anthropomorphic Test Device
CDC	Collision Deformation Code
CFR	Code of Federal Regulations, United States of America
CI	Confidence Interval
CIREN	Crash Injury Research and Engineering Network
ECE	Economic Commission for Europe
ECE-R94	ECE Regulation No. 94
ECE-R95	ECE Regulation No. 95
EES	Energy Equivalent Speed
EEVC	European Enhanced Vehicle-safety Committee
ETS	Equivalent Test Speed
Euro NCAP	European New Car Assessment Program
ESC	Electronic Stability Control
EUCAR	European Council for Automotive Research and Development
EVC	Enhanced Vehicle-to-Vehicle Crash Compatibility Group
FIA	Fédération Internationale de l'Automobile (*International Automobile Federation*)

FIMCAR	Frontal Impact and Compatibility Assessment Research Project
FMVSS	Federal Motor Vehicle Safety Standard, United States of America
FWDB	Full Width Deformable Barrier
FWRB	Full Width Rigid Barrier
GIDAS	German In-Depth Accident Survey
GTR	Global Technical Regulation
IHRA	International Harmonized Research Activities, also cited in the literature as International Harmonized Research Agenda
IIHS	Insurance Institute for Highway Safety
ISS	Injury Severity Score
J-NCAP	Japanese New Car Assessment Program
LTV	Light Truck Vehicle
MAIS	Maximum AIS
MDB	Mobile Deformable Barrier
MMR	Mean Mortality Rate
MPDB	Mobile Progressive Deformable Barrier
MPV	Multipurpose Passenger Vehicle
NCAP	New Car Assessment Program
NHTSA	National Highway Traffic Safety Administration, United States of America
NTDB	National Trauma Data Bank
ODB	Offset Deformable Barrier
PDB	Progressive Deformable Barrier
PEAS	Primary Energy Absorbing Structure
SAE	Society of Automotive Engineers
SEAS	Secondary Energy Absorbing Structure
StBA	German Federal Statistics Office (*Statistisches Bundesamt*)
SUV	Sports Utility Vehicle
TRIAS	Traffic Safety and Nuisance Research Institute's Automobile Type Approval Test Standard, Japan

TWG	EVC Technical Working Group
USA	United States of America
US-NCAP	United States New Car Assessment Program
VC-Compat	Vehicle Crash Compatibility Project
VDI	Vehicle Deformation Index
VDI 1	VDI Direction of Force
VDI 2	VDI Location of Damage
VDI 3	VDI Horizontal Description of Damage
VDI 4	VDI Vertical Description of Damage
VDI 6	VDI Degree of Deformation

Table of Contents

List of Figures

List of Tables

It is change, continuing change, inevitable change, that is the dominant factor in society today. No sensible decision can be made any longer without taking into account not only the world as it is, but the world as it will be...

Isaac Asimov (1920 – 1992)

Abstract

The objective of vehicle crash compatibility is the optimisation of vehicle design to minimise the total number of injuries and fatalities that occur in all collisions in the accident environment. It is hence distinguished from traditional perceptions of occupant protection in that it requires vehicle designs to be optimised to protect other road users in addition to the vehicle's own occupants. The aim of this thesis is to define an objective method to assess the compatibility of a front-to-front or front-to-side collision between two passenger vehicles.

Accident statistics from the German In-Depth Accident Survey (GIDAS) relational database are analysed to determine the significance of passenger vehicle occupant casualties with regards to other road users and also to set priorities for the assessment of compatibility between passenger vehicles. Collision obstacles, configurations, velocity, and vehicle mass are analysed with respect to the Abbreviated Injury Scale (AIS).

A method is defined to objectively measure compatibility by comparing the post-collision deformations from a vehicle-to-vehicle collision with the post-collision deformations from a series of vehicle-to-barrier collisions. The result is quantified with respect to injury data derived from the accident statistics.

Ideal models of horizontal and vertical structural homogeneity are developed and applied in front-to-front and front-to-side collision simulations between a mid-sized passenger car and a large Sports Utility Vehicle (SUV). Hence, for the first time, independent conclusions are able to be drawn based on the effects of ideal horizontal homogeneity and ideal vertical homogeneity. The effects of front-end

structural homogeneity are also investigated in combination with changes to the stiffness of various components in the vehicle side structure.

Finally, the findings of the simulations and the accident analysis are used to describe the necessary characteristics for a test procedure to assess a vehicle's compatibility. The merits of existing test procedures are discussed, and alternative concepts are proposed.

Chapter 1

Introduction

The quintessential subject of this thesis is personal mobility, which entails the use of a transport system to surmount distance. Mobility is measured in terms of the distance travelled and the time spent travelling, and is hence improved by a reduction in the time required to cover a given distance (Elvik & Vaa 2004).

The industrial revolution enabled the development of machines that increased mobility, but these machines introduced new risks, and by 1869 the world had experienced its first fatality in an automobile accident (Fallon & O'Neill 2005). By 2004, the number of annual traffic accident fatalities had risen to 1.3 million globally, and road traffic accidents accounted for 2.2% of all deaths (WHO 2008). Beyond the human cost, road traffic accidents also represent a substantial economic burden, which was estimated at 2.3% of Gross Domestic Product for Australia in 2003 (Connelly & Supangan 2006). The safety of personal mobility is therefore the more specific topic of this thesis.

Within the subject of safety, the research is further focussed on collisions between passenger vehicles. In such a collision, the design of each vehicle influences the safety of its own occupants and the occupants of the other vehicle (Appel 1973). The product of the vehicles' designs is described by the term 'compatibility', which encompasses the interaction that occurs in a collision between a particular pair of vehicles and the subsequent effect on the occupants' safety. Front-to-front and front-to-side collisions are the specific focus of the research, as

these are considered to be the most relevant for analysis (van Schijndel-de Nooij & Wismans 2008).

The principal goal of improving safety in front-to-front and front-to-side collisions is to reduce the harm associated with mobility, but improved safety may also be viewed as a mechanism to improve mobility since a journey can be more readily continued if the consequences of a collision are less severe.

1.1 Aims

The specific aims of this thesis are:

1. to identify factors that result in injuries and fatalities in collisions between passenger vehicles, including cars, light trucks, and vans,
2. to develop a method that is capable of objectively measuring compatibility in a collision between two passenger vehicles,
3. to identify design characteristics that improve compatibility between passenger vehicles, and
4. to identify tools that are capable of effecting improvements in vehicle design.

1.2 Research question

The primary research question addressed in this thesis is: **How can compatibility be objectively measured in front-to-front and front-to-side collisions?** In order to answer this question, the secondary questions addressed in each of the chapters are:

Chapter 2	What research has already been performed?
Chapters 3, 4, and 5	What are the boundary conditions?
Chapter 6	What needs to be measured?
Chapter 7	Which methods can be applied?
Chapters 8 and 9	Which results can be generated?
Chapter 10	How can this knowledge be applied?

1.3 Outline

In the literature review in Chapter 2, the context of compatibility is described within the broader field of transport safety research. This indicates both the scope of the research and the multitude of factors that may influence the outcome of a traffic accident. The second aspect of the literature review is the identification of the current vehicle design requirements regarding regulation tests and tests performed by consumer information programs such as the Australasian New Car Assessment Program (ANCAP). Finally, research on front-to-front and front-to-side collisions is reviewed, and answers regarding the research questions are identified.

In Chapter 3, German in-depth accident statistics are analysed to determine the significance of passenger vehicle occupant casualties with regards to other road users. Furthermore, passenger vehicle collisions are analysed to identify the most critical collision partners and collision directions.

In Chapter 4, the accident analysis is focussed on passenger vehicle frontal collisions, and the most critical collision partners are again identified. For frontal collisions with another passenger vehicle, the most critical collision direction of the collision partner is also investigated. Finally, for front-to-front collisions between two passenger vehicles, the most critical collision configurations are determined by analysing collision angles, damage locations, vehicle masses, and magnitudes of the Change in Velocity (Δv).

In Chapter 5, the accident analysis is focussed on passenger vehicle side collisions. This chapter follows a similar approach to that described above for Chapter 4, but the final analysis is directed towards identifying the most critical configurations for front-to-side collisions.

In Chapter 6, definitions of compatibility, a compatible collision, the properties of a compatible collision, and the properties of a compatible vehicle are investigated. The need for this chapter is driven by the disparity between the various definitions that are found in the literature.

In Chapter 7, vehicle assessment tools are compared and a method is defined to objectively measure compatibility in a front-to-front or front-to-side collision. The basis of this method is a comparison between the post-collision deformations measured in a vehicle-to-vehicle collision and the deformations measured in a series of vehicle-to-barrier collisions.

In Chapter 8, a method to simulate horizontal or vertical structural homogeneity is described. This method is applied in front-to-front collision simulations between a mid-sized passenger car and a large SUV, and the results are analysed using the method described in Chapter 7.

In Chapter 9, the same approach is applied to front-to-side collision simulations. In addition, the effects of front-end structural homogeneity are investigated in combination with changes to the vehicle side structure.

In Chapter 10, the findings of the thesis are used to describe the necessary characteristics for a test procedure to assess a vehicle's compatibility. The merits of existing test procedures are discussed, and alternative concepts are proposed.

Finally, in Chapter 11, conclusions are drawn and recommendations for further research are put forward.

Chapter 2

Literature Review

Research related to traffic safety is extensive, and hence the first aim of this literature review is to place the scope of the material covered in this thesis within the general body of knowledge. The second aim is to review the literature related to occupant protection and compatibility in front and side collisions.

The review is focussed on publications from 1998 onwards, although earlier publications are included if the results are considered significant. The research addressed in the review hence includes the first results of the International Harmonized Research Activities (IHRA) working groups, which were established in 1996, and all research since the last major change in occupant protection regulations – the introduction of the Economic Commission for Europe (ECE) regulations on front and side impact protection, ECE Regulation No. 94 (ECE-R94) and ECE Regulation No. 95 (ECE-R95), in 1998.

The literature review in this chapter is the product of a systematic analysis of all volumes of the International Journal of Crashworthiness, Accident Analysis and Prevention, Traffic Injury Prevention, the Stapp Car Crash Journal, and the Institution of Mechanical Engineers' Journal of Automobile Engineering as well as the proceedings of the International Technical Conferences on the Enhanced Safety of Vehicles. For an Australian perspective, the review includes the reports of the Monash University Accident Research Centre. Additional journals, confer-

ence proceedings, and reports are included on an ad hoc basis in the literature review if considered relevant. To limit the bias in the literature review, emphasis is placed on research performed in government, university, or other independent research programs. Research performed in the automotive industry is generally only cited if it represents a unique contribution to the body of knowledge. Independent research is often performed to either confirm or refute the observations from industry research programs, and hence these results are included instead.

2.1 The scope of traffic safety research

The collective goal of traffic safety research is to reduce the number of traffic accidents and the harm that they cause (Elvik & Vaa 2004). Nilsson (2004) proposed the three dimensional model shown in Figure 2.1 to describe the total harm caused by traffic accidents based. In this model, an increase in either exposure, risk, or consequence results in an increase in the total harm.

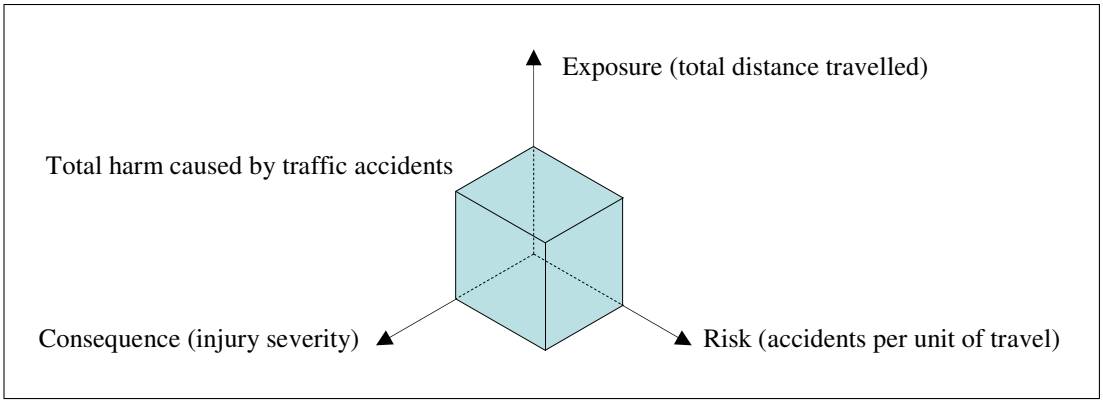

Figure 2.1: Model of the harm caused by accidents in a traffic environment. Adapted from Nilsson (2004).

In contrast to Nilsson's model, the scope of traffic safety research, which is described in Figure 2.2, is concentrated on injury severity and accident frequency. Reductions in exposure are rarely addressed as methods to reduce harm, since a reduction in exposure would imply a reduction in mobility. However, exposure is an important variable when considering a modal change between different forms of transport. For example, Bylow & Savage (1991) estimated that the deregulation

of the aviation industry in the United States of America (USA) led to a 2.2% reduction in annual automobile mileage and, due to the much lower frequency of airline accidents, has resulted in a reduction of approximately 200-300 fatlities per year.

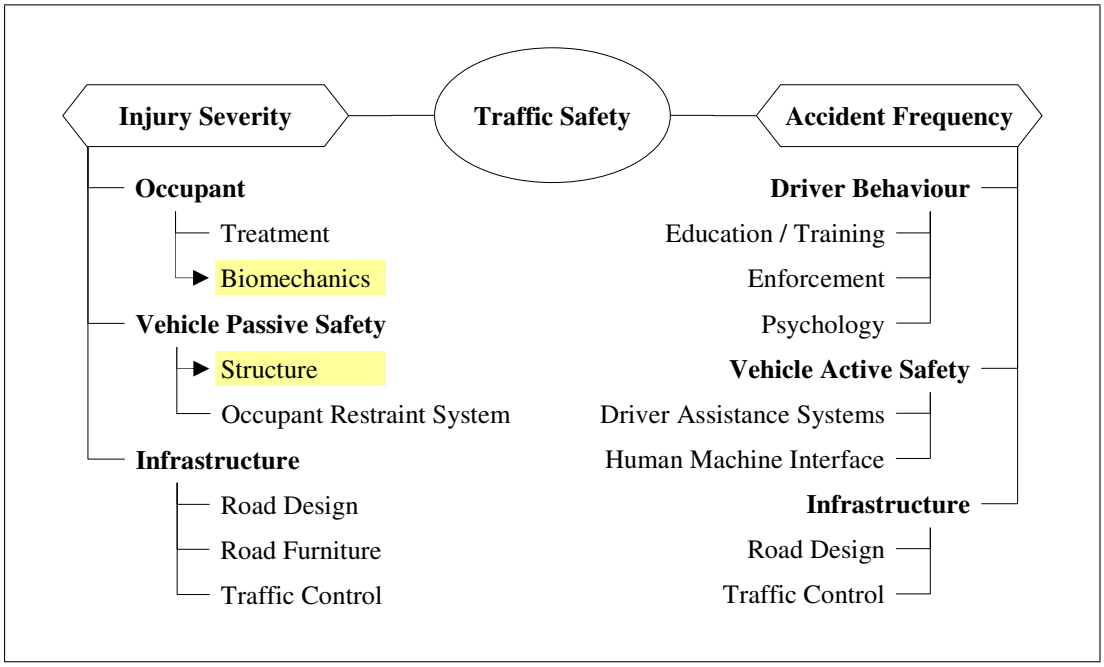

Figure 2.2: Scope of traffic safety research. The principal scope of this thesis addresses vehicle structure and occupant biomechanics.

Within the themes of injury severity and accident frequency, traffic safety research relates to one of three general aspects: human performance, vehicle design, and traffic infrastructure.[1] As shown in Figure 2.2, each of these topics can be further broken down into sub-topics, which themselves still summarise vast areas of research. In addition, accidentology can also be considered as an independent field of research, particularly with regards to the methods of accident analysis and reconstruction (for example Otte & Nehmzow 2002, Taschenmacher 2009).

The scope of this thesis is related to the outcome of collisions in terms of the risk of injury and fatality to passenger vehicle occupants. It therefore

[1]This breakdown of research topics is derived from the 'Haddon Matrix', which was originally designed to guide road safety policy (Haddon 1980). In its most simple form, the Haddon Matrix describes three factors that influence traffic accidents: human, vehicle, and environment, as well as three phases of an accident: pre-event, event, and post-event.

encompasses issues of biomechanics, such as the classification of injuries and the injury causation, as well as the design of vehicle structures. As far as possible, the remaining topics in Figure 2.2 are omitted from the scope, although all of these factors contribute to some extent in the event, or prevention, of a traffic accident.

2.2 Dynamic vehicle test procedures

Table 2.1: International regulatory requirements and consumer information tests for the protection of occupants in front and side collisions.

Usage[a]	**Configuration**	**Initial velocity (km/h)**		**Vehicle Δv (km/h)**[b]
		Vehicle	**Barrier**	
ECE-R94 Euro NCAP	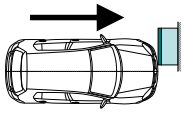	56 64	Fixed	64 74
FMVSS 208[c] US-NCAP	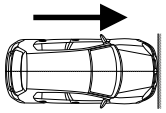	48 56	Fixed	55 64
ECE-R95 J-NCAP	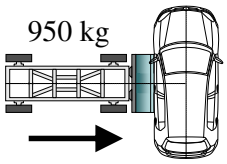	0	50 55	23 26
FMVSS 214 US-NCAP	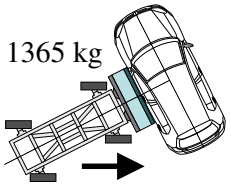	0	54 62	31 35
IIHS	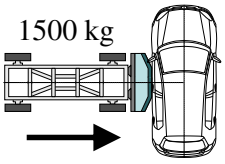	0	50	30

[a] Usage is listed according to the original application of the test procedure at the given test speed.

[b] The vehicle Δv is calculated based on the assumption of an inelastic collision with a Coefficient of Restitution (C_R) of 0.15 (Huang 2002). For the tests with mobile barriers, the calculation is based on the median vehicle mass of the German fleet (1385 kg) according to the GIDAS data from Chapters 4 and 5.

[c] Multiple test procedures are included in FMVSS 208. A 56 km/h test speed has been included since September 2007, but this test speed was first used in US-NCAP. The 48 km/h test speed is still used in FMVSS 208 as well as other regulations such as ADR 69 and TRIAS 47.

Table 2.1 describes the regulatory and consumer information test procedures that play a fundamental role in the design of current vehicles. The focus is limited to test procedures that are representative of vehicle-to-vehicle collisions involving the front or side of the vehicle, and hence lateral pole tests and rear-end tests are omitted. The focus is also limited to high speed tests, which are more critical for the design of the vehicle structure.[2] As shown in Table 2.1, the consumer information tests included in the various New Car Assessment Programs (NCAPs) are typically performed at higher speeds than the equivalent regulatory tests. However, all vehicles must meet the regulatory requirements whereas only a selection of vehicles are tested according to the NCAP requirements. A discussion of the factors that influence vehicle design should therefore include consideration of both sets of test conditions.

Table 2.2: Proposed test procedures for the assessment of occupant protection in front and side collisions.

Test name	**Configuration**	**Initial velocity (km/h)**		**Vehicle Δv (km/h)[a]**
		Vehicle	**Barrier**	
PDB	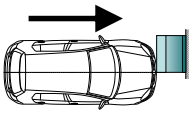	60	Fixed	69
FWDB	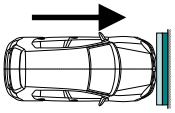	56	Fixed	64
AE-MDB	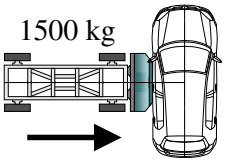	0	50	30

[a] See Footnote b to Table 2.1.

Table 2.2 describes three proposed test procedures that enjoy a significant level of development and are considered serious candidates for regulation. Although these test procedures are not yet used for compliance purposes, some

[2]Exceptions to this statement are low speed bumper tests such as the 49 CFR Part 581 Bumper Standard in the USA. These place requirements on the capabilities of the bumper system and hence indirectly dictate the vertical location of the supporting structures, which are typically also the structures that deform in a high speed collision.

manufacturers may be preemptively using them during the vehicle design process. This table is not intended to be an exhaustive list of proposed test procedures, and the multitude of proposals that have been superseded or deemed inappropriate in the past are omitted. The most noteworthy omission from Table 2.2 is a frontal Mobile Deformable Barrier (MDB), for which many proposals exist, but none are yet considered serious candidates for regulation.

2.3 Compatibility in front-to-front collisions

Research on collisions between small and large passenger vehicles had already begun at the beginning of the 1970s (Severy et al. 1971), and by the end of that decade, research was being actively directed towards the development of more compatible vehicle designs (Danner et al. 1980). By this time, it had been recognised that the compatibility of a vehicle is a product of its self-protection, which describes the functions of its design that protect its own occupants, and its partner-protection, which describes the functions of its design that protect other road users in the event of a collision (Appel 1973). It had also been found that the outcome of a vehicle-to-vehicle collision is influenced by the vehicles' mass ratio, their force-deformation characteristics, and the architecture of the energy absorbing structures (Seiffert et al. 1974). Danner et al. (1980) were therefore already able to propose constructive measures to improve compatibility, including lateral connections between the longitudinals, changes to deformation force levels in the crumple zone, and increased structural support in the passenger compartment.

These early findings remain relevant and reflect contemporary theory regarding the principal factors associated with compatibility. Terms that are now commonly used are vehicle mass, mass ratio, structural interaction, vehicle geometry, homogeneity, front-end force levels, stiffness, and compartment strength (Seiffert & Wech 2003, Faerber 2007, O'Brien et al. 2007, Meyerson et al. 2009, Yonezawa et al. 2009*a*).

2.3.1 Renaissance of compatibility research

Even during the development of the ECE-R94 test procedure in Europe, a "compatibility approach" (Lowne 1994, p15) was cited for future consideration, and three major research projects were initiated in 1997 with the support of the European Commission. The three research groups comprised the European governments in the European Enhanced Vehicle-safety Committee (EEVC), the automobile clubs in the International Touring Alliance (AIT) and Fédération Internationale de l'Automobile (FIA), and the automotive industry in the European Council for Automotive Research and Development (EUCAR) (Faerber et al. 1998, Klanner et al. 1998, Zobel & Schwarz 2001). Due to the similarity of vehicles in the European vehicle fleet, the projects concentrated on car-to-car compatibility, with the goal of identifying compatibility problems not only between different vehicle types, but also the "identification and quantification of incompatibilities between vehicles of similar mass and similar type" (Faerber et al. 1998, p651). European research has continued with a further EEVC project from 2001 to 2002 (Edwards et al. 2002), the Vehicle Crash Compatibility (VC-Compat) project from 2003 to 2006 (Edwards et al. 2007*b*), and the Frontal Impact and Compatibility Assessment Research (FIMCAR) project that began in October 2009 (CORDIS 2009).

Also in the mid 1990s, compatibility research was initiated by the National Highway Traffic Safety Administration (NHTSA) in the USA as a response to the growing issue of collisions between passenger cars and heavier vehicles such as Light Truck Vehicles (LTVs) (Hollowell & Gabler 1996). Research by NHTSA has continued and was supplemented by the Enhanced Vehicle-to-Vehicle Crash Compatibility (EVC) Technical Working Groups (TWGs) between 2003 and 2009. The EVC, which represented the North American automotive industry and vehicle importers, introduced voluntary standards in 2003 that place requirements on the Primary Energy Absorbing Structure (PEAS) and Secondary Energy Absorbing Structure (SEAS) of LTVs (EVC 2003). These remain the only standards or

regulations that directly address compatibility anywhere in the world, and have been attributed to a 19% reduction in the risk of car driver fatality in collisions with compliant LTVs (Baker et al. 2008).

Analysis of Japanese accident statistics found that compatibility between passenger cars should be the major focus of compatibility research there (Mizuno et al. 2001), but minicars and SUVs have also attracted significant attention (Mizuno & Kajzer 1998, 1999). Recent Japanese research has focussed predominantly on the adaptation of international compatibility assessment proposals to the Japanese vehicle fleet. In particular, Japanese research has focussed on the assessment of compartment strength (Mizuno et al. 2001, 2003, 2005*a*,*b*) and the alignment of vehicle structures including PEAS and SEAS (Arai et al. 2007, Mizuno et al. 2008, Yonezawa et al. 2009*a*).

The Australian vehicle fleet differs in mix from that of Europe, North America, and Japan, but it is not known to possess any unique vehicle characteristics or types. However, Australia maintained an active compatibility research program until the first half of this decade, and the Australian government pursued several unique lines of research, including Progressive Deformable Barrier (PDB) tests with constant initial kinetic energy[3] and tests with a PDB element mounted on a mobile trolley (Seyer et al. 2003*a*).

At the conception of IHRA in 1996, two separate working groups were formed to address frontal offset testing and compatibility (Lomanaco 1998, Rodgers 1998). However, these were merged in 2001 when it became apparent that the ongoing work of the frontal offset group was too heavily dependent on that of the compatibility group (O'Reilly 2003). The IHRA working groups did not produce any of their own results and acted instead as a forum to coordinate and exchange information between national research programs. However, the IHRA compatibility working group can be credited with two significant outcomes: the

[3]The initial velocity of each test vehicle was mass dependent such that its initial kinetic energy was 222 kJ, which represents the kinetic energy of a 1600 kg vehicle at 60 km/h. As shown in Table 2.1, the usual approach to vehicle testing is a constant test velocity for all vehicle masses.

identification of a common vertical zone for vehicle structures (O'Reilly 2003) and the definition of a test procedure to assess them (O'Reilly 2005).

Although IHRA was discontinued in late 2005, international research on compatibility has continued and it remains a topic of interest for researchers, regulators, and industry alike.

2.3.2 Research findings

The findings of research on front-to-front compatibility are summarised below in two major categories: statistical analyses and vehicle-to-vehicle crash tests. Published statistical analyses cover a broad range of variables, but the most attention has been directed towards the influence of vehicle type and mass. The published results of front-to-front vehicle crash tests are typically focussed on investigations of controlled variables including mass, stiffness, and geometry.

2.3.2.1 Analyses of vehicle type and mass

The volume of historical literature that addresses the effects that vehicle type and mass have on occupant protection and compatibility is considerable (see for example the literature review performed by Fildes et al. 1993). One of the more significant findings of this time was made by Evans & Frick (1993), who determined that the ratio of the injury risks in two colliding vehicles can be described by a power function of the vehicles' mass ratio. However, as stated in the introduction to this chapter, the review below is focussed on literature published since 1998.

In their analysis of crashworthiness in the Australian vehicle fleet, Newstead & Cameron (1999) deemed vehicle mass to have such a fundamental influence on a vehicle's safety that they adjusted their ratings to remove its effect. Their justification was that "the mass-adjusted index is of interest to regulators and the motor industry, as it shows whether particular models achieve good safety records by added mass rather than good design" (Broughton 1994, quoted in

Newstead & Cameron 1999, p13). In a complementary analysis of the aggressivity that vehicles exhibit towards their collision partners, it was shown that heavier vehicles tend to be more aggressive and that, even accounting for their masses, four-wheel-drives, passenger vans, and commercial vehicles tend to be more aggressive. However, only a weak relationship between crashworthiness and aggressivity was observed, which led to the conclusion that "vehicle mass is only playing a small part in the aggressivity dimension relative to total vehicle safety design" (Cameron et al. 1999, p139).

In Japan, an analysis of vehicle type determined that minicars and SUVs are the least compatible types of vehicles, since the former experiences the highest rate of fatalities of its own occupants and the later causes the highest rate of fatalities in collision partners (Mizuno & Kajzer 1999). However, this conclusion was based on the definition of compatibility "that passenger vehicles of disparate size provide an equal level of occupant protection in car-to-car collisions" (Mizuno & Kajzer 1999, p381). By reanalysis of Mizuno & Kajzer's results, it can be observed that the combined rate of fatalities in both vehicles is lower in collisions involving minicars than in collisions involving either large passenger cars, sports cars, 1-Box vehicles, or SUVs (see Mizuno & Kajzer 1999, Figure 9, p387). Mizuno & Kajzer's definition of compatibility hence appears flawed since it provides a poor rating of minicars even though collisions involving these vehicles result in a relatively low number of casualties.

A NHTSA study of data from the USA began with the pretext that "the compatibility of a vehicle is a combination of its crashworthiness and its aggressivity" (Gabler & Hollowell 2000, p19), but it then focussed exclusively on the evaluation of vehicles' aggressivity. It was observed that large pickups, vans, and SUVs are more aggressive than smaller vehicles, and a weak relationship could be observed between aggressivity and mass. Hence, although the authors claimed that the results "demonstrate a clear incompatibility" (Gabler & Hollowell 2000, p30), this conclusion is incongruent with the initial definition. More recent stud-

ies by the NHTSA have continued to focus on aggressivity and have reached similar conclusions (Austin 2005).

The Insurance Institute for Highway Safety (IIHS) also performed an analysis of data from the USA that compared the aggressivity of different vehicle types across a range of weight classes (Meyerson & Nolan 2001). Across all weight categories, they determined that pickups and utility vehicles account for more fatalities in collision partner vehicles than passenger cars do. However, this analysis was normalised with regards to fatalities per million registered vehicles per year, and hence it may have been biased by differing involvement rates for the different vehicle types.[4]

Kockelman & Kweon (2002) used ordered probit models to examine data from the USA and reached similar conclusions to those from the NHTSA and the IIHS. It was determined that drivers of heavy duty trucks experience lower injury severity in vehicle-to-vehicle collisions than drivers of passenger cars but that they also cause more severe injury to the drivers of collision partner vehicles.

Acierno et al. (2004) performed an in-depth analysis of 19 belted passenger car occupants and 6 belted LTV occupants that were involved in frontal car-to-LTV collisions. Injuries were classified according to the AIS, and the sample was taken from the Crash Injury Research and Engineering Network (CIREN) database. The results showed that 9/19 of the passenger vehicle occupants had AIS 2+ head injuries, 9/19 had AIS 2+ chest injuries, 6/19 had AIS 2+ abdomen injuries, 5/19 had AIS 2+ pelvis injuries, and 14/19 had AIS 2+ injuries to their extremities.[5] In contrast, none of the six LTV occupants had an AIS 2+ injury to the head, chest, or abdomen, but one sustained an AIS 2+ pelvis injury and the other five sustained AIS 2+ injuries to the lower extremities.

[4]As shown in Figure 2.1, involvement rate (accidents per unit of travel) is one of the three dimensions that contribute to the total harm in an accident environment. Statistics that are not controlled with respect to the involvement rate are therefore more representative of the total harm caused by a particular vehicle, but they are less representative of the harm caused in an individual collision.

[5]The nomenclature 'AIS 2+' is commonly used to describe an injury with an AIS score of 2 or greater. However, it does not include injuries with an AIS score of 9, since these injuries are of an unspecified nature (Gennarelli 1998).

An analysis of car-to-SUV and car-to-car collisions in the Netherlands determined that SUV occupants are less likely to be killed or seriously injured than passenger car occupants, but it was also observed that the occupants of vehicles that collide with SUVs experience a higher risk of being killed or seriously injured than the occupants of vehicles that collide with passenger cars (Margaritis et al. 2005).

An analysis of data from Great Britain also showed that the risk of fatality is higher for drivers of smaller vehicles than it is for the drivers of larger vehicles. It was also shown that the risk of fatality is higher for a driver colliding with a larger vehicle than a driver colliding with a lighter vehicle (Broughton 2008).

Fredette et al. (2008) combined an analysis of both vehicle type and mass using data from the Canadian vehicle fleet. It was determined that the drivers of the heavier vehicles in collisions experience a lower risk of fatality and that pickups are typically more aggressive than other vehicle types.

Martin & Lenguerrand (2008) analysed French data with respect to vehicle mass, and it was again determined that the risk of fatality is higher for the driver of a lighter vehicle when involved in a collision with a heavier vehicle. However, vehicle-to-vehicle collisions were also analysed using a holistic approach, and it was determined that the risk of a fatality occurring in a vehicle-to-vehicle collision is higher when there is a large difference between the involved vehicles' masses. Furthermore, it was found that the risk of fatality in a vehicle-to-vehicle collision is higher when the sum of the involved vehicles' masses is greater.

In an update of the earlier work by Newstead & Cameron (1999) and Cameron et al. (1999), their analyses of crashworthiness and aggressivity were complemented by an analysis of total secondary safety. The total secondary safety metric combines both crashworthiness and aggressivity into a single metric that considers the overall injury risk posed by a vehicle to its own occupants, unprotected road users, and occupants of other vehicles (Newstead et al. 2008). The rankings of different vehicle categories according to each of the three metrics are

summarised in Table 2.3. It was observed that "a strong relationship exists between crashworthiness and total secondary safety reflecting that crashworthiness is relevant to injury outcomes in all types of crashes" (Newstead et al. 2008, p77), and "a much weaker relationship [exists] between aggressivity and total secondary safety reflecting that aggressivity is only relevant to injury outcome in crashes between 2 light vehicles and involving unprotected road users" (Newstead et al. 2008, p78).

Table 2.3: The crashworthiness, aggressivity, and total secondary safety of various vehicle types in the Australian vehicle fleet ranked from safest (1) to least safe (10). Adapted from Newstead et al. (2008).

Ranking	**Vehicle safety ratings**		
	Crashworthiness	**Aggressivity**	**Total safety**
1	Medium SUV	Light car	Medium SUV
2	Large SUV	Small car	Large car
3	Large car	Medium car	Medium car
4	Commercial ute	Compact SUV	Compact SUV
5	Medium car	Large car	Small car
6	Compact SUV	MPV	Commercial ute
7	Commercial van	Medium SUV	MPV
8	MPV[a]	Commercial ute	Large SUV
9	Small car	Commercial van	Commercial van
10	Light car	Large SUV	Light car

[a] Multipurpose Passenger Vehicle (MPV)

An analysis of accident data from New Zealand also considered the overall injury risk posed by SUVs in terms of total secondary safety, and it was found that SUVs pose a relatively low injury risk per year of exposure, adjusted for distance driven. It was concluded that the higher aggressivity of SUVs is offset by a combination of their low collision involvement and good crashworthiness (Keall & Newstead 2008).

The literature clearly demonstrates that heavier vehicles offer less partner-protection than lighter vehicles, and that LTVs, SUVs, and MPVs typically offer less partner-protection than passenger cars. However, it is also clear that aggressivity only represents part of the issue of compatibility and that the self-protection of the

different vehicles should also be considered. Despite this, the literature addressing the total secondary safety of vehicles or the holistic outcome of vehicle-to-vehicle collisions is scarce.

2.3.2.2 Vehicle-to-vehicle collisions

Although vehicle type and mass have been the subject of extensive accident analyses, they have rarely been addressed as the primary variable in vehicle-to-vehicle tests. An early exception to this was a series of tests conducted by the NHTSA involving collisions between a passenger car and five other vehicles: another passenger car, a minivan, a SUV, a small pickup, and a large pickup (Summers et al. 1999, 2001). In these tests, the mass of the collision partner was found to correlate with the head, neck, and chest injury measures in the passenger car, but it was also observed that "even accounting for mass differences, there are additional factors that maybe affecting vehicle aggressivity" (Summers et al. 1999, p4). Most subsequent research has therefore focussed on identifying these additional factors.

2.3.2.2.1 Vertical structural alignment

The effects of vertical structural alignment have been investigated extensively in Europe, as early tests indicated that the misalignment of structural members had dominated the results by causing override/underride (Wykes et al. 1998).[6] In a collision between two similar MPVs, the vehicle with superior performance according to the European New Car Assessment Program (Euro NCAP) frontal testing procedure experienced underride and hence more compartment deformation than the vehicle that experienced override (Edwards et al. 2001*b*). The EEVC investigated the effects of vertical alignment in a collision with 100 mm ride height difference between two otherwise identical passenger cars (Wykes et al. 1998). The result was a substantial difference in vehicle deformation, although the mass and stiffness of the two vehicles were identical. In a subsequent test involving

[6] A vehicle is said to override another vehicle when its structural members pass over the top of the collision partner's structure in the event of a collision. Underride is the opposite.

a passenger car and a pickup, similarly poor interaction had been expected due to the vertical misalignment of the vehicles' structures. However, interaction occurred between the frame rail of the pickup and the suspension turret and engine mount of the passenger car, resulting in deformation similar to an earlier test involving two identical models of the passenger car. It was therefore concluded that "geometrical compatibility is not straightforward to asses" (Wykes et al. 1998, p668).

Series of tests performed in the USA have provided mixed results regarding vertical structural alignment. An initial set of tests that was performed by the IIHS compared the structural alignment and front-end stiffness of two LTVs. In a pair of frontal collisions with a passenger car, it was found that vertical alignment was the dominant effect (Meyerson & Nolan 2001). The NHTSA performed a subsequent set of collisions that compared new and old models of a large SUV in frontal collisions with a passenger car, but the results were inconclusive despite the lower structure of the newer model SUV. It was concluded that this was due to the greater mass and stiffness of the newer model SUV (Summers et al. 2003), and these results have subsequently been used to argue that "increasing the amount of structural engagement between a large vehicle and a small vehicle without regard to the structural forces and energy balance between the vehicles may produce undesirable results" (Verma et al. 2004, p585). The NHTSA attempted to show this with a subsequent set of tests in which pairs of pickups, SUVs, and MPVs with different front-end stiffnesses and different structural alignments were analysed in collisions with a passenger car. However, the results were again inconclusive and, at the relatively low collision severity used in the tests, increased override was observed to reduce the compartment accelerations and hence reduce the loadings on the Anthropomorphic Test Devices (ATDs) (Summers & Prasad 2005).

In a test performed by Seyer et al. (2003*b*) in Australia, it was observed that the effects of override/underride were stronger than those of vehicle mass.

The heavier of the two large cars in the test experienced underride, and its compartment was subsequently deformed to a greater degree than the compartment of the lighter, overriding car.

Recently, two series of tests were performed in Japan that involved a small passenger car colliding frontally with a SUV and a minicar colliding frontally with a large passenger car (Arai et al. 2007, Yonezawa et al. 2009*a*). Improvements in vehicle deformation and dummy injury measures were observed when the heights of the vehicles' structures were aligned.

In summary, it has been determined that vertical structural alignment is beneficial in severe collisions but that alignment alone does not guarantee compatibility. It has also been observed that misalignment may be beneficial in low severity collisions but, when analysed in the context of the entire accident environment, this may not offset the disbenefit observed in high severity collisions.

2.3.2.2.2 Horizontal structural alignment

The longitudinal structural members that act as the primary load paths in most vehicle designs cannot be located at the lateral extremities of the vehicle because this space is occupied by the front wheels. Hence, in some collision configurations, there may be a lateral misalignment between the vehicles' structures.

In a test performed by Mizuno et al. (2001) in Japan, a minicar and large car were aligned with 50% overlap of the width of the minicar. Due to the width of the front-end structures, the longitudinals of the vehicles did not interact with each other and instead crushed into the space between the wheel and the longitudinal of the collision partner. The 'fork effect'[7] was limited in this collision by interaction between the large car's crossbeam and the minicar's right front wheel. Although the deformation and injury measures in the minicar were generally higher, it was noted that the footwell intrusion and tibia injury measures in the large car were also very high (Mizuno et al. 2001).

[7]The 'fork effect' is the lateral equivalent of override/underride and occurs when longitudinal structural members pass by each other without interacting.

In a pair of European tests involving a large SUV and two models of mid-sized passenger cars, the relatively narrow width of the SUV's front-end structures resulted in lateral misalignment and minimal interaction between the vehicles' longitudinals in both tests, although the outcomes were otherwise quite different. In the first test, the lateral misalignment caused the SUV's bumper crossbeam to directly load the car's A-pillar. However, the effective interaction between the crossbeam and A-pillar was judged positively because it prevented the longitudinal from directly loading the footwell, which may otherwise have sustained significantly more deformation (Thomson et al. 2007). In the second test, the lateral misalignment and collision dynamics produced a partial 'glance off'[8] of the vehicles that resulted in an overall reduction in the loading of the car structure (Davies et al. 2006).

In summary, it has been observed that stiff lateral connections between the longitudinals are able to improve structural interaction in the event of lateral misalignment. Wider structures may also improve interaction, but it is not clear whether it would be more beneficial to promote glance off or structural interaction in low overlap collisions.

2.3.2.2.3 Multiple load paths

In an early European test involving a small and a mid-sized passenger car, it was observed that the connections between the front-end load paths were able to increase the stability of the structural elements undergoing crush and reduce the degree of override/underride (Wykes et al. 1998). In a subsequent test between two small passenger cars, one with a single front-end load path and one with dual load paths, it was observed that the vehicle with a single load path experienced less stable deformation of its front-end and more compartment deformation than the vehicle with dual load paths (Edwards et al. 2002). This was further

[8] Vehicles may 'glance off' each other in an offset collision with the effect that both maintain some forward velocity. Compared to a collision where the structures engage and one or both of the vehicles has a rearward velocity after the collision, glancing off each other leads to a much lower Δv for each vehicle, and substantially less kinetic energy must be dissipated.

investigated using two identical mid-sized passenger cars with a single load path design and ride heights that were modified to create a 60 mm vertical offset that would "promote any under/override that was likely to occur [in a real accident]" (Edwards et al. 2003*a*, p9). Tests were performed with the original vehicle designs and with the addition of a lower load path mounted forward of the engine subframe. The results showed a decrease in compartment deformation for the modified vehicles that was attributed to "the improved structural interaction and increased energy absorption of the frontal structure given by the additional load path and frontal connections" (Edwards et al. 2003*a*, p9).

During the initial phase of the VC-Compat project, a pair of tests was performed to compare the performance of a single load path vehicle in a collision with itself and in a collision with a dual load path vehicle. The two vehicle models had similar weights, and it was expected that the collision involving the vehicle with dual load paths would be more compatible. However, although it was observed that improved structural interaction occurred in the collision with the dual load path vehicle, the single load path vehicle experienced less compartment deformation in the collision with itself even though the collision had involved override/underride (Davies et al. 2005).

The VC-Compat consortium performed a second test series using newer model mid-sized passenger cars that subsequently provided the expected results (Thomson & Edwards 2005). It was observed that less override/underride occurred between the two identical vehicles with multiple load paths than between the two identical vehicles with a single load path. In a third collision performed in this test series, the single load path vehicle was tested against the multiple load path vehicle. It was observed that the single load path vehicle experienced less deformation than in the collision with itself and that the multiple load path vehicle was deformed to a similar extent as in the collision with itself (Davies et al. 2006).

These two mid-sized passenger cars were then used in a series of tests in-

volving a small, single load path passenger car. This test series had the objective of assessing the effect of single and multiple load path designs in collisions between vehicles of different masses. However, override/underride occurred in all tests due to the instability of the small car's front-end, and the compartment cell of the small car also collapsed in all of the tests, which prevented an accurate assessment of structural interaction (Thomson et al. 2007).

In a final set of tests investigating multiple load path designs, the VC-Compat consortium again used the two mid-sized passenger cars in collisions with a large SUV that itself had an additional lower load path. In the collision with the multiple load path passenger car, the lower load path of the SUV acted to limit the deformation of the car, but in the collision with the single load path passenger car, the SUV still induced significant override/underride (Davies et al. 2006, Thomson et al. 2007).

In Japan, a set of tests was performed using a mid sized passenger car and a minivan that were approximately equal in weight but had vertically misaligned primary structures (Mizuno et al. 2005*b*). In an initial test, some override/underride occurred, but its effect was limited by the lower crossbeam of the minivan, which interacted with the longitudinals of the passenger car. The test was then repeated with the crossbeam removed, and although the degree of override/underride increased, this time it was limited by interaction between the car structure and minivan engine (Mizuno et al. 2005*b*). These two tests were performed at relatively low severity, and it was observed that the compartment deformations were small. Hence, similar to the observations of Summers & Prasad (2005), it was found that the test without the minivan crossbeam resulted in lower dummy injury measures because the poorer structural interaction caused the compartment accelerations to be reduced (Mizuno et al. 2005*a*).

A subsequent set of tests was performed in Japan using a small passenger car and a SUV with 'blocker type' SEAS.[9] Tests were performed with and without the

[9] A 'blocker type' SEAS consists of an additional structure mounted below the primary load paths (Arai et al. 2007).

SEAS, and it was observed that the SEAS increased interaction with the passenger car wheel. Although "it was demonstrated that the SEAS of the [SUV] is quite effective for structural interaction improvement" (Mizuno et al. 2008, p536), the head, neck, and chest injury measures in the passenger car were higher in the test with the SEAS due to a 12 ms delay in the deployment of the restraint system (Mizuno et al. 2008).

The NHTSA performed a pair of tests between a passenger car and a new model MPV, which had a multiple load path design, and its predecessor model, which had fewer load paths (Patel et al. 2007). Vehicle mass was controlled in the tests and the vertical structural alignment of both MPVs was similar. The results showed that the newer design MPV induced higher injury measures in the passenger car despite the multiple load path design (Patel et al. 2007). The NHTSA concluded that a multiple load path design may reduce compatibility based on their assessment that the stiffness of both MPV models was similar (Patel et al. 2007, Table 2, p10) and hence their belief that the number of load paths was the only significant variable in the tests. However, significant doubt must be cast on this conclusion because the NHTSA's own results showed that their assessment of stiffness may be affected by the design of the barrier used to measure the forces and also that the newer model MPV may have been substantially stiffer than the older model (Patel et al. 2007, Table 1, p7). In a later test of blocker type SEAS, substantially better performance was observed in a pair of passenger car to LTV collisions when the SEAS was installed (Patel et al. 2009).

In summary, it has been observed that multiple load path designs typically improve structural interaction compared to single load path designs. However, as seen in the analyses of vertical alignment, improved interaction sometimes results in increased dummy injury measures in low severity collisions. It has also been observed that many different front-end components act as effective load paths. Furthermore, some of the results indicate that multiple load path designs may deform more stably than single load path designs.

2.3.2.2.4 Compartment strength

Even in collisions where structural interaction was good, the results have sometimes been observed to be incompatible due to the incongruence of the front-end force levels and the compartment strengths of the colliding vehicles.

In a Japanese test between a small car and a large car, the vertical alignment of the structures and the structural interaction observed in the collision were both good, but large deformations of the small car structure were still observed (Mizuno et al. 2001).

An Australian test between two small cars demonstrated that this issue is not just a product of vehicle mass. In that test, the heavier of the two cars sustained substantially greater compartment deformations due to poor compartment strength (Seyer et al. 2003*b*).

Similarly, a Japanese test involving a mid sized passenger car and a MPV, which were similar in weight and had vertically aligned primary load paths, resulted in good structural interaction but greater deformation of the MPV due to the higher stiffness of the car's front-end (Mizuno et al. 2005*b*).

In a pair of tests performed in Australia and Japan, a large passenger car was tested against new and old models of a small passenger car. In the first, Australian test, the old model of the small passenger car exhibited insufficient compartment strength and sustained large compartment deformations (Seyer et al. 2003*b*). Subsequently, the manufacturer of the small car modified the design to increase the compartment strength whilst leaving the front-end design otherwise unchanged. In the Japanese test with the newer model, the compartment remained stable and there was a generally large reduction in injury measures (Mizuno et al. 2005*a*). Interestingly, structural interaction was observed to be poor in both tests, but the increased compartment strength in the later test appeared to have also stabilised the deformation behaviour of the small car's front-end (Mizuno et al. 2005*a*).

In Europe, a test was performed with a minicar that had previously been

shown to perform well in collisions with much heavier passenger cars (Damm 2006). In a collision with itself, the minimal deformation zone of the minicar was ineffective and resulted in very high compartment decelerations and substantial footwell deformation (Damm 2006).

The NHTSA performed a series of tests with passenger cars and LTVs in which front-end stiffness matching was investigated whilst controlling vehicle weight and the vertical alignment of the structures (Patel et al. 2007). In the four tests with unmatched front-end stiffness, the dummy injury measures indicated a high risk of fatality, and in a single test with matched front-end stiffness, the dummy injury measures indicated a low risk of fatality (Patel et al. 2007). However, the results of this test series may have been biased by the use of two different passenger car models in the 'matched' and 'unmatched' tests.

In summary, it has been observed that a high strength passenger compartment is beneficial, and it is also apparent that the front-end force levels of vehicles should not be so high as to overwhelm the compartment strength of their collision partners. It has not been demonstrated that the dissipation of energy should be shared equally by collision partners, but it has been shown that all pairings of vehicles must be capable of dissipating the total collision energy within the deformation potential of their front-ends. If the severity of the collision exceeds the ability of the front-ends to dissipate the kinetic energy, then the compartment of one or both of the vehicles may be compromised.

The test results described above have been instrumental in the development of government policy and contemporary theory related to front-to-front compatibility. However, the mixed results clearly demonstrate the complexity of compatibility as a science and the difficulties of performing controlled tests. The methods used to evaluate the results are also open to criticism, since they range from subjective analyses of deformation behaviour and 'crash-aesthetics', which may be too idealised to reflect the multitude of possibilities that occur in the real accident environment (Zobel 1998), to highly objective dummy injury

measures, which may be too specific to reflect anything other than the exact test conditions.

2.3.3 Test and assessment proposals

Following the introduction of the Offset Deformable Barrier (ODB) test procedure, both as a 56 km/h test in ECE-R94 and a 64 km/h test in various NCAP programs, concerns were raised that the severity of the test procedure would lead manufacturers to build stiffer vehicles that would offer improved self-protection but could also act more aggressively in a vehicle-to-vehicle collision (Zeidler & Knöchelmann 1998). Early analyses by the IIHS found that redesigned vehicles retained similar stiffnesses in their front-ends, but that the compartment stiffness had been increased (Nolan & Lund 2001). However, later research performed by the NHTSA found that the redesigned vehicles that performed better in the 64 km/h ODB test were also more aggressive in oblique frontal offset collisions with a mid sized passenger car (Saunders & Prasad 2005). Conflicting positions also existed with regards to the speed appropriate for the test. Fildes et al. (2000) predicted a substantial benefit for the introduction of a 64 km/h regulatory test speed, but noted that further research of potential disbenefits was warranted. Edwards et al. (2001*a*) similarly recommended an increase in the ECE-R94 test speed to 65 km/h because it would be more representative of the accident environment. However, due to the stiffness concerns, the position in IHRA was to "review this issue again when more is known about the likely influence on compatibility" (Lomonaco & Gianotti 2001, p5).

2.3.3.1 Compartment strength test

The ODB test procedure has also been investigated extensively with an 80 km/h test speed that was designed to assess maximum compartment strength (Zobel & Schwarz 2001, Edwards et al. 2002, Mizuno et al. 2003, 2004, 2005*b*). However, this approach was ultimately abandoned because it was "thought that adequate

control of the compartment strength should be possible using a lower test speed [between 56 km/h and 64 km/h]" (Faerber 2007, p5).

2.3.3.2 Progressive Deformable Barrier

Based on the results of the AIT/FIA compatibility project, Klanner et al. (1998) proposed an alternative to the ODB used in ECE-R94. The proposed barrier was seen to be beneficial because it had higher stiffness, dissipated more energy, and did not 'bottom out',[10] but it was ultimately rejected by the EEVC because it "loaded the front of the car in an unrealistic way" (O'Reilly 2001, p6). However, the concept was further developed by Renault, and it evolved into what is now known as the Progressive Deformable Barrier (PDB) (Delannoy & Diboine 2001). Both the test procedure and barrier design of the PDB have subsequently undergone several design iterations, and the barrier has also been considered using a variable test speed (Seyer et al. 2003*b*), a mobile trolley (Seyer et al. 2003*b*, Schram & Versmissen 2007), and as a full width test (Delannoy et al. 2007). Several compatibility assessment criteria have been investigated for the PDB, including, for example, the Average Height Of Deformation (*AHOD*) and Average Depth Of Deformation (*ADOD*) described by Delannoy et al. (2005), but these were not verified in the VC-Compat project and "no formal compatibility assessment criteria with proposed thresholds have been published" (Faerber et al. 2007, p38). In late 2007, the French government formally submitted a proposal to amend ECE-R94 with the PDB test procedure (France 2007). The justification for the proposal was the issue of self-protection, since it was claimed that the test severity of the current ECE-R94 test procedure is lower for lighter vehicles and would be independent of vehicle mass if the PDB was introduced. However, during recent debate in the ad hoc group formed to address the French proposal, doubt regarding both the capability of the PDB and the benefit associated with the French objectives has been expressed by several countries (Castaing 2009).

[10] A barrier is said to 'bottom out' when the test vehicle crushes the deformable element completely and interacts directly with the rigid wall behind it.

2.3.3.3 Full Width Deformable Barrier

As discussed in Section 2.3.2.2, vehicle-to-vehicle tests performed in Europe identified a need to improve the frontal stiffness distributions of vehicles' front-end designs. Building on a recommendation from the IHRA to develop a harmonised full width test procedure (Lomonaco & Gianotti 2001), a Full Width Deformable Barrier (FWDB) was developed with the aim of measuring and assessing front-end forces (Edwards et al. 2003*b*). The Full Width Rigid Barrier (FWRB), which has been used in Federal Motor Vehicle Safety Standard (FMVSS) 208 since the 1970s, was seen as inappropriate for this task because the force measurements are distorted by inertial effects, and the flat, rigid surface is unable to load secondary load paths or generate shear forces in the connections between the load paths (Edwards et al. 2003*b*). The IHRA compatibility and frontal impact working group proposed the use of the FWDB to assess structural alignment (O'Reilly 2005), but this proposal remains unimplemented following the cessation of IHRA activities. Diverse assessment approaches have been investigated for the FWDB, and both Vertical Structural Interaction (VSI) and Horizontal Structural Interaction (HSI) metrics were proposed in the VC-Compat project (Edwards et al. 2007*b*). Performance limits were subsequently proposed by the EEVC compatibility and frontal impact working group (Faerber et al. 2007). However, repeatability and reproducibility tests performed in the Advanced Protection Systems (APROSYS) project found that the current metrics lack sufficient robustness (Edwards 2009).

2.3.3.4 Full Width Rigid Barrier

Despite the limitations listed above, the NHTSA has investigated several metrics based on force assessments with the FWRB (Swanson et al. 2003, Mostafa et al. 2005, Summers & Prasad 2005). Most recently, the NHTSA has evaluated the Average Height Of Force ($AHOF$) metric in the first 400 mm of vehicle deformation ($AHOF_{400}$) and a work stiffness metric known as $K_{W_{400}}$, which is also measured during the first 400 mm of vehicle deformation (Patel et al. 2007). The two metrics

were developed to measure structural alignment and initial stiffness, respectively, with the goal of encouraging similar structural characteristics across the vehicle fleet. The response from the automotive industry to both $AHOF_{400}$ and $K_{W_{400}}$ has been universally negative, with criticism of both the accuracy and side-effects of the metrics (Subramaniam et al. 2007, Hirayama et al. 2007, Uwai et al. 2007, Nusholtz et al. 2009).

In a pair of complementary research programmes in the USA and Japan, the assessment of vertical structural alignment has recently been investigated using a combination of the FWRB for PEAS and component level tests for SEAS (EVC 2009, Yonezawa et al. 2009*a*). Both research programmes investigated metrics similar to the VSI, which was originally defined for use with the FWDB. By adding additional tests for SEAS and only assessing the initial part of the vehicle deformation, the principal limitations of the FWRB were avoided. However, since the metrics proposed by the EVC and Yonezawa et al. are limited to the assessment of vertical alignment, the EVC concluded that there is "no evidence that [they] could provide a better compatibility assessment than the [EVC voluntary standard] already specifies" (EVC 2009, p5).

2.3.3.5 Mobile Deformable Barrier

Fixed barrier approaches are limited in their application to vehicle-to-vehicle compatibility because the test severity is typically representative of a collision with an identical vehicle, and hence the issues of mass and front-end stiffness imbalances are not addressed.[11] Several mobile barrier approaches have hence been developed, but none are considered as candidates for short or mid-term implementation. An oblique frontal offset test procedure was trialled in the USA and Japan (Ragland 1998, Mizuno et al. 2001), but several practical and technical issues led to the approach being discontinued (see Lomonaco & Gianotti 2001, Table 2, p6). In Australia, and more recently in Europe, the use of the PDB on

[11] A test velocity dependent on the vehicle mass would overcome this limitation, but is considered politically untenable.

a mobile trolley has been investigated in the co-linear frontal offset configuration (Seyer et al. 2003*b*, Schram & Versmissen 2007). The Australian research was discontinued due to repeatability issues, but the European research is expected to continue in the FIMCAR project (CORDIS 2009). Vehicle manufacturers have also developed various mobile barriers for the co-linear full overlap configuration (Takizawa et al. 2005, Verma 2007).

2.3.3.6 Geometric assessment

As discussed in Section 2.3.1, the only standards that currently address compatibility were introduced by the EVC in 2003. In their initial form, these standards were based on purely geometrical requirements that required the presence of either PEAS or SEAS within the 'bumper zone' defined in the 49 Code of Federal Regulations (CFR) Part 581 Bumper Standard (EVC 2003). The original requirements have subsequently been amended to define quasi-static performance requirements for SEAS (EVC 2006). Further research was performed by the EVC with the aim of identifying dynamic performance requirements that could replace the original geometric requirements. However, a satisfactory alternative could not be identified (EVC 2009). The NHTSA continues to pursue a similar research program, including the investigation of $AHOF_{400}$ for the assessment of PEAS as well as an over-ride barrier to control the stiffness of SEAS (Patel et al. 2009). In accordance with the EVC self-commitment, all LTVs sold in the USA by the BMW Group, Chrysler LLC, Ford Motor Company, General Motors, Honda, Hyundai Motor, Isuzu Motors, Kia Motors, Mazda, Mercedes-Benz USA, Mitsubishi Motors, Nissan, Subaru, Suzuki, Toyota, and Volkswagen Group have been in compliance with the requirements since September 2009 (EVC 2009).

2.4 Compatibility in front-to-side collisions

Research on compatibility in front-to-side collisions is not as extensive as that related to front-to-front collisions. An explanation for this may be that compatibil-

ity is a combination of self-protection and partner-protection (see Section 2.3), but although a balance must be sought for optimum results in front-to-front collisions, in an assessment of front-to-side compatibility, such as that proposed by Appel et al. (1991), the self-protection of the struck vehicle and the partner-protection of the striking vehicle have priority.[12] Furthermore, although some concepts of front-to-front compatibility advocate equal protection in both vehicles, it is generally accepted that the occupants of a struck vehicle in a front-to-side collision have an inherent disadvantage. Although the intricacies of front-to-side compatibility have always made it difficult to study, early research in this field was performed parallel to that of front-to-front compatibility and included the work of Seiffert et al. (1974), Danner et al. (1980), EEVC WG6 (1982), and Appel et al. (1991).

2.4.1 Harmonisation and demarcation of test procedures

Development of a dynamic side impact test procedure began in both Europe and the USA in the 1970s, and, by the early 1980s, the fundamental designs of the MDBs that would eventually be adopted into regulation had been developed and published (EEVC WG6 1982, Davis & Ragland 1980 cited in EEVC WG6 1982). However, validation of the barriers, development of ATDs, and specification of performance criteria were still necessary, and it was not until 1990 that the American test procedure was added to the existing quasi-static requirements in FMVSS 214. The European test procedure, which includes more complex designs of both the ATD and the MDB, was introduced as ECE-R95 in 1996.

The Japanese government adopted ECE-R95 as Traffic Safety and Nuisance Research Institute's Automobile Type Approval Test Standard (TRIAS) 47-3 in 1998, but when the Australian government introduced the Australian Design Rule (ADR) 72 in 1999, compliance with the requirements of either ECE-R95 or FMVSS 208 was accepted. Despite this, Australian regulators supported the devel-

[12] In a front-to-side collision, the 'struck' vehicle is the vehicle that experiences a side collision, and the 'striking' vehicle is the vehicle that experiences a frontal collision.

opment of a harmonised test procedure and had published such a proposal before ADR 72 even came into effect (Seyer et al. 1998). At the same time, the NHTSA published the results of their comparison of the two regulations, which identified the need to harmonise developments of future side impact ATDs and the need for FMVSS 214 to address collisions with LTVs (Samaha et al. 1998). The EEVC was also working on updates to ECE-R95, although these were primarily focussed on addressing limitations in the initial design of the MDB and the certification tests used during the manufacturing process (De Coo et al. 1998). Building on this background, an IHRA working group was founded in 1998 to coordinate the various research programs. The scope of the IHRA side impact working group also included a vehicle-to-pole test, out-of-position side airbag evaluation tests, and component level head impact tests, but because they have limited applicability to the issue of front-to-side compatibility, the review below is limited to the research on MDB test procedures.

The initial research of the IHRA group focussed on developing a harmonised test procedure, and hence research was performed to identify the properties of the MDBs that were most influential on dummy injury measures. Australian and Canadian researchers collaborated on a parametric study investigating the effects of the MDB mass, stiffness, stiffness distribution, ground clearance, configuration (crabbed or perpendicular), and collision velocity (Seyer et al. 2000). It was observed that increasing the test velocity and increasing the ground clearance of the barrier had the greatest effect on dummy injury measures, and that changing the stiffness and mass of the trolley was less influential. Seyer et al. (2000) found that the perpendicular configuration resulted in higher injury measures for the front seat dummy than the crabbed configuration, and this result was confirmed in tests performed in Japan (Yonezawa et al. 2001). The Japanese tests provided the opposite results for rear seated dummies, but Yonezawa et al. (2001) considered that a valid assessment of rear seat occupant protection would still be possible with a perpendicular test. The EEVC further investigated the effects of

the MDB mass, stiffness, profile, and ground clearance on rear seat dummies, but found that the front seat dummies were more sensitive to the changes (Lowne 2001).

Accident and fleet analyses were performed in both Japan and Europe and identified similar shortfalls with the ECE-R95 specification (Yonezawa et al. 2001, Edwards et al. 2001*a*). Both studies found that the median mass of the vehicle fleets was higher than the barrier mass and that the ground clearance of the barrier did not represent the height of current vehicles' longitudinals. Edwards et al. (2001*a*) were unable to correlate the latter point with accident data, but did determine that the test speed was too low. Yonezawa et al. (2001) determined that the test speed was correct, but found that the stiffness of the barrier was also too low in comparison to current vehicles' longitudinals. Based on these results, the IHRA side impact working group saw the need for "further research to define the test parameters of the [harmonised] MDB test" (Seyer 2001, p6).

By 2003, IHRA had abandoned the goal of a harmonised test procedure and was instead advocating a LTV-like barrier design for North America and a car-like barrier design for other markets (Seyer 2003). Catalysts for this shift were the introduction of the 'IIHS barrier', which was based on the FMVSS 214 barrier but designed to be more representative of the front-end geometry and ride height of a LTV (Arbelaez et al. 2002), and the initiation of work on the Advanced European Mobile Deformable Barrier (AE-MDB), which was being designed to be more representative of current model European and Japanese passenger cars than the existing MDB in ECE-R95 (Roberts & van Ratingen 2003). Although both the AE-MDB and IIHS test procedures used a 1500 kg barrier mass, 50 km/h test velocity, and perpendicular configuration (Dakin et al. 2003, Roberts & van Ratingen 2003), tests in Europe and Japan found that the geometry of the IIHS barrier face resulted in vehicle loadings that were not representative of a front-to-side collision between typical European or Japanese passenger cars (Roberts & van Ratingen 2003, Yonezawa et al. 2003).

The status quo has remained largely unchanged since 2003, despite calls from the automotive industry to adopt a harmonised test in the form of a Global Technical Regulation (GTR) (McNeill et al. 2005). Although the NHTSA identified an opportunity to update the FMVSS 214 barrier to be more representative of a LTV (Samaha & Elliott 2003), it took the view that "much research was [still] necessary to properly design a barrier that would accurately simulate the characteristics of the fleet" (Newgard et al. 2005, p10). Further research by the NHTSA to develop a new barrier has not been published, and vehicles designed for the North American market must therefore continue to perform well in both the FMVSS 214 test and the IIHS test. In Europe and Japan, development of the AE-MDB has continued through several iterations including the addition of a bumper element and the consideration of several stiffness distribution for the deformable element. Test results have been published for AE-MDB Version 1 (Roberts & van Ratingen 2003, Yonezawa et al. 2005), Version 2 (Ellway 2005, Matsui et al. 2007), Version 3.1 (Versmissen et al. 2007), Version 3.1J (Ueno et al. 2007), Version 3.3 (Fujiwara & Murayama 2007), Version 3.9 (Versmissen et al. 2007, Roussarie et al. 2007), and Version 3.10 (Fujiwara & Shigeta 2009), but there is still a lack of consensus regarding the preferred design.

2.4.2 Research findings

In addition to the design of the MDBs discussed in the previous section, the principal findings of research on front-to-side compatibility can be summarised in two major categories, which are broadly similar to those discussed for front-to-front compatibility in Section 2.3.2. Firstly, published statistical analyses cover a broad range of variables, but those most relevant to the issue of compatibility address the vulnerability and aggressivity of different vehicle types and design characteristics. Secondly, published results of front-to-side vehicle crash tests are typically focussed on investigations of controlled variables including mass, stiffness, geometry, and collision configuration.

2.4.2.1 Aggressivity and vulnerability

During the resurgence of compatibility research in the mid to late 1990s (see Section 2.3.1), the issue of front-to-side compatibility attracted a similar degree of interest to that of front-to-front compatibility.

In early results from Japan, comparisons with other passenger vehicles showed that minicars are less aggressive as striking vehicles and more vulnerable as struck vehicles and that the opposite is true for SUVs (Mizuno & Kajzer 1999). However, it has also been noted that passenger cars dominate the Japanese accident environment, representing approximately 57% of struck and striking vehicles (Yonezawa et al. 2001).[13] Early results from the NHTSA showed that the number of LTVs in the USA has increased substantially, but they also showed that there has been a disproportionately greater increase in the number of fatalities in LTV-to-car side collisions (Gabler & Hollowell 2000). The issue of aggressivity in collisions where the struck vehicle was a passenger car has also been analysed with respect to the ratio of driver fatalities in the striking and struck vehicles. Gabler & Hollowell (2000) found that the ratio is 1:6 for car-to-car collisions, whereas for LTV-to-car collisions the ratios range between 1:11 for small pickups to 1:23 for full size vans. These ratios were recalculated in more recent publications (Summers et al. 2001, 2003), with the most current results being 1:8 for car-to-car collisions, 1:22 for SUV-to-car collisions, and 1:39 for large pickup-to-car collisions. The NHTSA also calculated aggressivity ratings based on the number of fatalities in struck vehicles per 1000 front-to-side collisions that involved a particular type of striking vehicle (Summers et al. 2001). These range from 0.33 for minicars to 4.02 for large pickups. Similar ratings were calculated for vulnerability based on the number of fatalities in a particular type of struck vehicle per 1000 front-to-side collisions with any other vehicle. These range from 0.53 for minivans to 1.92 for subcompact cars and also include the much higher

[13] Vehicles not defined as 'passenger cars' in this study were 'buses', 'utility vehicles', 'vans', 'mini passenger cars', 'large trucks', 'trucks', and 'mini cargo' vehicles (Yonezawa et al. 2001, Figure 1, p2).

rate of 6.79 for minicars. Australian research found that larger striking vehicles are more aggressive, although it was not determined whether the cause of this aggressivity is due to mass or other size effects (O'Reilly 2001). In European research, influential factors were found to be the striking vehicle's bonnet height and the height difference between the striking vehicle's bumper and the struck vehicle's sill. A clear relationship between mass and aggressivity was not observed in Europe (O'Reilly 2001). Samaha & Elliott (2003) analysed the mean collision conditions for struck passenger vehicle occupants that sustained at least one AIS 3+ injury. The median Δv in a collision with a LTV was found to be 4 mph (6.4 km/h) higher than in a collision with a passenger car, and the median weight of colliding LTVs was found to be 800 lbs (363 kg) heavier. Using ordered probit models, Austin (2005) found that LTVs are more aggressive than passenger cars in a nearside collision with a passenger car. For vans, this was attributed to vehicle weight, but for pickups and utility vehicles the height of the vehicles' structures was also found to be significant.

The NHTSA analysed the risk of injury by body regions for passenger car occupants struck by a LTV and those struck by another passenger car (Samaha & Elliott 2003). It was found that the risk of AIS 3+ injury in a collision with a LTV is higher in all body regions, but the largest increase is for head injuries. LTVs were also analysed as struck vehicles, and it was found that LTVs are again the more aggressive collision partner, resulting in higher incidences of head, pelvis, and abdomen injuries (Samaha & Elliott 2003). Acierno et al. (2004) performed an in-depth analysis of 15 nearside passenger car occupants who sustained injuries in a collision with a LTV. It was found that 8/15 sustained AIS 2+ head injuries, 11/15 sustained AIS 2+ chest injuries, 5/15 sustained AIS 2+ abdomen injuries, 8/15 sustained AIS 2+ pelvis injuries, and 2/15 sustained AIS 2+ injuries to the extremities. The "injuries were attributed to intrusion of the door panels, B-pillar, and in some cases direct contact with the impacting vehicle" (Acierno et al. 2004, p765). Scarboro et al. (2007) performed a broader analysis of AIS 3+ injuries for

car-to-car, car-to-LTV, LTV-to-car, and LTV-to-LTV front-to-side collisions. The results indicated that LTV-to-car collisions produce a higher incidence of chest injuries, but reanalysis of the published data shows that the observed differences are not significant at the 95% confidence level.[14] Injury distributions in Japan were analysed with respect to the type of striking vehicle, and it was found that larger vehicles cause a higher proportion of head and thorax injuries and a lower proportion of neck and 'other' injuries (Yonezawa et al. 2009*b*).[15] No apparent trend was observed for abdomen and pelvis injuries.

Based on time series data from the USA from 1975 to 2000, Abdel-Aty & Abdelwahab (2004) investigated the mix of LTVs and cars in the vehicle fleet and their influence on the accident statistics. It was predicted that the total number of fatalities in front-to-side collisions would increase by 12% by 2010 and that the number of fatalities in LTV-to-car front-to-side collisions would increase by 32% by 2010. However, "this analysis assumes the continuation of the current trends and not taking into consideration any drastic changes in consumer preferences and/or other effects [sic]" (Abdel-Aty & Abdelwahab 2004, p462). The EVC voluntary standards on the alignment of LTV structures, which were phased in between 2003 and 2009, have been shown to reduce the fatality risk of nearside passenger car drivers by 19% (Baker et al. 2008) and therefore represent a change that should avert at least part of the decline that was predicted by Abdel-Aty & Abdelwahab.

2.4.2.2 Vehicle-to-vehicle collisions

Front-to-side compatibility has been investigated using full scale tests between two vehicles, tests with MDBs as surrogates for the striking vehicle, and collision simulations. This section is focussed on the results of full scale tests, since these are the most reliable representation of the accident environment.

[14] Exact p-values cannot be calculated without the exact case numbers. However, conservative estimates of the data (Figure 5, p7) clearly indicate that the observations made by Scarboro et al. are not significant ($p > 0.05$).

[15] The vehicle classifications used by Yonezawa et al. (2009*b*) were 'minicar', 'passenger car', '1-Box or SUV', and 'large vehicle or truck'.

A parametric study of mass, stiffness, and the vertical height of structural members was performed by the IIHS using large American sedans and LTVs (Nolan et al. 1999). An unexpected result was that the tow hooks mounted on the frame rails of one of the LTVs had a significant influence on the interaction between the vehicles. Also, it was found that an absolute increase in deformation did not necessarily result in higher injury measures, but rather that the manner of deformation was more important. Analysis of this test series within IHRA concluded that the lateral bending of the striking vehicles' front-end structures, which was attributed to the forwards motion of the struck vehicles, reduced the striking vehicles' effective frontal stiffness (O'Reilly 2001). Nolan et al. (1999) concluded that improved engagement with the side structures of the struck vehicle would result in improved compatibility. For the nearside occupant's head, it was determined that a higher bonnet increased the risk of head contact and injury: "the key issues are height of the intruding structure and the extent of intrusion, which is greatest for the heavier, stiffer, and more massive vehicles" (Nolan et al. 1999, p10).

The NHTSA performed a series of five tests between a passenger car and five other vehicles: another passenger car, a minivan, a SUV, a small pickup, and a large pickup (Summers et al. 1999, 2001). However, the injury measures for the struck driver did not show a strong correlation with either the weight of the striking vehicles or the aggressivity ratings that had been derived from accident data. The NHTSA subsequently performed a parametric test series to investigate the effects of structural height and vehicle weight (Summers et al. 2001). Car-to-car and large SUV-to-car tests were performed, but it was found that "there is not a simple or direct relationship between the striking vehicle's weight and the measured probability of injury. Side impact compatibility also involves tradeoffs between the injury location both between the head, thorax, and pelvis injury measures, and between the front and rear seat occupants. Simple changes to the striking vehicle do not lead directly to a reduction in the injury criteria of the

struck occupants" (Summers et al. 2001, pp7-8).

In Japan, a test series was performed using a mid-sized passenger car as the struck vehicle and a SUV, minivan, and 1-Box as striking vehicles, which were all ballasted to a test weight of 1500 kg (Yonezawa et al. 2003). The results were mixed, but the minivan, which had the lowest longitudinal heights, appeared to be the least aggressive. A later test series performed in Japan by Yonezawa et al. (2009*a*) included a mid-sized passenger car as the struck vehicle and a 1-Box and the same mid-sized passenger car as the striking vehicles. The car-to-car combination was tested in both the moving-to-stationary and the moving-to-moving configurations, whilst the 1-Box-to-car combination was only tested in the moving-to-stationary configuration. The 1-Box, which was heavier than the car, was judged to be more aggressive even though it produced the lowest head injury measures. Yonezawa et al. attributed the lower head injury measures to the flat deformation pattern caused by the 1-Box, which heavily loaded the struck dummy's thorax but produced kinematics that reduced the loading on the head. The moving-to-stationary configuration resulted in greater deformations and higher dummy injury levels than the moving-to-moving configuration, although the dummy kinematics were judged to be similar. Yonezawa et al. concluded that the deformation mode of the car's front-end in the moving-to-moving test was less stiff due to the sideways deformation of the structure and hence confirmed the earlier conclusions based on the IIHS tests.

Within the EEVC and the APROSYS project, a series of tests using four different striking vehicles and six different struck vehicles was performed to produce baseline data for the development of the AE-MDB (Lowne 2001, Ellway 2005, Versmissen et al. 2007). A small SUV, which was the heaviest of the striking vehicles, produced the greatest degree of intrusion and typically the highest dummy injury measures in the struck vehicles. Within the test series, it was found that the bumper crossbeams of the striking vehicles were stiffer than the centre regions of the AE-MDB v1 and AE-MDB v2. The higher stiffness of the crossbeams

led to increased interaction with the struck vehicles' B-pillars, and hence the AE-MDB v3.1 and AE-MDB v3.9 were both developed with a bumper beam element (Versmissen et al. 2007). Although these tests did not specifically address the issue of compatibility, they did highlight the interaction between bumper cross-beams and B-pillars.

2.4.3 Assessment of front-to-side compatibility

As stated previously, the compatibility research projects of the mid to late 1990s initially attached a similar degree of importance to both front-to-front and front-to-side compatibility. The NHTSA stated their intent to "determine the effect that different striking vehicle front end characteristics have on side struck vehicle occupant responses" (Hollowell & Gabler 1996, p5), whilst the EEVC stated that "effort will be concentrated on the most important impact types: car to car frontal and side impacts" (Faerber et al. 1998, p650). These two positions were reflected in IHRAs initial objective "to develop internationally agreed test procedures designed to improve the compatibility of car structures in front to front and front to side car to car impacts" (Rodgers 1998, p636).

However, by 2001, IHRA had determined that front-to-side compatibility was "a complex area" (O'Reilly 2001, p9). For the struck vehicle, it was concluded that the optimisation of self-protection with respect to the current vehicle fleet was the most appropriate strategy. For the striking vehicle, it was concluded that front-to-front compatibility strategies "that encourage homogeneity and good interaction with sill and passenger compartment pillars [sic]" (O'Reilly 2001, p9) would also be beneficial for front-to-side compatibility. A proposal to optimise the stiffness distribution for front-to-side compatibility in the first 100 mm of front-end deformation was considered a "speculative possibility" (O'Reilly 2001, p10), but in 2003 the IHRA compatibility working group reported that "a set of requirements aimed especially at side impact compatibility is not being worked on" (O'Reilly 2003, p4).

More recently, front-to-side compatibility was addressed in the APROSYS project, and an assessment concept for front-end structures was proposed (Thompson et al. 2007). The APROSYS assessment concept advocated the control of vertical load distributions so that interaction with the sill would be encouraged and loading of nearside occupants' upper bodies would be discouraged. The assessment of the initial phase of vehicle deformation was suggested, but the definition of the desired vertical load distribution and the specification of performance limits were still identified as future research.

Chapter summary

In Section 2.1, the scope of the thesis is defined within the broader scope of traffic safety research. In Section 2.2, the dynamic vehicle test procedures that are currently used in regulations and consumer information tests are listed. These place critical demands on the design of vehicles and hence influence the compatibility of the current vehicle fleet. Finally, in Sections 2.3 and 2.4, the literature related to the background, research findings, and assessment proposals for front-to-front and front-to-side compatibility are discussed. The results of the literature review are summarised below with regards to the research questions that are defined in Chapter 1.

What are the boundary conditions of front-to-front and front-to-side compatibility? In numerous studies, it has been observed that larger, heavier vehicles are more aggressive and that smaller, lighter vehicles are more vulnerable in both front-to-front and front-to-side collisions. However, analyses addressing the total harm associated with particular vehicles, i.e. a measure of the total number of injuries and fatalities in a collision independent of which of the two vehicles they occur in, are scarce. French statistics show that the total risk of injury in a collision is higher when the vehicles' weights differ by more than 340 kg or when the sum of the involved vehicles' weights is greater. Australian statistics

show that collisions involving medium SUVs result in the lowest incidences of fatalities or serious injuries and that collisions involving light cars result in the highest incidences. It is also shown that there is a strong correlation between a vehicle's total safety and its crashworthiness – reflecting the fact that the vehicle's own occupants are always involved in the collision.

What needs to be measured to assess front-to-front and front-to-side compatibility? Compatibility is a product of self protection and partner protection. In front-to-front collisions, the properties of vehicle design associated with compatibility are vehicle mass, structural interaction, vehicle geometry, homogeneity, front-end force levels, stiffness, and compartment strength. In front-to-side collisions, the mass and stiffness of striking vehicles are less influential than their geometry and stiffness distribution.

Which methods can be applied to assess front-to-front and front-to-side compatibility? Compatibility has been assessed using dummy injury measures, deformation assessments, and subjective assessments of vehicle deformation. The ambiguity of these methods is problematic because it can lead to different interpretations of experiments that should be designed to provide objective results.

Which results can be generated regarding front-to-front and front-to-side compatibility? In front-to-front collisions, it has been shown that the vertical alignment of the structures is essential in severe collisions, but that alignment alone does not guarantee compatibility. Stiff lateral connections have been observed to be beneficial for avoiding the fork effect, but it is not clear whether interaction or glance off should be encouraged in low overlap collisions. Multiple load path designs have been seen to behave more stably and improve structural interaction compared to single load path designs. However, many different front-end components have been observed to act as effective load paths. It has been

shown that a stiff passenger compartment is essential and that the front-end force levels should not be so high as to overload the passenger compartment of the collision partner. In front-to-side collisions, it has been shown that interaction with the struck vehicle's sill reduces the loading on the occupants. It has also been observed that a higher bonnet on the striking vehicle increases the risk of head injury in the struck vehicle. In many tests, reduced loading in one body region corresponded to increased loading in another. A uniform loading of the struck vehicle has therefore been deemed preferable to minimise the risk of severe injuries in any particular body region.

How can the knowledge of front-to-front and front-to-side compatibility be applied? Proposals to address front-end design include an increase in the test velocity of the current ECE-R94, but concern has been raised that this may aggravate the aggressivity/vulnerability disparity between heavy and light vehicles. Metrics for the assessment of compatibility are available for neither the PDB nor the FWDB, and concern has also been raised that the intrinsic characteristics of the PDB may enable vehicle designs that reduce compatibility. By its design, the FWRB has very limited capacity to address vehicle design characteristics beyond the alignment and stiffness of primary structures, and even this is contentious. Several designs of MDBs have been investigated, but their development remains in a relatively early phase. The only implemented standard that addresses compatibility in front-end design is the EVC self-commitment, which applies to LTVs in the North American market and specifies the geometrical alignment of PEAS and, if applicable, the geometrical alignment and performance of SEAS. Of the few proposals that exist to specifically address front-to-side compatibility, the optimisation of the struck vehicle's self protection with respect to the current vehicle fleet is the only strategy that is currently being pursued. For the striking vehicle, it is expected that front-to-front compatibility improvements will also be beneficial in front-to-side collisions.

Chapter 3

Preliminary Statistical Analysis

In order to judge the potential benefit offered by any change in vehicle design, it is important to first understand the existing situation in the traffic accident environment. Predictions can then be made with respect to both the benefits and the side effects that may occur. To achieve this, statistics are analysed in this chapter using data from the GIDAS relational database, which consists of data collected within two defined areas around the German cities of Hanover, Lower Saxony, and Dresden, Saxony (Otte et al. 2003). Although the absolute quantity of these data is limited to about 1000 accidents per region per year, their use is appropriate for this study because they consist of in-depth information derived from on-the-scene investigation and accident reconstructions. The use of in-depth data is widely considered as preferable to the abundant but elementary information available in national accident statistics (Hill et al. 2001, Farmer 2003). The data also consist of a mixture of urban, rural, and motorway traffic and are composed of accidents that involved a modern fleet of vehicles and well developed infrastructure. The data therefore represent the state-of-the-art in road transport and are a good basis for predictions of the future. The database, important variables and categorisations used within this chapter are further described in Appendix A.

In this chapter, an overview of the German accident environment is presented, which provides a basis for the detailed analysis of front and side collision

statistics in Chapters 4 and 5, respectively. The aims of this chapter are to identify the relationship between injury severity and the risk of fatality for persons in the database and to provide an overview of the road users and collision types in the database.

With the exception of the data in Table 3.1 and Figure 3.2,[16] the statistics presented in Chapters 3, 4, and 5 are limited to belted passenger vehicle occupants. This reflects current European road safety policy (*Directive 2003/20/EC*) and reduces scatter in the statistics.

3.1 Injury and fatality in the GIDAS dataset

The Abbreviated Injury Scale (AIS) is an ordinal scale used to classify an individual injury according to its survivability (Gennarelli 1998). Therefore, if each person in a group has a single coded injury, it is straightforward to predict what percentage will be fatally injured. However, for the analysis of traffic accidents, aggregate injuries also need to be taken into consideration, and hence it is common practice in technical publications to analyse a person's Maximum AIS (MAIS).[17] From a medical perspective though, this approach is imperfect because the AIS risk of fatality for a single injury is not applicable to a person with multiple injuries or even a polytrauma. To overcome this ambiguity and to compare the published mortality rates with the outcome of injuries recorded in the GIDAS database, this section includes an analysis of persons with single and multiple injuries that was performed in cooperation with Dr. Mirko Junge of Volkswagen Group Accident Research.

In Figure 3.1, AIS mortality rates are determined for the GIDAS data using persons with a single coded injury. To ensure the quality of the data, persons are only included if the AIS code and AIS identifier match according to the 1998

[16] Table 3.1 and Figure 3.2 include data from the entire accident environment (including, for example, pedestrians), and hence it is relevant to consider both belted and unbelted persons.

[17] The MAIS is defined as the AIS level of the most severe, i.e. maximum, injury that is coded. The absolute number of coded injuries at each AIS level is not taken into consideration.

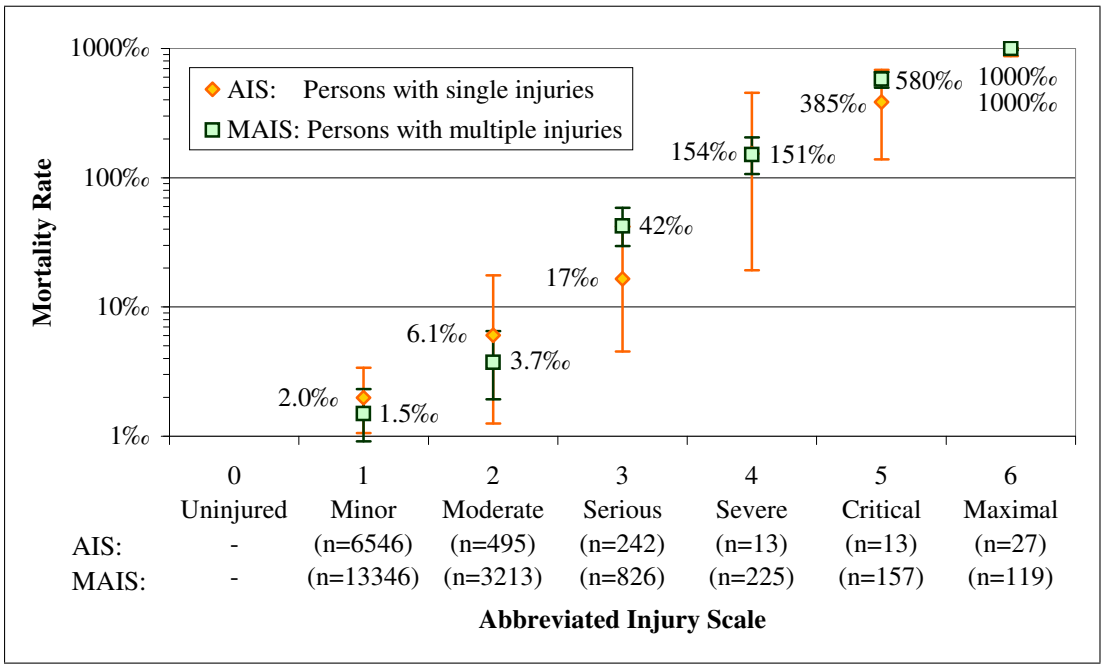

Figure 3.1: Mortality rates for each degree of AIS and MAIS injury, derived from GIDAS data. The error bars show the 95th percentile binomial confidence intervals of the mortality rates. A significant difference between the mortality rates of the AIS and the MAIS classifications is not observed at any of the injury levels.

edition of the AIS codebook (Gennarelli 1998). Permillage figures and binomial confidence intervals are shown in Figure 3.1 based on the number of recorded fatalities. The results derived from GIDAS are very similar to those published in the 2005 edition of the AIS-codebook (Gennarelli & Wodzin 2005), which are 7‰, 8‰, 35‰, 150‰, 400‰, and 790‰ for AIS 1 to AIS 6, respectively.[18,19] The only significant differences between the published data and the AIS data from GIDAS are the higher mortality rate for an AIS 1 injury ($p < 0.001$) and the lower mortality rate for an AIS 6 injury ($p = 0.004$).

To determine a mortality rate for each level of MAIS, persons with one or more coded injuries are classified according to their most severe injury. To en-

[18]Note that mortality rates are quoted in deaths per 1000 persons throughout this thesis. This is indicated by the use of the permil symbol (‰), which should not be confused with that of the percent (%).

[19]Note that a fatality is only recorded in the GIDAS database if it occurs within 30 days of the accident. This is consistent with the reporting of national accident statistics in Germany but different to the published AIS survivability rates, which are derived from the National Trauma Data Bank (NTDB) data from the USA and Puerto Rico. The NTDB data define the injury outcome at the point of hospital discharge, regardless of the length of stay. However, hospital discharge does not imply recovery and the 'hospital discharge disposition' variable in the NTDB includes the possibility of transfer to another hospital or care facility (American College of Surgeons 2008).

sure the quality of the data, persons are omitted if, for any of their injuries, the AIS code and AIS identifier do not match according to the 1998 edition of the AIS codebook (Gennarelli 1998). The mortality rates and their associated 95^{th} percentile binomial confidence intervals are shown in Figure 3.1.

Due to the small number of cases in which only one injury is sustained, the AIS levels provide large confidence intervals, and the null hypothesis, that the AIS and MAIS classifications are equivalent, cannot be rejected with 95% confidence at any of the AIS levels ($p_1 = 0.657$, $p_2 = 0.727$, $p_3 = 0.184$, $p_4 = 1.000$, $p_5 = 0.389$, and $p_6 = 1.000$ for the AIS/MAIS levels 1 to 6, respectively).

By comparing the MAIS mortality rates from the GIDAS data with the published AIS mortality rates, it can be observed that they are similar at AIS levels 3 and 4. Both MAIS 1 and 2 injuries in the GIDAS database are more survivable than the AIS 1 and 2 injuries given in Gennarelli & Wodzin (2005) ($p < 0.001$ and $p = 0.004$, respectively), whereas the MAIS 5 and 6 injuries are less survivable ($p < 0.001$ in both cases). These variations in the survivability rates can be attributed to differences in both the sampling methods[20] and the sample populations in the GIDAS and NTDB databases.[21] Since the MAIS mortality rates in Figure 3.1 are defined using the same data as the rest of the accident analysis, they are used as the reference values in the remainder of the thesis.

3.2 The German accident environment

In this section, the German accident environment is analysed to provide a statistical context for the discussion of passenger vehicle compatibility. The significance

[20]For example, the two databases apply different methods to determine whether an injury was fatal (see also Footnote 19). The 30 day limit applied to GIDAS data ensures that a very high proportion of accident related fatalities are recorded, whereas the NTDB classification does not indicate whether a patient, who is transfered to another hospital, dies of their injuries at a later time.

[21]For example, the two different sets of data are based on the care provided in two different hospital systems. The NTDB data are sampled exclusively from trauma centres, whereas the GIDAS data do not place any limits on where the injuries are treated. MacKenzie et al. (2006) found that the treatment of severely injured patients in Level 1 trauma centres resulted in a 25% reduction in mortality compared to nontrauma centres. Furthermore, the GIDAS data is limited to traffic related injuries.

of passenger vehicle occupants is compared to other road users, and the importance of passenger vehicle to passenger vehicle collisions is compared with other collision types. Finally, the significance of front and side collisions is investigated.

3.2.1 Types of road users involved in accidents

The GIDAS database includes an entry for each person that is involved in a road accident in which at least one person is injured. In Figure 3.2a, all road users involved in accidents between 1996 and 2005 are grouped according to their modes of transport.[22,23] These groupings are shown in the form of a traditional pie chart, but within each mode of transport, the risk of sustaining a particular degree of injury is shown along the radial axis of the pie segments. The statistics are presented in this way because it concisely shows both the size of each group and their respective injury risks. As a result, the goal of reducing the overall number of traffic fatalities and injuries can be approached more effectively: problems with a high risk but low frequency or those with a high frequency but low risk can be quickly identified and do not attract undue attention.

The MAIS levels in Figure 3.2 are grouped into four classifications: MAIS 0-1, MAIS 2, MAIS 3, and MAIS 4-6. The MAIS 0 and MAIS 1 classifications are combined because it is contested that a person classified with MAIS 0 is truly uninjured. The AIS 1 classification consists mostly of minor injuries such as light bruising and superficial scratches (Gennarelli 1998), and it is unlikely that a person involved in a traffic accident would remain completely free of these types of injuries. Classifications of MAIS 0 in traffic accidents may therefore be seen as under-reporting, which is a broadly acknowledged problem in accident statistics (Hauer 2006, Yamamoto et al. 2008). The MAIS 4, 5, and 6 classifications are

[22]The range of 1996 to 2005 is used in order to cover a decade of accident statistics, and the choice represents the best distribution of cases and vehicles in the GIDAS database, which is described in Tables A.2a and A.2b in Appendix A. The use of contemporary accident data provides the most relevant basis for the prediction of future risks (Evans 2003), and the same range of data was also utilised by Martin & Lenguerrand (2008) in their recent analysis of French accident statistics.

[23]The definition of each mode of transport is given in Table A.1.

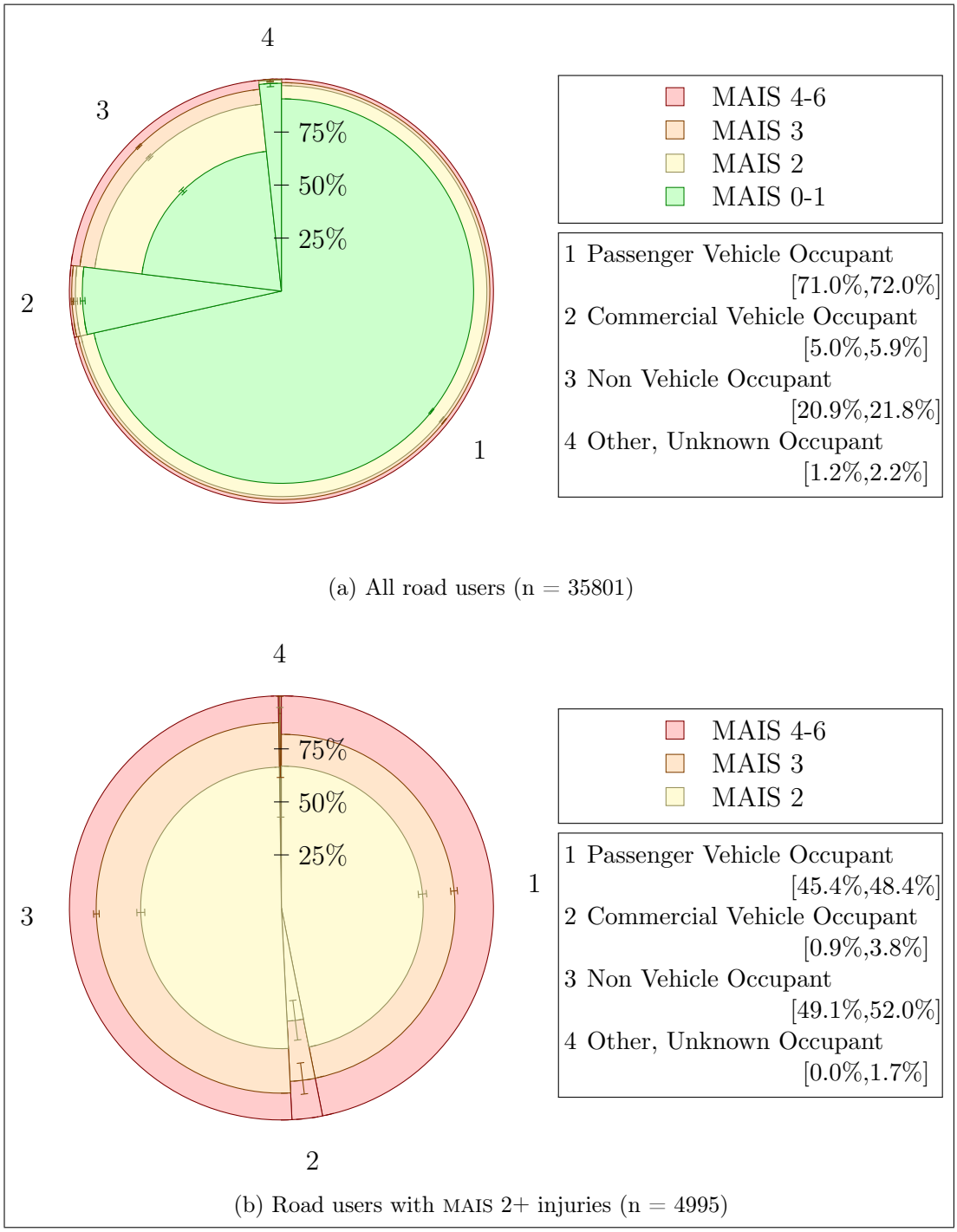

(a) All road users (n = 35801)

(b) Road users with MAIS 2+ injuries (n = 4995)

Figure 3.2: Injury risk to persons involved in traffic accidents in Germany between 1996 and 2005. The data are grouped according to the mode of transport. The error bars show the 95th percentile binomial confidence intervals of the risk of MAIS 2+, MAIS 3+, or MAIS 4+ injury. The percentage ranges in the legends show the 95th percentile multinomial confidence intervals of the distribution of traffic participants.

combined because, as shown in Figure 3.1, each of these injury classifications represents a genuine risk of fatality, and, according to the Injury Severity Score (ISS) rating,[24] a MAIS 4+ classification always corresponds to an ISS ≥ 16 classification and is hence defined as a polytrauma (Baker et al. 1974).

In the figure legend, the distribution of road users is described using 95^{th} percentile multinomial confidence intervals, which are calculated based on the major segments of the pie chart. At the centre of each segment, on the border between each level of injury, error bars show the range of the 95^{th} percentile binomial confidence intervals for the risks of MAIS 2+, MAIS 3+, and MAIS 4+ injuries. It is common practice to consider injuries at or a above a particular level, as this simplifies the process of defining risk functions (see for example Javouhey et al. 2006, Newgard et al. 2005), and hence a binomial approach is appropriate. The methods used to calculate the multinomial and binomial confidence intervals are described in Appendix C.

The data in Figure 3.2 are plotted twice: both with and without the MAIS 0-1 classification. The former, in Figure 3.2a, shows the distribution of all coded road users that are involved in a collision in which at least one person is injured, and the latter, in Figure 3.2a, shows the distribution of all road users that sustain a MAIS 2+ injury in a collision.

In Figure 3.2a, it can be seen that the German accident environment is dominated by passenger vehicle occupants,[25] which comprise approximately 71% of all involved persons. The next most significant group are 'non vehicle occupants' (pedestrians, bicyclists, moped riders, and motorcyclists[26]), which repre-

[24]The Injury Severity Score (ISS) is a method used to assess trauma severity and is used to define the term 'polytrauma'. The ISS is based on the AIS ratings of injury severity and is calculated by first determining the injury with the highest AIS score in each of six body regions: head and neck, face, chest, abdomen, extremity, and external. The three body regions with the highest scores are then selected, and the ISS is calculated as the sum of the squares of these three scores. A polytrauma is defined as an ISS score ≥ 16 (Baker et al. 1974).

[25]As noted at the beginning of the chapter, the data in Figure 3.2 include both belted and unbelted occupants.

[26]Although bicycle, moped, and motorcycle riders do indeed possess a vehicle, with minor exceptions their vehicle does not offer them a space within which they are protected. They are therefore classified together with pedestrians as non vehicle occupants.

sent approximately 22% of involved persons. A further 5.4% of persons involved in accidents are occupants of commercial vehicles, and those remaining are the occupants of other or unknown vehicle types, including rail transport. The confidence intervals show that the differences in the sizes of each of these four groups is significant.

This initial breakdown indicates that passenger vehicle occupants are the most significant group in the statistics, but it fails to take account of the significantly different injury risks that the different groups encounter when they are involved in an accident. The raw number of persons involved in accidents only shows each road user's exposure to the traffic environment. The risk of injury to a road user when he or she is involved in an accident is, however, related to the nature and conditions of the accident, rather than the frequency with which that type of accident occurs. For example, 9% of passenger vehicle occupants sustain MAIS 2 injuries or higher whereas 34% of non vehicle occupants and only 6% of commercial vehicle occupants sustain injuries at this level. The difference between the risk of MAIS 2+ injury for these three populations is significant at the 95% confidence level.

Assuming that commercial vehicles tend to be larger and heavier than passenger vehicles and that these are in turn larger and heavier than the vehicles (if any) of the non-occupants, a final observation from Figure 3.2a is that the likelihood of receiving a higher level of injury increases as the size or weight of the vehicle type decreases. Such an observation indicates that larger vehicles are either inherently safer for their occupants or that larger vehicles increase the injury risk of their collision partners. The classification of vehicle types in Figure 3.2 is too broad to make definitive conclusions about the role of vehicle mass or size, and hence vehicle mass is one of the aspects of compatibility that is investigated in more detail in Chapters 4 and 5.

In Figure 3.2b, which shows the distribution of MAIS 2+ injured road users, it can be seen that passenger vehicle occupants do not dominate the statistics.

In stark contrast to Figure 3.2a, passenger vehicle occupants make up 47% of persons that sustain MAIS 2+ injuries, and non vehicle occupants represent 51%. Of the remaining MAIS 2+ injuries, 2% are sustained by commercial vehicle occupants and 0.2% by other or unknown road users. As such, when equating the effects of MAIS 2+ injuries, traffic accidents involving injury to non vehicle occupants represent a slightly larger problem than traffic accidents involving injury to passenger vehicle occupants ($p = 0.012$).

The distribution of injury severity is, however, different for each group of road users, and it can be seen in Figure 3.2b that the risk of sustaining MAIS 4-6 injuries is higher for passenger vehicle occupants than it is for non vehicle occupants ($p < 0.001$). As shown in Figure 3.1, these injuries are associated with a much higher mortality rate.

To determine which group of traffic participants is more significant in terms of fatalities, three sets of data are presented in Table 3.1. In the first column, the German national accident statistics from 1996-2005 are shown (StBA 2006). This includes all German traffic fatalities from this time period and hence represents the population from which GIDAS is a sample. In the second column, fatalities recorded in GIDAS between 1996 and 2005 are also presented. Although these data are collected from the same time period, the GIDAS sampling methods have the obvious effect that the absolute number of fatalities is two orders of magnitude less than the German Federal Statistics Office (StBA) data. In the third column of Table 3.1, the MAIS injury data from Figure 3.2 are combined with the mortality rates shown in Figure 3.1 to estimate the number of injuries that are fatal. To enable a direct comparison between the two sets of GIDAS data, the recorded fatalities are limited to persons with a known MAIS in the range MAIS 0 to MAIS 6. The results show a clear similarity between the two sets of GIDAS data and also a good correlation with the StBA data. This reflects the results of previous studies that have determined that GIDAS data are representative of the StBA national statistics (Hautzinger et al. 2004). It is therefore concluded

Table 3.1: Comparison between the distribution of fatally injured road users in the StBA national accident statistics (StBA 2006) and the GIDAS database for accidents occurring between 1996 and 2005. The 95th percentile multinomial confidence intervals are given for the distribution of fatally injured road users from the GIDAS database.

Type of Road User	**Recorded Fatalities**				**Estimate**	
	StBA[a]		**GIDAS**[b]		**GIDAS**[c]	
Passenger Vehicle	42521	(59%)	277	[54%, 62%]	266.61	(56%)
Commercial Vehicle	2569	(3.6%)	13	[0.0%, 7.5%]	12.72	(2.7%)
Non Vehicle Occupant	26179	(36%)	185	[34%, 44%]	193.27	(41%)
Other, Unknown	740	(1.0%)	1	[0.0%, 4.9%]	1.32	(0.3%)

[a] The StBA dataset represents the entire population of fatally injured road users in Germany, and hence exact percentages are calculated instead of confidence intervals.

[b] Fatalities recorded for persons with injuries in the range MAIS 0 to MAIS 6.

[c] Estimate calculated by multiplying the number of persons at each level of MAIS injury by the mortality rate at that injury level. Based on a population of 35035 involved persons.

that the use of MAIS injuries and their associated fatality risks is a valid tool for estimating the distribution of fatally injured persons. Furthermore, for small datasets, the estimated distribution of fatalities may be more representative of the total population than the recorded distribution because it is based on all injured persons rather than the very small set consisting of those that are fatally injured.

Considering the StBA data in Table 3.1, passenger vehicle occupants represent 59% of fatalities, non vehicle occupants represent 36% of fatalities, commercial vehicle occupants represent 3.6% of fatalities, and other and unknown persons represent 1.0% of fatalities. The issue of injuries to non vehicle occupants is a significant one, and one that should be addressed in any general consideration of road safety, however the remainder of this thesis focuses on the protection of passenger vehicle occupants.

3.2.2 Passenger vehicle collision partners and obstacles

In the previous section, it is shown that the occupants of passenger vehicles comprise the largest group of fatally injured road users. In this section, the obstacles

and collision partners of passenger vehicles are investigated.[27] Figure 3.3 shows the distribution of passenger vehicle occupants grouped according to the type of collision partner or obstacle they collided with. The distribution of the injuries sustained by the passenger vehicle occupants in these collisions is also shown.

In order to focus the results on more modern vehicle designs, the data are limited to the occupants of passenger vehicles that were built between 1996 and 2005, inclusive. It should, however, be noted that the age of the vehicles in the sample is not evenly distributed.[28]

Typically, a traffic accident is not a simple event where a single collision is responsible for bringing all involved parties from their initial velocity to rest. For a complete record of an accident, major collisions, minor collisions, and events such as braking and skidding are recorded separately in the GIDAS database. As a hypothetical example, a car may clip a kerbstone, collide with another vehicle, skid towards the side of the road, impact with a tree, and then finally come to rest in a ditch. Each of these events would be coded separately in the database with details on the change in velocity, direction, deformation, and so on (Otte et al. 2003). Due to the overwhelming number of multiple collision accidents, it is not practical to ignore these accidents and only use those with a single collision. A process has therefore been developed by Volkswagen Group Accident Research to analyse the database and select the most severe collision based on the Δv, weighted according to the direction of impact.[29] Due to the unpredictable nature of traffic accidents, the process is not infallible, but the results are satisfactory. The process is also

[27] The definitions of each of the collision partners and obstacles are given in Tables A.1 and A.2, respectively.

[28] The distribution of the dates of manufacture of the passenger vehicles in the dataset is shown in Figure A.2a. See also Footnote 22.

[29] Accidents involving rollover are an exception to this approach, and in these cases the rollover is always used to classify the accident. This approach does not provide useful results for the analysis of rollover severity because secondary collisions may be more severe than the simple rolling of the vehicle. For example, if a rolling vehicle collides with its roof against a tree, the high severity of the accident is likely to come from the collision with the tree rather than the rolling motion that preceded it. An in-depth analysis of the statistics is therefore appropriate for the analysis of rollover severity. However, since analysing rollover severity is not the objective of this thesis, all collisions involving rollover are grouped together, and front, side, rear, and oblique collisions are considered separately.

significantly more efficient than individually considering each collision for the 54,364 persons in the database and is hence applied to the analyses in this thesis.

In Figure 3.3a, it can be seen that the majority of passenger vehicle occupants are involved in collisions with other passenger vehicles. Also, although collisions with non vehicle occupants make up 29% of cases, the passenger vehicle occupants have a very low risk of MAIS 2+ injury in these collisions.

In collisions with other passenger vehicles, only 6% of passenger vehicle occupants receive MAIS 2+ injuries. This represents a lower risk of MAIS 2+ injury than that experienced in collisions with commercial vehicles ($p < 0.001$), other vehicles ($p = 0.010$), poles, posts, and trees ($p < 0.001$), walls and barriers ($p < 0.001$), and ground surfaces and ditches ($p < 0.001$). Only a collision with a non vehicle occupant represents a lower risk of MAIS 2+ injury to a passenger vehicle occupant than a collision with another passenger vehicle ($p < 0.001$).

In Figure 3.3b, the data are limited to MAIS 2+ injuries. For an analysis of higher levels of injury severity, this diagram is more appropriate because it removes the bias that may be present in the sample of MAIS 0-1 injuries. In a low severity collision with another passenger vehicle, the likelihood that an uninjured person will be entered into the GIDAS database is higher because an injury in either vehicle means that all persons are entered into the database. However, in a similarly low severity collision with a roadside object, that uninjured person would not be entered into the database because the entire accident would be judged to be injury-free. The reporting of low severity injuries is also higher in vehicle-to-vehicle collisions because there is a greater chance of being able to claim damages for personal injury. As a result, the number of MAIS 0-1 injuries may be disproportionately high in collisions with other passenger vehicles, meaning that the estimate of the risk of MAIS 2+ injury in these collisions may be disproportionately low.

The distribution of passenger vehicle occupants in Figure 3.3b is significantly different to that in Figure 3.3a. At the 95% confidence level, the propor-

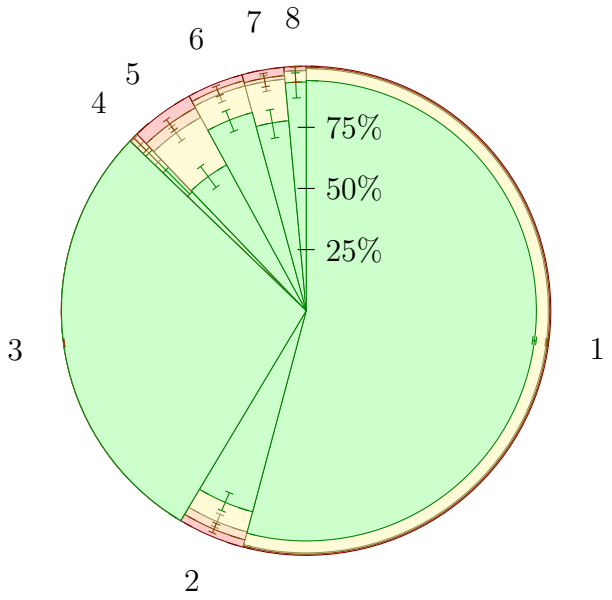

MAIS 4-6	
MAIS 3	
MAIS 2	
MAIS 0-1	

1 Passenger Vehicle	[53.0%,55.3%]
2 Commercial Vehicle	[3.3%,5.6%]
3 Non Vehicle Occupant	[27.4%,29.8%]
4 Other Vehicle	[0.0%,1.8%]
5 Pole, Post, Tree	[3.0%,5.4%]
6 Wall, Barrier	[2.5%,4.9%]
7 Ground, Ditch	[1.6%,4.0%]
8 Other, Unknown	[0.3%,2.6%]

(a) All belted passenger vehicle occupants (n = 7402)

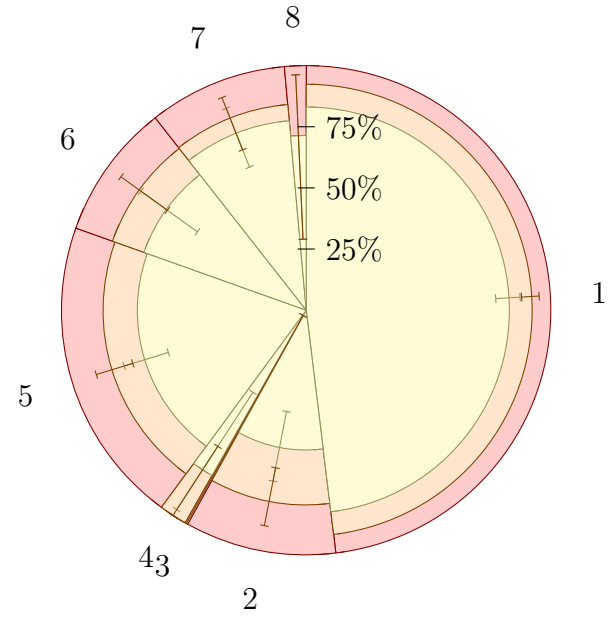

MAIS 4-6	
MAIS 3	
MAIS 2	

1 Passenger Vehicle	[43.8%,52.7%]
2 Commercial Vehicle	[5.7%,14.6%]
3 Non Vehicle Occupant	[0%,4.9%]
4 Other Vehicle	[0.0%,6.5%]
5 Pole, Post, Tree	[16.1%,25.0%]
6 Wall, Barrier	[4.7%,13.6%]
7 Ground, Ditch	[4.9%,13.8%]
8 Other, Unknown	[0.0%,6.1%]

(b) Belted passenger vehicle occupants with MAIS 2+ injuries (n = 491)

Figure 3.3: Injury risk to belted occupants of passenger vehicles with a date of manufacture between 1996 and 2005. The data are grouped according to the object struck. The error bars in show the 95$^{\text{th}}$ percentile binomial confidence intervals of the risk of MAIS 2+, MAIS 3+, or MAIS 4+ injury. The percentage ranges in the legends show the 95$^{\text{th}}$ percentile multinomial confidence intervals of the distribution of struck objects.

tion of passenger vehicle occupants involved in collisions with passenger cars and non vehicle occupants is lower, and the proportion involved in commercial vehicle collisions, pole, post, and tree collisions, and ground surface and ditch collisions is higher. Hence, although the clear majority of passenger vehicle occupants are involved in collisions with other passenger vehicles, collisions between two passenger vehicles only cause about 48% of MAIS 2+ injuries. The range of the 95th percentile multinomial confidence interval, from 43.8% to 52.7%, indicates that the true proportion may be more or less than half.

Figure 3.3b also shows that the risk of MAIS 3+ injury is relatively low in collisions between two passenger vehicles. This observation is significant with respect to collisions with commercial vehicles ($p = 0.007$) but not significant with respect to collisions with poles, posts, and trees ($p = 0.054$), walls and barriers ($p = 0.200$), and ground surfaces and ditches ($p = 0.622$). The risk of a MAIS 4+ injury in a collision between two passenger vehicles also appears to be lower than in other collision types, but this observation is not statistically significant ($p \geq 0.087$).

The general conclusion that can be drawn from Figure 3.3 is that the compatibility between passenger vehicles is relatively good, since these collisions represent a lower risk of MAIS 2+ injury than most other collision types (excluding collisions with non vehicle occupants). Furthermore, although approximately 50% of MAIS 2+ injuries to passenger vehicle occupants occur in collisions with other passenger vehicles, the other 50% occur in collisions where passenger vehicle compatibility is of absolutely no relevance. When considering improvements to compatibility, it is therefore essential that the protection of occupants in other collision types is not diminished.

3.2.3 Passenger vehicle collision direction

In the previous section, it is shown that belted occupants of modern passenger vehicles are involved in collisions with other passenger vehicles at a relatively

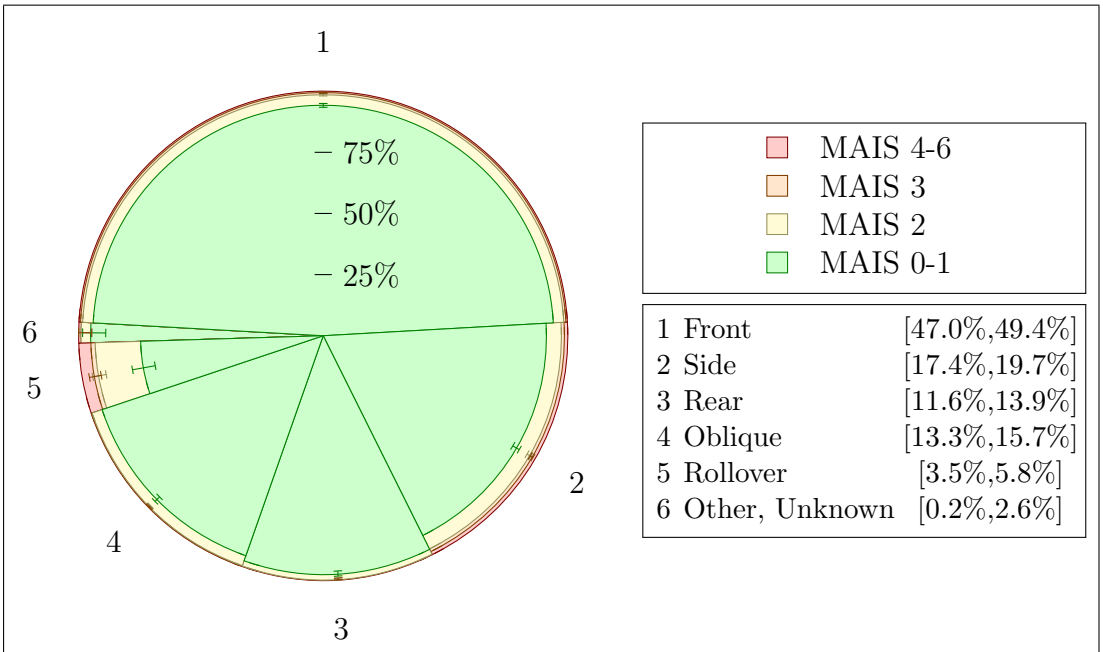

(a) All belted passenger vehicle occupants (n = 7402)

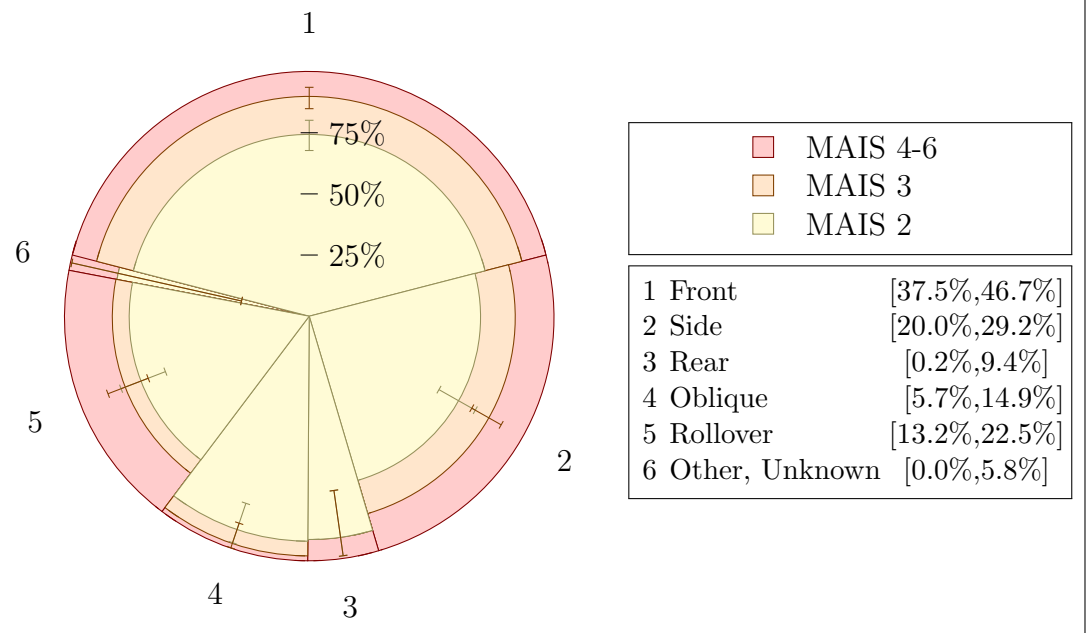

(b) Belted passenger vehicle occupants with MAIS 2+ injuries (n = 491)

Figure 3.4: Injury risk to belted occupants of passenger vehicles with a date of manufacture between 1996 and 2005. The data are grouped according to the collision direction. The error bars show the 95$^{\text{th}}$ percentile binomial confidence intervals of the risk of MAIS 2+, MAIS 3+, or MAIS 4+ injury. The percentage ranges in the legends show the 95$^{\text{th}}$ percentile multinomial confidence intervals of the distribution of collision directions.

high frequency but that they experience a relatively low risk of injury in these collisions. In this section, the same set of data is analysed with regards to the direction of impact rather than the collision partner. To minimise scatter in the results, the directions of impact are defined taking into account both the VDI Direction of Force (VDI 1) and the VDI Location of Damage (VDI 2), and accidents involving rollover are categorised separately.[30] The results are shown in Figure 3.4, which is presented in the same format as the previous two figures.

In Figure 3.4a, it can be seen that almost half of passenger vehicle collisions are frontal, which may be attributed to a passenger vehicle's typically forwards direction of travel. Side collisions are the next most frequent, followed by oblique collisions and rear collisions. Collisions involving rollover are relatively infrequent, but they clearly have a higher risk of injury. With the exception of oblique collisions and rear collisions, this order of collision frequencies given above is significant at the 95% confidence level.

The side collisions in Figure 3.4a can also be analysed separately as either left collisions or right collisions, but the distribution does not indicate a significantly higher proportion on either side. The difference in the risk of MAIS 2+ injury is also not statistically significant ($p = 0.225$), and hence the results in Figure 3.4 are combined into the single category of side collisions.

The lowest risk of a MAIS 2+ injury occurs in either oblique collisions or rear collisions ($p = 0.068$). The risk of a MAIS 2+ injury in a frontal collision is higher than that in a rear collision ($p = 0.001$), but the difference to an oblique collision is not significant ($p = 0.326$). In a side collision, the risk of a MAIS 2+ injury is greater than that in a frontal collision ($p = 0.009$) but lower than that in a collision involving a rollover ($p < 0.001$).

If oblique collisions are ignored, the results above show that the risk of a MAIS 2+ injury increases in the order of rear collisions, frontal collisions, side collisions, and collisions involving rollover. However, this does not necessarily

[30] The definition of each collision direction is given in Table A.3.

mean that the rear-end of a passenger vehicle is safer than its front or side, since the results do not take into account the distribution of collision severities. If it is assumed that a passenger vehicle usually travels forwards, it follows that a passenger vehicle usually has a forwards velocity vector when involved in a collision.[31] Irrespective of the speed, the typical forwards velocity vector of a vehicle adds to its Δv in the event of a frontal collision and reduces its Δv in a rear collision. Hence, it can be assumed that the distribution of Δv values in rear collisions is lower than that in frontal collisions. As such, Figure 3.4a does not indicate that a rear collision with a particular Δv is safer than a frontal collision at the same Δv. However, Figure 3.4a does indicate that rear collisions, over the distribution of severities at which rear collisions occur, are safer than frontal collisions, over the distribution of severities at which frontal collisions occur. Continuing with the assumption that passenger vehicles usually have forward velocity vectors, it follows that side collisions generally occur with higher values of Δv than rear collisions and lower values of Δv than frontal collisions. Therefore, since Figure 3.4a indicates that frontal collisions, over the distribution of severities at which frontal collisions occur, are safer than side collisions, over the distribution of severities at which side collisions occur, it can be concluded that for a given Δv a frontal collision in a passenger vehicle is safer than a side collision. To determine which collision velocities are critical for occupant injury, the Δv of passenger vehicle front and side collisions are investigated in more detail in Chapters 4 and 5.

The distribution of MAIS 2+ injuries is summarised in Figure 3.4b, which shows that the largest proportion of MAIS 2+ injured passenger vehicle occupants is involved in frontal collisions, followed by side collisions, collisions involving rollover, oblique collisions, and rear collisions. At the 95% confidence level, the proportion of side collisions is indistinguishable from that of collisions involving rollover ($p = 0.208$), the proportion of collisions involving rollover is indistinguish-

[31] This assumption represents an extreme simplification of the accident environment. It is only included for demonstrative purposes.

able from that of oblique collisions ($p = 0.136$), and the proportion of oblique collisions is indistinguishable from that of rear collisions ($p = 0.363$). Otherwise the order of the distribution is significant ($p \leq 0.003$). Therefore, apart from the increased significance of collisions involving rollover, the order of the collision directions in Figure 3.4b is identical to that in Figure 3.4a.

Significant differences in the risk of a MAIS 3+ injury are only observed when comparing oblique collisions to frontal collisions ($p = 0.042$) and side collisions ($p = 0.025$). A significant difference in the risk of a MAIS 4+ injury is only observed when comparing oblique collisions to collisions involving rollover ($p = 0.036$). When compared to frontal collisions, the risk of a MAIS 4+ injury in either a side collision ($p = 0.350$) or a collision involving rollover ($p = 0.164$) is not significantly different at the 95% confidence level.

From a broader perspective, it can be concluded from Figure 3.4b that the majority of MAIS 2+ injuries occur in front collisions, side collisions, and collisions involving rollover. Although a rollover may in some cases be initiated by a collision between two passenger vehicles, the rollover itself is a separate event during which it is only the rolling vehicle that can offer any protection to its occupants. Despite the obvious significance of collisions that involve rollover, it does not make sense to consider them further in a discussion of vehicle-to-vehicle compatibility because they are purely a self-protection issue. It should also be noted that the analysis performed in this thesis does not distinguish between the rollovers and the other events that occur during each accident. A more in-depth analysis of accidents involving rollover would be necessary to determine the relative severity of the rollover event compared to preceding and subsequent collision events.

Chapter summary

In Section 3.1, a relationship between the risk of fatality and the MAIS classification is established based on data from the GIDAS database. In Section 3.2, this

relationship is shown to be a valid tool for estimating the distribution of fatally injured persons within a subset of the data.

In Section 3.2.1, the distribution and risk of injury are analysed for each group of road users in the German accident environment. Passenger vehicle occupants are the most significant in terms of the absolute number of involved persons (71%) as well as the number of fatalities (59%). Non vehicle occupants are the most significant in terms of MAIS 2+ injuries, making up 51% of the MAIS 2+ injured persons compared to 47% for passenger vehicle occupants.

The collision partners and obstacles of passenger vehicles are analysed in Section 3.2.2. Although 45% of MAIS 2+ injuries occur in collisions with other passenger vehicles, the risk of MAIS 3+ injury in these collisions is lower than that in collisions with commercial vehicles.

The directions of passenger vehicle collisions are analysed in Section 3.2.3. The majority of MAIS 2+ injuries occur in front collisions (42%), side collisions (24%), and collisions involving rollover (18%). However, in order to focus on the improvement of compatibility in passenger vehicle to passenger vehicle collisions, the analysis in the following chapters is limited to front and side collisions.

Chapter 4

Frontal Collision Statistics

In Chapter 3, it is shown that almost half of the road users that sustain MAIS 2+ injuries are passenger vehicle occupants and that the largest portion of these injuries are sustained in frontal collisions. In this chapter, passenger vehicle frontal impacts are analysed in detail with a particular focus on front-to-front collisions between two passenger vehicles.

The aims of this chapter are: to determine, with respect to other frontal collisions, the significance of front-to-front collisions between passenger vehicles; to determine the most appropriate collision configuration to use for the simulations in Chapter 8; to determine the severity of front-to-front collisions with respect to deformation, velocity, and vehicle weight; and to compare the severity of front-to-front collisions with other frontal collision types. Finally, a relationship between velocity and the risk of fatality in a frontal collision is determined.

As is the case for the data presented in Sections 3.2.2 and 3.2.3, the data in this chapter refer to the belted occupants of passenger vehicles with a date of manufacture between 1996 and 2005. The collision directions that are described in this chapter are defined in Table A.3 and take into account both the VDI Direction of Force (VDI 1) and VDI Location of Damage (VDI 2).

4.1 Overview of frontal collisions

In this section, the risk of injury to belted passenger vehicle occupants in frontal collisions is analysed with respect to their collision partners and obstacles. For the subset of collisions where the collision partner is another passenger vehicle, the risk of injury is also analysed with respect to the collision direction of the other vehicle.

4.1.1 Collision partners and obstacles in frontal collisions

Figure 4.1a shows the distribution of collision partners and obstacles in passenger vehicle frontal collisions and the distribution of injuries to all belted passenger vehicle occupants involved in these collision. This figure is remarkable in its similarity to the distribution of obstacles and collision partners in Figure 3.3a, which includes all collision directions. The only significant difference is an increase in the number of collisions with other passenger vehicles from 54% for all collisions to 57% for frontal collisions. Furthermore, there are no significant differences between the risks of injuries observed in Figure 4.1a and the risks of injuries observed in Figure 3.3a.

A similar situation is true for Figure 4.1b, except that in this case there are no significant differences when compared with Figure 3.3b: neither with the distribution of collision partners and obstacles nor with the risks of injury.

It can therefore be concluded from Figure 4.1 that the likelihood of colliding with another passenger vehicle is slightly higher in a frontal collision than for all collision types, but that the risk of injury is not significantly different. However, it should be noted that almost half of all collisions are frontal collisions (see Figure 3.4), and hence the distribution of the former heavily influences that of the latter.

Using the approach developed in Section 3.2.1 to determine the distribution of fatally injured passenger vehicle occupants, it can be estimated that 38% of fatalities occur in collisions with other passenger vehicles, 24% in collisions with

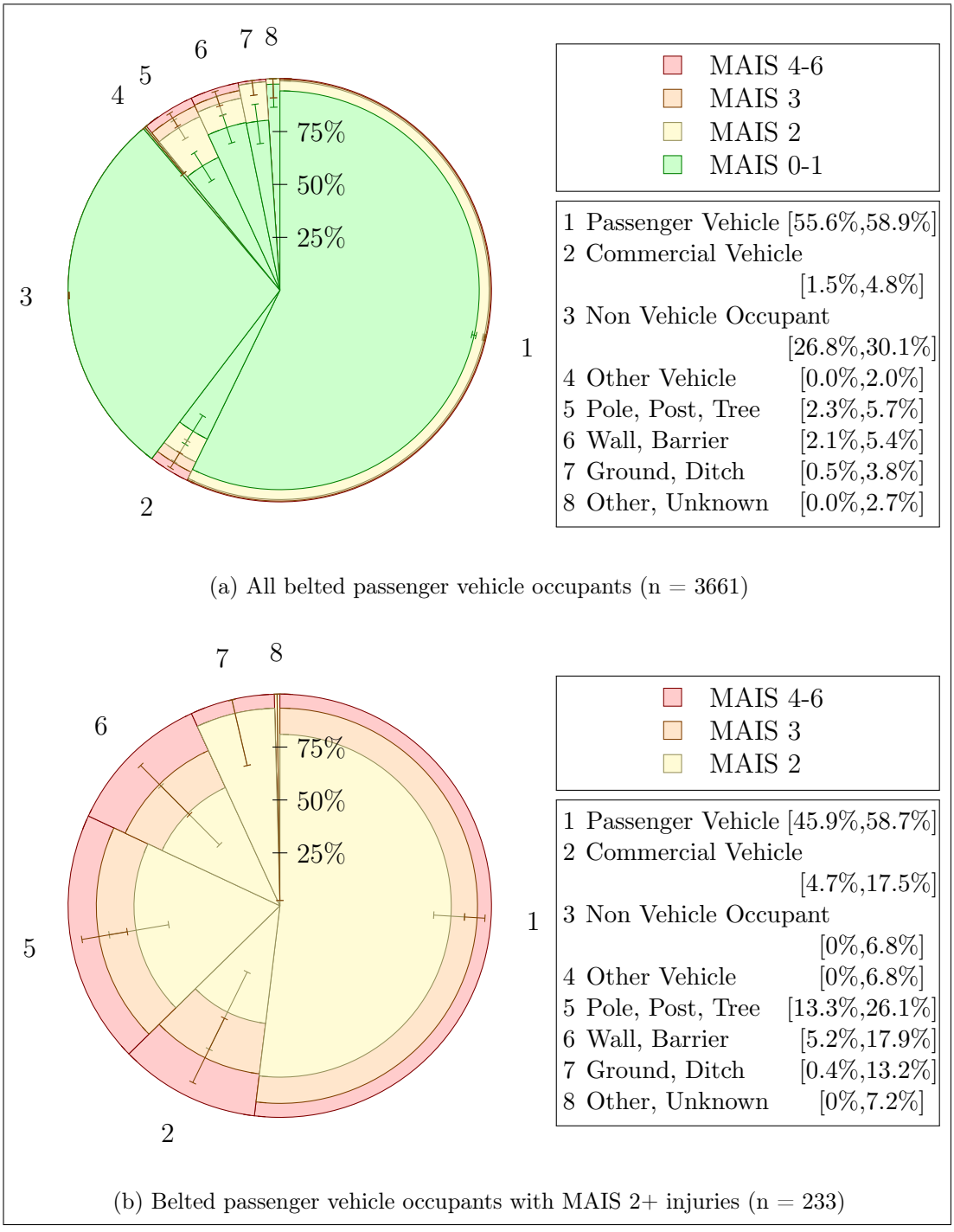

(a) All belted passenger vehicle occupants (n = 3661)

(b) Belted passenger vehicle occupants with MAIS 2+ injuries (n = 233)

Figure 4.1: Injury risk to belted passenger vehicle occupants involved in frontal collisions. The data are grouped according to the object struck. The occupants' vehicles have a date of manufacture between 1996 and 2005. The error bars show the 95th percentile binomial confidence intervals of the risk of MAIS 2+, MAIS 3+, or MAIS 4+ injury. The percentage ranges in the legends show the 95th percentile multinomial confidence intervals of the distribution of struck objects.

commercial vehicles, 17% in collisions with walls and barriers, 14% in collisions with poles, posts, and trees, and 7% in collisions with ground surfaces and ditches.

4.1.2 Collision partner direction in frontal collisions with other passenger vehicles

In the section above, it is shown that for passenger vehicle frontal collisions, the majority of collision partners are other passenger vehicles. In this section, the injury risk in the first passenger vehicle (the one that experiences a frontal collision) is analysed with respect to the collision direction of the passenger vehicle with which it collides. As is the case with the occupants' vehicles, the dates of manufacture of the collision partner vehicles are also limited to between 1996 and 2005 so that the compatibility between modern passenger vehicles can be analysed. The results are shown in Figure 4.2.

In contrast to Figure 3.4, where collisions involving the rear of the passenger vehicle are observed to be a relatively infrequent occurrence, in Figure 4.2a it can be seen that front-to-rear collisions between passenger vehicles are relatively frequent, representing approximately 42% of passenger vehicle frontal collisions where the collision partner is another passenger vehicle. Front-to-front and front-to-side collisions are the next most frequent, representing 25% and 24% of frontal collisions, respectively. Frontal collisions with the oblique directions on the collision partner and frontal collisions that result in a rollover of the collision partner are relatively infrequent. The results for front-to-side collisions in Figure 4.2a can also be considered separately as either front-to-left or front-to-right collisions. However, the differences between the proportions are not significant at the 95% confidence level ($p = 1.000$), each representing approximately 12% of frontal collisions.

This distribution of collision configurations appears reasonable: in normal traffic the vehicle in front faces in the same direction, and hence a collision with its rear-end is the most likely outcome. In general, with the exception of in-

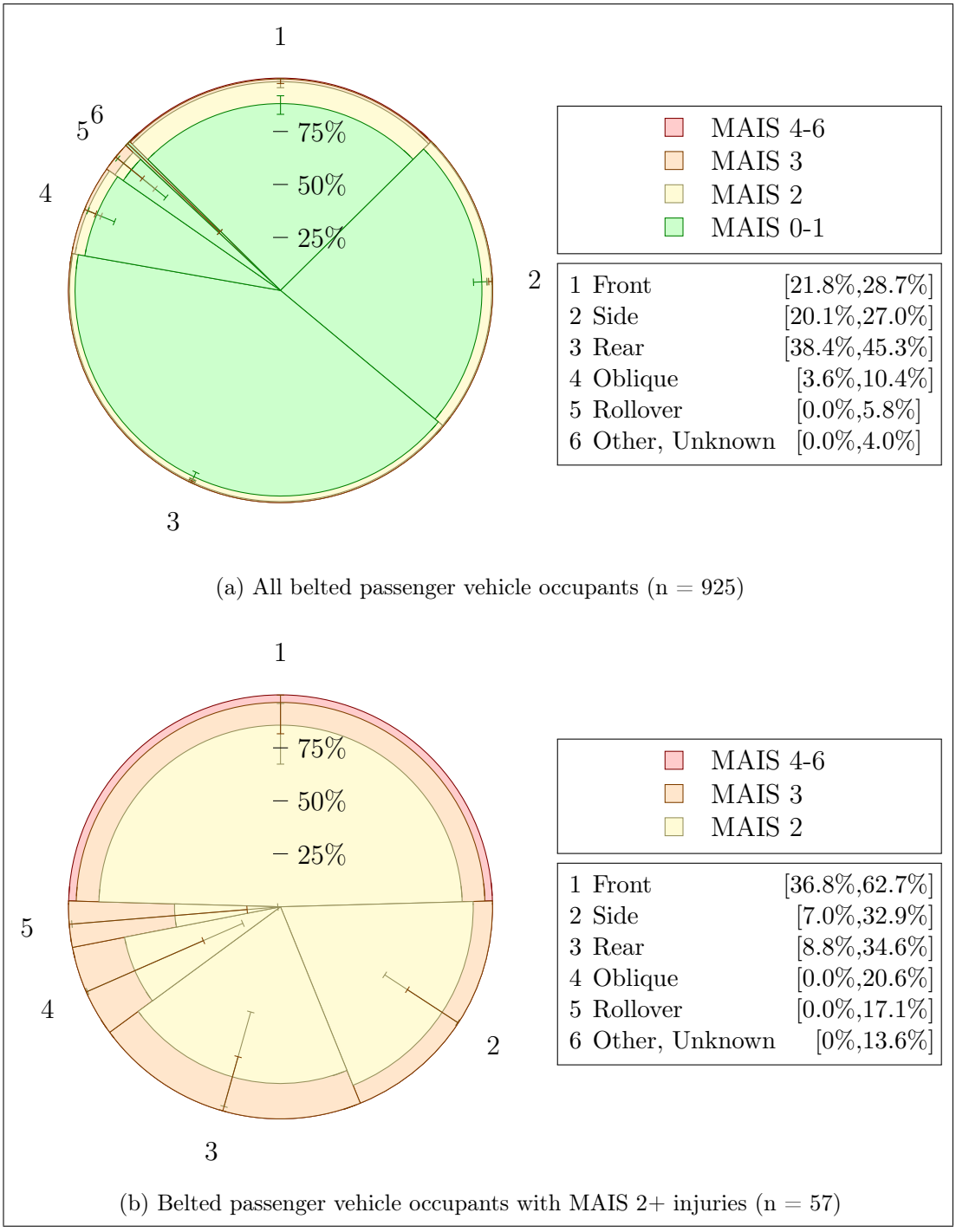

(a) All belted passenger vehicle occupants (n = 925)

(b) Belted passenger vehicle occupants with MAIS 2+ injuries (n = 57)

Figure 4.2: Injury risk to belted passenger vehicle occupants involved in frontal collisions with other passenger vehicles. The data are grouped according to the collision directions of the collision partner vehicles. The data are limited to collisions where both vehicles have a date of manufacture between 1996 and 2005. The error bars show the 95th percentile binomial confidence intervals of the risk of MAIS 2+, MAIS 3+, or MAIS 4+ injury. The percentage ranges in the legends show the 95th percentile multinomial confidence intervals of the distribution of collision directions.

tersections, two vehicles should not be in the same place facing in two different directions. However, when a vehicle leaves the correct lane or incorrectly negotiates a crossroad, then the result may be a front-to-front or front-to-side collision.

For an occupant involved in a frontal collision, the risk of sustaining a MAIS 2+ injury in a collision with the front of another passenger vehicle is significantly higher than it is in a collision with the rear of another passenger vehicle ($p = 0.004$) but not significantly higher than it is when colliding with the side of another passenger vehicle ($p = 0.079$). The effect of these differences in the risk of sustaining a MAIS 2+ injury are shown in Figure 3.4b. Front-to-front collisions are the most frequent cause of MAIS 2+ injuries ($p = 0.020$), representing approximately 49%, followed by front-to-rear and front-to-side collisions, representing approximately 21% and 19%, respectively. The higher risk of injury in a front-to-front collision may be attributed to the higher severity of a front-to-front collision: even assuming an equal distribution of initial velocities for all collision types, front-to-front collisions are generally more severe because more energy must be dissipated when the initial velocity vectors of the two vehicles are opposed.

Since the front-to-front collision configuration is responsible for approximately half of the MAIS 2+ injuries experienced by belted passenger vehicle occupants when they collide frontally with another passenger vehicle, the following conclusion can be drawn: For the improved protection of passenger vehicle occupants in frontal collisions, the interaction with the front-end of the collision partner's vehicle is of principal interest.

4.2 Detailed analysis of front-to-front collisions

One of the objectives of this chapter is to establish the most appropriate simulation and crash test configurations to use for the analysis of compatibility between passenger vehicles. In this section, the front-to-front collision configuration is

analysed with respect to VDI Direction of Force (VDI 1), VDI Horizontal Description of Damage (VDI 3), Change in Velocity (Δv), and the mass of the colliding vehicles. The results in this section are analysed and presented without differentiation according to the occupant's seating position. On the one hand, this may negatively influence the results by introducing scatter, for example due to differences between restraint systems, but, on the other hand, it has the positive effect of introducing a bias that reflects the relative significance of each seating position. Based on the available data, the results described below are not significantly different to those from separate analyses of drivers, front seat passengers, and rear seat passengers.

4.2.1 Direction of force and location of damage

In Figure 4.3, the risk of injury to passenger vehicle occupants involved in front-to-front collisions is shown with respect to VDI 1 (Figure 4.3a) and VDI 3 (Figure 4.3b). In order to analyse the data from the perspective of both self-protection and partner-protection, the figures include the distribution of injuries based on the VDI 1 and VDI 3 of both the occupant's vehicle (lower part of each sub-figure) and the collision partner (upper part of each sub-figure). As a consequence, each involved person is included twice in Figure 4.3a and twice in Figure 4.3b.[32] In contrast to previous figures, which are in the form of a complete pie chart, the data in Figure 4.3 are presented in the form of partial segments to symbolise the front-to-front nature of the collisions. Despite the difference in the art of presentation, each of the four individual charts in Figure 4.3 represents 100% of involved persons.

In Figure 4.3a, no significant differences in the risks of injury can be seen with respect to the VDI 1 of either the occupant's vehicle or the collision partner. For both, however, there is a significantly higher proportion of VDI 1 = 12

[32]Note that the inclusion of all vehicle occupants leads to non-significant differences between the distributions of VDI 1 and VDI 3 in the upper and lower parts of Figures 4.3a and 4.3b, respectively. If the analysis were to be performed with matching pairs of drivers, the upper and lower diagrams would have symmetrical distributions of VDI 1 and VDI 3.

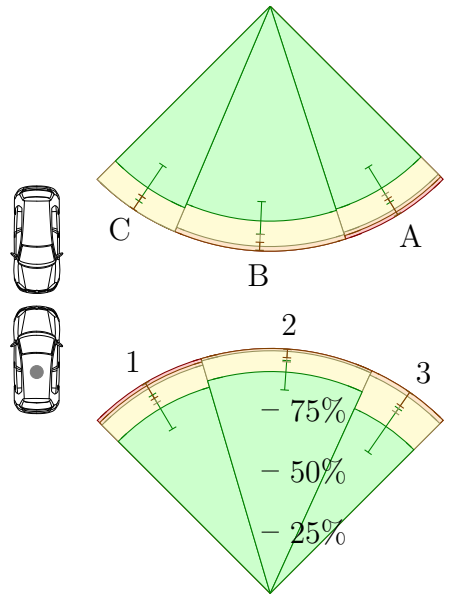

MAIS 4-6
MAIS 3
MAIS 2
MAIS 0-1

Collision partner	
A VDI1 = 11	[23.2%,36.9%]
B VDI1 = 12	[38.6%,52.4%]
C VDI1 = 1	[17.6%,31.4%]
Occupant's vehicle	
1 VDI1 = 11	[24.9%,38.6%]
2 VDI1 = 12	[38.6%,52.4%]
3 VDI1 = 1	[15.9%,29.6%]

(a) Belted passenger vehicle occupants grouped according to the direction of the collision force acting on each vehicle (Collision partner n = 233, Occupant's vehicle n = 233)

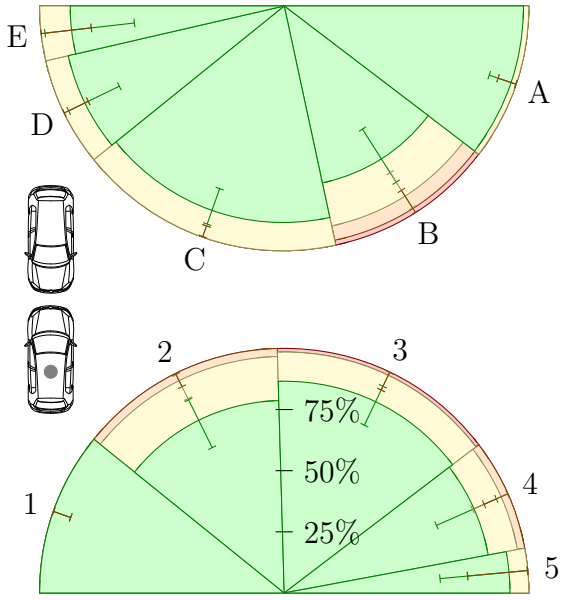

MAIS 4-6
MAIS 3
MAIS 2
MAIS 0-1

Collision partner	
A Left < 33%	[14.0%,27.5%]
B Left 33% - 66%	[15.8%,29.3%]
C All, Centre	[28.4%,41.9%]
D Right 33% - 66%	[7.7%,21.2%]
E Right < 33%	[0.5%,14.0%]
Occupant's vehicle	
1 Left < 33%	[14.9%,28.5%]
2 Left 33% - 66%	[20.7%,34.4%]
3 All, Centre	[23.4%,37.1%]
4 Right 33% - 66%	[8.1%,21.8%]
5 Right < 33%	[0.0%,12.8%]

(b) Belted passenger vehicle occupants grouped according to the horizontal location of damage on each vehicle (Collision partner n = 222, Occupant's vehicle n = 222)

Figure 4.3: Injury risk to belted passenger vehicle occupants involved in front-to-front collisions with other passenger vehicles. The data are grouped according to VDI 1 and VDI 3. The data are limited to collisions where both vehicles have a date of manufacture between 1996 and 2005. The error bars show the 95th percentile binomial confidence intervals of the risk of MAIS 2+, MAIS 3+, or MAIS 4+ injury. The percentage ranges in the legends show the 95th percentile multinomial confidence intervals of the distributions of VDI 1 and VDI 3 values.

collisions than VDI 1 = 1 collisions or VDI 1 = 11 collisions (occupant's vehicle: $p \leq 0.024$, collision partner: $p \leq 0.050$). For the assessment of front-to-front compatibility, it is therefore concluded that the most appropriate test configuration is a collision where VDI 1 = 12.

In Figure 4.3b, it can be seen that collisions with damage on the right side of the vehicle front-end occur significantly less often. The most frequent collisions appear to be those with damage over the full width of the vehicle, followed by those with up to 66% damage to the left front and those with up to 33% damage to the left front. The only significant differences in the risk of MAIS 2+ injuries occur between these latter two collision types, and collisions resulting in up to 66% damage to the left front are more severe. This result is significant for damage to both the occupant's vehicle ($p = 0.013$) and that of the collision partner ($p = 0.023$). It is therefore concluded that the most appropriate test configuration for the assessment of front-to-front compatibility is either with full overlap or with 33% to 66% overlap on the driver's side of the vehicle.[33]

No significant differences between the risks of injuries associated with any VDI 1 or VDI 3 can be observed between the occupant's vehicle and the collision partner in Figure 4.3. Although this does not prove that the distributions are the same, the results do not indicate that any particular collision configuration is more or less severe from the perspective of self-protection or partner-protection.[34] It is therefore concluded that a symmetrical test configuration is appropriate.

Typically, front-to-front crash tests are performed with the vehicles moving directly towards each other with either 100% overlap or 50% overlap on the driver's side (see the literature cited in Section 2.3.2.2).[35] The conclusions from Figure 4.3 support the use of either or both of these standard configurations.

[33]Note that VDI 3 describes the region of damage and not the collision overlap. It is reasonable to assume that the region of damage always exceeds the degree of overlap in a collision.

[34]An example hypothesis is that a collision resulting in a particular type of damage to one of the vehicles represents a high risk of injury to the vehicle's own occupants but a low risk of injury to the occupants of the other vehicle.

[35]In the event that the two vehicles have different widths, the overlap is usually 50% of the narrower vehicle.

4.2.2 Change in velocity (Δv)

Collision Δv is a relevant measure of severity because it not only indicates the energy that must be dissipated by the vehicle structure but also the loading on the occupants and the restraint system. Analysis of Δv is preferable to an analysis of the initial velocity of a vehicle because it takes into account the residual velocities, rebound, and any differences in the initial momentum of the two colliding vehicles.

The data in Figure 4.4 are presented using box plots to show the median MAIS that occurs at a particular Δv (Figure 4.4a) and the median Δv at which a particular MAIS occurs (Figure 4.4b).[36] The boxed area indicates the 25^{th} and the 75^{th} percentiles of the data, and the whiskers indicate the 10^{th} and the 90^{th} percentiles. Due to the ordinal scale of MAIS and the limited volume of the data, one or more of the percentiles can occur at the same value, which results in an atypical box plot. The dataset does not contain any cases with MAIS = 4, MAIS = 5, or $\Delta v > 70$ km/h, and hence box plots cannot be included in Figure 4.4 for these categories.

The data in Figures 4.4a and 4.4b are analysed using two different approaches because, although the collision Δv is independent of the injuries that occur, by defining MAIS as the independent variable in Figure 4.4b, the median Δv that causes a particular degree of injury can be determined. This may then be used to define an appropriate test speed. For example, although Figure 4.4a shows that the expected level of injury does not reach MAIS 2 until a collision Δv of 60 km/h, Figure 4.4b shows that MAIS 2 injuries typically occur at a Δv of 37 km/h. The reason for this apparent contradiction is that lower severity injuries occur more frequently.[37] In order to effectively decrease the number of MAIS 2+ injuries, it may be more effective to focus on the values of Δv at which the most MAIS 2+ injuries occur, rather than simply focussing on the Δv values at which they become more frequent than the MAIS 0-1 injury levels.

[36] In Figure 4.4a the Δv values are collected into categories, such that a Δv of 1 to 10 is given as '10', a Δv of 11 to 20 is given as '20', and so on.

[37] See for example the distribution of injuries in Figure 3.2a

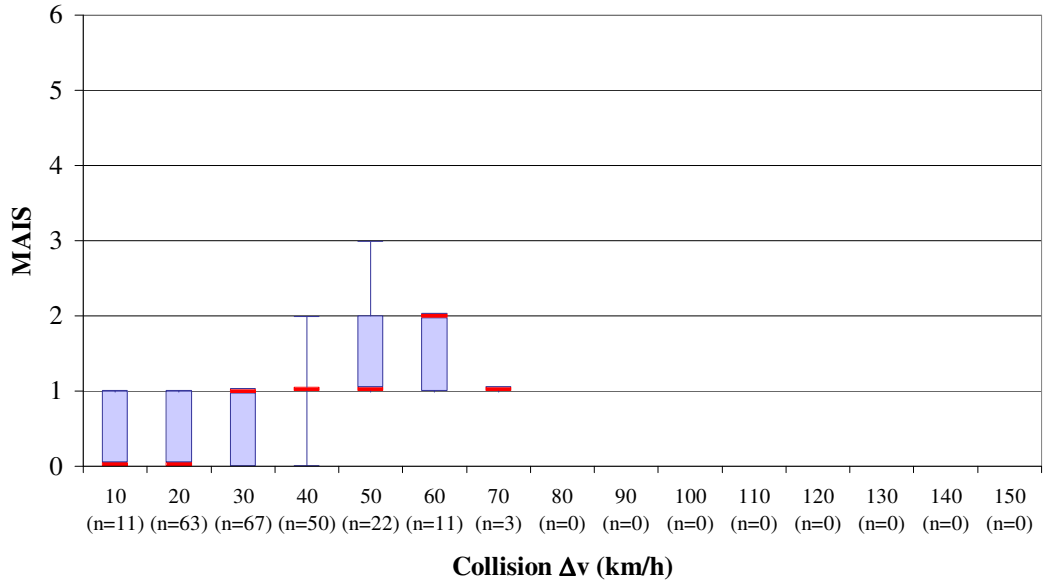

(a) Degree of injury with respect to the collision Δv (n = 227)

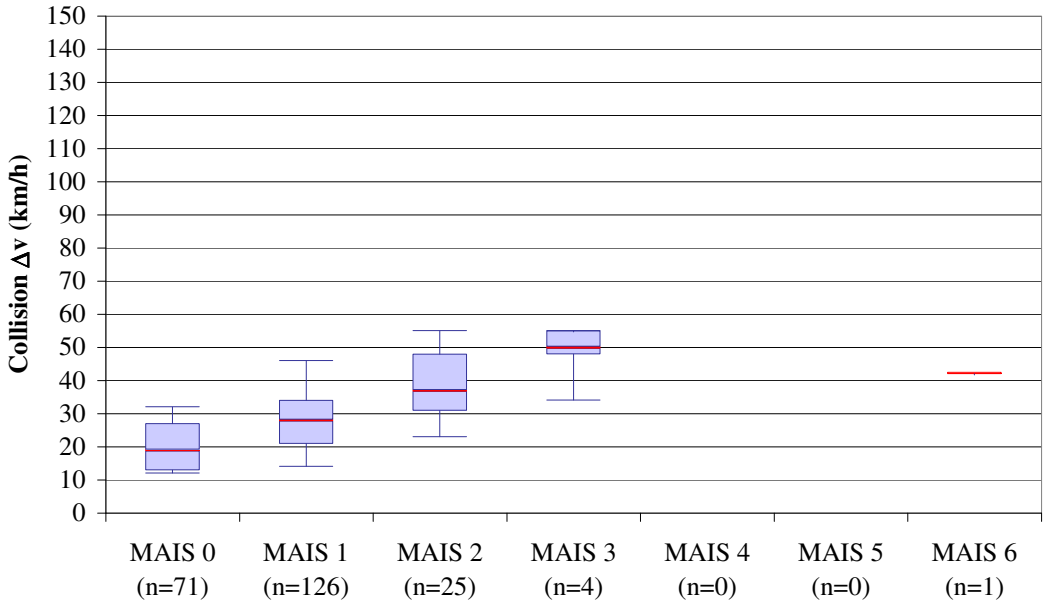

(b) Collision Δv with respect to the degree of injury (n = 227)

Figure 4.4: Comparison between collision Δv and the degree of injury to belted passenger vehicle occupants involved in front-to-front collisions with other passenger vehicles. The data are limited to collisions where both vehicles have a date of manufacture between 1996 and 2005. The box plots show the 10^{th}, 25^{th}, 50^{th}, 75^{th}, and 90^{th} percentiles of the data.

A significant, positive relationship between Δv and MAIS can be observed in Figure 4.4a (Jonckheere-Terpstra Test, $p < 0.001$).[38] However, due to the limits placed on the dataset that is shown in Figure 4.4, only 227 persons from the GIDAS database are included, none of the Δv values exceed 70 km/h, and only four cases of MAIS 3+ injury are included. As a result, a relationship defining the level of MAIS to be expected at a particular Δv cannot be defined. In Figure 4.4b, a similar positive relationship between MAIS and Δv is observed and is again significant (Jonckheere-Terpstra Test, $p < 0.001$). The median Δv at which MAIS 2 injuries occur is 37 km/h and the median Δv at which MAIS 3 injuries occur is 50 km/h.

Due to the limited data available for collisions between two modern passenger vehicles, the relationship between Δv and MAIS is revisited in Section 4.3 using a larger dataset.

4.2.3 Collision mass ratio

The effect of vehicle mass on occupant protection is a frequent topic of discussion in safety related publications. Depending on the perceptions of the author, the focus is typically directed towards either the aggressiveness of larger, heavier passenger vehicles (for example, Brieter 2008) or the inferior safety of smaller, lighter passenger vehicles (for example, IIHS 2009). However, the analysis of collision outcomes based on risk ratios is also criticised because it does not distinguish between positive and negative behaviour. For example, Dreyer et al. (1981) showed that the perceived 'inferior' safety of lighter vehicles may in fact be attributed to their high level of partner protection and the correspondingly low level of injuries and fatalities that occur in the vehicles with which they collide. An alternative approach to the analysis of vehicle mass is therefore applied in this section.[39]

[38] Jonckheere-Terpstra test statistics are calculated using the method described by van de Wiel et al. (1999).

[39] The data are presented in Figure 4.5a using an approach similar to the analysis of risk ratios. The same data are presented in Figure 4.5b using the alternative approach. Both approaches are used in order to demonstrate the potential for conflicting observations and conclusions.

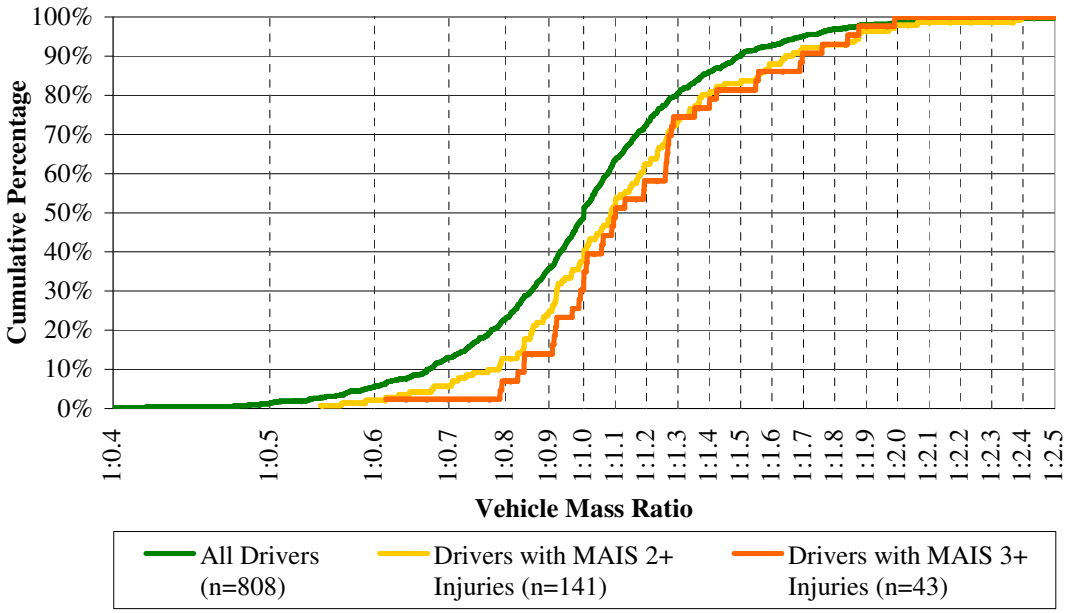

(a) Cumulative distribution with respect to vehicle mass ratio. A vehicle mass ratio of 1:2.0 indicates that the mass of the collision partner's vehicle is double that of the driver's vehicle's mass.

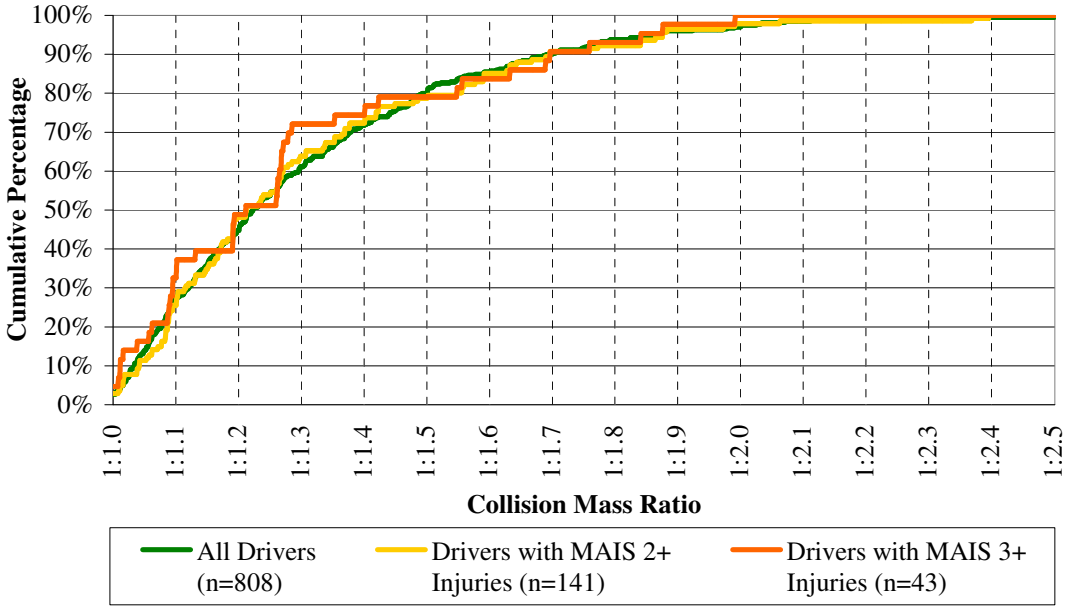

(b) Cumulative distribution with respect to collision mass ratio. A collision mass ratio of 1:2.0 indicates that the heavier vehicle's mass is double that of the lighter vehicle's mass.

Figure 4.5: Cumulative distributions of belted drivers involved in front-to-front collisions with other passenger vehicles. The distributions are based on the estimated total vehicle weight of each vehicle. The data are limited to collisions where both vehicles have a date of manufacture between 1981 and 2005.

The effect of vehicle weight on injury risk is investigated in this section by comparing the degree of injury to the ratio of the colliding vehicles' masses. The variable used for the analysis is the estimated total vehicle mass, which includes the mass of the occupants and payload and hence reflects the true mass, momentum, and kinetic energy at the time of the collision. The dataset used in the analysis consists of front-to-front collisions between two passenger vehicles where both vehicle masses are known, the MAIS of both drivers is known, and both drivers were belted. Due to these limits, the set of drivers of vehicles with dates of manufacture between 1996 to 2005 is reduced to n = 126, and only 16 of these cases have MAIS 2+ injuries. This prevents any significant observations from the data, and hence the case selection criteria used for Figure 4.5 include vehicles with dates of manufacture from an expanded date range from 1981 to 2005. Based on the expanded set of data, the cumulative distributions in Figure 4.5 are plotted to show the difference between the distribution of all drivers and the distribution of drivers with MAIS 2+ and MAIS 3+ injuries.

In Figure 4.5a, the cumulative distribution is plotted using the mass ratio of each vehicle when compared to its collision partner. As such, for the hypothetical case of a collision between a 1500 kg vehicle and a 1200 kg vehicle, the driver of the first vehicle would be plotted with a vehicle mass ratio of 1:0.8, and the driver of the second vehicle would be plotted with a vehicle mass ratio of 1:1.25. In Figure 4.5a, it can be seen that 23% of belted drivers experience front-to-front collisions where their vehicle has a mass ratio of less than 1:0.8 and, since the distribution is based on matching pairs, 23% experience a mass ratio of more than 1:1.25. However, when the distributions of injuries in Figure 4.5a are considered, it can be seen that the mass ratios less than 1:0.8 account for only 13% of MAIS 2+ injuries and 7% of MAIS 3+ injuries whereas the mass ratios greater than 1:1.25 account for 33% of MAIS 2+ injuries and 42% of MAIS 3+ injuries. This result reflects observations from the literature (see Section 2.3.2.1) and indicates that the drivers of lighter vehicles are more frequently injured in front-to-front collisions

than the drivers of heavier vehicles. The differences between the distribution of all drivers and the distribution of drivers with MAIS 2+ injuries are significant (Kolmogorov-Smirnov test, p = 0.015).[40]

Although this result indicates that the belted drivers of lighter vehicles have a higher risk of MAIS 2+ injury than the belted occupants of heavier vehicles, mass is not the only factor that influences injury risk. For example, in 20% of the cases included in Figure 4.5a, a higher level of MAIS is recorded for the driver of the heavier vehicle.

When considering the effect of vehicle mass on the traffic accident environment, it is necessary to analyse the data on a collision basis rather than a vehicle basis. By considering the data at the collision level, it is possible to determine whether collisions between vehicles with unequal masses are responsible for a disproportionately high number of injuries when compared to collisions between vehicles with equal masses. Under the null hypothesis, which is that collisions between vehicles with unequal masses are equivalent to collisions between vehicles with equal masses, it may be concluded that higher mass ratios do not represent a higher risk of injury to the community as a whole, even if they represent an increased risk of injury to one of the involved individuals.

To investigate this hypothesis, the cumulative distributions in Figure 4.5b plot the injury data for each of the drivers with respect to the mass ratio of the lighter vehicle to the heavier vehicle in the collision. Hence, for the hypothetical collision between the 1200 kg and 1500 kg vehicles discussed above, both drivers would be plotted with a collision mass ratio of 1:1.25.

The results in Figure 4.5a show a clear similarity between the distribution of all drivers and the distribution of drivers with MAIS 2+ injuries. However, due to the relatively small number of drivers with MAIS 3+ injuries, it is not clear whether higher collision mass ratios result in a higher, lower, or equivalent risk of MAIS 3+ injury.

[40]Kolmogorov-Smirnov test statistics are calculated with StatPlus 2008 software.

The differences between the distribution of all drivers and the distribution of drivers with MAIS 2+ injuries are not significant (Kolmogorov-Smirnov test, p = 0.801). The lack of a significant difference cannot be taken as proof of the null hypothesis. However, if it were to be assumed that the null hypothesis was true, then the data in Figure 4.5b would support the conclusion that the total risk of injury to all occupants in a collision is independent of the relationship between the masses of the vehicles involved. Therefore, from a societal perspective, there would be no further reason for an assessment of mass with regards to compatibility in front-to-front collisions between passenger vehicles.

4.3 Relationship between Δv and mortality rate

The final aim of this chapter is to determine a function to relate the mechanical severity of the collision to the injury severity of the vehicle occupants. The relationship between Δv and MAIS is investigated in Figure 4.4a, but MAIS data cannot be used to define a continuous function because the AIS is an ordinal scale and, for example, an injury of MAIS 3.5 is meaningless. However, the mortality rate for each value of MAIS is determined in Chapter 3, and, since the mortality rate is a continuous scale, these results are applied again in this section.

Due to the relatively small quantity of data available for passenger vehicle to passenger vehicle collisions in Figure 4.4, it is not practical to define a relationship based on these data alone. In particular, the lack of very high severity collisions is problematic. Therefore, a dataset is used that includes the front-to-front collisions from Section 4.2.2 as well as frontal collisions with commercial vehicles and frontal collisions with fixed obstacles. The data are again limited to belted occupants of passenger vehicles with dates of manufacture between 1996 and 2005 and, to further limit scatter in the results, only include occupants aged from 16 to 60 years old.

To check the correlation between the expanded dataset and the results for front-to-front collisions, Figure 4.6 is plotted for comparison to Figure 4.4. These

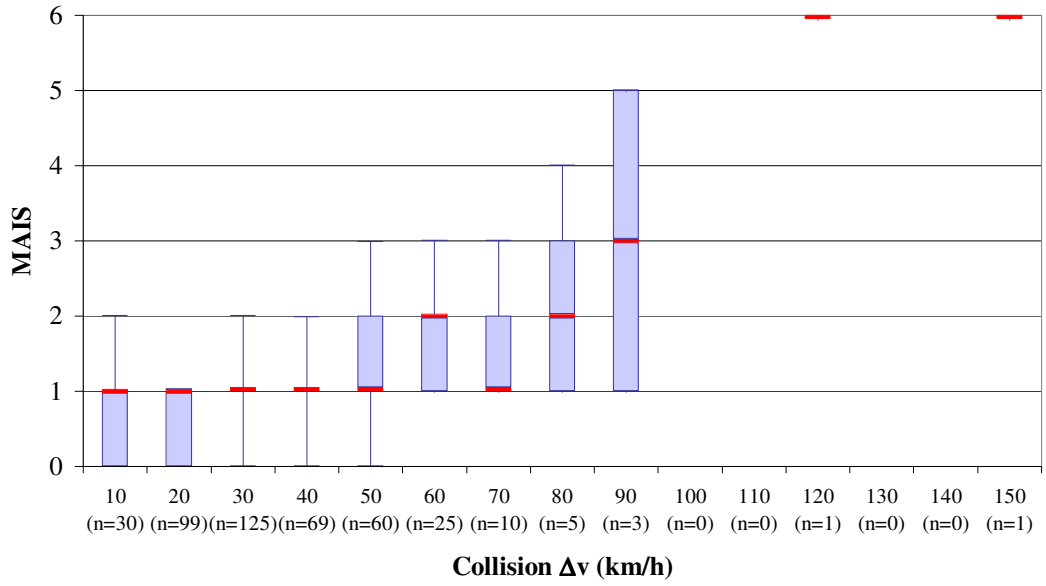

(a) Degree of injury with respect to the collision Δv (n = 428)

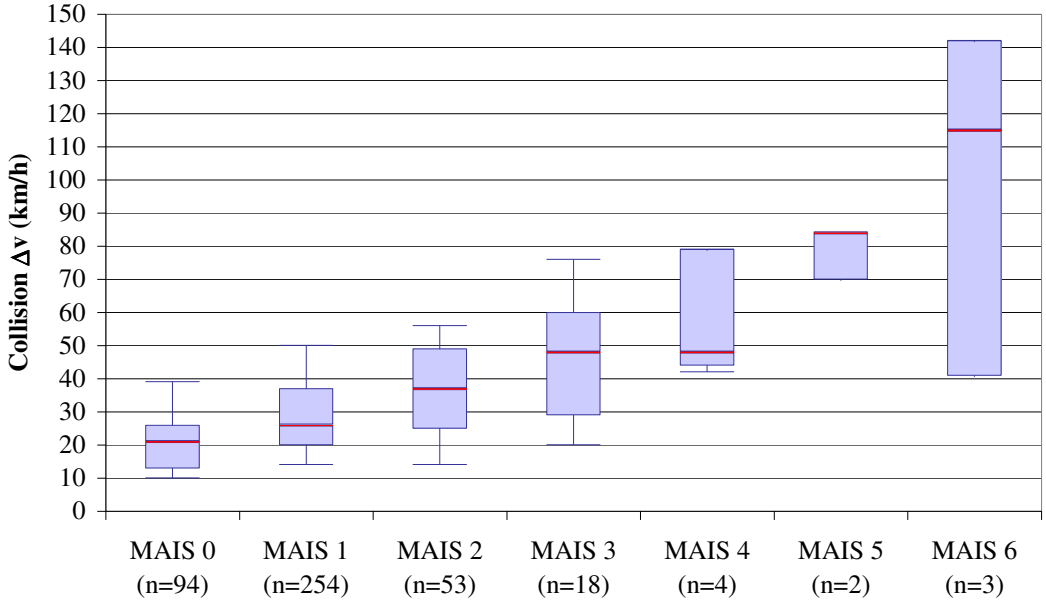

(b) Collision Δv with respect to the degree of injury (n = 428)

Figure 4.6: Comparison between collision Δv and the degree of injury to belted passenger vehicle occupants involved in frontal collisions. The data are limited to occupants aged between 16 and 60. They are also limited to occupants of vehicles that have a date of manufacture between 1996 and 2005. The data are limited to frontal collisions with either commercial vehicles or fixed objects or front-to-front collisions with other passenger vehicles that have a date of manufacture between 1996 and 2005. The box plots show the 10^{th}, 25^{th}, 50^{th}, 75^{th}, and 90^{th} percentiles of the data.

datasets are compared using an adaptation of the Mann-Whitney U-Test and the Jonckheere-Terpstra Test. In order to calculate this statistic, each category of Δv and MAIS is at first treated as an independent sub-population and, similar to a Mann-Whitney U-Test, the median from Figure 4.4 is compared to the median from Figure 4.6. For example, the distribution of injuries in the 60 km/h Δv category from Figure 4.4a is compared to that of Figure 4.6a to determine whether or not the median level of the MAIS values is significantly different between the two samples. At this point, a p-value could be calculated for each of the categories using a Mann-Whitney U-Test (van de Wiel et al. 1999). However, this does not reflect the true situation because each individual p-value would be calculated using only a part of the entire distribution. The pertinent question in this comparison is to determine whether or not the distribution of MAIS values in Figure 4.6a or the distribution of the Δv values in Figure 4.6b are generally higher or lower than the equivalent distributions in Figure 4.4. Therefore, a single statistic is calculated by summing the differences across the categories in each figure. This approach is equivalent to the treatment of multiple samples in a Jonckheere-Terpstra Test (van de Wiel et al. 1999). Finally, the result is compared to a probability generating function and a p-value is calculated. The theorem underlying this statistic is described in Appendix D.

For the calculation of the statistic comparing Figure 4.4a to Figure 4.6a, only categories up to a Δv of 70 km/h are used. This limit is dictated by the lack of data on front-to-front collisions at higher velocities and the necessity of having data in the sub-populations of both datasets in order to compare the median values. Based on the seven categories up to a Δv of 70 km/h, the median level of MAIS is significantly higher in Figure 4.6a than in Figure 4.4a ($p = 0.022$). However, by direct comparison of the means in each figure, it can be observed that the differences are limited to the 10 km/h and 20 km/h sub-populations. This observation is tested by performing the statistical test separately on the ranges 10 to 20 km/h and 30 to 70 km/h. These separate tests identify a significant

difference in the 10 to 20 km/h range (p = 0.009) but no significant difference is observed in the 30 to 70 km/h range (p = 0.211). These results indicate that the two datasets may be similar at Δv values above 20 km/h, but that the dataset used in Figure 4.4a, which only includes vehicle-to-vehicle collisions, has more uninjured occupants at Δv values below 20 km/h than the dataset used in Figure 4.6a, which includes both vehicle-to-vehicle collisions and single vehicle collisions. This outcome is indicative of the GIDAS database, which only includes accidents where at least one person is injured. Since a lone driver who remains uninjured in a collision will never be entered into the database if he or she collides with a tree, but may be entered into the database if he or she collides with another vehicle, there is a degree of bias in the database caused by over-reporting of uninjured occupants in vehicle-to-vehicle collisions. However, given that this difference is only observed at low values of Δv and that the mortality rate for MAIS 1 injuries is also very low, it is concluded that the results in Figure 4.6a are sufficiently representative of those in Figure 4.4a and a valid basis for a definition of the relationship between Δv and mortality rate.

Similar to the method described above, in order to calculate the statistic comparing Figure 4.4b to Figure 4.6b, the sub-populations for MAIS 4 and MAIS 5 are excluded since these data are not present in Figure 4.4b. Based on the five sub-populations for MAIS 0-3 and MAIS 6, the statistical test does not identify a significant difference between the two datasets (p = 0.406). The bias identified in Figure 4.4a is not present in Figure 4.4b because, although there are relatively fewer uninjured occupants in Figure 4.4 than in Figure 4.6, the value of Δv at which an occupant remains uninjured is independent of the sample size. This result confirms the conclusion that the data in Figure 4.6 is a valid basis for the following analysis.

In Section 4.2.2, insufficient data are available to analyse the relevance of the 56 km/h regulatory test speed, which corresponds to a Δv of 64.4 km/h when the collision has a Coefficient of Restitution (C_R) of 0.15 (Huang 2002). In Figure 4.6a,

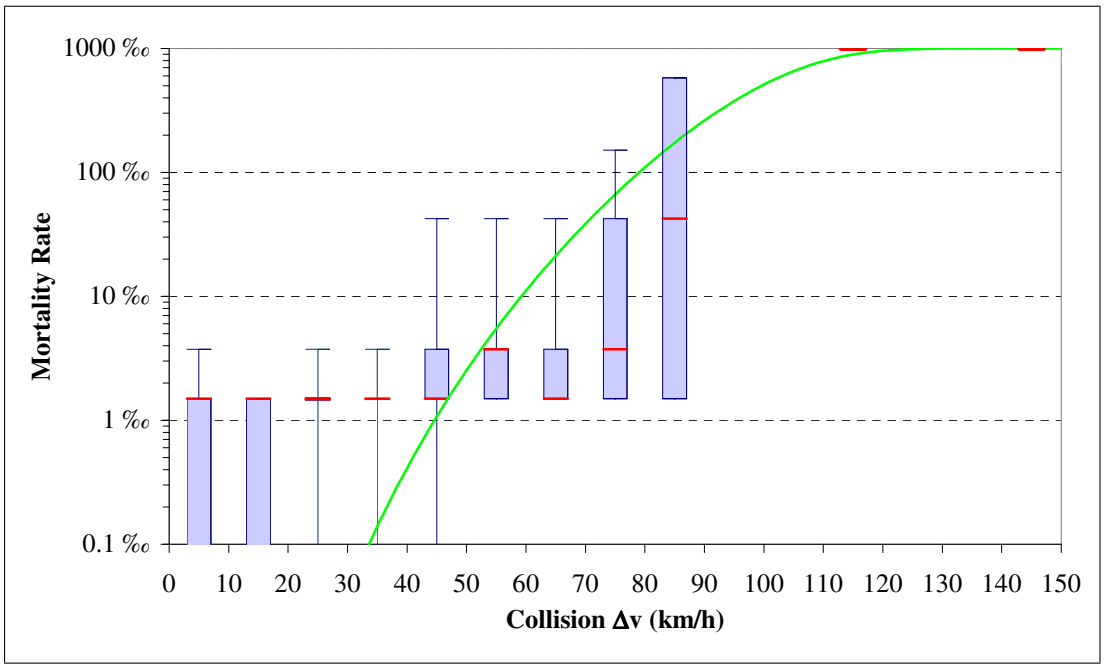

Figure 4.7: Comparison between collision Δv and the degree of injury to belted passenger vehicle occupants involved in frontal collisions. The data are limited to occupants aged between 16 and 60. They are also limited to occupants of vehicles that have a date of manufacture between 1996 and 2005. The data are limited to frontal collisions with either commercial vehicles or fixed objects or front-to-front collisions with other passenger vehicles that have a date of manufacture between 1996 and 2005. The box plots show the 10^{th}, 25^{th}, 50^{th}, 75^{th}, and 90^{th} percentiles of the data. The curve is calculated to show the best fit to the data (n = 428, $R^2 \approx 0.543$).

it can be seen that the 70 km/h category of Δv, which includes collisions with Δv values between 61 km/h and 70 km/h, typically causes a MAIS 1 injury. However, in Figure 4.6b, it can be seen that a Δv of 64.4 km/h is at the 89^{th} percentile of the Δv values that cause MAIS 3 injuries. It can therefore be concluded that a collision at the regulatory test speed typically causes minor injuries, but it is also higher than the speeds at which many serious injuries occur.[41]

Using the mortality rates calculated in Section 3.1 for each level of MAIS, the data in Figure 4.6a can be converted into a relationship between Δv and mortality rate as shown in Figure 4.7. The calculation of this type of relationship between Δv and risk is common in the literature (see for example Stanzel & Page 2006, Wood et al. 2007). Although the distribution of Δv is continuous

[41] According to the AIS definitions, an AIS 1 injury is 'minor' and an AIS 3 injury is 'serious'.

in Figure 4.7, box plots showing 10 km/h intervals are used to make the results easier to interpret. Using the original values of Δv, a curve is plotted in Figure 4.7 to describe the risk of fatality at any given value of Δv. The equation of the curve takes the form of a Weibull risk function (Juckett & Rosenberg 1993):

$$y(x) = 1 - e^{-(x/\lambda)^k} \tag{4.1}$$

where k describes the shape of the curve and λ describes its scale. The use of this equation provides the typical 'S' form of a risk curve, although this form is not apparent in Figure 4.7 due to the logarithmic scale on the y-axis. The values of k and λ in Equation 4.1 are defined to provide the curve with the lowest Coefficient of Variance (R^2), where:

$$R^2 \approx 1 - \frac{\sum_i (y_i - f_i)^2}{\sum_i (y_i - \hat{\bar{y}})^2} \tag{4.2}$$

The values f_i in Equation 4.2 refer to the values of the actual data, which in the case of Figure 4.7 means the mortality rate associated with each occupant's injury. For each f_i, the corresponding value of Δv is substituted into Equation 4.1 (as x) in order to determine the values of y_i. It should be noted that Equation 4.2 is an approximation of R^2 since the population mean $\bar{y}$ is unknown, and the sample mean $\hat{\bar{y}}$, which is the mean derived from the values f_i, is used in its place. The curve shown in Figure 4.7 has the coefficients $k = 8.142$ and $\lambda = 104.2$, which gives a coefficient of variance $R^2 \approx 0.543$.

Using the curve in Figure 4.7, it can be estimated that belted passenger vehicle drivers involved in frontal collisions with a $\Delta v = 45$ km/h experience a 1‰ mortality rate. A 10‰ mortality rate is experienced by those involved in collisions with a $\Delta v = 59$ km/h. Those involved in collisions with a $\Delta v = 79$ km/h experience a 100‰ mortality rate, and those involved in collisions with a $\Delta v = 130$ km/h have a mortality rate approaching 1000‰. A test speed of 56 km/h, which corresponds to a $\Delta v = 64.4$ km/h when $C_R = 0.15$ (Huang 2002), is hence representative of a collision with a mortality rate of 20‰. Based on the curve in Figure 4.7,

it is also observed that the database bias at Δv values below 20 km/h has little or no influence on the results, since the mortality rate decreases below 0.1‰ for Δv values below 34 km/h.

The curve in Figure 4.7 provides interesting results when used to analyse the effect of mass ratio. For example, for a front-to-front collision between two vehicles with a mass ratio of 1:1 and a collision velocity of 100 km/h, each vehicle has a $\Delta v = 57.5$ km/h, and hence the risk of fatality for each of the drivers is 7.9‰.[42] For a mass ratio of 1:2, the same collision velocity results in a risk of fatality of 0.3‰ for the driver of the heavier vehicle and 79‰ for the driver of the lighter vehicle. The mean risk of fatality in the second collision is therefore 40‰, which is clearly higher than the mean risk of fatality observed in the first collision. These results correlate with those in Figure 4.5a but appear to contradict the conclusions derived from Figure 4.5b.

However, the curve in Figure 4.7 is not linear, and hence it provides different results at different degrees of collision severity. For a mass ratio of 1:1 and a collision velocity of 200 km/h, the risk of fatality to each driver is 893‰. For a mass ratio of 1:2, the risk of fatality is 79‰ for the driver of the heavier vehicle and slightly under 1000‰ for the driver of the lighter vehicle. The mean risk of fatality in the second collision is therefore 540‰, which is substantially lower than the mean risk of fatality observed in the first collision.

The results at these two collision velocities show that the risk of fatality may be dependent on the mass ratio of the vehicles but that the dependency is not direct. This result therefore supports the analysis of collision mass ratio in Section 4.2.3, since Figure 4.5b includes the entire distribution of collision velocities that occur in the accident environment. The conclusion from the end of Section 4.2.3 is hence corrected to state that the total risk of injury to all occupants is independent of the relationship between the masses of the vehicles involved, but this is only valid when considered across the entire range of collision velocities that occur in the accident environment.

[42] It is assumed that $C_R = 0.15$ (Huang 2002).

Chapter summary

This chapter focusses on passenger vehicle frontal collisions and the injuries experienced by belted passenger vehicle occupants that are involved in these collisions. All statements below are made in this context.

In Section 4.1.1, it is shown that 57% of frontal collisions involve another passenger vehicle, which is a significant increase over the 54% of all collisions that are shown in Chapter 3 to involve another passenger vehicle. Frontal collisions involving another passenger vehicle are further analysed in Section 4.1.2, and it is shown that front-to-front collisions occur in 25% of cases but are responsible for 49% of MAIS 2+ injuries. It is therefore concluded that the front-end of the collision partner is of particular interest when considering compatibility.

In Section 4.2.1, front-to-front collisions are analysed with respect to the direction of force and location of damage on the front-end. It is shown that the existing vehicle-to-vehicle test designs (front-to-front with parallel velocity vectors and either 50% or 100% overlap) are appropriate for the analysis of compatibility.

In Section 4.2.2, collision severity is analysed in front-to-front collisions, and a positive relationship between the collision Δv and the MAIS injury level sustained by belted occupants is determined. Furthermore, it is shown that the median velocity at which MAIS 2 injuries occur is $\Delta v = 37$ km/h and that the median velocity at which MAIS 3 injuries occur is $\Delta v = 50$ km/h.

The relative mass of the vehicles involved in front-to-front collisions is analysed in Section 4.2.3, and it is shown that the drivers of lighter vehicles involved in front-to-front collisions have a higher risk of sustaining a MAIS 2+ injury. However, it is also shown that the lower risk of injury experienced by the drivers of heavier vehicles has a balancing effect such that the overall risk of injury is independent of the mass ratio between the vehicles involved. It is therefore concluded that, when the outcome is viewed from a societal perspective, heavier vehicles do not reduce the safety of front-to-front collisions between passenger vehicles.

The mortality rates calculated in Chapter 3 for each level of MAIS are applied

in Section 4.3 to define a function relating the Δv of frontal collisions to the mortality rate for belted occupants. For example, it is shown that a Δv of 64 km/h corresponds to a 20‰ risk of fatality for a belted occupant.

Chapter 5

Side Collisions Statistics

In Chapter 3, it is shown that almost half of the road users that sustain MAIS 2+ injuries are passenger vehicle occupants and that a substantial proportion of these injuries occur in side collisions. In this chapter, passenger vehicle side collisions are analysed with a particular focus on front-to-side collisions between two passenger vehicles.

The aims and approach used in this chapter are identical to those used for the analysis of frontal collisions in Chapter 4. Hence, to avoid unnecessary repetition, detailed descriptions of the methods used in this chapter are omitted. The data given in this chapter refer predominantly to persons who experience a side collision. The only exception to this occurs in the analysis of vehicle mass in Section 5.2.3.

Previous studies on side collisions have shown that the risk of injury is higher for struck-side occupants than it is for non-struck-side occupants (Farmer et al. 1997), and that the presence of other passengers in adjacent seating positions also affects the risk of injury (Frampton et al. 2000). However, since the aim of this chapter is to describe the general situation in side collisions, neither of these factors is controlled in the analysis. Based on the available data, the analyses performed in this chapter do not show any significant differences between struck-side and non-struck-side occupants, and hence these results are not further

discussed.[43]

Electronic Stability Control (ESC) has been shown to have a large potential to improve occupant protection (see Ferguson 2007, for a review of recent literature), which has led to the adoption of various policies to mandate its fitment in future vehicles. It has also been shown that one of the effects of ESC is that it alters the distribution of collision configurations and types, particularly with regards to side collisions with poles (Rieger et al. 2005). However, based on the dataset comprising all collision types in Figure 3.3a, the ESC fitment rate is only 18%. The results in this chapter may therefore misrepresent the traffic accident environment of the future.

As in Chapter 4, the data in this chapter refer to the belted occupants of passenger vehicles with dates of manufacture between 1996 to 2005 except where otherwise stated. Collision directions are again defined according to Table A.3, which refers to both VDI 1 and VDI 2.

5.1 Overview of side collisions

In this section, the risk of injury to belted passenger vehicle occupants involved in side collisions is analysed with respect to their collision partners and obstacles. For the subset of collisions where the collision partner is another passenger vehicle, the risk of injury is also analysed with respect to the collision direction of the other vehicle.

5.1.1 Collision partners and obstacles in side collisions

Figure 5.1a shows the distribution of collision partners and obstacles in passenger vehicle side collisions and the distribution of injuries to all belted passenger vehicle

[43]The inability to observe significant differences between the struck-side and non-struck-side occupants does not preclude the presence of bias in the combined dataset. However, the smaller size of the struck-side and non-struck-side datasets prevents any improvement in the quality of the analysis and typically reduces the significance of the observations. It is therefore concluded that the use of the combined dataset is more relevant with regard to the aim of the chapter and more useful for determining significant results.

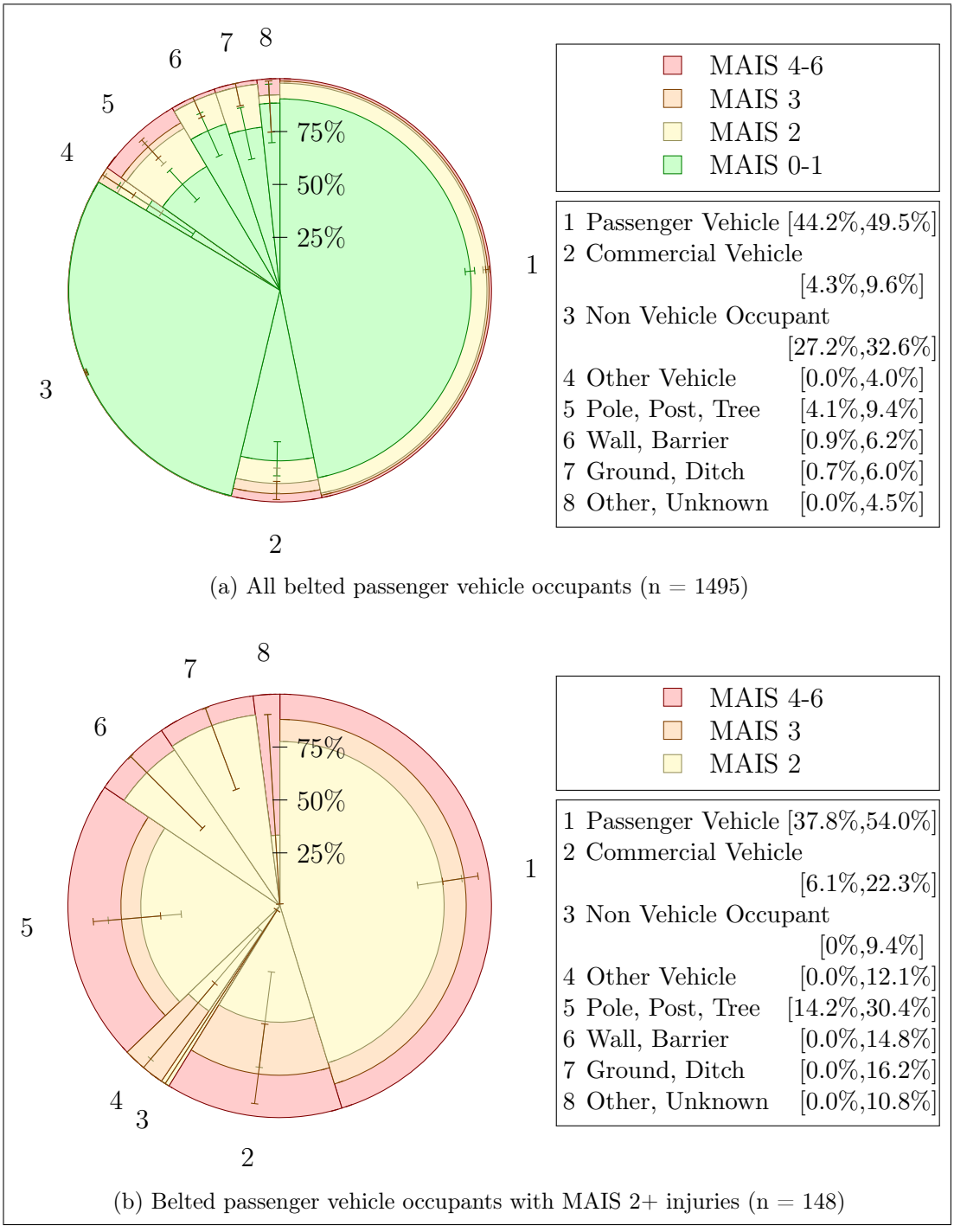

(a) All belted passenger vehicle occupants (n = 1495)

(b) Belted passenger vehicle occupants with MAIS 2+ injuries (n = 148)

Figure 5.1: Injury risk to belted passenger vehicle occupants involved in side collisions. The data are grouped according to the object struck. The occupants' vehicles have a date of manufacture between 1996 and 2005. The error bars show the 95$^{\text{th}}$ percentile binomial confidence intervals of the risk of MAIS 2+, MAIS 3+, or MAIS 4+ injury. The percentage ranges in the legends show the 95$^{\text{th}}$ percentile multinomial confidence intervals of the distribution of struck objects.

occupants involved in these collisions. When compared to the frontal collisions in Figure 4.1a, the only significant difference observed in the distribution of collision partners is a decrease in the number of collisions with other passenger vehicles from 57% for frontal collisions to 47% for side collisions. However, although side collisions with other passenger vehicles are less frequent, they represent a significantly higher risk of sustaining a MAIS 2+ injury ($p = 0.017$).

When the distribution of MAIS 2+ injured occupants is compared for frontal collisions and side collisions, there are no significant differences observed between Figure 4.1b and Figure 5.1b. This applies to both the distribution of collision partners and obstacles as well as the risks of injury.

It is therefore concluded from Figure 5.1 that the likelihood of having a side collision with another passenger vehicle is lower than in a frontal collision, but that the risk of sustaining a MAIS 2+ injury is higher. As a result, the proportion of MAIS 2+ injuries that occurs in collisions with other passenger vehicles is similar for both side collisions and frontal collisions.

Using the approach developed in Section 3.2.1 to determine the distribution of fatally injured passenger vehicle occupants, it can be estimated that 39% of fatalities occur in collisions with other passenger vehicles, 34% in collisions with poles, posts, and trees, and 20% in collisions with commercial vehicles. The estimated proportion of fatalities that occur in side collisions with poles, posts, and trees is therefore substantially higher than that in frontal collisions. However, Rieger et al. (2005) estimated that the standard fitment of ESC would lead to a substantial reduction in lateral pole collisions compared to other pole collisions. Hence, although side collisions with poles, posts, and trees are significant for passenger vehicles with a date of manufacture between 1996 and 2005, they are likely to be less relevant for future vehicle fleets.

5.1.2 Collision partner direction in side collisions with other passenger vehicles

In the section above, it is shown that for passenger vehicle side collisions other passenger vehicles make up the largest portion of collision partners. In this section, the collision direction of the partner vehicle is investigated with respect to the risk of injury in the vehicle that experiences the side collision. The results are shown in Figure 5.2.

Front-to-side collisions are predominant in Figure 5.2a, comprising approximately 61% of the collisions where a passenger vehicle collides with the side of another passenger vehicle ($p < 0.001$). Oblique collisions are the next most frequent type with approximately 24% ($p = 0.014$). Side-to-side collisions appear to be the third most frequent configuration, but a difference between the proportion of these collisions and those of rear and rollover collisions cannot be discerned at the 95% confidence level ($p = 0.145$).

The distribution in Figure 5.2a supports the hypothesis that a passenger vehicle typically travels in a forwards direction. Under this hypothesis, a side collision occurs when two vehicles cross paths and one of them collides frontally with the side of the other. The high proportion of oblique-to-side collisions may be attributed to front-to-side collisions where the velocities of the two vehicles lead to a lateral force being applied to the front of the collision partner,[44] and the side-to-side collisions may be attributed to lane departure events that occur in multi-lane traffic environments.

Significant differences in the risks of MAIS 2+ injury are not observed with regards to the collision direction of the striking vehicle. The raw data indicate that there is a higher risk in front-to-side collisions, but this is not statistically significant with respect to either oblique-to-side collisions ($p = 0.688$) or side-to-side collisions ($p = 0.357$).

[44] An 'oblique' collision is defined as any combination of VDI Direction of Force (VDI 1) and VDI Horizontal Description of Damage (VDI 3) that does not correspond to either a front, side, or rear collision. See Table A.3.

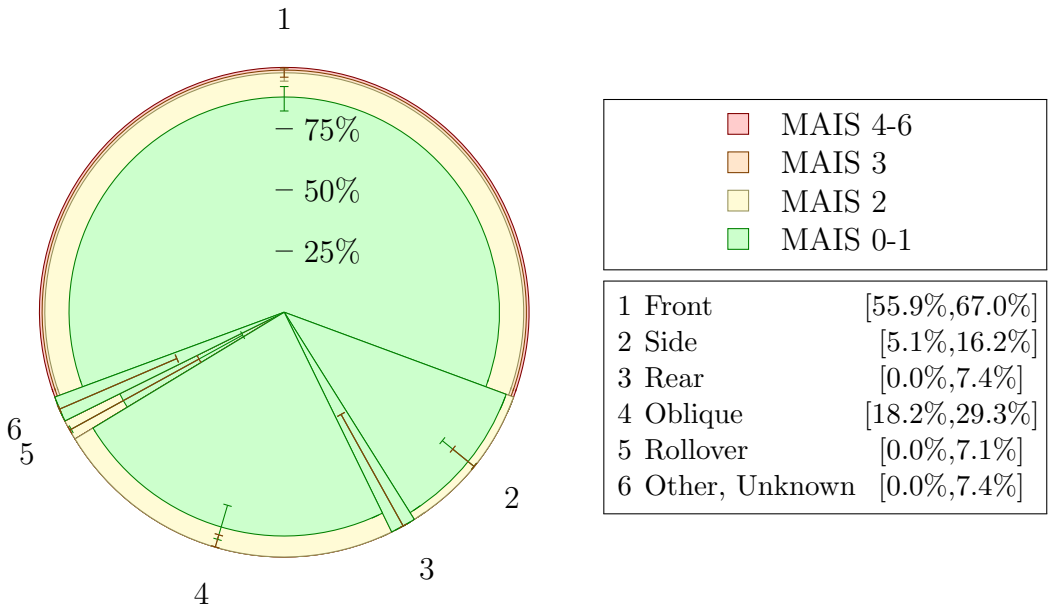

(a) All belted passenger vehicle occupants (n = 297)

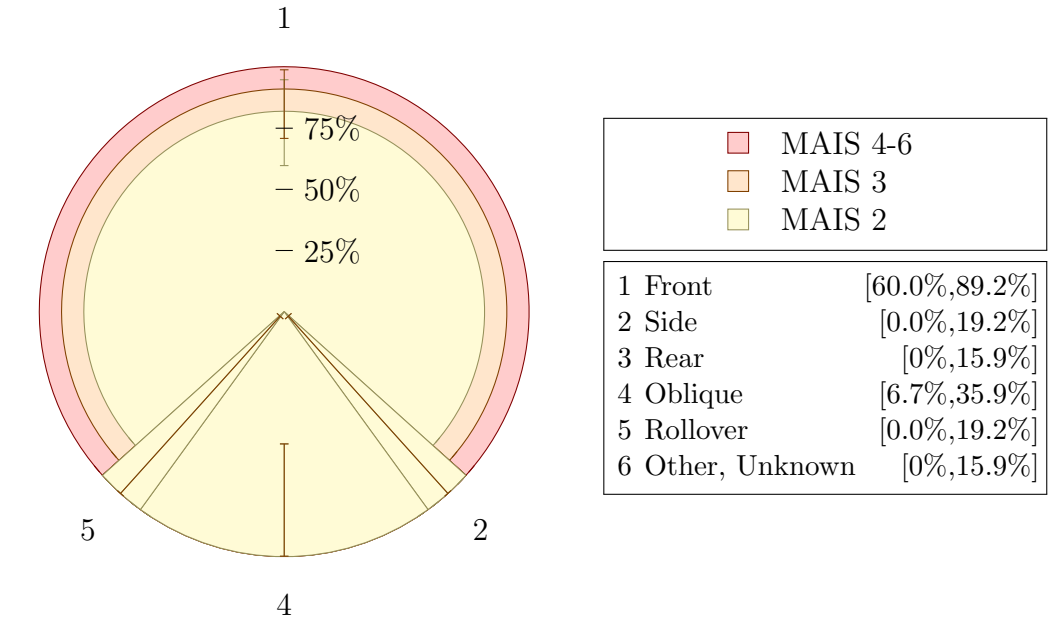

(b) Belted passenger vehicle occupants with MAIS 2+ injuries (n = 30)

Figure 5.2: Injury risk to belted passenger vehicles occupants involved in side collisions with other passenger vehicles. The data are grouped according to the collision directions of the striking vehicles. The data are limited to struck vehicle occupants and collisions where both vehicles have a date of manufacture between 1996 and 2005. The error bars show the 95$^{\text{th}}$ percentile binomial confidence intervals of the risk of MAIS 2+, MAIS 3+, or MAIS 4+ injury. The percentage ranges in the legends show the 95$^{\text{th}}$ percentile multinomial confidence intervals of the distribution of collision directions.

By comparing the results in Figures 4.2a and 5.2a, the relative severity of a front-to-side collision can be compared for the occupants of the striking vehicle (Segment 2 in Figure 4.2a) and the occupants of the struck vehicle (Segment 1 in Figure 5.2a). Although the raw results indicate a higher risk of MAIS 2+ injury in the side collision, this observation is not significant ($p = 0.096$).

The focus of the analysis in Figure 5.2b is limited to occupants with MAIS 2+ injuries, but the conclusions are the same as those above: the largest proportion of injuries occur in the front-to-side configuration ($p < 0.001$), which makes up approximately 73% of cases. No significant differences in the risk of injury in side collisions are observed, but it is conspicuous that MAIS 3+ injuries only occur in front-to-side collisions.

The statistics show clearly that the front-to-side collision configuration is the most frequent form of side collision with another passenger vehicle. Since frontal collisions are defined as collisions involving deformation to the vehicle's front-end (see Table A.3), it is concluded that the front-end of the collision partner's vehicle is of major interest for the improvement of compatibility and the increased protection of occupants involved in side collisions. This parallels the conclusion that is drawn with respect to frontal collisions in Section 4.1.2. The optimum design of a vehicle front-end is therefore a compromise between self-protection and also partner-protection in collisions with either the front or side of other passenger vehicles.

5.2 Detailed analysis of front-to-side collisions

The purpose of this section is to identify the most appropriate simulation and crash test configurations to use for the analysis of compatibility in front-to-side collisions. The analysis is performed with respect to VDI Direction of Force (VDI 1), VDI Horizontal Description of Damage (VDI 3), Change in Velocity (Δv), and the mass of the colliding vehicles. As is the case with the analysis of frontal collisions in Chapter 4, the results are presented without differentiation according

to the occupant's seating position. Based on the available data, the analyses performed in this section do not show any significant differences between struck-side and non-struck-side occupants. Therefore, although it may introduce some scatter, the results in this section are presented utilising all occupants irrespective of their seating position.

5.2.1 Direction of force and location of damage

Figure 5.3a shows the risk of injury to belted struck vehicle occupants with respect to the VDI 1 of the occupant's vehicle and that of the collision partner. Since a side collision may involve either the left or the right of the vehicle, a direction of force perpendicular to the vehicle can be recorded as either VDI 1 = 3, if the collision occurres on the right, or VDI 1 = 9, if the collision occurres on the left. Therefore, these two values are grouped together in the diagram, and the same is done for VDI 1 $\in \{2, 10\}$ and VDI 1 $\in \{4, 8\}$.[45]

Due to the relatively low number of cases, significant differences in the risk of sustaining a MAIS 2+ injury cannot be identified between the categories of VDI 1 in Figure 5.3a. For the collision partner's vehicle, the raw data indicate a higher risk for VDI 1 = 12, but this is not significant with respect to either VDI 1 = 1 ($p = 0.263$) or VDI 1 = 11 ($p = 0.276$). For the occupant's vehicle, a higher risk is indicated for VDI 1 $\in \{3, 9\}$, but this is again not significant with respect to either VDI 1 $\in \{2, 10\}$ ($p = 0.369$) or VDI 1 $\in \{4, 8\}$ ($p = 0.803$). No category of VDI 1 occurs in a higher proportion of collisions for the collision partner ($p \geq 0.843$), but for the occupant's vehicle a VDI 1 $\in \{2, 10\}$ occurs in approximately 63% of cases, which is significantly larger than the portion of cases that occur with either VDI 1 $\in \{3, 9\}$ or VDI 1 $\in \{4, 8\}$ ($p < 0.001$). For the assessment of front-to-side compatibility, it is therefore concluded that the direction of force of the striking vehicle is not critical within the range VDI 1 $\in \{11, 12, 1\}$, but the struck vehicle should have a direction of force approximately 30° forward of the perpendicular.

[45] The VDI Direction of Force (VDI 1) is described in detail in Figure A.3.

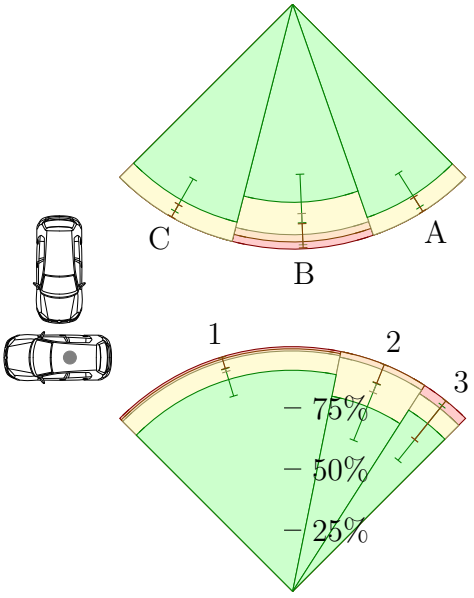

MAIS 4-6
MAIS 3
MAIS 2
MAIS 0-1

Front of collision partner	
A VDI1 = 11	[20.9%,36.7%]
B VDI1 = 12	[29.7%,45.5%]
C VDI1 = 1	[26.4%,42.2%]
Side of occupant's vehicle	
1 VDI1 ∈ {2, 10}	[56.0%,70.1%]
2 VDI1 ∈ {3, 9}	[17.0%,31.1%]
3 VDI1 ∈ {4, 8}	[7.1%,21.2%]

(a) Belted struck vehicle occupants grouped according to the direction of the collision force acting on each vehicle (Collision partner n = 182, Occupant's vehicle n = 182)

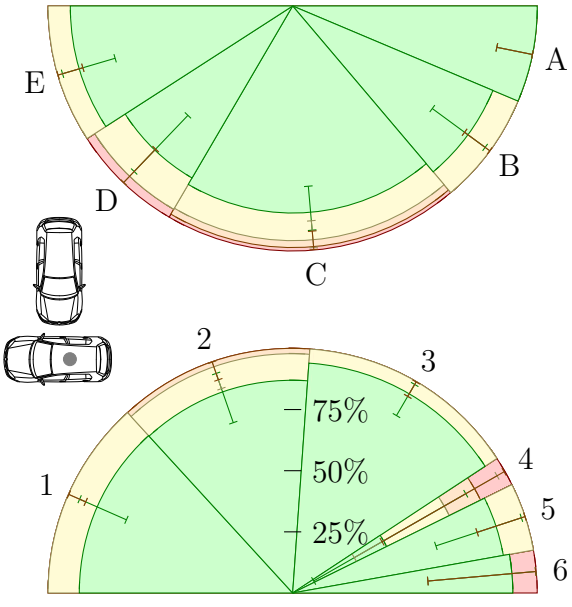

MAIS 4-6
MAIS 3
MAIS 2
MAIS 0-1

Front of collision partner	
A Left < 33%	[5.5%,20.3%]
B Left 33% - 66%	[7.7%,22.5%]
C All, Centre	[32.0%,46.8%]
D Right 33% - 66%	[7.7%,22.5%]
E Right < 33%	[11.0%,25.8%]
Side of occupant's vehicle	
1 Front	[19.1%,34.3%]
2 Front incl Comp	[18.5%,33.8%]
3 Compartment	[21.9%,37.1%]
4 Entire side	[0.0%,11.9%]
5 Rear incl Comp	[1.7%,16.9%]
6 Rear	[0.0%,13.6%]

(b) Belted struck vehicle occupants grouped according to the horizontal location of damage on each vehicle (Collision partner n = 181, Occupant's vehicle n = 178)

Figure 5.3: Injury risk to belted passenger vehicle occupants involved in front-to-side collisions with other passenger vehicles. The data are grouped according to VDI 1 and VDI 3. The data are limited to struck vehicle occupants and collisions where both vehicles have a date of manufacture between 1996 and 2005. The error bars show the 95th percentile binomial confidence intervals of the risk of MAIS 2+, MAIS 3+, or MAIS 4+ injury. The percentage ranges in the legends show the 95th percentile multinomial confidence intervals of the distributions of VDI 1 and VDI 3 values.

Similar to the results for VDI 1, no significant differences in the risk of sustaining a MAIS 2+ injury can be observed with respect to the VDI 3 of the collision partner in Figure 5.3b. However, the proportion of collisions that involve deformation to the entire width of the front-end is significantly greater than that for any of the partial deformation categories ($p = 0.004$). For the occupant's vehicle, the risk of MAIS 2+ injury in a collision that deforms the entire side of the vehicle is higher than that in a collision which only deforms the compartment ($p = 0.036$). This result is unexpected, since it could be anticipated that deformation to the compartment would result in high loading on the occupants and hence a high risk of injury. However, by analysing the VDI Degree of Deformation (VDI 6) values for these collision, it can be observed that the severity of the collisions that only deform the compartment is typically lower than the collisions that deform the entire vehicle side.[46]

At the 95% confidence level, the proportion of collisions that cause deformation to either the front, the front including the compartment, or the compartment is significantly greater than the proportion of collisions that cause deformation to either the rear, rear including the compartment, or the entire side ($p < 0.001$). It is therefore concluded that the most appropriate test configuration for the assessment of compatibility involves deformation to the entire width of the vehicle colliding frontally and deformation to the compartment of the vehicle colliding laterally, including possibly some deformation forward of the compartment.[47]

The standard test configuration that has been used for most of the recent front-to-side collision research (see the literature cited in Section 2.4.2.2) involves a collision aligned with the passenger compartment and perpendicular velocity vectors for the two colliding vehicles. This configuration correlates reasonably well with the values of VDI 1 and VDI 3 that are significant in the accident environment.

[46]For collisions that lead to deformation of the compartment, the VDI 6 values occur in the range VDI 6 $\in \{1, 3\}$ with a median of VDI 6 = 2. For collisions that lead to deformation of the entire side, the VDI 6 values occur in the range VDI 6 $\in \{3, 5\}$ with a median of VDI 6 = 3.

[47]The VDI Horizontal Description of Damage (VDI 3) is described in detail in Figure A.5.

5.2.2 Change in velocity (Δv)

In comparison to an analysis of just the initial velocity of the colliding vehicles, Δv is particularly relevant for the analysis of collision severity in side collisions. By measuring the change in the velocity vector of the vehicle, both the initial velocity of the vehicle, which may not be in a sideways direction, and the impulse caused by the collision itself are taken into consideration.

As is the case for the front-to-front collisions in Figure 4.4a, the front-to-side data in Figure 5.4a are dominated by the MAIS 0 and MAIS 1 injury levels. Also, the dataset only includes three occupants with MAIS 3+ injuries, and the median injury level does not exceed MAIS 1 except in the 60 km/h Δv category, which only includes one case. A positive relationship between MAIS and Δv is measurable (Jonckheere-Terpstra Test, $p < 0.001$), but a relationship defining the level of MAIS to be expected at a particular Δv cannot be defined due to the absence of very high severity collisions from the dataset. In Figure 5.4b, the relationship between MAIS and Δv is again positive (Jonckheere-Terpstra Test, $p < 0.001$). The median Δv at which MAIS 2 injuries occur is 39 km/h, and the three MAIS 3+ injuries occur at a median Δv of 47 km/h.

Similar to the analysis of frontal collisions, the relationship between Δv and MAIS is also addressed in Section 5.3 using a larger dataset.

5.2.3 Collision mass ratio

The analysis in Figure 5.5 is performed using front-to-side collisions between two passenger vehicles where both vehicle masses are known. The data in Figure 5.5a are limited to belted struck vehicle drivers with a known level of MAIS, but they are not limited with regards to the belt use or injury level of the driver of the striking vehicle. Both drivers are included in Figure 5.5b, and hence the data are limited to cases where the MAIS of both drivers is known and where both

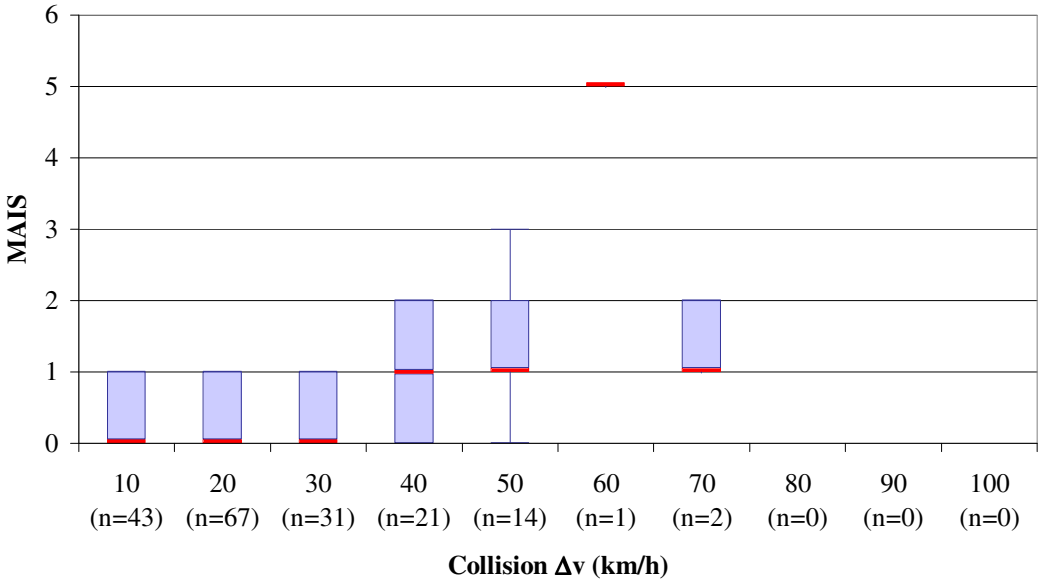

(a) Degree of injury with respect to the collision Δv (n = 179)

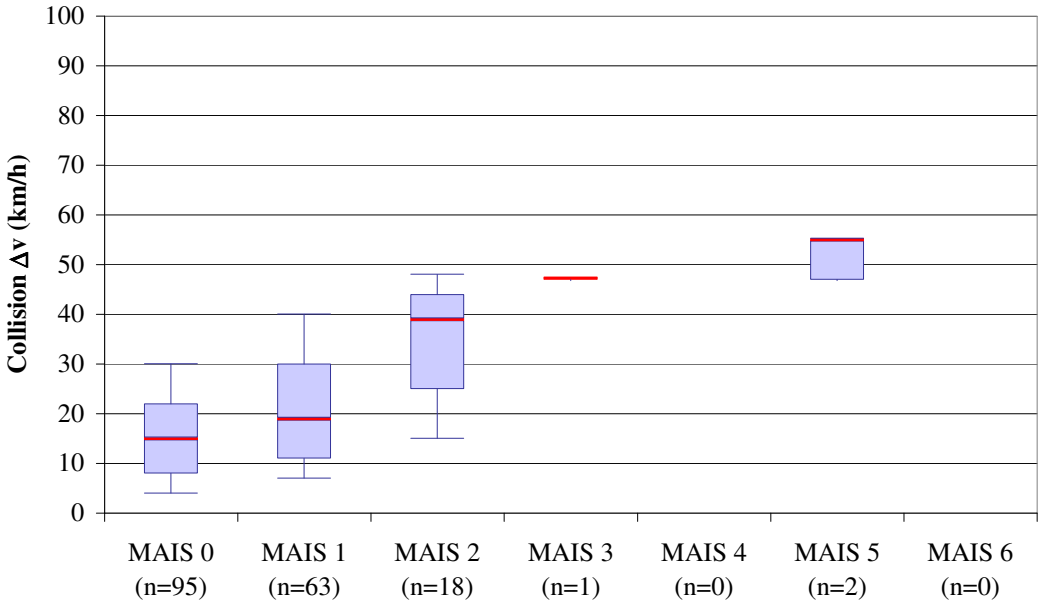

(b) Collision Δv with respect to the degree of injury (n = 179)

Figure 5.4: Comparison between collision Δv and the degree of injury to belted passenger vehicle occupants involved in front-to-side collisions with other passenger vehicles. The data are limited to struck vehicle occupants and collisions where both vehicles have a date of manufacture between 1996 and 2005. The box plots show the 10^{th}, 25^{th}, 50^{th}, 75^{th}, and 90^{th} percentiles of the data.

drivers were belted.[48] As is the case for Figure 4.5, the dates of manufacture of the vehicles are limited between 1981 and 2005.

In Figure 5.5a, the cumulative distribution is plotted using the mass ratio of the struck vehicle compared to the striking vehicle. The difference between the distribution of all drivers and the distribution of drivers with MAIS 2+ injuries shows that belted drivers face a higher risk of injury when the vehicle with which they collide is heavier (Kolmogorov-Smirnov test, $p < 0.001$). Similarly, the differences between the distribution of all drivers and the distribution of drivers with MAIS 3+ injuries is also significant (Kolmogorov-Smirnov test, $p = 0.004$). The same conclusion is reached in Chapter 4 for drivers involved in front-to-front collisions.

Unlike the even distribution of drivers involved in front-to-front collisions in Figure 4.5a, Figure 5.5a indicates that only 46% of the struck vehicle drivers are in the heavier of the two vehicles. This is likely to be an artefact of the GIDAS database and the requirement that all cases include at least one injury. Front-to-side collisions where the struck vehicle is heavier arise less frequently in the database because, as shown above, the occupants of a heavier struck vehicle have a relatively low risk of injury and, as observed in Figure 4.2, the occupants of the striking vehicle also have a relatively low risk of injury. Therefore, it is more likely that all occupants of both vehicles remain uninjured and that the accident is excluded from the database.

In Figure 5.5b, the data are analysed at the collision level and hence include the drivers of both vehicles. In contrast to the results for front-to-front collisions, Figure 5.5b indicates that front-to-side collisions between two vehicles with unequal masses result in higher risks of MAIS 2+ injury than similar collisions between equally heavy vehicles. This observation is significant (Kolmogorov-Smirnov test, $p = 0.005$). In contrast, the differences between the distribution of all drivers and the distribution of drivers with MAIS 3+ injuries are not signifi-

[48] Figure 5.5b is the only point in this chapter where the occupants of the striking vehicles are included in the data. Otherwise the analysis is limited to the occupants of the struck vehicle.

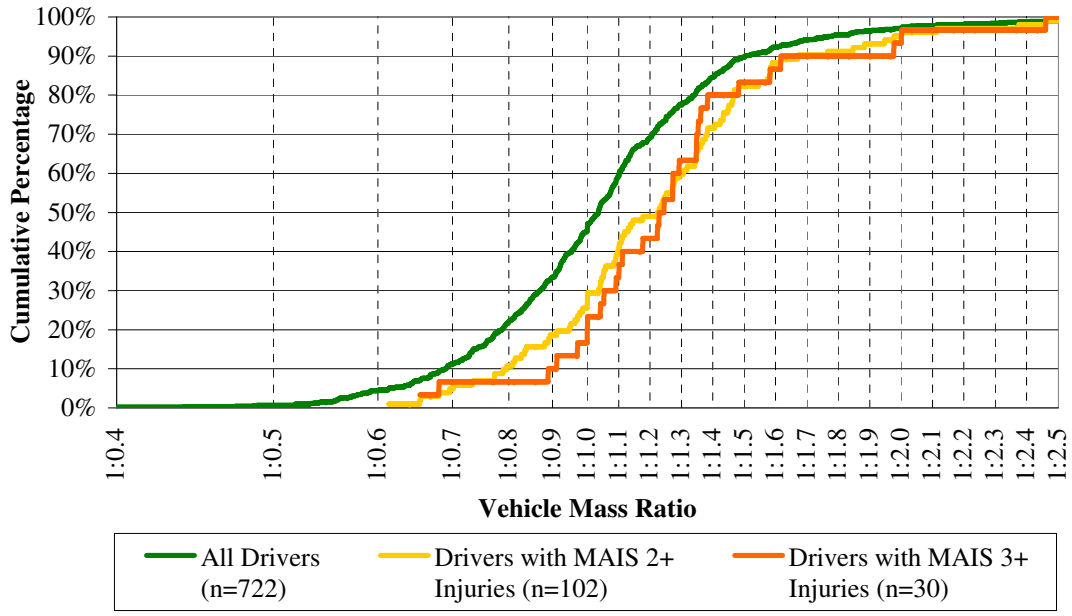

(a) Cumulative distribution with respect to vehicle mass ratio. Limited to drivers of the struck vehicle. A vehicle mass ratio of 1:2.0 indicates that the striking vehicle's mass is double that of the struck vehicle's mass.

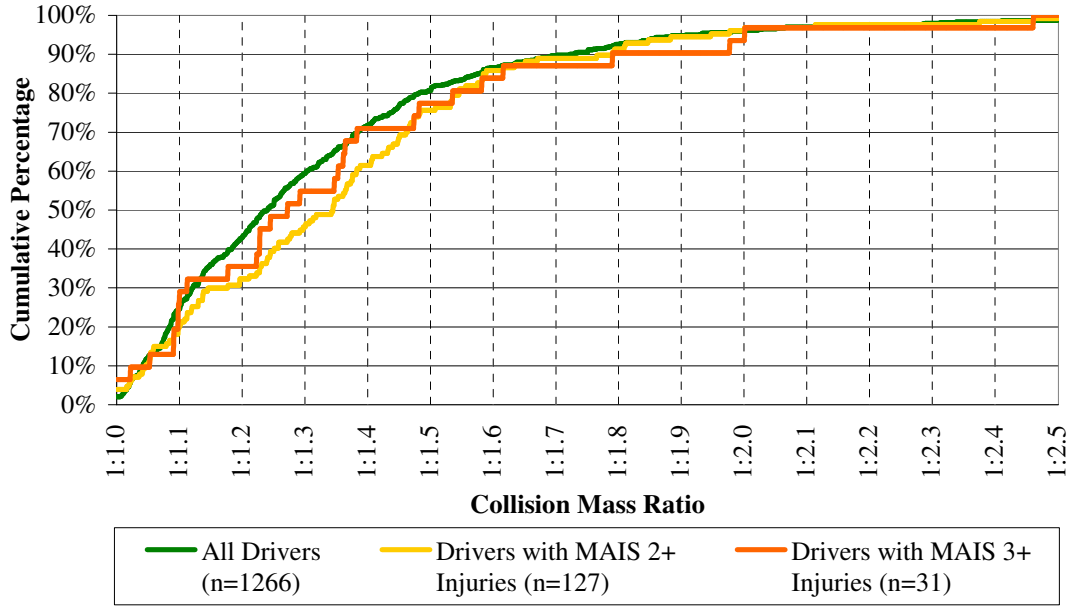

(b) Cumulative distribution with respect to collision mass ratio. Includes drivers of both vehicles. A collision mass ratio of 1:2.0 indicates that the heavier vehicle's mass is double that of the lighter vehicle's mass.

Figure 5.5: Cumulative distributions of belted drivers involved in front-to-side collisions with other passenger vehicles. The distributions are based on the estimated total vehicle weight of each vehicle. The data are limited to collisions where both vehicles have a date of manufacture between 1981 and 2005.

cant (Kolmogorov-Smirnov test, p = 0.453), although this can be attributed to the small number of belted drivers with MAIS 3+ injuries. From both an individual and a societal perspective, it is concluded that compatibility in front-to-side collisions is typically dependent on vehicle mass.

It is hypothesised above that the distribution of front-to-side collisions in the GIDAS database may be 'missing' a number of accidents in which all occupants remain uninjured because a heavier vehicle is struck in the side by a lighter vehicle. To determine whether these missing cases have an effect on the analysis, the datasets in Figure 5.5 can be supplemented with pseudo cases with two uninjured drivers. A balance between the heavy and light vehicles in the subsets of struck and striking vehicles can hence be achieved. However, the analysis of this modified distribution does not contradict any of the conclusions reached above.

5.3 Relationship between Δv and mortality rate

The final aim of this chapter is to determine a relationship between Δv and the mortality rate of passenger vehicle occupants involved in side collisions. However, the complexity of the data for side collisions exceeds that for the frontal collisions that are analysed in Section 4.3. The results are inconclusive for several combinations of collision partners and obstacles, additional limitations on VDI 3, additional limitations on occupant age, and separate consideration of struck-side and non-struck-side occupants. A major limitation on the ability to define an acceptable curve is the absence of very severe, high speed collisions involving modern vehicles. Without these cases, it is impossible to estimate where the risk of fatality approaches 1000‰. The results also appear to be dependent on a multitude of factors that contribute to the occupants' injuries. Furthermore, although this analysis focuses only on Δv, the literature cites the initial velocity of the striking vehicle as another indicator of severity for struck-side occupants (Tingvall et al. 2003). A broader multivariate analysis using a larger dataset is therefore recommended for further research in this area.

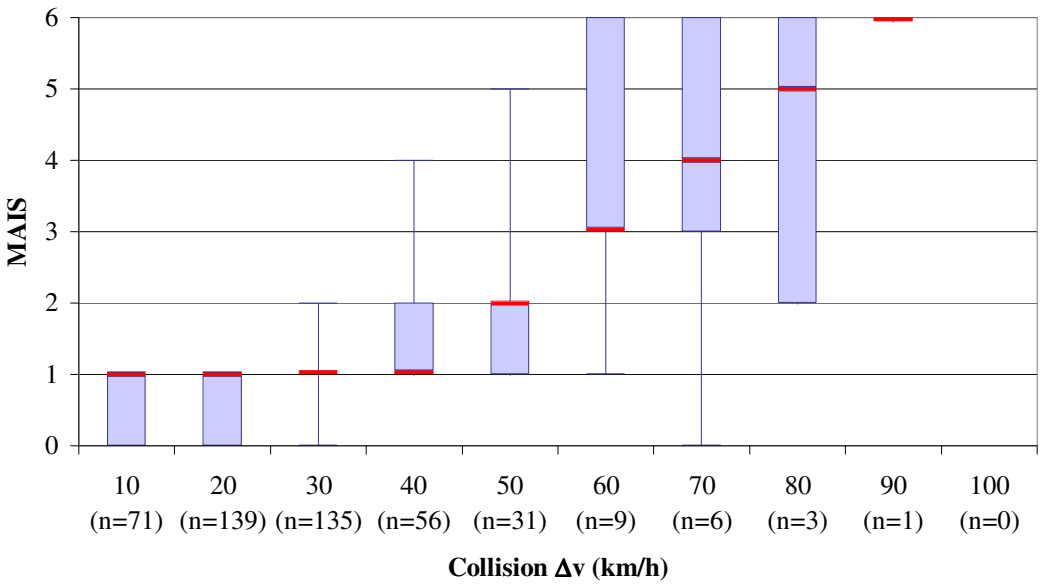

(a) Degree of injury with respect to the collision Δv (n = 451)

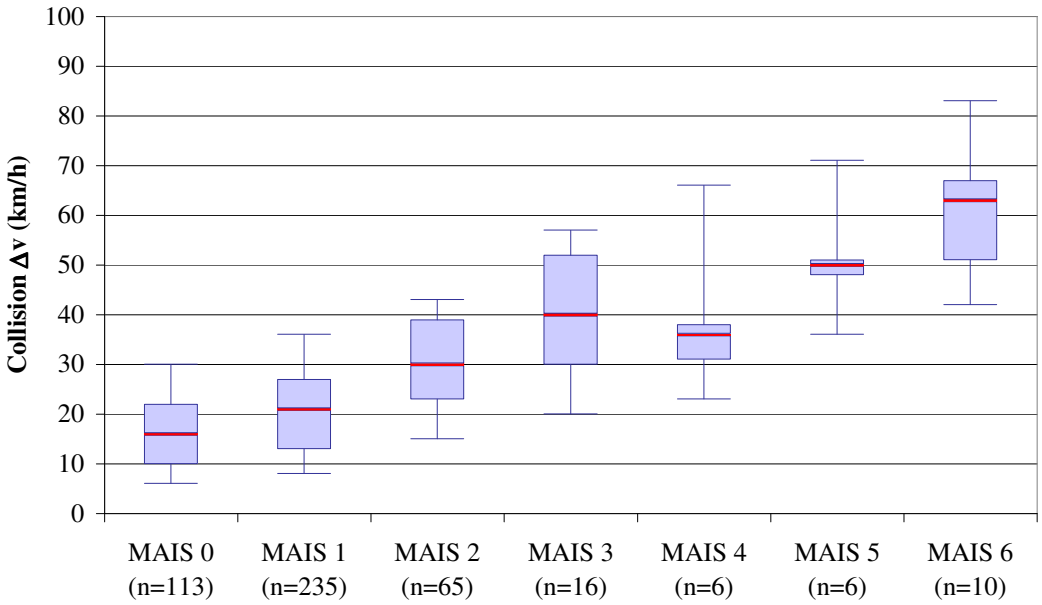

(b) Collision Δv with respect to the degree of injury (n = 451)

Figure 5.6: Comparison between collision Δv and the degree of injury to belted passenger vehicle occupants involved in front-to-side collisions with other passenger vehicles. The data are limited to struck-side, struck vehicle occupants aged between 16 and 60. They are also limited to collisions where VDI 3 indicates that the passenger compartment is deformed. The date of manufacture of the vehicles is not limited. The box plots show the 10^{th}, 25^{th}, 50^{th}, 75^{th}, and 90^{th} percentiles of the data.

For illustrative purposes, a dataset including vehicles of all ages is analysed in Figure 5.6. The data include belted struck-side occupants aged 16 to 60 years, and are limited to front-to-side collisions where VDI 3 indicates that the passenger compartment is deformed. Because the results include many older vehicles, they are not considered to be representative of modern vehicle designs.

In comparison to the results in Figure 5.4a, the results in Figure 5.6a predict a higher level of MAIS for a given Δv. This observation is significant according to the statistical test described in Section 4.3 ($p < 0.001$). This may reflect an improved level of occupant protection in more modern passenger vehicles, since the datasets are based on different ranges of vehicle manufacturing date. In contrast, the differences between the datasets used in Figures 5.4b and 5.6b are not significant ($p = 0.232$). For the MAIS 2 injuries, the median Δv in Figure 5.4b is 39 km/h, but the median Δv in Figure 5.6b is only 30 km/h. This may again reflect the different ranges of vehicle manufacturing date used in the two datasets, but it may also be an artefact of the small quantity of data used in Figure 5.4b. The mean Δv at which the MAIS 2 injuries occur in Figure 5.4b is 34 km/h, which is also the midpoint between the 25^{th} and 75^{th} percentiles of the data. It is hence concluded that a Δv of 34 km/h is more representative of the MAIS 2 cases in Figure 5.4b.

In Figure 5.7, the MAIS data from Figure 5.6a are plotted in terms of the expected mortality rates, and a curve is defined to determine the rate of mortality for any given Δv. The curve is defined according to Equation 4.1 and, with the coefficients $k = 5.787$ and $\lambda = 71.40$, the correlation with the data results in a coefficient of variance $R^2 \approx 0.343$.[49] Using this curve, it can be estimated that belted struck-side occupants involved in front-to-side collisions with a $\Delta v = 22$ km/h experience a 1‰ mortality rate. A 10‰ mortality rate is experienced by those involved in collisions with a $\Delta v = 32$ km/h. Those involved in collisions with a

[49] This value of R^2 indicates a weak correlation with the data, but it is stronger than the correlation described by Wood et al. (2007) for their analysis of the relationship between Δv and risk and is hence considered an acceptable basis for the analysis.

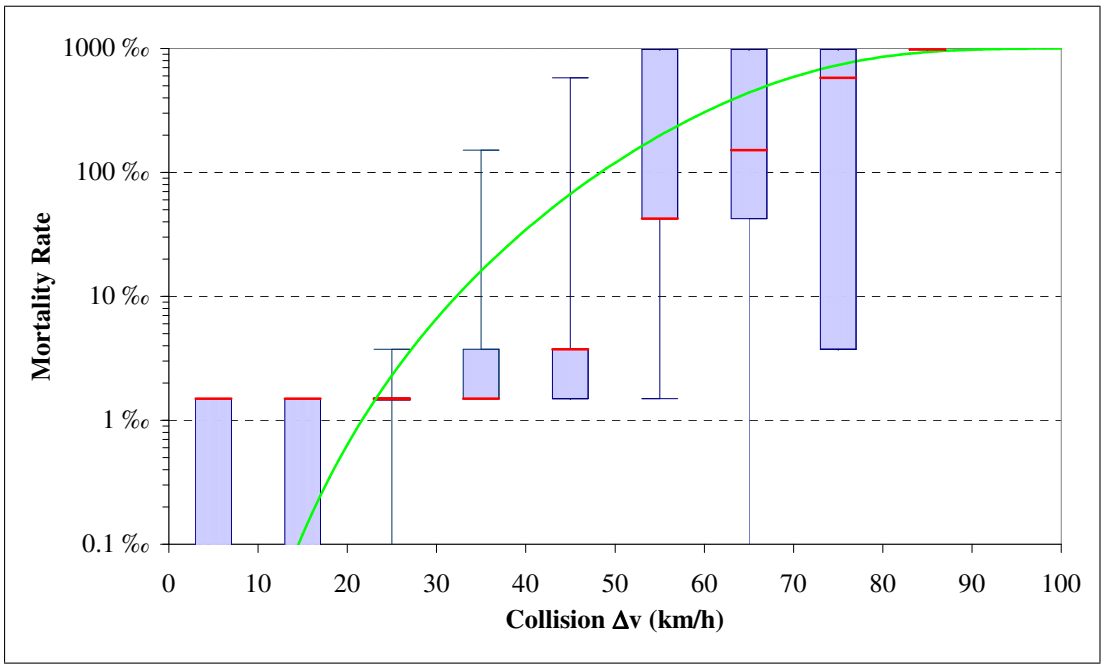

Figure 5.7: Comparison between collision Δv and the degree of injury to belted passenger vehicle occupants involved in front-to-side collisions with other passenger vehicles. The data are limited to struck-side, struck vehicle occupants aged between 16 and 60. They are also limited to collisions where VDI 3 indicates that the passenger compartment is deformed. The date of manufacture of the vehicles is not limited. The box plots show the 10^{th}, 25^{th}, 50^{th}, 75^{th}, and 90^{th} percentiles of the data. The curve is calculated to show the best fit to the data (n = 451, $R^2 \approx 0.343$).

$\Delta v = 48$ km/h experience a 100‰ mortality rate, and those involved in collisions with a $\Delta v = 100$ km/h have a mortality rate approaching 1000‰. A striking vehicle velocity of 48 km/h, which corresponds to a $\Delta v = 27.6$ km/h when the vehicles are equally massive and $C_R = 0.15$ (Huang 2002), represents a 4.1‰ risk of fatality for a belted struck-side occupant.

The results in Figure 5.7 do not provide valid results for a modern vehicle. However, in order to illustrate the compatibility measurement procedure described in Chapter 7, the results in Figure 5.7 are applied. Conclusions based on this procedure can be considered valid after further research is conducted to redefine Figure 5.7.

Chapter summary

This chapter focusses on passenger vehicle side collisions and the injuries experienced by belted passenger vehicle occupants when involved in these collisions. All statements below are made in this context. A degree of bias may be present due to the consolidation of struck-side and non-struck-side occupants, but the separated datasets would be too small to effectively account for this bias, and the consolidated dataset is more representative of the general situation in side collisions.

In Section 5.1.1, it is shown that 47% of side collisions involve another passenger vehicle, which is significantly less than the 57% of frontal collisions that are shown to involve another passenger vehicle in Chapter 4. However, the risk of sustaining a MAIS 2+ injury is significantly higher in a side collision than in a frontal collision. Side collisions involving another passenger vehicle are further analysed in Section 5.1.2, and it is shown that front-to-side collisions occur in 61% of cases and are responsible for 73% of MAIS 2+ injuries. It is therefore concluded that the front-end of the collision partner is of particular interest when considering compatibility.

In Section 5.2.1, front-to-side collisions are analysed with respect to the direction of force and location of damage for both the occupant's vehicle and that of the collision partner. It is concluded that the existing vehicle-to-vehicle test design (front-to-side with perpendicular velocity vectors) is appropriate for the analysis of compatibility.

In Section 5.2.2, collision severity is analysed in front-to-side collisions, and it is shown that there is a positive relationship between the collision Δv and the MAIS injury level sustained by belted occupants. The median velocity at which MAIS 2 injuries occur is $\Delta v = 39$ km/h, but this result is reviewed in Section 5.3, and it is concluded that the mean velocity of $\Delta v = 34$ km/h is more representative of the dataset.

The relative mass of the vehicles involved in front-to-side collisions is anal-

ysed in Section 5.2.3, and it is shown that the drivers of lighter vehicles involved in front-to-side collisions have a higher risk of sustaining a MAIS 2+ injury. The total risk of injury in a front-to-side collision, including the belted drivers of both vehicles, is higher when the vehicles have unequal masses. It is therefore concluded that vehicle mass has an influence on compatibility in front-to-side collisions from both an individual and a societal perspective.

The mortality rates calculated in Chapter 3 for each level of MAIS are applied in Section 5.3 to define a function relating the Δv of front-to-side collisions to the mortality rate of belted struck-side occupants. Hence, it could be found that a Δv of 27.6 km/h corresponds to a 4.1‰ risk of fatality for a belted struck-side occupant. However, the dataset used in Section 5.3 is not limited to vehicles with dates of manufacture between 1996 and 2005 and is hence not considered valid for the analysis of modern vehicles. The results derived from this function, including those in Chapter 9, are presented with the caveat that further research needs to be performed to validate them.

Chapter 6

Definition of a Compatible Vehicle

The objective of this chapter is to define the properties and attributes of a compatible vehicle. To determine these, definitions for 'compatibility' and a 'compatible collision' are also discussed. In the first section, a general definition of compatibility is selected, which acts as a guide for the following sections. In the second section, a definition is proposed for determining whether any particular collision is compatible or incompatible. In reaching this proposal, various alternative viewpoints are also discussed and critically analysed. In the third section, the properties of a compatible collision are discussed, and in the fourth section, the properties of a compatible vehicle are defined.

As shown in Figure 6.1, this chapter begins with the definition of a goal for compatibility, and then describes the factors that contribute to achieving that goal. Hence, the order of this chapter is opposite to the order of causation in the accident environment.

In defining compatibility and a compatible collision, the term 'optimisation' is used extensively with regards to the design of vehicles. In this context, it is assumed that the resources available for allocation to vehicle safety features are limited, and an optimised application of these resources results in a reduced number of injuries and fatalities.

Additional safety benefits may be obtained through the allocation of addi-

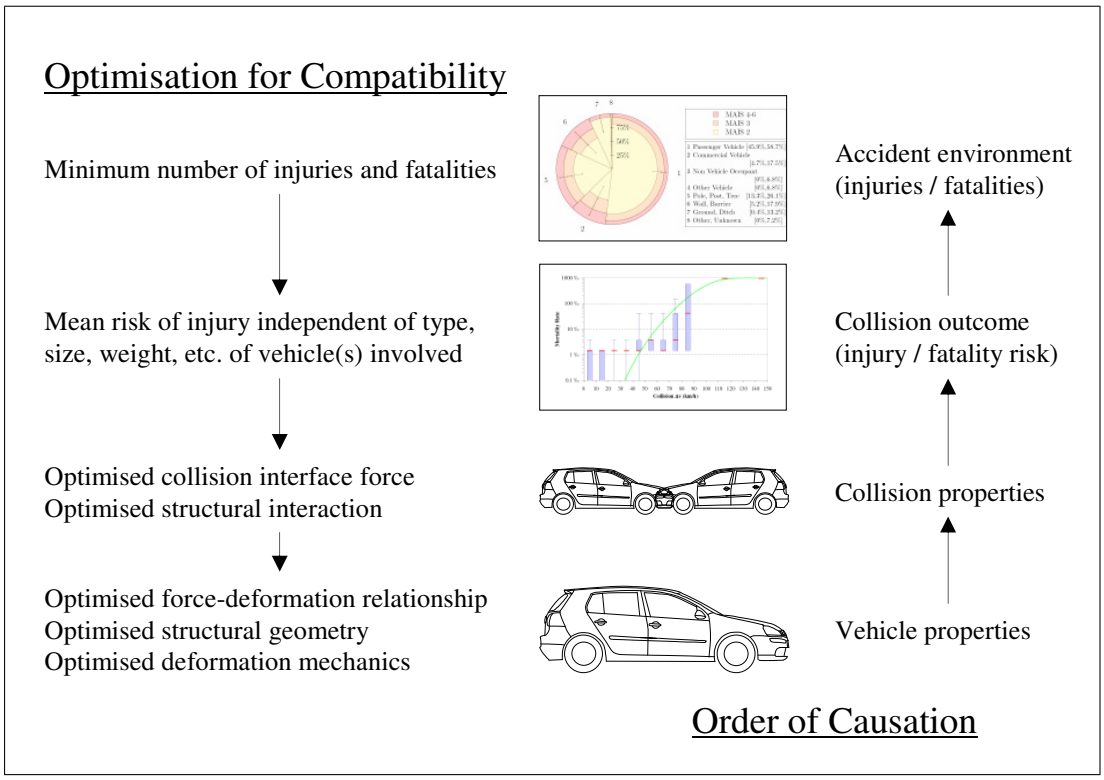

Figure 6.1: Summary of concepts described in Chapter 6.

tional resources, but discussion of this is intentionally avoided. The purpose of this chapter is to address the issue of optimisation, and a discussion of the allocation of additional resources would only raise questions of efficiency. The consideration of efficiency, in terms of cost-benefit analyses, is advocated in the literature (Elvik 2003), and it has even been argued that an excessive and inefficient allocation of resources to traffic safety programs would lead to socio-economic costs that would result in an increase in fatalities (Elvik 1999).[50] Future improvements in compatibility may indeed result in additional costs, but this does not change the ultimate goal, which is to ensure that the costs are optimally invested for maximal societal benefit.

6.1 Definition of compatibility

Many different interpretations of 'compatibility' exist within the field of vehicle safety (see for example van der Sluis 2000, Barbat 2005), and hence it is neces-

[50] For example, money spent on traffic safety programs cannot be spent on preventing disease.

sary to define this principle for the context of this thesis. In its broadest sense, compatibility refers to the ability of two or more things to harmoniously or effectively interact with each other. Although a traffic accident may not seem like an event where one can find harmony, if two vehicles are designed so that their structures interact effectively in the event of a collision, the risk of occupant injury may be reduced. Therefore, a first attempt to define compatibility could be:

> *Vehicle compatibility* is the optimisation of vehicle design to minimise the number of injuries and fatalities that occur in vehicle-to-vehicle collisions.[51]

However, in Chapter 3, it is shown that collisions with other passenger vehicles only account for half of the MAIS 2+ injuries sustained by passenger vehicle occupants. If the optimisation of vehicle designs were to be limited to 'vehicle compatibility', a degradation of safety could occur in other situations, and therefore the total number of injuries and fatalities could increase. This type of goal conflict can be illustrated using the example of the bullbar. If the interaction between a kangaroo and a vehicle were to be considered, the fitment of a bullbar would be justifiable according to the definition that 'kangaroo compatibility' is the optimisation of vehicle design to minimise the number of injuries and fatalities that occur in collisions with kangaroos.[52] However, to focus purely on collisions with kangaroos would be to neglect the negative influence that a bullbar has in collisions with pedestrians and bicyclists, where the protection of both the vehicle occupants and the non vehicle occupants is important. Similarly, to focus purely on 'vehicle compatibility' may encourage some vehicles to reduce their safety in collisions with poles, walls, or heavy vehicles. It is therefore proposed to avoid a focus on 'vehicle compatibility' and instead use a more

[51] Please note that this definition is rejected in the following paragraph and is *not* the definition of 'compatibility' that is referred to in subsequent sections and chapters.

[52] In the case of a collision with a kangaroo, it is assumed that the condition of the kangaroo after the collision is unimportant. Alas, poor Skippy.

general definition that does not encourage the optimisation of vehicle design to a particular collision partner or obstacle, but rather to the accident environment as a whole:

> *Compatibility* is the optimisation of vehicle design to minimise the number of injuries and fatalities that occur in all collisions in the accident environment.

It is important to note that although this definition includes all collision types, including single vehicle accidents, it differs from the traditional definition of vehicle safety because, rather than focussing purely on the protection of a vehicle's own occupants, it also extends to the protection of collision partners.

6.2 Definition of a compatible collision

In this section, the definition of 'compatibility' from above is applied with respect to individual collisions, and various definitions are put forward to describe whether any particular collisions can be considered compatible or incompatible. With the focus on a single collision, the goal to minimise the number of injuries and fatalities can be addressed using three alternative fields of observation: the vehicle, the collision, or the accident environment. In other words, an observer may analyse a collision by considering either the risk of injury in each involved vehicle, the risk of injury in the collision as a whole, or the outcome of the collision in the context of the entire accident environment. Depending on the chosen field of observation, a compatible collision occurs when the design of the involved vehicle(s) results in the minimum risk of injury in either the vehicle, the collision, or the accident environment.[53] A flow chart outlining the approach taken in this section is given in Figure 6.2.

[53]Minimum risk is discussed here with a dependency on the severity of the collision. For a particular vehicle, it should therefore be interpreted as the minimum risk of injury measured across all collision severities and weighted according to their relative frequencies.

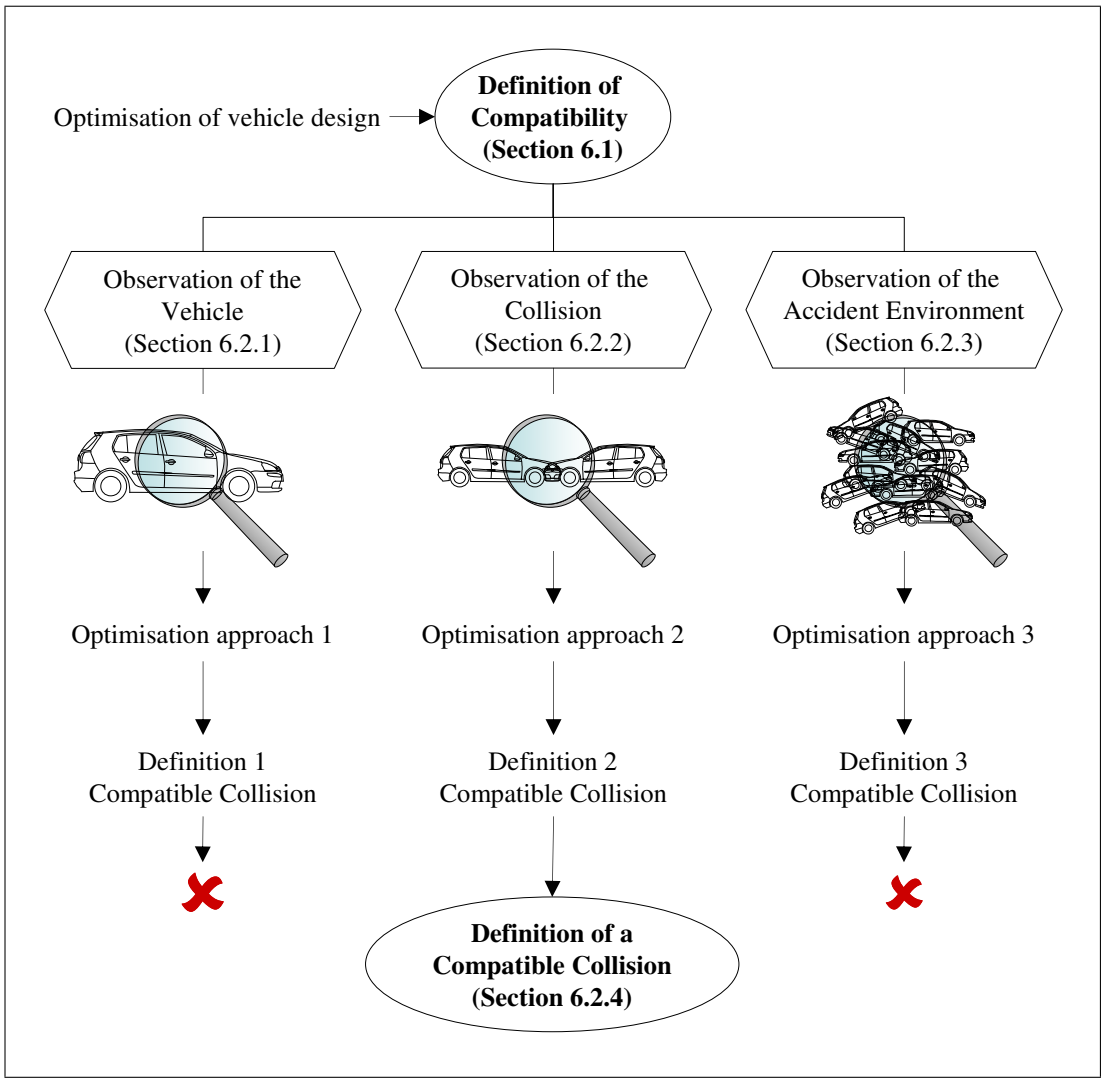

Figure 6.2: Outline of the approach used in Section 6.2 to determine the most appropriate definition of a compatible collision.

6.2.1 Observation of the vehicle

If an individual vehicle is observed, the outcome of a collision can only be considered compatible if the occupants of the vehicle experience some minimum risk of injury. If a different vehicle were to be involved in an identical collision, the outcome would again only be considered compatible if the occupants of the second vehicle experienced the same minimum risk of injury as the occupants of the first vehicle. Applying this approach to an entire fleet of vehicles leads to the conclusion that the risk of injury in a compatible collision is independent of the vehicle being occupied.

Vehicle design regulations, which demand that all vehicles provide a minimum level of occupant protection in a collision with a wall or barrier, have led to the design of a vehicle fleet where there is a similar risk of injury in any vehicle involved in a single vehicle collision. For example, Chauvel et al. (2009) showed that the severity of injuries sustained in single vehicle collisions is similar across all classes of vehicle mass. In the current accident environment, single vehicle collisions can therefore be considered compatible. Designing vehicles to achieve this goal is relatively straightforward, since the optimisation of a particular vehicle's design only affects the protection of its own occupants. However, in a collision between two passenger vehicles, the design of both vehicles affects the risk of injury to both vehicles' occupants.

In the case of a front-to-front collision between two passenger vehicles, the collision is fundamentally identical for both vehicles.[54] Therefore, expanding on the conclusion above, the vehicle-to-vehicle collision would be compatible if the risk of injury were to be the same for the occupants of each vehicle, irrespective of the size, mass, type, or any other properties of either vehicle. This therefore leads to the more general definition that the risk of injury in a compatible collision is independent of all of the vehicles that are involved. Hence, this would require, for example, identical risks of injury in a collision between a minicar and a large SUV. In Figures 4.5a and 5.5a, it is shown that front-to-front and front-to-side collisions in the current vehicle fleet can be considered incompatible from this perspective.

6.2.2 Observation of the collision

If an individual collision is observed, its total severity can be represented by the mean risk of injury experienced by all involved persons. For single vehicle collisions, observation of the vehicle and observation of the collision are hence

[54] In a collision between two vehicles with unequal masses, the Δv of each vehicle is different. However, this is a product of the vehicles themselves rather than the collision. Since the approach velocity is the same for both vehicles, the initial conditions of the collision are considered identical.

equivalent. However, for vehicle-to-vehicle collisions, the risks of injury in each vehicle are combined and not assessed independently. For example, if two vehicles were to collide, with the driver of one of the vehicles experiencing a 25% risk of injury and the driver of the other vehicle experiencing a 75% risk of injury, then the mean risk of injury for the collision would be 50%. When observing another collision, where the drivers of both vehicles experience a 50% risk of injury, the outcome would be considered identical. According to this approach, a vehicle-to-vehicle collision is hence considered compatible if the mean risk of injury is at some minimum level, irrespective of differences in the risk of injury to each individual. Expanding this to an entire fleet of vehicles leads to the definition that the mean risk of injury in a compatible collision is independent of the vehicles that are involved.[55]

As discussed in Section 6.2.1, regulatory tests have achieved this independence for single vehicle collisions. Furthermore, the data in Figure 4.5b show that the mean risk of injury in front-to-front collisions between two passenger vehicles is independent of the their mass ratio, and hence, at least with respect to vehicles' mass ratios, front-to-front collisions are also compatible. The data in Figure 5.5b show that front-to-side collisions are currently incompatible, since the mean risk of injury is dependent on the involved vehicles' mass ratios.

6.2.3 Observation of the accident environment

If the entire accident environment is observed, the outcome of a single collision must be considered in the context of all other collisions, and a compatible collision is one that occurs when the fleet is optimised to achieve the minimum overall risk of injury to all persons. In this context, an increased risk of injury in a particular vehicle or in a particular collision may actually correspond to an improvement

[55]In other words, for a particular collision configuration and collision severity, a compatible collision occurs when the mean risk of injury is at some minimum value. This value is independent of the vehicles involved, so, for example, the mean risk of injury in a collision between a minicar and a SUV should be the same as the mean risk of injury in a collision between two mid-sized cars.

in compatibility. In contrast to the previous two sections, it must therefore be assumed that the risk of injury in a compatible collision is dependent on the vehicles involved.

For example, consider a hypothetical vehicle fleet consisting of minicars and large SUVs and an accident environment consisting of vehicle-to-wall and vehicle-to-vehicle collisions as described in Table 6.1. For this fleet, 'Scenario 1' represents a design where the collisions are compatible according to the definition from Section 6.2.2, and the mean risk of injury in the accident environment is 50%. 'Scenario 2' is an alternative design where more is invested in the protection of the minicar drivers and less in the protection of the SUV drivers. Under these circumstances, the collisions would be considered incompatible according to the definitions from both Section 6.2.1 and Section 6.2.2. However, the mean risk of injury in the accident environment is reduced to 48%, which represents a clear improvement according to the original definition of compatibility from Section 6.1.

Table 6.1: Model showing two optimisation points for a simple vehicle fleet.

Accident environment		**Scenario 1**	**Scenario 2**
Collision	**Frequency**[a]	**Risk of injury**	**Risk of injury**[b]
Minicar-to-wall	5	50%	45%
SUV-to-wall	3	50%	55%
Minicar-to-minicar	8	50% ; 50%	45% ; 45%
SUV-to-SUV	2	50% ; 50%	55% ; 55%
SUV-to-minicar	8	25% ; 75%	30% ; 70%
Mean risk of injury		**50%**	**48%**

[a] The frequencies are representative of a vehicle fleet in which minicars are twice as frequent as SUVs and an accident environment in which vehicle-to-vehicle collisions are twice as frequent as vehicle-to-wall collisions.

[b] Scenario 2 represents an optimisation point where the the risk of injury in the SUVs is 5% higher than in Scenario 1 and the risk of injury in the minicars is 5% lower. In comparison to a hypothetical 'current' situation, it may be assumed that the risks of injury in both Scenario 1 and Scenario 2 represent a reduction in the risks of injury in all collisions for both minicar and SUV occupants. Therefore, Scenario 2 does not necessarily represent a reduction in the level of protection for SUV occupants: The benefit for the SUV occupants under Scenario 2 is simply not as great.

The problem with this approach is that the composition of the vehicle fleet and the accident environment are dynamic, and hence the optimum design of the fleet will vary over time.[56] Indeed, even the introduction of the optimised vehicles may change the composition of the vehicle fleet to such an extent that they are no longer optimal. Furthermore, in order to define the regulations that enforce the optimisation of the fleet, assumptions must be made about its future composition and that of the accident environment. If these assumptions prove to be false, the result could be an overall reduction in safety. For example, if there were to be an unanticipated increase in the number of SUVs and SUV collisions in the fleet described in Table 6.1, the risks of injury described by Scenario 2 would lead to a worse overall outcome because the SUVs would be 'optimised' to provide less protection. Such an approach is clearly too precarious to be appropriate for vehicle safety policy.

An additional issue is that vehicle fleets and accident environments vary around the world and, even if the global fleet and global accident environment were used to define the optimum, the effect in each individual vehicle market may be positive or negative.[57] The use of a global approach could therefore contradict the 1998 Agreement on Global Technical Regulations (GTRs), which precludes the adoption of GTRs that lower the level of occupant protection in the jurisdiction of any of the contracting parties (UN-ECE 1998, §1.1.4). An alternative would be a market-specific approach, but this too would contradict the goal of harmonised vehicle regulations (UN-ECE 1998, §1.1.6) and may result in vehicle development costs that outweigh the benefits. This does not mean that the goals of vehicle safety and regulatory harmonisation are contradictory, but it does mean that care must be taken when choosing the appropriate point for optimisation.

[56] For example, the increasing adoption of driver assistance systems may affect the composition of the accident environment, and the introduction of alternative propulsion systems may affect the composition of the vehicle fleet.

[57] For example, if the global accident environment were similar to the example shown in Table 6.1, but one country had a higher proportion of SUVs in its domestic fleet, then Scenario 2 would be beneficial on a global scale but detrimental in that country.

6.2.4 Definition of a compatible collision

The definition of compatibility in Section 6.1 is based on the consideration of the entire accident environment, and hence the definition of a compatible collision should ideally also be based on the observation of the entire accident environment. However, a definition has little purpose unless it can be applied and used to guide improvements in vehicle design. As described in Section 6.2.3, a definition based on the observation of the entire accident environment is not sufficiently robust. In contrast, a definition based on the observation of either vehicles or collisions would be immune to changes in the vehicle fleet and accident environment because, in either case, the risk of injury in a particular collision should be independent of the vehicles involved. These two definitions are equivalent for single vehicle collisions, and hence their differences regarding the treatment of vehicle-to-vehicle collisions are discussed below.

For the purpose of the discussion, it is assumed that the frequency, severity, and types of vehicle-to-vehicle collisions that are experienced by any model of vehicle are independent of its type, size, weight, or any other characteristic of its design. Then, for any particular collision type, the collision can be characterised for each vehicle, and it can be assumed that all vehicle types will have the same frequency of that collision, the same collision severities, and the same distribution of collision partners. For example, the two vehicles involved in a front-to-side collision could be classified as having a 'frontal collision with the side of another vehicle' and a 'side collision with the front of another vehicle'. According to the definition of a compatible collision based on the observation of the vehicle, the risks of injury in all 'frontal collisions with the side of another vehicle' should be the same, and the risks of all 'side collisions with the front of another vehicle' should also be the same, irrespective of the vehicles involved.[58] This would therefore imply that the mean risk of injury in all front-to-side collisions would also be the same, hence also satisfying

[58]This risk is relative to the severity of the collision. See also Footnotes 53 and 54.

the definition of a compatible collision based on the observation of the collision.

The logic applied above to the example of a front-to-side collision is equally applicable to all other collisions types, and hence it can be stated that the observation of the vehicle always has a goal that satisfies the observation of the collision. However, as observed with regards to vehicle mass ratios in front-to-front collisions in Figure 4.5, the opposite is not true. The two definitions therefore present alternative goals for achieving an optimum compatibility. Given a hypothetical vehicle fleet optimised according to the observation of the vehicle, many alternative vehicle fleets could be designed to give an equivalent outcome based on the observation of the collision. If any of these alternatives were to be less costly to implement than the original, resources could be reallocated to increase the overall level of safety and hence achieve an increase in compatibility according to the original definition in Section 6.1. This represents a Kaldor-Hicks optimisation rather than a Pareto optimisation, but the goal of maximising societal benefit would nonetheless be achieved.[59]

Mass is one of many characteristics of a vehicle's design, but it is critical for any discussion of compatibility because the occupants of a heavier vehicle have an intrinsic mechanical advantage in a vehicle-to-vehicle collision (Wood 1997). This arises because momentum must always be conserved in a collision, and hence the occupants of a heavier vehicle will always experience a lower Δv than the occupants of a lighter vehicle. There is no theoretical obstacle to the neutralisation of this advantage, but the goal of mass independent injury risks in both single vehicle and vehicle-to-vehicle collisions could only be realised at tremendous expense.[60] Given that the masses of passenger vehicles will remain

[59]The Pareto and Kaldor-Hicks efficiencies are measures of economic efficiency. A Pareto optimisation occurs when at least one person has a benefit and nobody is disadvantaged. A Kaldor-Hicks optimisation occurs when the benefit received by an individual or group exceeds the combined loss experienced by all other individuals or groups (Adler & Posner 2000).

[60]One proposal for achieving this goal is 'stiffness-matching' (see for example Swanson et al. 2003). However, this would necessitate changes such as the lengthening of crumple zones in heavier vehicles, which would ultimately lead to increased weight, cost, fuel consumption, and emissions (O'Brien et al. 2007).

inhomogeneous in the foreseeable future, it is concluded that the observation of the vehicle cannot provide the optimum definition of a compatible collision. The following definition of a compatible collision is therefore proposed based on the observation of the collision:

> When evaluated for all involved persons, the mean risk of injury in a *compatible collision* is independent of the vehicle(s) involved, irrespective of its(their) type, size, weight, or any other design characteristic.

Considered alone, this definition may be misinterpreted to imply that, for example, all collisions would be compatible if there were always a 100% risk of injury. The definition of a compatible collision must therefore always be interpreted within the context of the definition of compatibility. Furthermore, since compatibility refers to the optimisation of vehicle design, the mean risk of injury in a compatible collision should always be equal to the mean risk of injury measured in the equivalent design load cases (i.e. crash tests). The comparison of real or realistic collisions with design load cases is a widely accepted method, which is used in both the development of test procedures and research on vehicle collision performance (see for example Lowne 1994, Thomson et al. 2007, Versmissen et al. 2007, EVC 2009).

The definition may also be misinterpreted to imply that the safety systems in all vehicles should be the same. However, the objective of the definition is that each collision's outcome is independent of the vehicles' designs, and this requires that the safety systems in each vehicle be tailored to its type, size, weight, and other characteristics. Furthermore, the ability for vehicle manufacturers to use different combinations and implementations of safety systems encourages research and development, which may enable long term improvements in the overall level of safety for the entire vehicle fleet.

6.3 Properties of a compatible collision

In the previous section, a compatible collision is defined in terms of its outcome, which is the mean risk of injury to the involved occupants. In this section, the mechanical properties of a vehicle collision are described, and their influence on occupant injury risk is discussed.

The properties discussed in this section are the collision interface force and structural interaction. The published test results, which are discussed in Chapter 2, show that the collision interface force and structural interaction are properties of all collisions; both compatible and incompatible. In order to achieve a compatible outcome, the optimums of both the collision interface force and the degree of structural interaction must be achieved.

6.3.1 Collision interface force

The collision interface force describes the pair of forces that acts on a vehicle and the obstacle or collision partner with which it collides (Edwards et al. 2001*b*), as described by Newton's third law of motion. As a result of these forces, the vehicle is deformed according to its stiffness and decelerated according to its mass. These two events are described by Hooke's law and Newton's second law of motion, respectively. The deformation of the vehicle dissipates kinetic energy, which is dependent on both the vehicle's mass and its velocity. In general terms, deformation continues until the vehicle's kinetic energy is dissipated (Wood & Walsh 2002).

Although the collision interface force is the same for a pair of colliding vehicles, differences in either the masses or stiffnesses lead to differing effects of the collision interface force: A stiffer vehicle deforms less than its collision partner, and a heavier vehicle is less severely decelerated. The collision interface force must be optimised for occupant protection, since higher forces result in higher decelerations but also allow more energy to be dissipated within a given length. Both excessive decelerations and compartment deformation have been

shown to increase the risk of occupant injury (Kullgren 1999, Augenstein et al. 2005, Tencer et al. 2005).

6.3.2 Structural interaction

Structural interaction describes the efficiency with which vehicle structures are deformed during a collision (Thomas 2006). A vehicle's structure consists of multiple load paths, each with multiple modes of deformation. If these load paths are not engaged, or if they are deformed in a sub-optimal failure mode, less energy is dissipated per measure of deformation, and a greater degree of deformation is necessary in order to dissipate the vehicle's kinetic energy (Thomas 2006).

Structural interaction modifies the effective stiffness of a vehicle and hence influences the collision interface force. Reduced structural interaction therefore has the potential to reduce compartment decelerations. However, if it is assumed that a vehicle's restraint system protects the occupant and is designed under conditions of maximal structural interaction, then the effects of a reduction in structural interaction would be marginal. It is therefore always preferable to maximise structural interaction in a collision (Thomas 2006).

Although the homogeneous, linear crush of the vehicle structure that occurs in a laboratory test with a flat, rigid barrier may be considered to represent the effective maximum of structural interaction, other deformation patterns may be equally effective (Zobel 1998). For example, homogeneous, linear crush of the vehicle front-end results in some load paths being completely crushed before others. Even with a less efficient deformation mode, an inhomogeneous crush pattern may be capable of dissipating an equal quantity of energy if the other load paths are engaged to a greater degree. Zobel therefore criticised the focus on what he described as "crash-esthetics" (Zobel 1998, p729), which may be theoretically correct but practically irrelevant.

6.4 Properties of a compatible vehicle

In the previous section, the mechanical properties of a vehicle collision are described. This section describes the influence that a vehicle's design has on the properties of a collision. Since the properties of a collision influence its outcome, which can be evaluated as being compatible or incompatible according to the definition in Section 6.2.4, this section describes the physical characteristics of vehicle designs that can be optimised to achieve compatibility.

Based on the literature in Chapter 2 and the discussion of collision properties in the previous section, there are three vehicle design properties that significantly influence compatibility: the general relationship between force and deformation, the geometry of the vehicle structure, and the mechanics of the vehicle's load paths.

6.4.1 Force-deformation relationship

The relationship between force and deformation may be referred to as stiffness, but this can be misleading for an analysis of injury risk, which is attributable to compartment intrusions and decelerations but has no direct link to the gradient of a force-deformation curve. Due to the high risk of injury caused by compartment deformation (Augenstein et al. 2005, Tencer et al. 2005), the relationship between force and deformation is often discussed separately for the crumple zone and the passenger compartment. For example, Edwards et al. (2007*b*) described these as 'frontal force levels' and 'compartment strength' in the context of frontal collisions. However, in the context of a compatible collision, as defined in Section 6.2.4, the outcome may be considered optimal even if the risk of injury in each of the two colliding vehicles is different. This implies that the degree of deformation of the vehicles may also be different, and it is therefore appropriate to consider a continuous relationship between force and deformation that extends between the crumple zone and passenger compartment.

For single vehicle collisions, the force-deformation relationship presents a

relatively simple optimisation to minimise occupant loadings. This optimisation is dependent on the vehicle mass, the depth of the crumple zone, and the severity of the collision, and it must also consider the optimisation of the restraint system. To ensure the maximum dissipation of energy in the crumple zone, the deformation forces should be maximised within the limits designated by the maximum decelerations that can be safely managed by the restraint system. If the kinetic energy of the collision is high enough to exhaust the dissipation potential of the crumple zone and hence cause deformation of the passenger compartment, there will be an acute risk of injury to the occupants. Higher deformation forces are therefore preferable in the passenger compartment, since this minimises the degree of deformation required to dissipate the remaining kinetic energy. An optimised vehicle design is therefore characterised by moderate force levels in the crumple zone and high force levels in the passenger compartment.

For vehicle-to-vehicle collisions, differences in the force-deformation relationships must be balanced so that the deformations and accelerations in each vehicle still result in a compatible collision. Hence, in a severe collision where one of the vehicles has an inherent advantage,[61] it is essential that the forces required to deform the crumple zone of the vehicle in the advantageous position are not higher than the forces required to deform the passenger compartment of the vehicle in the disadvantageous position. This relationship between crumple zone and compartment deformation forces was described by Zobel (1998) as the 'bulkhead principle'.

The benefit that could be achieved by increasing the force levels in the crumple zones of lighter vehicles is limited by the need to also manage these forces in less severe collisions. The further optimisation of the force-deformation relationship for vehicle-to-vehicle collisions would therefore need to take into consideration the force-deformation characteristics of all possible collision partners as well as the relative risk of injury in each vehicle.

[61] For example, in a collision between a heavier and a lighter vehicle or in a front-to-side collision.

6.4.2 Vehicle structural geometry and mechanics

The geometry and deformation mechanics of a vehicle structure are critical for ensuring that structural interaction occurs. The geometry of the structure should encourage initial alignment of the load paths, and the deformation mechanics of the structure should encourage the engagement of the load paths over the duration of the collision.

To ensure that good structural interaction occurs in the broadest possible spectrum of collisions, 'interaction zones' have been proposed, within which passenger vehicle structures should interact with collision partners and other important obstacles such as roadside barriers and truck under-run protection. For example, the IHRA Phase 1 Compatibility Test Procedure includes a 'common interaction zone' between a height of 330 mm and 580 mm, and the AutoAlliance Commitment on Enhancing Vehicle-to-Vehicle Crash Compatibility requires alignment of vehicle structures within the 'Bumper Zone' between a height of 16" to 20" (O'Reilly 2005, Barbat 2005). According to this principal, vehicles should be designed so that the optimal deformation of the vehicle's structures occurs when collision forces are applied to the vehicle within the interaction zone. Critical for achieving this goal are both the geometrical alignment of deformable structures with the interaction zone and their ability to continue to react forces even under dynamic loading and deformation.

Several open questions remain with regards to the optimisation of vehicle structural geometry and mechanics, and even a definition of the ideal conditions remains elusive. For example, it has been argued that a large vertical range for the interaction zone would benefit collision mechanics (Thomson et al. 2007), but also that a correctly located narrow vertical range would benefit structural alignment (O'Brien et al. 2007). The extent to which a vehicle's structure should be homogeneous, the degree with which structures should overlap the interaction zone, and the proportion of a vehicle's collision forces that should be reacted within the interaction zone are also issues for which no optimum is defined.

Chapter summary

Vehicle properties affect collision properties, which affect the outcomes of the collision, which contribute to make up the accident environment. However, as shown schematically in Figure 6.1, these issues are described in the opposite order in this chapter because it is focussed on motivating the optimisation of vehicle design.

In Section 6.1, a definition of compatibility is proposed that consideres not only vehicle-to-vehicle collisions but also collisions with other obstacles and collision partners. The definition also takes into consideration the risk of injury to all road users:

> *Compatibility* is the optimisation of vehicle design to minimise the number of injuries and fatalities that occur in all collisions in the accident environment.

In Section 6.2, a definition for a compatible collision is proposed by considering the collision as a single event. As such, the mean risk of injury in the collision is taken as the critical measure, rather than the risks of injury in each individual vehicle:

> When evaluated for all involved persons, the mean risk of injury in a *compatible collision* is independent of the vehicle(s) involved, irrespective of its(their) type, size, weight, or any other design characteristic.

In Section 6.3, the properties of a compatible collision are described in terms of the collision interface force and structural interaction. Finally, in Section 6.4, the properties of a compatible vehicle are described in terms of structural geometry, deformation mechanics, and the relationship between force and deformation.

Chapter 7

Measurement of compatibility

Various approaches have been proposed and used to analyse vehicle-to-vehicle collisions in other publications and research projects, but robustness issues tend to limit their applicable scope. The purpose of this chapter is to define a robust procedure to determine if the definition of a 'compatible collision' from Chapter 6 is satisfied. In order to evaluate the outcome of the simulations that are described in later chapters, a procedure is described that is applicable to different collision configurations and different combinations of vehicles. Furthermore, it is designed to filter out the localised effects that may arise in a parametric study but do not necessarily represent a change in safety.

In the first section of the chapter, various tools that are used to estimate injury risk in a collision are discussed and compared. In the second section, procedures to assess both front-to-front and front-to-side compatibility are proposed, and their application to vehicle-to-vehicle collision simulations is demonstrated.

7.1 Tools for measuring compatibility

In Chapter 6, the critical measure for assessing a compatible collision is defined as the mean risk of injury for all of the participants in a collision. In this section, tools are described that can be used to estimate the risk of injury in an individual

vehicle. It is relatively straightforward to average the results from individual vehicles to determine the collision mean. The tools range from direct estimations of biomechanic loadings with an ATD to abstract forms of measurement using vehicle accelerations, forces, deformation, and energy.

7.1.1 Anthropomorphic Test Devices

The most direct way to assess occupant injury risk in a collision is with an ATD, which is also known as a crash test dummy. The forces, moments, accelerations, and displacements measured by an ATD can be used to calculate the risk of injury to individual body parts and therefore for a collision as a whole. Since ATDs can be used in any vehicle, their measurements are able to compare different collisions without ambiguity.

However, this strength of an ATD is also a weakness: An ATD provides an exact assessment of the events that occur in a particular collision, and these events cannot necessarily be generalised. An ATD assesses a vehicle as an entire system and is sensitive to the behaviour of all its components. This is appropriate in a regulatory test, where a vehicle has been designed to meet specific performance criteria, but inappropriate for research applications, where the general behaviour of the vehicle is under investigation. In the latter case, the behaviour of a particular component may be trivial in the context of the research program, but it may also have a substantial influence on the ATD results. Two such examples from international research projects are given below.

In 2006, a pair of crash tests was performed by the EVC to compare the effects of vertical alignment between passenger car and LTV structures (Verma 2007). A significant but unexpected outcome of these tests was that the passenger car's airbags deployed differently in the two tests and hence provided different levels of restraint to the ATDs. As a consequence, the results were ambiguous because the effect of the vehicles' structures could not be distinguished from that of the restraint system. Although the ATD measurements clearly showed which

of the two collisions represented a higher risk of injury, it was unclear whether the result could be attributed to the structural alignment or just the restraint system behaviour.

A similar degree of ambiguity arose in the test results for one of the vehicles used extensively by the VC-Compat project. Due to the failure of the driver and passenger seat rails in some of the tests, the ATD measures varied substantially and did not correlate with the structural performance of the vehicle. Consequently, although the ATD measures were able to indicate the increased risk of injury as a result of the seat rail failures, they were not relevant for the analysis of front-end geometry and forces, which was the true purpose of the test series (Davies et al. 2006). In significant reports on the vehicle-to-vehicle tests performed in the VC-Compat project (see for example Faerber et al. 2007, Thomson & Edwards 2005) ATD measures have been completely omitted, and the authors have focussed exclusively on indirect measures of injury risk such as deformation and the compartment deceleration pulse.

Given the potential ambiguity in research results derived from ATDs, it is concluded that an indirect assessment of a vehicle's occupant protection would be a more robust approach.

7.1.2 Dynamic point measurement

The dynamic measurement of a point on the vehicle structure is typically performed using either an accelerometer or a film-based measurement of displacement. In either case, simple mathematical calculations enable the determination of accelerations, velocities, and displacements, and, if the measurement point can be treated as a lumped mass, forces and work can also be determined.

The analysis of accelerations is broadly used in both design and research (see for example Subramaniam et al. 2007, Schram 2008), but the application to the latter is limited by the interdependent effect that compartment accelerations and restraint system design have on the risk of occupant injury. Since a vehicle's

restraint system could be optimised to manage a range of compartment accelerations, the measurement of compartment acceleration alone does not provide a reliable and repeatable estimate of occupant injury risk.

Force is the product of acceleration and mass, and hence a force based analysis is also dependent on the performance of the restraint system. A force based assessment of frontal compatibility was proposed by Schwarz (2002), but it encouraged higher force levels in lighter vehicles and would have hence only functioned if the performance of these vehicles' restraint systems was also increased.

By measuring the accelerations of two separate points in a vehicle structure, the A-pillar and the B-pillar, Thomas (2006) proposed a method to calculate the quantity of energy dissipated in the passenger compartment. Thomas showed that this approach could be used to optimise structural interaction in an offset front-to-front collision between two identical vehicles, but significant errors were identified in collisions between different vehicle types. Attempts to adapt Thomas' method to a more general set of conditions have shown that an increase in its scope is impracticable.

To be applicable to a wide range of vehicles and collision types, analysis of Thomas' method has shown that an approach based on dynamic point measurement needs to be robust regarding motion in all six degrees of freedom. This greatly exceeds the complexity of the single degree of freedom analyses described above, especially when the measurement points are located on deforming structures.

7.1.3 Static point measurement

In contrast to the dynamic measures described in the previous section, static measures provide less detail but are much more robust. The objective of a static measurement of the structure is to determine the post collision deformations, and particular focus is directed towards compartment deformations since these

directly influence the risk of occupant injury (Augenstein et al. 2005, Tencer et al. 2005).

A particular advantage of a static measurement approach is that a large number of points can be analysed with relatively low marginal costs. Even the analysis of real world collisions is possible, although the likely absence of exact pre-collision data makes such an assessment subject to errors in the range of the vehicle's manufacturing tolerances.

The major limitation of static measurements is that they cannot include the effect of compartment accelerations on the risk of occupant injury. However, if it is assumed that compartment deformations become the dominant cause of injury under conditions where the compartment is directly loaded, then this limitation becomes irrelevant. It has also been shown that the separate optimisation of vehicle structures and restraint systems is an effective approach to crashworthiness design (Liao et al. 2008), and hence changes to the restraint system could potentially be used to compensate for any increases in compartment accelerations that may occur. Even accounting for these factors though, there remains a possibility that an optimisation based on static measurements would not account for all aspects of crashworthiness. At collision severities where the passenger compartment is not deformed, or in the hypothetical case of a perfectly rigid compartment, static point measurements are meaningless and an alternative must be used.

Based on these factors and the limitations of the ATD and dynamic point measurement approaches, it is concluded that the measurement of compartment deformations is the most appropriate basis for the assessment of a compatible collision.

7.2 Proposed measurement procedure

The method described in this section and its application to the simulations in the following chapters are based on two fundamental assumptions. Firstly, it is as-

sumed that all vehicles currently offer equivalent occupant protection in standard collision configurations dependent on the Δv of the collision. This assumption corresponds to risk curves like those in Figures 4.7 and 5.7 and also reflects the principal of vehicle regulations, which are designed to ensure that all vehicles offer a minimum level of protection at the regulation test speed.

Secondly, it is assumed that compartment deformation is the cause of injury in these collisions. This assumption is supported by numerous studies of injury causation in both front and side collisions (Eigen & Glassbrenner 2003, Augenstein et al. 2005, Tencer et al. 2005, Conroy et al. 2008, Coimbra et al. 2008, Schiff et al. 2008), although other studies also show correlations with factors including collision velocity and accelerations. The second assumption implies that there is a relationship between compartment deformation and injury risk that is dependent on the collision configuration, but, since different vehicles have different restraint systems, it may be unique for each individual vehicle design. Hence, the combination of the first and second assumptions implies that, for each current vehicle design, there is a unique relationship between Δv and compartment deformation.[62] However, in accordance with the first assumption, this relationship only applies to standard collision configurations such as crash tests. In a vehicle-to-vehicle collision, where a vehicle's deformation is dependent on both the collision velocity and the design of the collision partner, only the second assumption remains valid.

To utilise these assumptions, the Equivalent Change in Velocity ($E\Delta v$) is defined as a measure of post-collision compartment deformation. For any given collision, $E\Delta v$ describes a hypothetical Change in Velocity (Δv) that would be required in a vehicle-to-barrier collision in order to cause an equivalent degree of

[62] Wood et al. (2007) investigated the relationship between Δv and the risk of fatality based on the assumption that vehicle deformation is the sole cause of injury. They found that their model underestimated the risk of fatality, and hence concluded that inertial effects are also important. The method described in this chapter differs from the approach of Wood et al. (2007) because it focuses on correlation rather than causation. Hence, deformation is used as a proxy variable that describes both the deformations and inertial effects that arise in the standard collision configurations.

compartment deformation. The $_E\Delta v$ is therefore similar to the Energy Equivalent Speed (EES) and Equivalent Test Speed (ETS) measures that are common in the literature, but it has two significant differences. Firstly, it is based on compartment deformation rather than total vehicle deformation, since the former is more relevant to occupant injury. Secondly, it is based on the collision Δv, since this is the most accurate measure of severity that is available in the accident statistics.

Building upon the two assumptions above and the definitions from Chapter 6, the following procedure is proposed for the measurement of compatibility in a passenger vehicle collision:

1. Measure the compartment deformations for each vehicle involved in a particular collision.
2. Identify a standard test configuration for each vehicle from Step 1 that is representative of the collision that it experienced. For example, for a co-linear front-to-front collision, the FWRB test configuration may be considered representative for both vehicles involved.
3. Collect accident data that are representative of each of the test configurations identified in Step 2. Use these data to define risk curves with respect to the collision Δv.
4. Perform a series of tests using the same vehicle models as those involved in the collision from Step 1. Perform the tests using the configurations identified in Step 2 over a range of test speeds. Measure the compartment deformations after each test and determine a relationship between compartment deformation and collision Δv.
5. Compare the deformations from Step 1 with the relationship from Step 4 to determine the $_E\Delta v$. The $_E\Delta v$ is defined as the Δv in the standard test configuration that would be necessary to deform the vehicle to the same extent as was measured in Step 1.
6. For each vehicle, compare the $_E\Delta v$ values from Step 5 with the correspond-

ing risk curves from Step 3 to estimate the risk for the occupants of each vehicle.

7. Calculate the mean risk for the collision.
8. To form a basis for comparison, calculate a nominal mean risk for the collision from Step 1. The nominal mean risk is based on the principal that the mean risk of injury in a compatible collision should be equal to the mean risk of injury measured in an equivalent design load case (i.e. crash test configuration). Hence:
   (a) Determine the closing velocity for the vehicles in Step 1. In this case, the closing velocity is the relevant measure of collision severity because, unlike Δv, it is independent of the vehicles' mass ratio.
   (b) Using the closing velocity and the test configurations from Step 2, calculate a nominal Δv for each vehicle.
   (c) Using the risk curves from Step 3, calculate nominal risks based on the nominal values of Δv.
   (d) Finally, average these to determine the nominal mean risk.
9. The definition of a compatible collision is satisfied if the calculated mean risk from Step 7 is less than or equal to the nominal mean from Step 8.

The procedure and its application in this thesis are described in further detail in the following sections.[63]

An additional assumption, which is applied in this thesis but is not necessary for the general application of the measurement procedure, is that the relationship between deformation and injury risk remains valid even when minor changes are made to a vehicle's design. This addresses situations in which the modifications to the vehicle either increase or decrease its safety. Such a change would invalidate the first assumption, and hence the use of risk curves based on accident data from the current vehicle fleet would also become invalid. However, contingent on the assumption that the changes are minor and the restraint system is unchanged,

[63] It should be noted that the sections below are arranged thematically and do not follow the precise order of the procedure described above.

the relationship between risk and deformation for an unmodified vehicle may also be applied to a modified vehicle. However, Step 4 in the method described above should always be performed with unmodified vehicles. This provides a relationship between deformation and Δv that is still valid in combination with the relationship between Δv and risk from Step 3.

7.2.1 Collision configurations

This section describes the selection of the collision configurations that are analysed in Chapters 8 and 9. These collisions are hence the inputs to the first step of the compatibility measurement procedure. This section also describes the selection of the accident data that is required for the third step and the calculation of the nominal mean risk that is described in the eighth step.

Although the definition of a compatible collision from Chapter 6 and the compatibility measurement procedure described at the beginning of Section 7.2 may be applied to both vehicle-to-vehicle and single vehicle collisions, the accident analysis in Chapters 4 and 5 shows that front-to-front and front-to-side collisions between passenger vehicles are of primary interest.[64]

In Chapter 4, it is shown that a frontal test configuration with parallel velocity vectors and either 50% or 100% overlap correlates with the accident data, and a collision Δv of approximately 64 km/h is of relevance to occupants that are severely injured. Therefore, as shown in Figure 7.1, front-to-front compatibility is analysed in two test configurations, which both have a closing speed of 112 km/h, since this results in the desired Δv in a collision between identical vehicles with a C_R of 0.15.

In these collision configurations, the relationship between mortality rate and Δv in Figure 4.7 is used as the estimate of risk according to Step 3 of the compatibility measurement procedure. Since these data are based on mortality

[64]In Chapter 4, it is shown that front-to-front collisions are compatible with respect to the vehicles' mass ratios. However, mass ratio is only one aspect of compatibility and the further analysis of front-to-front collisions is still justified.

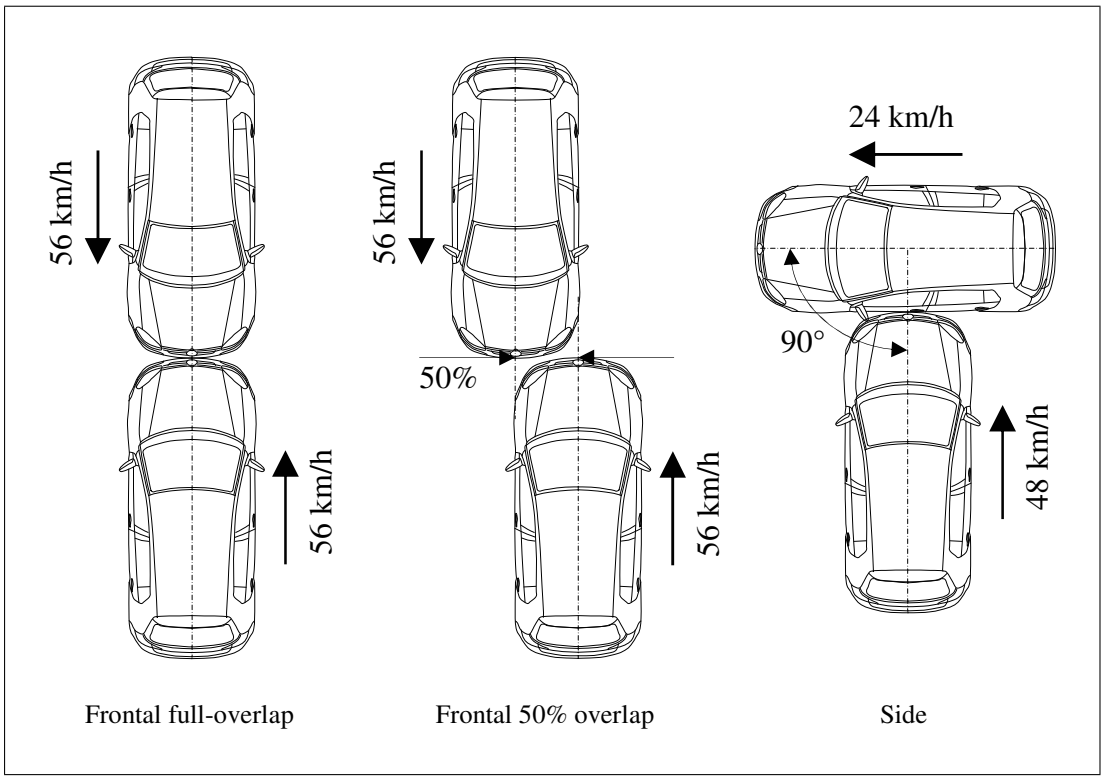

Figure 7.1: Front-to-front and front-to-side configurations used in the analysis of compatible collisions.

rates, the 'mean risks' in Steps 7 and 8d are calculated in terms of a Mean Mortality Rate (MMR). Therefore, assuming a Δv of 64 km/h in two identical vehicles, the nominal MMR in these collision configurations is 20‰.

In Chapter 5, it is shown that a side collision with a direction of force forward of the perpendicular is the most representative of the accident environment, and it is also shown that a collision Δv of 34 km/h is of relevance to occupants with MAIS 2 injuries. These conditions could be achieved with either a crabbed collision, where the struck vehicle is stationary and the striking vehicle collides at an angle, or with a collision in which both vehicles are moving forwards with perpendicular velocity vectors. However, research has shown that a crabbed collision results in reduced loading to the front seat occupants when compared to a perpendicular collision (Newgard et al. 2005). Hence, as shown in Figure 7.1, the configuration with both vehicles moving is used.

The test configuration chosen for the analysis of front-to-side collisions is used extensively in side impact research and continues to be used as the reference

collision for the development of the AE-MDB (Ellway et al. 2006). In this configuration, the struck vehicle has a forwards velocity of 24 km/h, and the striking vehicle has a forwards velocity of 48 km/h. At the initial point of contact, the vehicles are aligned perpendicularly, and the centre-line of the striking vehicle is aligned with the reference point of the front seat in the struck vehicle.

It should be noted that this test configuration does not satisfy the goal of a lateral $\Delta v = 34$ km/h unless the mass ratio of the collision exceeds 1:1.6. Assuming that the colliding vehicles have equal masses and the collision has a C_R of 0.15, then the lateral Δv is 28 km/h. The velocity vectors before and after the collision also indicate a direction of force that is only marginally forward of the perpendicular. However, the chosen configuration and velocities are representative of the current level of design requirements and are hence a relevant point at which to perform the analysis. The simulations performed in Chapter 9 have a mass ratio of 1:1.9, and hence the Δv measured in these collisions is approximately 36 km/h.

In the front-to-side collision configuration, the risk in the vehicle colliding frontally is taken from the relationship between mortality rate and Δv in Figure 4.7, and the risk in the vehicle colliding laterally is taken from the relationship in Figure 5.7. In a collision between identical vehicles, the front and side collisions occur with Δv values of 28 km/h. Hence, the nominal mortality rate in the frontal collision is 0.02‰, and the nominal mortality rate in the side collision is 4.08‰.[65] Consequently, the nominal Mean Mortality Rate (MMR) in this collision configuration is 2.0‰. Although this value is an order of magnitude less than the nominal MMR for the front-to-front collision configuration, as stated above the severity of the front-to-side collision configuration is representative of the current level of design requirements and is hence a relevant point at which to perform the analysis.

[65] At this level of collision severity, the nominal mortality rate in the frontal collision is three orders of magnitude lower than the nominal mortality rate in the side collision. Its influence on the mean mortality rate is hence minimal. For ease of calculation, the analysis of the striking vehicle could be omitted without reducing the accuracy of the result. However, to thoroughly demonstrate the method in this thesis, the frontal deformation data are also presented.

7.2.2 Reference deformation points

This section describes the selection of the deformation measurement points that are used in the first and fourth steps of the compatibility measurement procedure. Although simulation results or data from three-dimensional scanning equipment could be used to measure the deformation of the entire vehicle compartment, such a result is complex to assess, subject to multiple interpretations, and difficult to compare for different vehicle designs. Therefore, the definition of a limited number of intrusion points is a compromise that is both practical and robust.

The measurement points need to be common to all vehicles, simple to locate, reproducible, and relevant to occupant injury. Also, to ensure robustness, they need to cover the broadest possible area in which deformation is likely to occur. To assess the front-to-front and front-to-side collisions that are defined in Figure 7.1, the points shown in Figure 7.2 are used. For the assessment of compartment deformation in the frontal collisions, measurement points are defined on the bulkhead, and for the side collisions they are defined on the B-pillar and doors.

In Figure 7.2a, the instrument panel crossbeam points are relevant for head and chest injuries because deformation here leads to loading of the occupant through the airbag. The A-pillar points are another good indicator of instrument panel displacement and are hence relevant for head, chest, tibia, and pelvis injuries. Deformation of the footrest or footwell crossbeam points leads to direct loading of the occupants' feet, and deformation of EEVC points B1 and B2 leads to direct loading of the occupants' heels.[66] The brake pedal attachment point is a good indicator of pedal displacement, which may also lead to loading of the occupants' lower legs.

In Figure 7.2b, three points are located on the inner skin of each door, which are directly aligned with the chest, abdomen, and pelvis of a 50^{th} percentile male occupant. These points assess direct loading of the occupant. An additional point is defined on each door and, similar to the approach taken by Abe et al. (2005),

[66] The 'EEVC points' shown in Figure 7.2a are defined in Euro NCAP (2003).

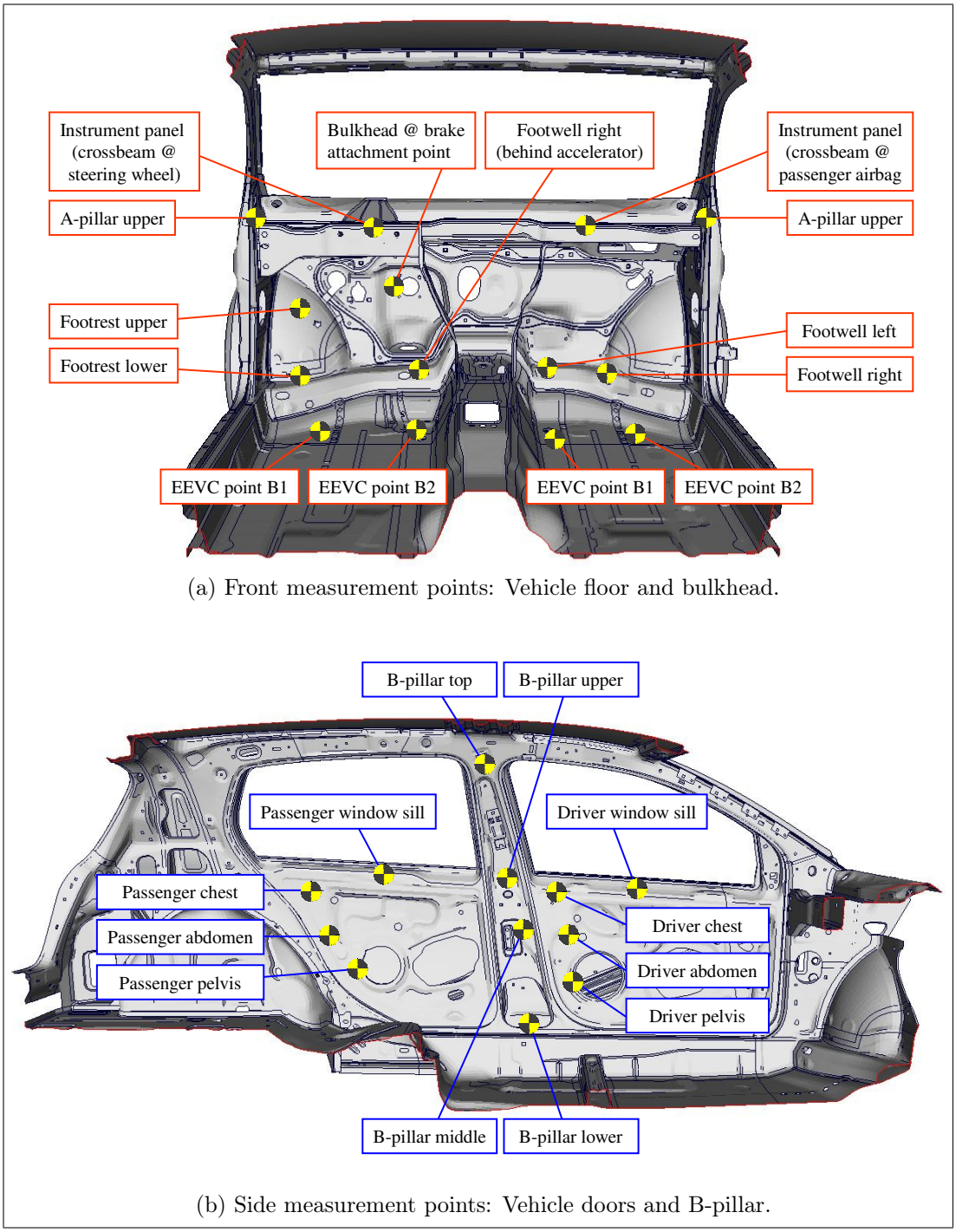

(a) Front measurement points: Vehicle floor and bulkhead.

(b) Side measurement points: Vehicle doors and B-pillar.

Figure 7.2: View of a passenger vehicle structure showing the deformation measurement points for the assessment of compatibility in frontal and lateral collisions.

four points are defined on the B-pillar. On each door, the additional point is located in the middle of the door at the window sill. On the B-pillar, the top point is located where the B-pillar is attached to the roof and the lower point is located where it is attached to the sill. The upper point is aligned with the window sill and the middle point is located approximately half way between the upper and lower points. These additional points increase the area of assessment and are placed in locations that should be easy to identify in almost all vehicle designs. They are also relevant to occupant injury risk in a broad range of collisions, even though they do not align perfectly with a standard seating position.

In the event that a 2-door vehicle is tested, the rear passenger door points could be replaced with measurement points on the panel between the B-pillar and C-pillar. However, this configuration is not investigated in this thesis.

7.2.3 Reference deformation data

This section describes the selection of standard test configurations according to the second step of the compatibility measurement procedure and the generation of reference deformation data according to the fourth step. Simulations in this thesis are performed with models of a mid-sized passenger car and a large SUV, and hence reference deformation data are required for each vehicle in each of the collision configurations defined in Section 7.2.1. The vehicle models used for the simulations are validated with respect to both front and side crash tests, but their construction is not a component of this thesis.

For the 50% overlap front-to-front collisions, the data are derived from the ECE-R94 test configuration.[67] In Figure 7.3, the results are plotted for simulations performed at 8 km/h intervals. The deformable barrier used in the ECE-R94 test configuration dissipates energy as it deforms, which lowers the effective collision severity for the vehicle. To remove this effect, the Δv values used in Figure 7.3

[67] Although the ECE-R94 test specification requires that the barrier overlaps 40% of the vehicle width, this arrangement was itself determined based on vehicle-to-vehicle reference tests with 50% overlap (Lowne 1994) and is hence considered appropriate.

are reduced to only reflect the proportion of the kinetic energy that is dissipated through vehicle deformation.

For the 100% overlap front-to-front collision configuration, the data are derived from full width rigid barrier collisions. The results are plotted in Figure 7.4 for simulations performed at 8 km/h intervals. In this case, the actual Δv values are used in the denominator, since a rigid barrier does not dissipate energy.

For the front-to-side collision configuration, all simulations in Chapter 9 are performed with the SUV colliding frontally into the side of the passenger car. Hence, the SUV data from Figure 7.4b are again utilised, and additional data are generated for the passenger car using the AE-MDB test configuration.[68] The results are plotted in Figure 7.5 for simulations performed at 5 km/h intervals. Although the AE-MDB has a deformable barrier face that is capable of dissipating energy, a correction is inappropriate for this collision configuration because both the vehicle and the trolley are mobile. Hence, Figure 7.5 is also plotted using the actual Δv values measured in the simulations.

Figures 7.3 and 7.4 show similar results for both vehicles. In both full overlap and offset collisions, insignificant deformation occurs at Δv values up to 40 km/h. This correlates with the results in Figure 4.7, which show that the mortality rate in collisions with a Δv less than 45 km/h is less than 1‰. Hence, although the deformation data cannot provide a reliable estimate of $E\Delta v$ below 40 km/h, this is effectively irrelevant for the calculation of a mortality rate. At velocities greater than 40 km/h, there is a progressive increase in the deformations until an approximately linear relationship between Δv and deformation is observed. In this final stage, the front-end of the vehicle is completely deformed and the compartment is being directly loaded. The data shown in Figures 7.3 and 7.4 are limited to those velocities that are considered relevant to the analysis in Chapters 8 and 9. Hence this final, linear stage of deformation is not shown for all measurement points.

[68] At the time of writing, the AE-MDB v3.9 appears to be the most likely candidate for introduction into regulation, and hence its stiffness characteristics are used.

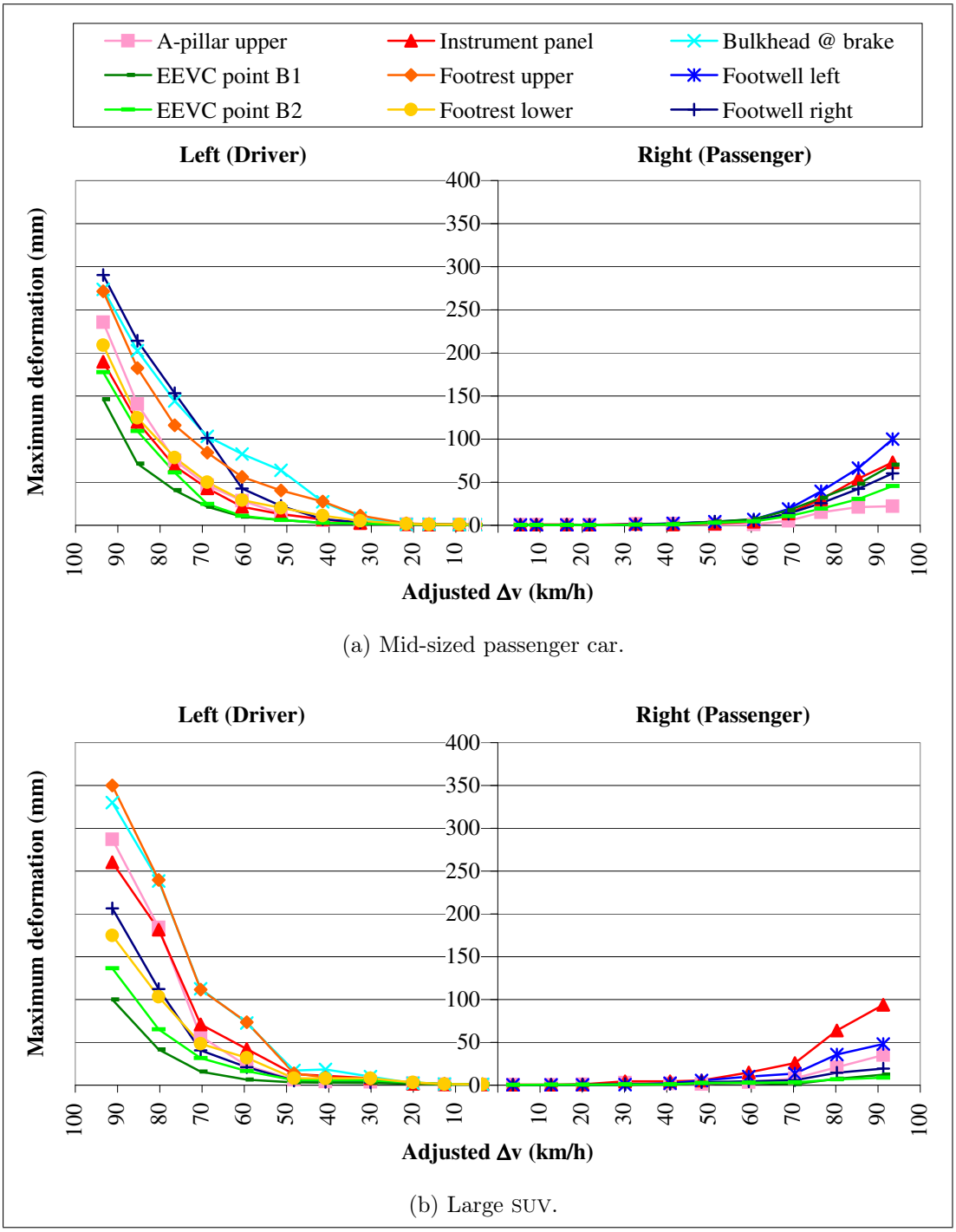

(a) Mid-sized passenger car.

(b) Large SUV.

Figure 7.3: Compartment deformation in frontal vehicle-to-barrier simulations using the ECE-R94 test configuration over a range of test speeds. Adjusted Δv calculated to correct for energy dissipated by ECE-R94 barrier face.

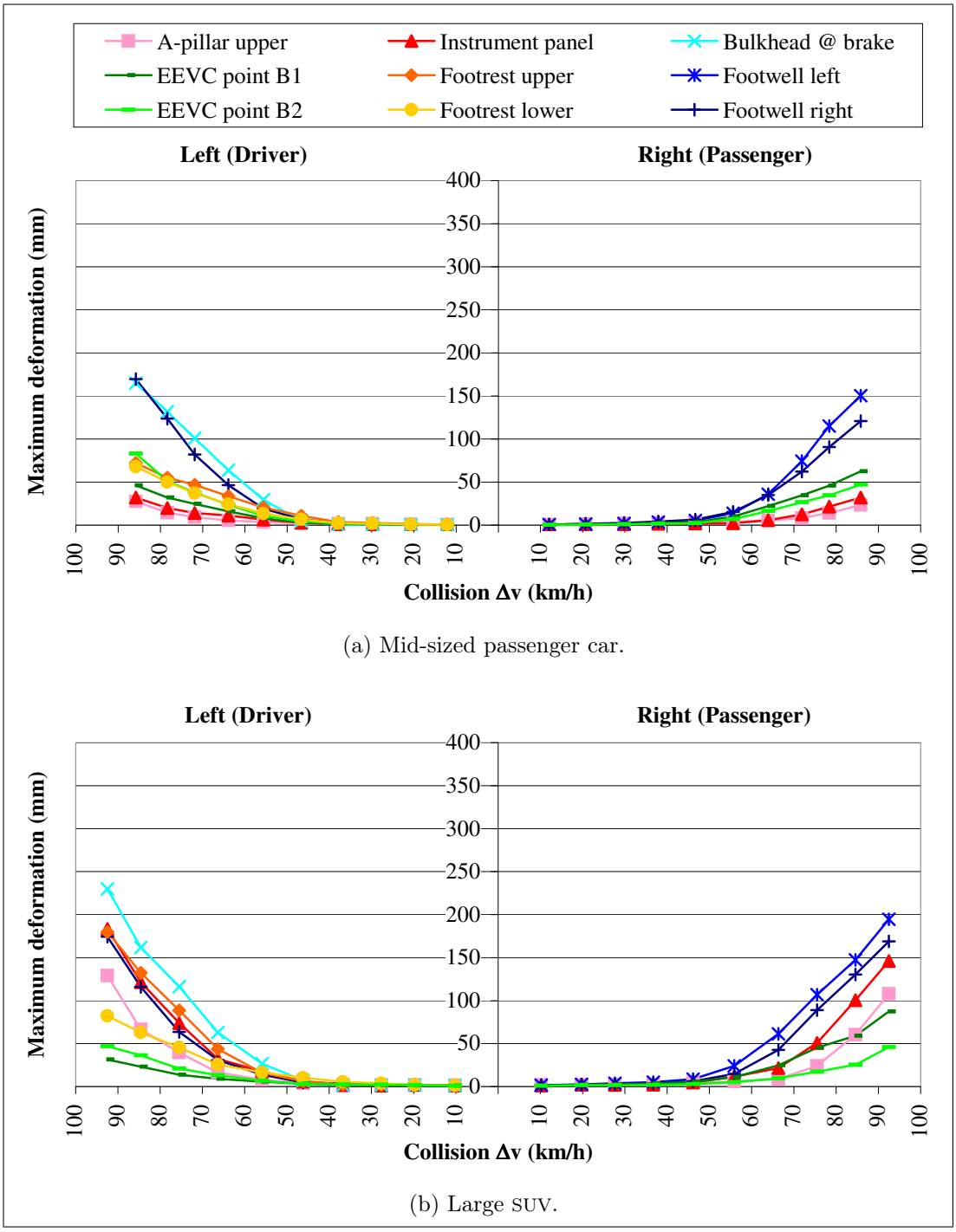

(a) Mid-sized passenger car.

(b) Large SUV.

Figure 7.4: Compartment deformation in frontal vehicle-to-barrier simulations using a full width rigid barrier test configuration over a range of test speeds.

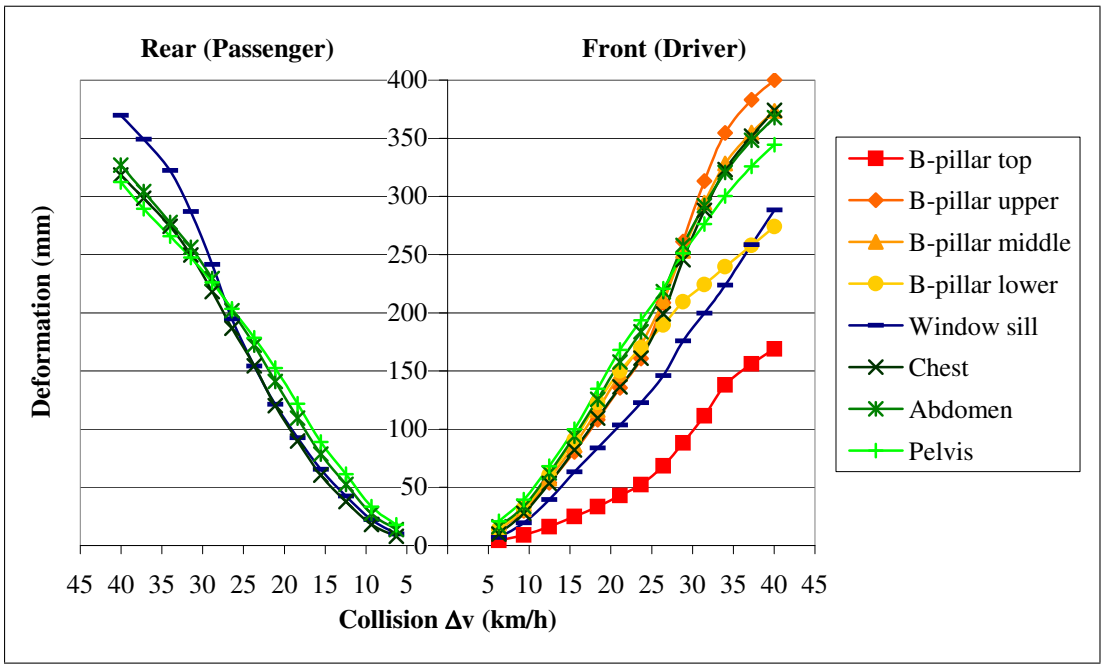

Figure 7.5: Side deformation in a mid-sized passenger car for vehicle-to-barrier simulations over a range of test speeds using the AE-MDB.

Figures 7.3 and 7.4 show generally higher measures of deformation in the SUV than the passenger car, but this does not contradict the assumption that both vehicles offer equivalent levels of occupant protection. For example, the SUV's restraint system may offer more protection against compartment deformations. Also, the extensive differences between the two vehicles mean that there is more absolute distance between the bulkhead and the occupants in the SUV.

A comparison between the driver's side data in Figures 7.3 and 7.4 shows higher measures of deformation in partial overlap collisions, but this does not necessarily invalidate the use of the same risk curve for both collision configurations. Although lower measures of deformation occur in full overlap collisions, these are typically accompanied by more severe compartment accelerations. Research has indicated that the risk of injury in partial overlap and full overlap frontal collisions is different (Stanzel & Page 2006), but the calculation of separate risk curves is not possible using the limited dataset from Section 4.3, and hence the relationship from Figure 4.7 is applied to both configurations.

In Figure 7.3, it can be seen that the deformation of the passenger side of the vehicle is insignificant up to a Δv of approximately 70 km/h. This is due to

the offset nature of the collisions. Although the deformations begin to increase at higher velocities, the test configuration proposed in Section 7.2.1 results in Δv values of approximately 64 km/h. Therefore, the passenger side deformations in offset collisions are of little use for measuring the severity of the collision and are hence omitted from further analysis.[69,70]

In Figure 7.5 it can be seen that the deformation of the vehicle side is generally similar at all of the measurement points. Exceptions are that substantially less deformation occurs at the top of the B-pillar and relatively less deformation occurs at the bottom of the B-pillar at higher speeds. The former is caused by the distance between the top of the B-pillar and the contacting surface of the AE-MDB, and the latter is due to the support afforded by the floorpan of the vehicle. Another notable effect is that there is more deformation at the middle of the rear door than the middle of the front door. In contrast to the data for frontal collisions in Figures 7.3 and 7.4, the deformation of the side structure is observed even at low values of Δv due to the absence of a side crumple zone.

The cost of performing full scale crash tests is prohibitive, and hence the generation of results like those given in Figures 7.3, 7.4, and 7.5 is only practical using simulation. Indeed, even the time and cost of performing the simulations is considerable. The cost of these data is particularly pertinent because the results are only used for reference purposes and are not the primary focus of the research. However, the ODB test procedure is performed at speeds of 40 km/h, 56 km/h, and 64 km/h during certification and consumer testing and could hypothetically be used to generate the data without additional cost.[71] A drawback of these three tests is that they provide a relatively small range of velocities. However, a

[69] In an offset collision, the deformation to the driver's side indicates the severity of the collision, the resulting deceleration of the vehicle, and hence also the risk of injury to the passenger. The driver's side deformations may therefore be considered relevant for both occupants.

[70] Analysis of the 50% overlap collisions in Chapter 8 indicates that the use of passenger side data would actually be valid for the calculation of $_E\Delta v$, but this may not be reproducible for other vehicle designs.

[71] The test specifications for these three tests vary with regards to the required vehicle weight and equipment. Also, because they are performed in different markets, vehicles may be localised to an extent that they cannot be considered equivalent. Comparable, valid results are therefore not currently available.

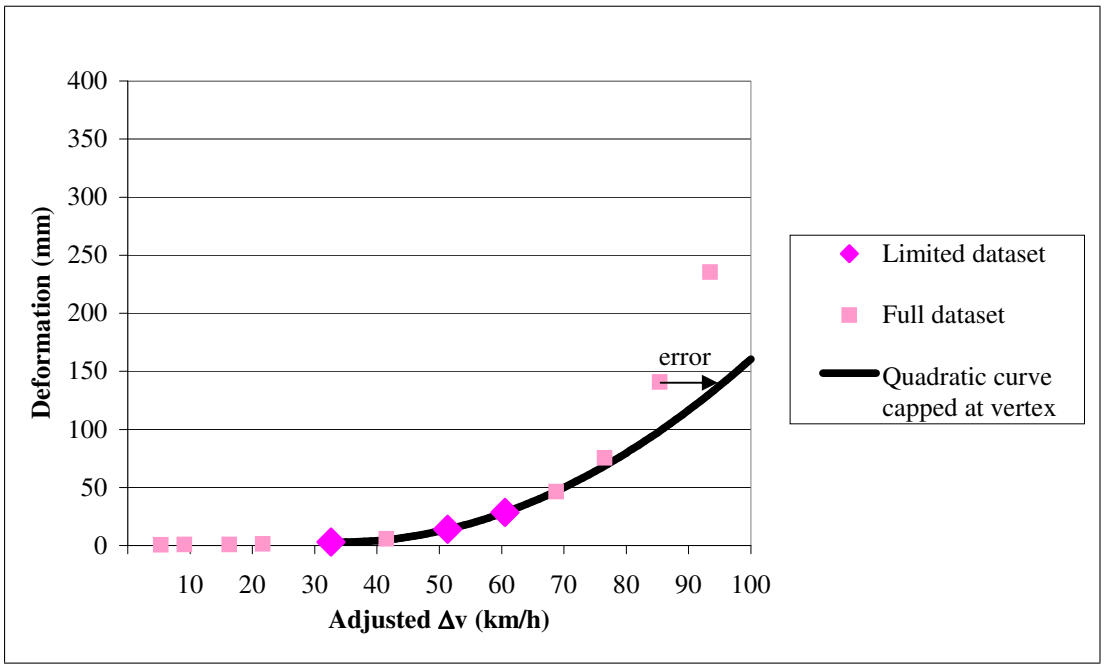

Figure 7.6: Example curve based on deformation data from the 40 km/h, 56 km/h, and 64 km/h vehicle-to-barrier simulations with the mid-sized passenger car in the ECE-R94 test configuration. Adjusted Δv calculated to correct for energy dissipated by ECE-R94 barrier face. Deformations measured at the A-pillar upper point on the driver's side.

broader range of Δv values can be analysed by extrapolating the results. To test whether these data would be valid for the analysis of collisions over a broad range of Δv, quadratic curves can be fitted to the results of the 40 km/h, 56 km/h, and 64 km/h simulations.[72] For example, Figure 7.6 shows the curve calculated for the driver's side A-pillar upper point in the passenger car. To test the validity of this approach, the deformation data from the other simulations can then be used to predict the collision velocities based on the curves. In the example in Figure 7.6, it can be seen that the curve estimates a higher Δv value than that which is actually necessary to cause the 141 mm of deformation to the A-pillar upper point. When assessed for all measurement points, the passenger car curves provide a reasonable degree of accuracy for test speeds up to 80 km/h, with errors in the $E\Delta v$ of up to 16%. However, the SUV curves result in an error of 18% at

[72] Quadratic curves are used for pragmatic reasons: because the results are not linear at these velocities and because a quadratic equation is simple to define based on three points of data. Alternative curves do not achieve a substantial improvement in either the accuracy or the validity of the estimates.

a test speed of 72 km/h and 23% at a test speed of 80 km/h. For both vehicles, estimates cannot be made for test speeds below 40 km/h because the quadratic curves are typically invalid. Although these results do not support the use of extrapolated data beyond the available range of test speeds, further investigation of this approach may be warranted.

In almost all cases, including in this thesis, the analysis must be based on a finite number of reference collisions, and hence a method is required to estimate the relationship between Δv and deformation at intermediate velocities. For this thesis, linear interpolation is applied.[73]

7.2.4 Consolidation of measurement points

The fifth step of the method described at the beginning of Section 7.2 requires the calculation of a single $_E\Delta v$, which can then be converted into a risk in Step 6. However, since the compartment deformation is measured at multiple points, multiple values of $_E\Delta v$ must be calculated. Several approaches for the consolidation of these values are conceivable, including the use of an average, a weighted average, or a maximum. When taking an average, the possibility also exists to first convert the individual values of $_E\Delta v$ into risks, which produce different results because the risk curves are not linear. The weighted averaging of the $_E\Delta v$ values is the most conservative of these approaches, and hence this method is applied using the approach described below.

For both front and side measurement points, weighting is applied to equalise the effect on various body regions. For the front deformation points, the averaging process begins on the drivers side by averaging the results from the upper and lower footrest points to provide a single value for the front of the left foot. Similarly, the accelerator and brake points are averaged for the right foot. These two results are then averaged with the corresponding footwell points to give a

[73] Linear interpolation is used for the pragmatic reason that it is simple and also because the relationship between deformation and Δv does not appear to follow any obvious trends. Neither quadratic nor exponential interpolation are appropriate across the entire range of data.

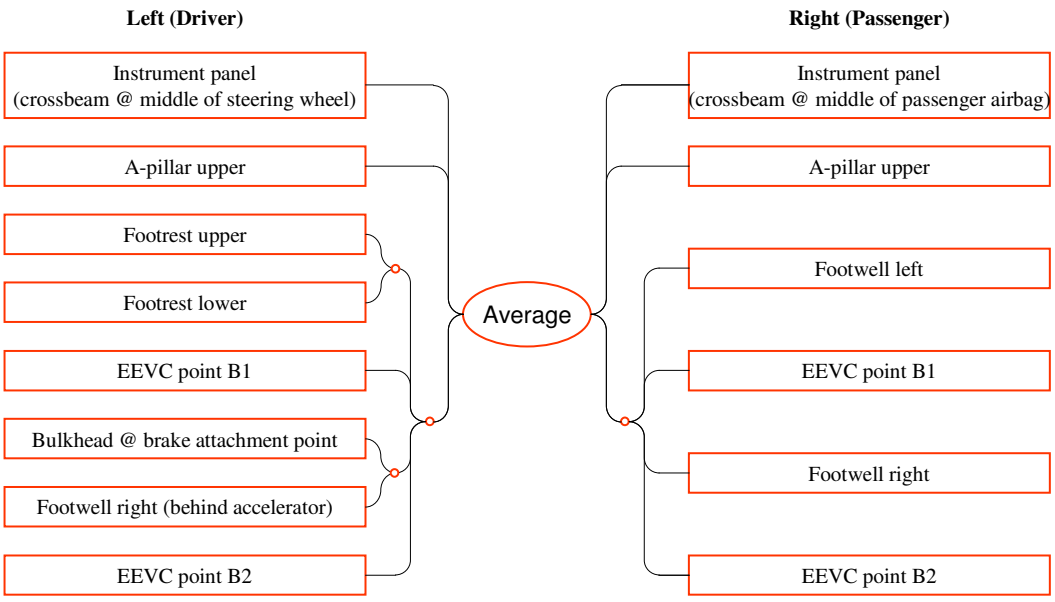

(a) Consolidation of frontal deformation data.

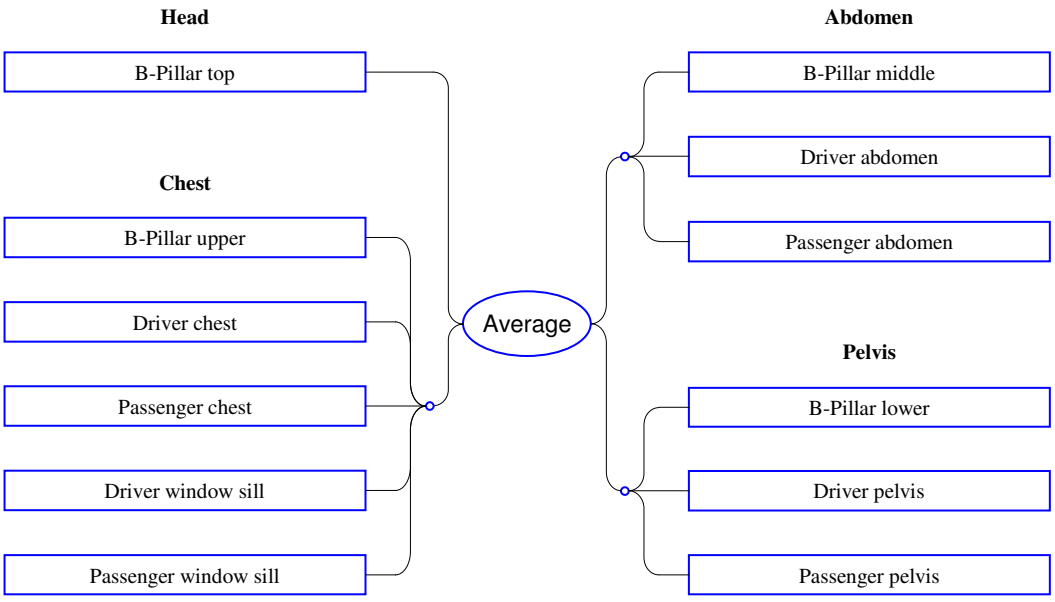

(b) Consolidation of lateral deformation data.

Figure 7.7: Process of averaging $E\Delta v$ values calculated from deformation measurements on the front and side of the passenger compartment.

single value for the driver's feet and lower legs. This value is then averaged with those of the instrument panel crossbeam and A-pillar on the driver's side to give a single value for the driver. On the passenger's side, the process is similar, except that there are only four points for the feet, and these are averaged in a single step.

For the side deformation points, the B-pillar top point is of relevance to head injury and is hence left alone. The B-pillar upper, window sill, and chest points are collected for both the driver and rear passenger due to their relevance to chest injury. The B-pillar middle and abdomen points are collected for their relevance to abdomen injury, and the B-pillar lower and pelvis points are collected for their relevance to pelvis injury. This weighting places more emphasis on the front seating position, since deformation of the B-pillar more directly affects the front seated occupants. However, given the imbalance between front to rear occupancy rates (Cuerden et al. 2007), this is considered desirable.

The two averaging processes are shown schematically in Figure 7.7, with each circle (○ or ○) representing an intermediate point where the values are averaged, and the large 'Average' circles in the centres providing the final, consolidated values of $E\Delta v$.

7.2.5 Example analyses

To demonstrate the compatibility measurement procedure, each of the collision configurations described in Section 7.2.1 is analysed in this section for the mid-sized passenger car and large SUV introduced in Section 7.2.3. Vehicle-to-vehicle crash tests involving this exact combination of vehicles are not available for validation purposes, but comparisons with similar collisions involving other mid-sized passenger cars and large SUVs indicate that the results are representative of these types of collisions. In each of the tables below, the values in the 'Mortality rate' row are the results of Step 6 of the compatibility measurement procedure and the value in the 'Mean Mortality Rate' row is the result of Step 7.

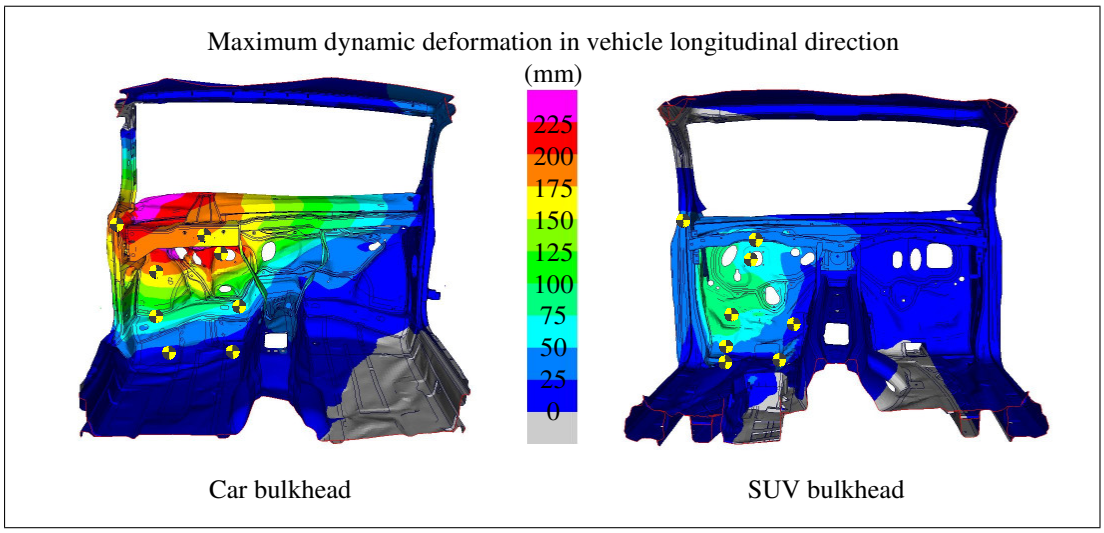

Measurement point	Mid-size car		Large SUV	
	Defo. (mm)	**$E\Delta v$ (km/h)**	**Defo. (mm)**	**$E\Delta v$ (km/h)**
Driver's side:				
Instrument panel crossbeam	183	92	39	58
A-pillar upper	228	92	28	61
Footrest upper	187	85	79	60
Footrest lower	95	79	39	64
Bulkhead at brake attachment	196	84	71	59
Footwell right	69	64	15	55
EEVC point B1	22	68	23	72
EEVC point B2	20	65	28	68
Driver weighted average		85		61
Mortality rate		180‰		13‰
Mean Mortality Rate (MMR)				97‰

Figure 7.8: Deformation profile and measurement point results of a front-to-front collision simulation between a mid-sized passenger car (1470 kg) and a large SUV (2834 kg) with 50% overlap of the car width (1759 mm) and 112 km/h approach speed.

In Figure 7.8, the bulkhead deformations of both vehicles in the 50% offset frontal collision are shown. The nominal Δv of this collision configuration is 64 km/h, and although the $E\Delta v$ of the passenger car exceeds this value by 21 km/h, the $E\Delta v$ of the SUV is only 3 km/h lower. As a consequence, the mean mortality rate in this collision is 4.9 times higher than the nominal mean of 20‰, and it is hence concluded that this collision is incompatible according to Step 9

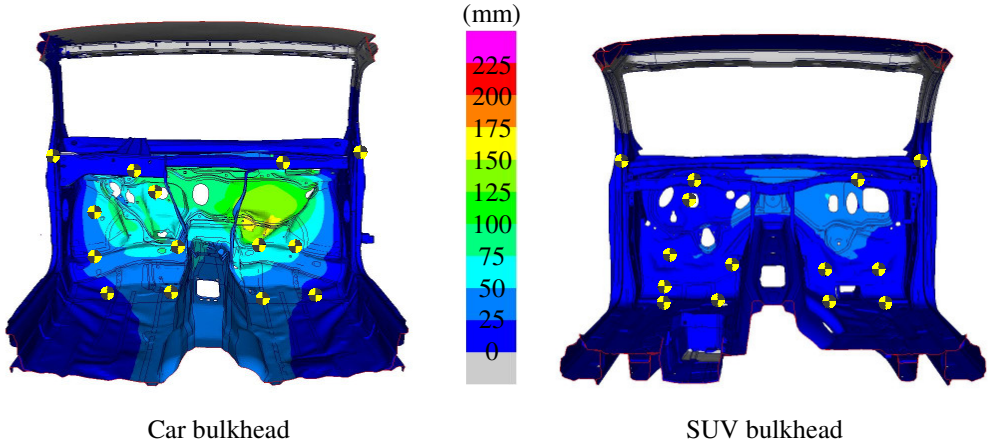

Measurement point	Mid-size car		Large SUV	
	Defo. (mm)	$E\Delta v$ **(km/h)**	**Defo. (mm)**	$E\Delta v$ **(km/h)**
Driver's side:				
Instrument panel crossbeam	14	71	11	51
A-pillar upper	12	74	3	34
Footrest upper	43	69	7	48
Footrest lower	30	67	13	51
Bulkhead at brake attachment	81	67	11	48
Footwell right	56	65	10	52
EEVC point B1	21	69	4	49
EEVC point B2	33	69	5	52
Driver weighted average		71		45
Passenger's side:				
Instrument panel crossbeam	12	71	7	49
A-pillar upper	14	77	4	46
Footwell left	64	69	19	52
Footwell right	55	69	14	54
EEVC point B1	31	69	10	53
EEVC point B2	24	69	4	52
Passenger weighted average		72		49
Vehicle weighted average		72		47
Mortality rate		46‰		1.6‰
Mean Mortality Rate (MMR)				24‰

Figure 7.9: Deformation profile and measurement point results of a front-to-front collision simulation between a mid-sized passenger car (1470 kg) and a large SUV (2834 kg) with 100% overlap and 112 km/h approach speed.

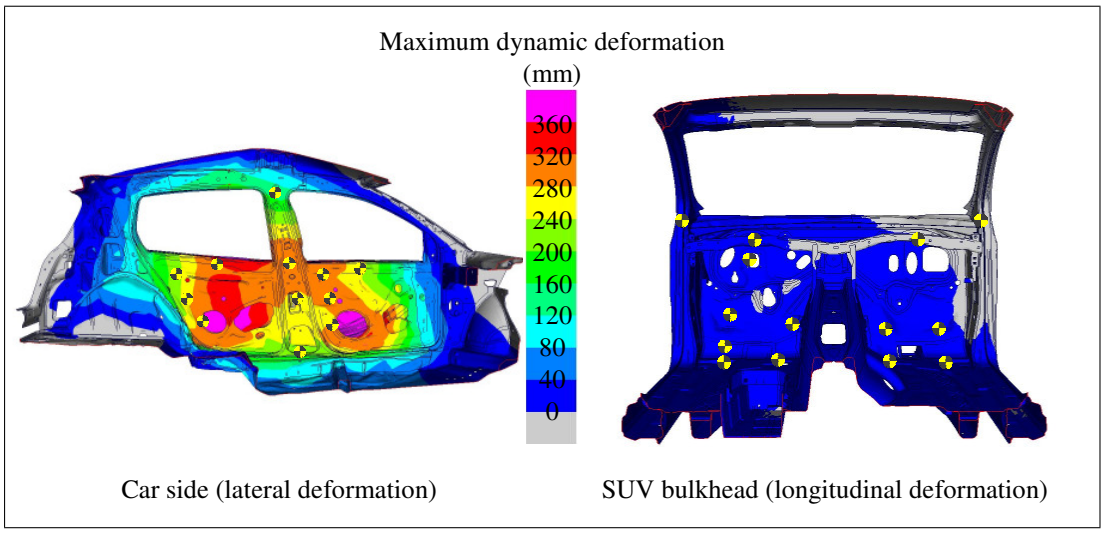

Figure 7.10: Deformation profile of a front-to-side collision between a large SUV (2834 kg, striking vehicle, 48 km/h) and a mid-sized passenger car (1470 kg, struck vehicle, 24 km/h). The locations of the measurement points used in Table 7.1 are shown.

of the compatibility measurement procedure.

The $E\Delta v$ values calculated for the individual measurement points vary over a range from 64 km/h to 92 km/h for the passenger car and 55 km/h to 72 km/h for the SUV. This demonstrates the variability that can arise in the results and the absolute necessity of a large number of measurement points.

In Figure 7.9, the bulkhead deformations of both vehicles in the 100% overlap frontal collision are shown. The nominal Δv of this collision configuration is again 64 km/h, and although the $E\Delta v$ of the passenger car exceeds this value by 8 km/h, the $E\Delta v$ of the SUV is 17 km/h lower. Due to the non-linear form of the function that is used to define the risk curve, the 8 km/h higher $E\Delta v$ of the passenger car leads to a 26‰ increase in the mortality rate of its occupants, and the 17 km/h lower $E\Delta v$ of the SUV leads to a 18‰ decrease in the mortality rate of its occupants. Hence, although the mean $E\Delta v$ is lower than 64 km/h, the mean mortality rate for the collision is 1.2 times higher than the nominal rate of 20‰, and it is again conlcuded that the collision is incompatible.

In Figure 7.10, the deformations of both vehicles in the front-to-side collision are shown. The nominal Δv of this collision is 28 km/h for both vehicles, but

Table 7.1: Measurement point results of a front-to-side collision between a large SUV (2834 kg, striking vehicle, 48 km/h) and a mid-sized passenger car (1470 kg, struck vehicle, 24 km/h).

Measurement point	**Mid-size car**		**Large SUV**	
	Defo. (mm)	$E\Delta v$ **(km/h)**	**Defo. (mm)**	$E\Delta v$ **(km/h)**
Doors and B-pillar:				
B-pillar top	150	36		
B-pillar upper	304	30		
B-pillar middle	273	30		
B-pillar lower	207	28		
Driver window sill	227	34		
Driver chest	293	31		
Driver abdomen	305	32		
Driver pelvis	293	33		
Rear passenger window sill	312	33		
Rear passenger chest	217	28		
Rear passenger abdomen	258	31		
Rear passenger pelvis	293	37		
Side weighted average		33		
Bulkhead on driver's side:				
Instrument panel crossbeam			1	18
A-pillar upper			3	34
Footrest upper			2	16
Footrest lower			2	13
Bulkhead at brake attachment			1	13
Footwell right			2	20
EEVC point B1			1	18
EEVC point B2			2	19
Driver weighted average				23
Bulkhead on passenger's side:				
Instrument panel crossbeam			0	3
A-pillar upper			1	5
Footwell left			3	17
Footwell right			1	9
EEVC point B1			2	15
EEVC point B2			1	8
Passenger weighted average				7
Vehicle weighted average		33		15
Mortality rate		10.9‰		0.0‰
Mean Mortality Rate (MMR)				5.4‰

this equates to a 4.08‰ mortality rate in the side collision and a 0.02‰ mortality rate in the frontal collision. The measurement point results in Table 7.1 show that the $E\Delta v$ experienced in the side collision is 5 km/h higher than the nominal Δv, resulting in a 7‰ increase in the mortality rate. But although the $E\Delta v$ of the SUV is 13 km/h lower than the nominal value, the mortality rate cannot decrease below zero, and hence a maximum reduction of 0.02‰ is achievable.[74] Consequently, although the mean $E\Delta v$ is again observed to be lower than the nominal Δv for the collision configuration, the mean mortality rate is 2.7 times higher than the nominal rate of 2.0‰. It is therefore concluded that this collision is also incompatible.

The three examples presented in this section demonstrate different starting points for an optimisation of compatibility. In the 50% offset frontal collision, a substantial reduction in the $E\Delta v$ of both vehicles is necessary. In the 100% overlap frontal collision, little additional benefit can be achieved by reducing the $E\Delta v$ of the SUV, and hence efforts must be directed towards the passenger car. Finally, in the front-to-side collision, even the nominal Δv presents practically zero risk for the SUV occupants, and hence compatibility can only be achieved in this collision by reducing the car's $E\Delta v$ to the same level as the nominal Δv.

Chapter summary

In Section 7.1, the use of ATDs, dynamic measurement data, and static measurement data are discussed as potential methods to assess the risk of injury in a vehicle collision. It is concluded that the use of deformation data provides the most robust approach.

In Section 7.2, a procedure to test the definition of a compatible collision is introduced. The essence of this procedure is the comparison of compartment deformation data from the collision of interest with data from a series of reference

[74] This outcome supports the previous statement in Footnote 65, that the analysis of the striking vehicle could be omitted without reducing the accuracy of the result.

collisions in order to determine an $_E\Delta v$ for each involved vehicle. The $_E\Delta v$ values are then converted to a measure of risk, which is finally used to test the compatibility of the collision. A formal validation of the method is not performed, but the results are considered valid because the approach is derived from observations from previous research. A formal validation would require detailed research in the field of physical trauma and is hence considered to exceed the scope of this thesis.

The $_E\Delta v$ used in the compatibility measurement procedure differs from the EES and ETS measures that are common in the literature in that it is based on compartment deformations rather than total vehicle deformation and is also related to the collision Δv. It is therefore more relevant to occupant injury and utilises the most accurate measure of collision severity that is available in the accident statistics.

Three vehicle-to-vehicle collision configurations are analysed using a mid-sized passenger car and a large SUV and all three collisions are found to be incompatible. These three collisions form the basis of the analysis in the following chapters.

Chapter 8

Front-to-Front Collision Simulations

In Chapter 6, the geometry and deformation mechanics of vehicle structures are identified as properties that influence compatibility. The aim of this chapter is to demonstrate the effects of modified geometry and deformation mechanics in front-to-front collision simulations. By using simulation techniques rather than full-scale testing, a large range of variables are able to be investigated for a fraction of the cost of a single vehicle-to-vehicle test. The use of front-to-front collision simulations is an accepted tool for the research of compatibility, and a broad range of results have been published by both the automotive industry (for example Loo et al. 2003, Fujii et al. 2003) and independent research institutes (for example Jenefeldt 2008, Park et al. 2009).

Taking advantage of the possibilities offered by a virtual environment, models of perfectly homogeneous front-end structures are used in this chapter to compare the benefits of horizontal and vertical homogeneity using the compatibility measurement procedure described in Chapter 7.

The theory underlying the concepts of horizontal and vertical homogeneity is described in Section 8.1, and the methods used to perform the modelling and simulations are described in Section 8.2. The results according to the assessment method from Chapter 7 are given in Section 8.3, and they are discussed in Sections 8.4 and 8.5 for horizontal and vertical homogeneity, respectively.

8.1 Theory: Properties of structural homogeneity

Within the context of vehicle-to-vehicle compatibility, the concept of homogeneity has been used in the literature as a method to evaluate a vehicle's geometry and deformation mechanics and hence predict whether good structural interaction will occur in a collision with another vehicle. Both a weak and a strong interpretation of the 'homogeneity' concept arise in the literature, although the differences are rarely discussed.

The weak interpretation of homogeneity regards the way a vehicle applies forces in a collision and is often used to describe the force distribution measured in a vehicle-to-barrier test. This interpretation is based on the hypothesis that a vehicle that applies forces more homogeneously will be a more compatible collision partner and "should provide a more homogeneous front-end against which the other car's structure can react" (Edwards et al. 2003*b*, p3). According to this interpretation, an ideal vehicle front-end behaves like the honeycomb elements used to construct crash test barriers.[75]

The strong interpretation of homogeneity regards the way a vehicle reacts forces in a collision. This interpretation is based on the hypothesis that a vehicle that is able to react forces similarly, irrespective of where they are applied, provides better protection to its occupants and that "to achieve good structural interaction [vehicle designs need to] increase the number of active load paths into the main energy absorbing structures" (Edwards et al. 2001*a*, p4). In this case, an ideal vehicle front-end is equally capable of reacting the forces applied by a wide object, such as another vehicle, or a narrow object, such as a tree or pole, even if localised loading occurs away from the main load paths.

The second interpretation is considered stronger because a vehicle that is able to react forces homogeneously is also able to apply forces homogeneously, but the opposite is not true. The second, stronger interpretation of homogeneity is

[75]See for example the homogeneous force distribution achieved by a Mobile Progressive Deformable Barrier (MPDB) in a collision with a rigid barrier (Schram & Versmissen 2007, Figure 8, p4).

applied in this chapter because it encourages vehicle designs that are compatible in a broader range of collisions.

The concepts of horizontal and vertical structural homogeneity independently describe the ability of a vehicle to distribute loads in the vertical and horizontal directions. The intent of these definitions is to separately assess components such as the bumper crossbeam, which distributes loads horizontally, and the subframe, which distributes loads vertically (Edwards et al. 2007*a*). However, due to the limits imposed by research using real vehicles, the two concepts have not yet been considered independently.

Horizontal homogeneity describes the ability of a vehicle structure to transfer loads in a horizontal direction to the main load paths. In the horizontal plane, the main load paths of a passenger vehicle front-end typically consist of the two longitudinals that support the motor. If a load is applied between or outboard of the longitudinals,[76] some other part of the vehicle structure should be capable of transferring that load to the longitudinals. In the literature, bumper crossbeams are often promoted for this purpose, although components such as the engine and wheels have also been found to be effective in some crash tests. Horizontal homogeneity may be particularly important when the offset of a front-to-front collision precludes direct interaction between the longitudinals of two colliding vehicles.

Vertical homogeneity describes the ability of a vehicle structure to transfer loads in a vertical direction to the main load paths. In the vertical plane, the main load paths of a passenger vehicle typically consist of the upper longitudinal, which supports the top of the front suspension, the main longitudinal, which supports the motor, and a subframe that may also support the motor and lower suspension links. In a collision, the main longitudinal is typically designed as the primary load path. If a load is applied above or below the longitudinals, the secondary load paths and vertical connections to the primary load path should

[76] This condition is often described as the 'fork effect'.

be capable of transferring or supporting that load. Vertical homogeneity may be particularly important when the heights of the longitudinals of two colliding vehicles are not aligned or when their deformation mechanics leads to a dynamic offset.

8.2 Methods

The test and assessment method used for the simulations is described in Chapter 7 and is based on co-linear front-to-front simulations with an approach velocity of 112 km/h using models of a mid-sized passenger car and a large SUV. The homogeneity of the vehicles' structures is varied between the simulations and the effects are assessed in various collision configurations. The two sections below describe the test matrix and the method used to model the homogeneous structures.

8.2.1 Test matrix

The matrix in Table 8.1 describes the variables that are investigated in the simulations and includes cross-references to the relevant sections of the discussion. Four 'standard' simulations, which form the core of the test matrix, are highlighted in yellow in Table 8.1. In these simulations, a homogeneous region 250 mm in height and covering the entire width of each vehicle is assessed. Simulations of both horizontal and vertical homogeneity are performed in the 50% overlap and 100% overlap collision configurations.

Additional simulations are performed to determine the effect of a 500 mm high homogeneous region and a 'narrow' homogeneous region that only extends between the vehicles' longitudinals. The effects of structural homogeneity are also analysed for a SUV structure raised by 125 mm and for collisions in the 33% and 66% overlap collision configurations. In each of the collision configurations, 'basis' simulations are performed using vehicle models with inhomogeneous structural characteristics.

Table 8.1: Front-to-front collision simulations: Test matrix including cross references to the discussion.

Shield homogeneity:		**Horizontal**				**Vertical**		**Basis models without crossbeams**
Shield width:		**Entire vehicle width**		**Narrow**		**Entire vehicle width**		
Shield height:		**250 mm**	**500 mm**	**250 mm**		**250 mm**	**500 mm**	
Standard SUV ride height	**33% overlap**	Section 8.4.1 Section 8.4.4 Figure 8.6	–	Section 8.4.4 Figure 8.6		–	–	Section 8.4.1
	50% overlap	Section 8.4 Section 8.4.4 Figure 8.3	–	Section 8.4.4		Section 8.5 Section 8.5.3 Figure 8.10	Section 8.5.3 Figure 8.10	Section 8.4 Section 8.5 Section 8.5.3 Figure 8.3
	66% overlap	Section 8.4.1 Section 8.5.1 Figure 8.4 Figure 8.8	–	–		Section 8.5.1 Figure 8.8	–	Section 8.4.1 Section 8.5.1 Figure 8.4
	100% overlap	Section 8.4 Section 8.4.3	Section 8.4.3	–		Section 8.5 Section 8.5.2 Section 8.5.3 Figure 8.7	Section 8.5.3	Section 8.4 Section 8.5 Section 8.5.3 Figure 8.7
125 mm raised SUV ride height	**100% overlap**	Section 8.4.2 Section 8.4.3 Figure 8.5	Section 8.4.3	–		Section 8.5.2 Section 8.5.3 Figure 8.9	Section 8.5.3	Section 8.4.2 Section 8.5.2 Section 8.5.3 Figure 8.5 Figure 8.9

The various sizes of the homogeneous regions reflect the assessment areas defined in metrics such as the HSI and VSI (Edwards et al. 2007*a*). Correspondingly, the homogeneous regions are centred at 455 mm of ground clearance.

In order to focus on the most relevant outcomes, several combinations of model variants and collision configurations are omitted from the test matrix in Table 8.1, and only the simulations that produce the primary findings of the front-to-front simulations are included.

8.2.2 Modelling of homogeneous structures

To create an inhomogeneous basis arrangement against which the vehicles with homogeneous characteristics can be compared, the bumper crossbeams of the passenger car and SUV models are removed so that the ability of the vehicles to transfer local loads to the longitudinals is minimised. To avoid an unrealistic instability of the front end, the longitudinals are connected by beam elements that maintain the relative distance between the forward most points of the longitudinals, but do not interact with any other components in the vehicle or the collision partner.

The combination of both horizontal and vertical homogeneity was simulated by Thomas (2006), who modelled a thin, flat, rigid shield in the front-end of a vehicle structure. Thomas found that structural homogeneity leads to an improvement in compatibility in offset frontal collisions, but he did not distinguish between horizontal and vertical homogeneity. In order to model horizontal and vertical homogeneity independently, the approach used by Thomas is adapted so that the thin shields are highly flexible in one axis and rigid in the other. The material used for the shields is a mono-directional ply with very high stiffness in the ply direction and very low stiffness in the normal direction.[77] The shields are further stiffened using rigid nodal connections in the ply direction.[78]

[77] The stiffness moduli in the ply and normal directions differ by four orders of magnitude.

[78] The shields used in this thesis are an improvement on those presented previously by O'Brien (2008) and are considered to be more realistic in their deformation behaviour.

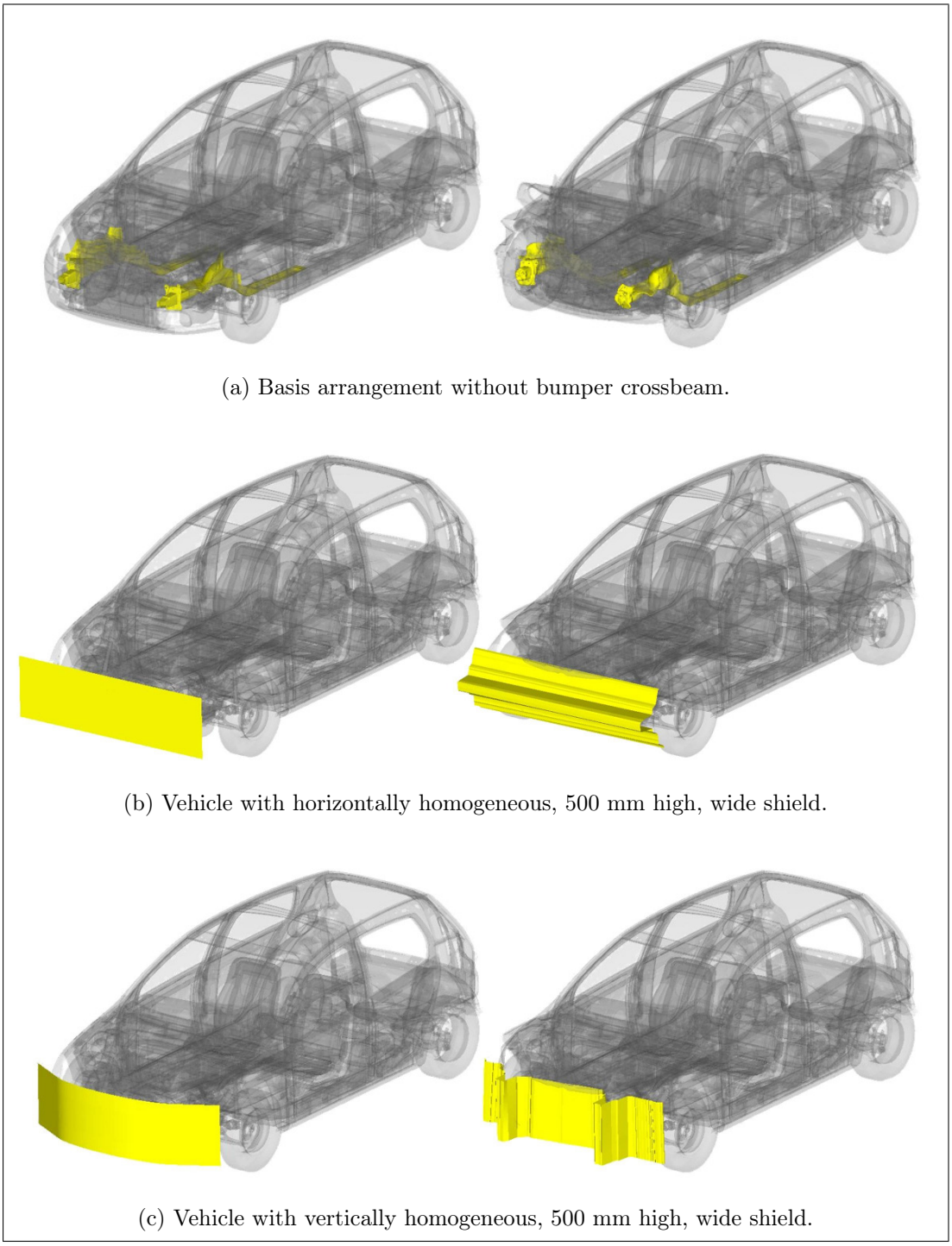

(a) Basis arrangement without bumper crossbeam.

(b) Vehicle with horizontally homogeneous, 500 mm high, wide shield.

(c) Vehicle with vertically homogeneous, 500 mm high, wide shield.

Figure 8.1: Typical behaviour of the passenger car with and without homogeneous shields. The figures on the left show the vehicle model before the collision and the figures on the right show the deformation during a collision with a deformable barrier. The deformable barriers are omitted from the figures to avoid obstructing the view of the homogeneous shields.

To model the vehicles with homogeneous characteristics, shields are positioned in the space that is normally occupied by the bumper crossbeam. The vertically homogeneous shields are curved in the horizontal plane to follow the contour of the original bumper crossbeams, but straight in the vertical direction to enable a homogeneous transfer of forces. In contrast to the vertically homogeneous shields, the horizontally homogeneous shields are modelled as a flat plane.

Movement of the shields in the vertical and lateral directions is limited with respect to the vehicles' local coordinate systems, but movement in the collision direction is free depending on contact with other parts of the vehicle and the collision partner. Rotation tangent to the direction of homogeneity is permitted, as is the rotation of the horizontal shield about the vertical axis. Other rotations are limited. The control of the shields' movements and the connections to the vehicles' structures are provided by beam-like elements that link each shield to the base of the relevant vehicle's B-pillar.[79] Apart from the connections at each end, all contacts between these beam elements and the vehicles' structures are ignored in the simulation.

The geometry and behaviour of the shields are demonstrated in Figure 8.1. In Sections 8.4 and 8.5, figures showing the ideal homogeneous shields, main load paths, engine, wheels, and the compartment bulkhead of each vehicle are used to highlight the interaction between the two vehicles. In Figure 8.2, the location and pre-collision geometry of these components are shown within the total vehicle structure.

8.3 Simulation results

The results of the front-to-front simulations are summarised in Table 8.2 and are further discussed Sections 8.4 and 8.5.

[79]The B-pillars are used because of the high stiffness of the components, the fact that they remain undeformed in the front-to-front collisions, and their relative proximity to the vehicles' centres of gravity.

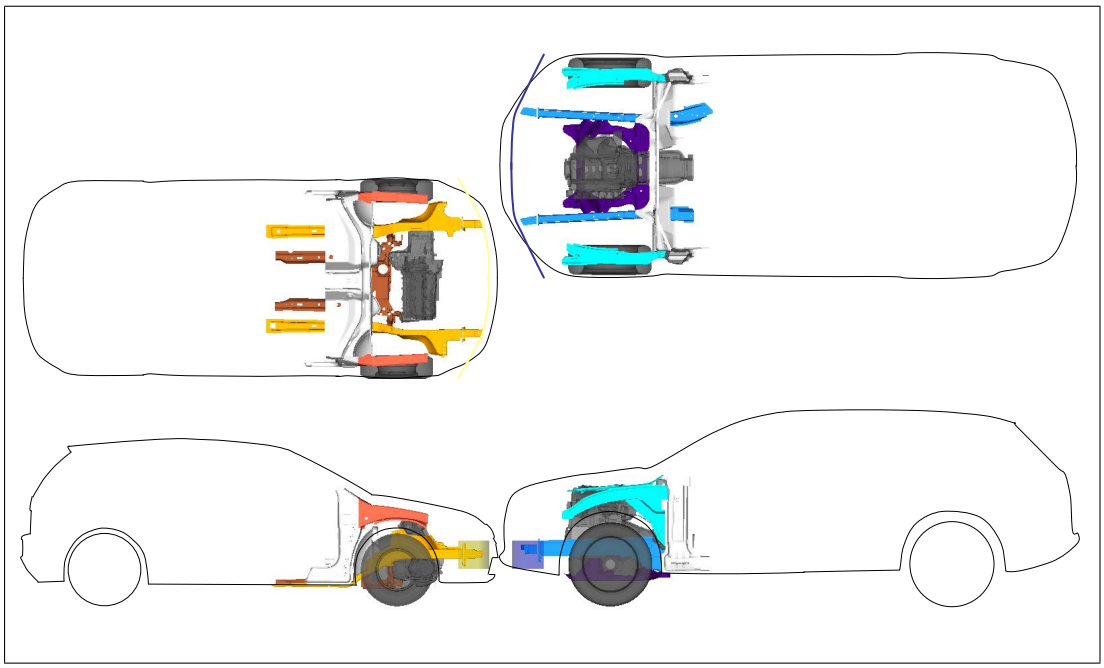

Figure 8.2: Geometry of the mid-sized passenger car and large SUV prior to the 50% overlap collision simulation. The ideal homogeneous shields, main load paths, engine, wheels, and the compartment bulkhead are visible within the outlines of the vehicles.

The mass of the shields ranges between 2.2 kg and 8.1 kg, compared to the 4.3 kg and 5.1 kg of the original vehicles' bumper crossbeams. Compared to the basis models without bumper crossbeams, the addition of the shields results in an increase in the initial kinetic energy of up to 1.0 kJ. In contrast, the deformation of the shields themselves results in the dissipation of up to 2.8 kJ. If this difference were to be subtracted from the initial kinetic energy of the passenger car, the effect would be a 0.3 km/h reduction in its initial velocity of 56 km/h. Since this is well within the ±1 km/h tolerance common to most physical crash tests, it is concluded that the presence of the shields does not adversely affect the results and that the simulations with and without the shields are comparable.

8.4 Discussion: Horizontal homogeneity

Horizontal homogeneity is analysed in the 50% and 100% overlap configurations using 250 mm high shields covering the entire width of each vehicle. In comparison to the basis simulations, a substantial reduction in the mean mortality rate is

Table 8.2: Results of front-to-front collision simulations between various variants of a mid-sized passenger car and a large SUV with 112 km/h approach speed. In each simulation, the same type of shield is added to both the car and the SUV. The shields modelled in the simulations represent the maximum theoretical performance for vertically homogeneous or horizontally homogeneous vehicle structures.

Shield properties			**Car** $E\Delta v$ **(km/h)**	**SUV** $E\Delta v$ **(km/h)**	**Collision MMR**
Homogeneity	**Height**	**Width**			
33% overlap collision configuration:					
Basis model[a]	–	–	99.3	61.9	253‰
Horizontal	250 mm	Wide	83.2	61.9	81.3‰
Horizontal	250 mm	Narrow	92.6	62.0	167‰
50% overlap collision configuration:					
Basis model	–	–	86.2	61.8	103‰
Horizontal	250 mm	Wide	80.3	61.6	63.5‰
Horizontal	250 mm	Narrow	86.3	58.3	101‰
Vertical	250 mm	Wide	80.4	64.1	66.6‰
Vertical	500 mm	Wide	80.8	63.8	68.3‰
66% overlap collision configuration:					
Basis model	–	–	80.9	58.6	64.7‰
Horizontal	250 mm	Wide	74.7	57.5	36.2‰
Vertical	250 mm	Wide	75.0	60.2	39.1‰
100% overlap collision configuration:					
Basis model	–	–	72.4	49.3	26.4‰
Horizontal	250 mm	Wide	72.8	45.8	26.9‰
Horizontal	500 mm	Wide	72.8	46.3	27.1‰
Vertical	250 mm	Wide	68.7	49.2	17.6‰
Vertical	500 mm	Wide	68.8	48.8	17.9‰
100% overlap collision configuration, 125 mm raised SUV:					
Basis model	–	–	94.8	44.4	186‰
Horizontal	250 mm	Wide	89.8	33.6	129‰
Horizontal	500 mm	Wide	89.1	37.3	122‰
Vertical	250 mm	Wide	72.2	46.5	25.3‰
Vertical	500 mm	Wide	72.7	45.7	26.6‰

[a] Basis models without homogeneous shields and without bumper crossbeams.

measured in the 50% overlap configuration, with benefit observed in both the car and the SUV, but a slight increase in the mean mortality rate is observed in the 100% overlap configuration, with the disbenefit in the car outweighing the benefit in the SUV.

The basis simulations in both configurations exhibit similar behaviour. In the 50% overlap configuration, the left longitudinals of both vehicles are aligned and remain engaged throughout the collision. Similarly, in the 100% overlap configuration, the left and right longitudinals of both vehicles are aligned and also interact throughout the collision. Likely due to differences in the force-deformation relationships of the two vehicles' longitudinals, the car's longitudinals are deformed to a greater degree than the SUV's longitudinals.

With the addition of the horizontally homogeneous shields, the transfer of loads through the vehicles' front-ends is altered such that the direct and exclusive interaction between the longitudinals no longer occurs. Instead, loads are also supported by the wheels, motor block, and other components. As a consequence, in both the 50% overlap and 100% overlap configurations, the car's longitudinals are deformed to a lesser degree than in the basis simulations, and the SUV's longitudinals are deformed to a greater degree. This is shown for the 50% overlap configuration in Figure 8.3. Although the force-deformation relationships of the individual deformable components is not altered, this result shows that the addition of the horizontally homogeneous shields leads to a different distribution of loads and hence an effective increase in the forces required to deform the front-end of the car. It is therefore concluded that a horizontally homogeneous structure is effective even when the primary load paths of the vehicles are perfectly aligned.

The addition of the horizontally homogeneous shields appears to reduce the effective vertical homogeneity of the vehicles in the 100% overlap configuration. Although the longitudinals interact in the basis simulation, a degree of override/underride occurs in the simulation with the horizontally homogeneous shields. This can be observed both in the interaction between the longitudi-

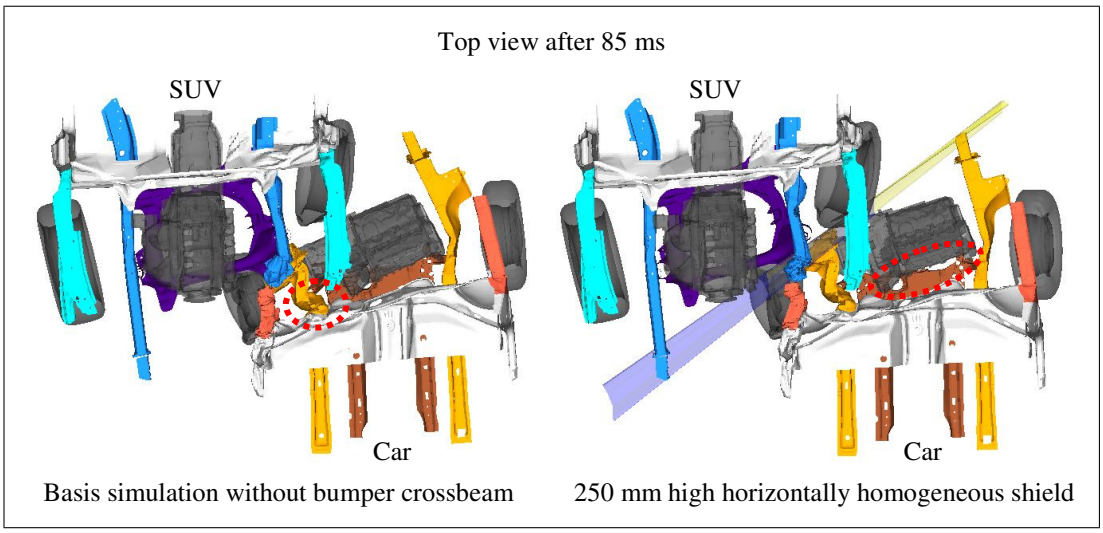

Figure 8.3: Horizontal homogeneity in a 50% overlap collision simulation between a car and SUV. The ideal homogeneous shields, main load paths, engine, wheels, and the compartment bulkhead are visible. The greater degree of deformation to the car's longitudinal is highlighted on the left, and the reduced degree of crush to the car's front-end is highlighted on the right.

nals and the dive angles of the vehicles during the collision. As a consequence, deformation of the car upper A-pillar and instrument panel is increased and deformation in the car footwell is reduced, which on balance results in a 0.4 km/h increase in the car's $E\Delta v$.

8.4.1 Alternative overlap configurations

In Section 8.1, it is stated that horizontal homogeneity is particularly important when the collision overlap precludes direct interaction between the vehicles' longitudinals. However, both the 50% overlap and 100% overlap simulations with the basis models result in interaction between the longitudinals of the car and the SUV. Therefore, additional simulations are performed with 33% and 66% overlap, since the statistical analysis in Section 4.2.1 also identifies this range of overlap as relevant for the analysis of front-to-front compatibility. For the measurement of compatibility, the procedure used for the 50% overlap configuration is applied and, for efficiency, the reference vehicle-to-wall deformation data for the 50% overlap configuration are also utilised. In absolute terms, these reference data

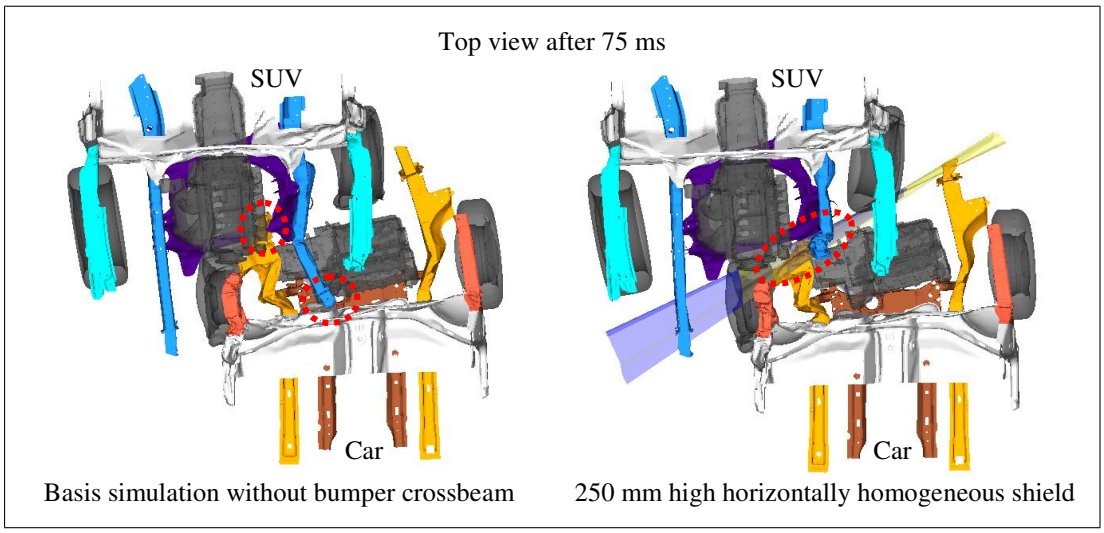

Figure 8.4: Horizontal homogeneity in a 66% overlap collision simulation between a car and SUV. The ideal homogeneous shields, main load paths, engine, wheels, and the compartment bulkhead are visible. The lack of interaction between the longitudinals is highlighted on the left, and the increased interaction is highlighted on the right.

are only valid for collisions with 50% overlap, and they are applied in this section with the knowledge that the absolute results are incorrect, but still a useful basis for comparison. The simulations are performed using the 250 mm high, wide shields, and substantial reductions in the mean mortality rates are measured in both configurations as a consequence of reductions in the car's $E\Delta v$.

The basis simulations in both configurations exhibit similar behaviour, with no interaction occurring between the car and SUV longitudinals. These structures are therefore only supported by secondary load paths and the compartment of the collision partner. The car longitudinal is supported by the SUV's left wheel in the 33% overlap configuration and, after penetrating the SUV's radiator, is supported by the engine subframe in the 66% overlap configuration. In both cases, the SUV's secondary load paths are able to support the forces necessary to deform the car's longitudinal. In contrast, the SUV's longitudinal directly loads the A-pillar of the car in the 33% overlap configuration and, after penetrating the car's radiator and passing over the gearbox, almost comes into contact with the car's bulkhead in the 66% overlap configuration.

With the addition of the horizontally homogeneous shields, a crossover between the vehicles' longitudinals is prevented, and hence they are both deformed to a greater degree in both the 33% overlap and the 66% overlap configurations. The different patterns of deformation are shown for the 66% overlap simulations in Figure 8.4.

In the 50% overlap and 100% overlap configurations, the primary load paths are loaded in the basis simulations and the addition of the shields transfers part of this load to the secondary load paths. In contrast, in the 33% overlap and the 66% overlap configurations, the secondary load paths are loaded more heavily in the basis simulations and the addition of the shields transfers part of this load to the primary load paths. It is therefore concluded that a horizontally homogeneous structure is also effective at reducing the severity of a front-to-front collision when the primary load paths of the vehicles have a lateral offset.

8.4.2 Alternative vertical alignment

The effect of horizontal homogeneity is also simulated with the driving height of the SUV raised by 125 mm.[80] Similar to the previous section, this represents a case where the primary load paths of the vehicles are not aligned. The simulation is performed in the 100% overlap configuration using the 250 mm high, wide shields. In comparison to the basis simulation without bumper crossbeams, a substantial reduction in the mean mortality rate is measured, but the result is still more than six times higher than the nominal rate for a front-to-front collision with an approach speed of 112 km/h.

Due to the vertical offset between the primary structures, the longitudinals of the SUV pass over the longitudinals of the car in the basis simulation.

[80] In contrast to a physical test, the driving height of the simulation model is increased by moving the entire vehicle and its ground surface. The SUV's suspension remains unchanged. The car model is not affected by the presence of the second ground surface because there is no contact defined between these two entities. Forces between two objects are only calculated by PamCrash simulation software if a 'contact' between them is defined (ESI Group 2008). If no contact is defined, the objects may pass through or occupy the same space without influencing each other.

Consequently, the forward sections of the longitudinals remain undeformed. Deformation of the car's longitudinals only occurs rearward of the engine mounting points as a result of interaction between the car's motor block and the SUV's engine subframe, and deformation of the SUV's longitudinals only occurs in bending as a result of the SUV overriding the car. The longitudinals of the SUV come within 67 mm of direct contact with the car's bulkhead.

Although the addition of the horizontally homogeneous shields does not completely compensate for the vertical offset between the primary load paths, the interaction between primary and secondary load paths is improved. As shown in Figure 8.5, the SUV's longitudinals are able to interact with the car's upper longitudinals, and the car's longitudinals are able to interact with the SUV's engine subframe. This reduces the severity of the car's deformation, but not to the extent observed in a collision with interaction between the primary load paths. It is therefore concluded that a horizontally homogeneous structure only has limited effectiveness when the primary load paths of the vehicles are not vertically aligned.

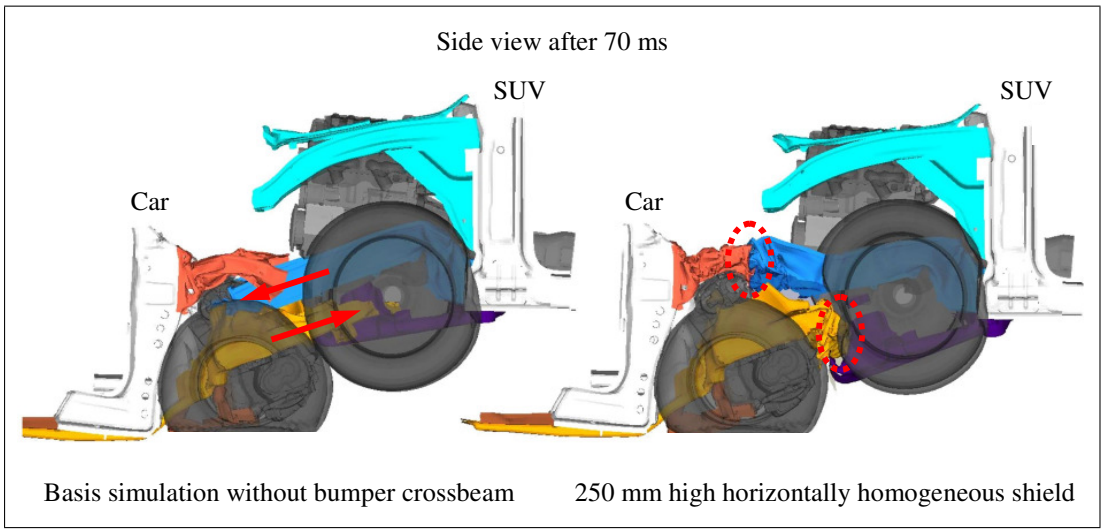

Figure 8.5: Horizontal homogeneity in a 100% overlap collision simulation between a car and SUV with 125 mm raised driving height. The ideal homogeneous shields, main load paths, engine, wheels, and the compartment bulkhead are visible. The lack of interaction between the longitudinals is highlighted on the left, and the interaction between primary and secondary load paths is highlighted on the right.

8.4.3 Alternative height of homogeneous region

The optimum height of a horizontally homogeneous region is investigated by comparing a 250 mm high shield with a 500 mm high shield in the 100% overlap configuration. Both the standard driving height and the 125 mm raised driving height, which is also used in Section 8.4.2, are analysed. In comparison to the simulations with 250 mm high shields, the simulations with 500 mm high shields lead to a slight increase in the mean mortality rate measured in the collision simulation with standard driving heights and a marginal reduction in the collision simulation with modified driving heights.

The differences between the simulations at the normal driving height are slight, with the maximum difference between deformation measures being 2 mm. The only differences observed in the deformation of the front-ends are a slight increase in the deformation of the SUV's subframe and a similar increase in the deformation of the car's upper longitudinals. These changes both correlate with the increased height of the homogeneous region, but the overall effect of the 500 mm homogeneous region is negligible. The differences between the simulations with the raised driving height are also slight, with the only substantial difference between deformation measures being a 7 mm reduction at the left upper A-pillar in the car. This is attributed to improved interaction between the SUV's right longitudinal and the car's left upper longitudinal, which is deformed to a greater degree than in the collision simulation with the 250 mm high shield. From these simulations, it is concluded that an increase in the range of the horizontally homogeneous region from 250 mm to 500 mm does not represent a substantial improvement in compatibility and is therefore not justified.

8.4.4 Alternative width of homogeneous region

The optimum width of a horizontally homogeneous region is investigated by comparing a 250 mm high shield covering the entire width of the vehicle to a 250 mm high shield covering only the space between the longitudinals. Simulations are

performed in the 50% overlap configuration and the 33% overlap configuration, which is also used in Section 8.4.1. In comparison to the simulations with the wide shields, the simulations with narrow shields lead to a substantial increase in the mean mortality rate due to increases in the car's $E\Delta v$ in both collision configurations.

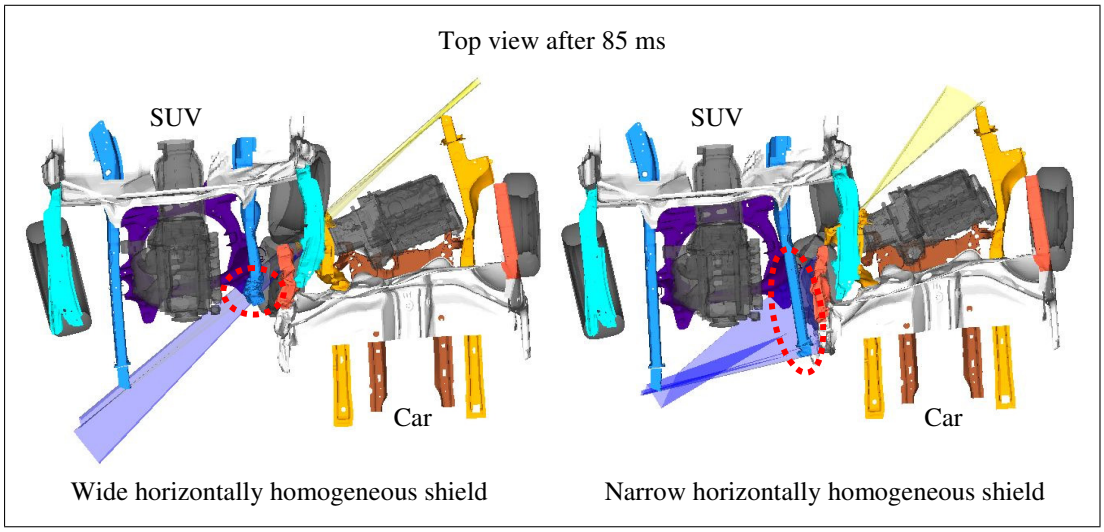

Figure 8.6: Horizontal homogeneity in a 33% overlap collision simulation between a car and SUV. The ideal homogeneous shields, main load paths, engine, wheels, and the compartment bulkhead are visible. The deformation of the SUV's longitudinal is highlighted on the left, and the lack of deformation is highlighted on the right.

As shown in Figure 8.6, in the 33% overlap configuration, the combination of the low overlap and narrow shields mean that the SUV's and car's shields do not interact with each other and the SUV's longitudinal remains effectively undeformed. Although the narrow shield averts the direct interaction between the SUV's longitudinal and the car's A-pillar that can be observed in the basis simulation, the load path including the SUV's wheel and the car's longitudinal is more heavily loaded. Due to a lack of deformation in the SUV's longitudinal, the collision energy is dissipated by increased deformation of the car's compartment and, to a lesser degree, the SUV's footwell.

In the 50% overlap configuration, the narrow shields interact at the beginning of the collision, but then the longitudinals deform and translate laterally so that each longitudinal passes between the longitudinal and wheel of the collision

partner. As in Section 8.4.2, this means that the primary load paths of each vehicle can only interact with the secondary load paths of the collision partner. The SUV's longitudinal is deformed to a lesser degree than in the simulation with the wide shield, and the car's longitudinal and upper longitudinal are deformed to a greater degree. From these simulations, it is concluded that a wider horizontally homogeneous region is more compatible.[81]

8.5 Discussion: Vertical homogeneity

Vertical homogeneity is analysed in the 50% overlap and 100% overlap configurations using 250 mm high shields covering the entire width of each vehicle. In comparison to the basis simulations, substantial reductions in the mean mortality rate are measured in both collision configurations, primarily as a result of reductions in the car's $_E\Delta v$. Since the mean mortality rate in the 100% overlap configuration with the vertically homogeneous shield is less than the nominal rate of 20‰, it satisfies the definition of a compatible collision from Chapter 6.

Although the longitudinals of the car and SUV are aligned and also interact in the 50% overlap basis simulation, the addition of the vertically homogeneous shields induces a lateral displacement of the longitudinals that causes them to pass by each other and enter the space between the wheel and longitudinal of the collision partner. As a consequence, both vehicles' longitudinals remain largely undeformed. A similar lateral displacement of the longidtudinals is observed in the 50% overlap configuration with the narrow, horizontally homogeneous shields in Section 8.4.4, and a similar lack of deformation to the longitudinals is observed in the basis 100% overlap simulation with raised SUV driving height in Section 8.4.2. However, in contrast to those simulations, in the simulation with the vertically homogeneous shield, sufficient energy is dissipated by components whose loading does not result in increased deformation of the car's passenger compartment.

[81] It should be noted that the wide, horizontally homogeneous shield is an extremely hypothetical model that greatly exceeds the stiffness of any practical vehicle structure.

The interaction that occurs in this simulation would be classified as poor according to subjective criteria,[82] and may result in poorer results at higher velocities. However, the analysis shows that the vertically homogeneous shield leads to a reduction in compartment deformation measures, and the collision velocity is relevant in the accident environment. Objectively, this result must therefore be assessed positively. Despite this, it is difficult to draw conclusions regarding vertical homogeneity from this simulation, since the outcome is primarily due to unstable interaction in the horizontal direction and not due to the homogeneous transfer of loads in the vertical direction.

In the basis 100% overlap simulation, the left longitudinal of each vehicle is deformed to a lesser degree than the right longitudinal, and, with the addition of the vertically homogeneous shields, this difference is increased. In the SUV, this results in slightly higher compartment deformations on the passenger's side and slightly lower deformations on the driver's side. In the car, the compartment deformations are generally reduced, but the reduction is greater on the driver's side. The addition of the vertical shields, and hence the support of the longitudinals by secondary load paths, increases the effective force-levels of the left side longitudinals in comparison to the right side longitudinals of the collision partner.

The principal benefit from the addition of the vertically homogeneous shields is due to a reduction in the override/underride in comparison to the basis simulation. With the addition of the shield, the generation of vertical forces between the SUV and the car is minimised, and hence the dive angle of the car is reduced. As shown in Figure 8.7, this reduces the loading on the upper longitudinals of the car and leads to a reduction in the upper A-pillar and instrument panel deformations. By reducing the dive angle of the car, the collision is more representative of a vehicle-to-barrier collision, in which the collision interface is always vertical. This

[82] Similar interaction has been observed and criticised in other analyses of compatibility in 50% overlap configurations between SUVs and passenger cars (see for example Brieter 2008, Edwards et al. 2007*b*).

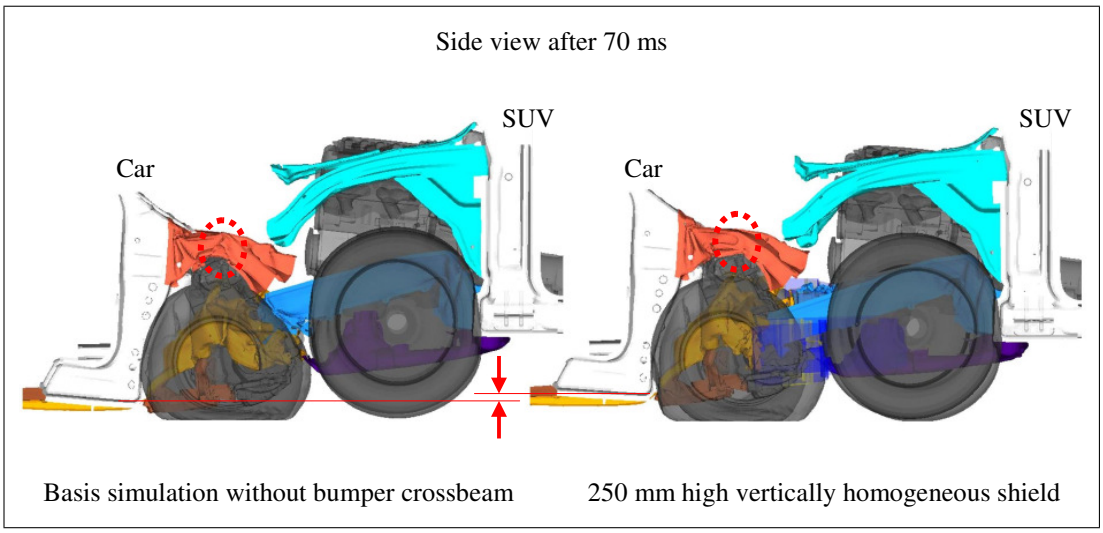

Figure 8.7: Vertical homogeneity in a 100% overlap collision simulation between a car and SUV. The ideal homogeneous shields, main load paths, engine, wheels, and the compartment bulkhead are visible. The difference between the deformation of the car's upper longitudinal and the degree of dive of the car are highlighted.

result shows that the alignment observed in the basis collision simulation is not sufficient to eliminate the transfer of vertical forces across the collision interface, but that this is achieved by the addition of a more vertically homogeneous structure. It is therefore concluded that a vertically homogeneous structure is effective even when the primary load paths of the vehicles are geometrically aligned.

8.5.1 Alternative overlap configurations

Due to the inconclusive results for vertical homogeneity in the 50% overlap configuration, the analysis in this section also includes vertical homogenity in 33% overlap and 66% overlap configurations. The final simulation matrix includes these combinations, although they had initially been excluded because it had been expected that the horizontally homogeneous shields would be more relevant in the 33% and 66% overlap configurations, which are characterised by the lateral misalignment of the vehicles' longitudinals.

In the 33% overlap configuration, the vertically homogeneous shield causes the SUV's longitudinal to glide off the car's A-pillar without engaging it significantly. It is not clear whether this is a realistic behaviour for a vehicle with

an ideally vertically homogeneous strucuture or simply an artefact of the shield model. The compatibility measurement procedure indicates that this is the most compatible of the 33% overlap configurations, but since the glide off is questionable, the result is omitted from the analysis and is not included in Table 8.2. Despit this, this simulation supports the hypothesis that even a partial glide off is effective in low overlap configurations.

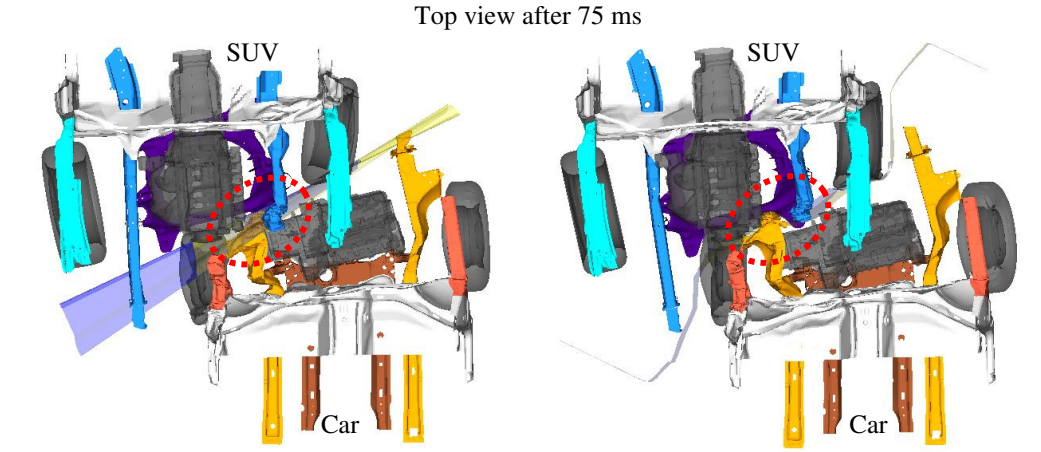

Figure 8.8: Comparison between horizontal and vertical homogeneity in 66% overlap collision simulations between a car and SUV. The ideal homogeneous shields, main load paths, engine, wheels, and the compartment bulkhead are visible. The similar degree of interaction between the longitudinals and the secondary load paths is highlighted in both cases.

It would be reasonable to expect that the 66% overlap configuration with the vertically homogeneous shield would be similar to the basis simulation. However, the compatibility measurement procedure indicates that the results are actually very similar to the simulation with the horizontally homogeneous shields. As shown in Figure 8.8, although the vertically homogeneous shield cannot increase the interaction between the primary load paths of the vehicles, which have a lateral offset, the vertically homogeneous shields enable the SUV's left longitudinal to interact with the car's engine and also enable the car's left longitudinal to interact more effectively with the SUV's subframe. Based on this result, it is concluded that a vertically homogeneous structure approaches a similar degree

of effectiveness to that of a horizontally homogeneous structure even in collision configurations where the primary structures are not in lateral alignment.

8.5.2 Alternative vertical alignment

The effect of vertical homogeneity is also simulated with the driving height of the SUV increased by 125 mm in the 100% overlap configuration. The simulation uses the 250 mm high, wide shields, and the mean mortality rate is measured at a level equivalent to the basis 100% overlap simulation with equal driving heights.

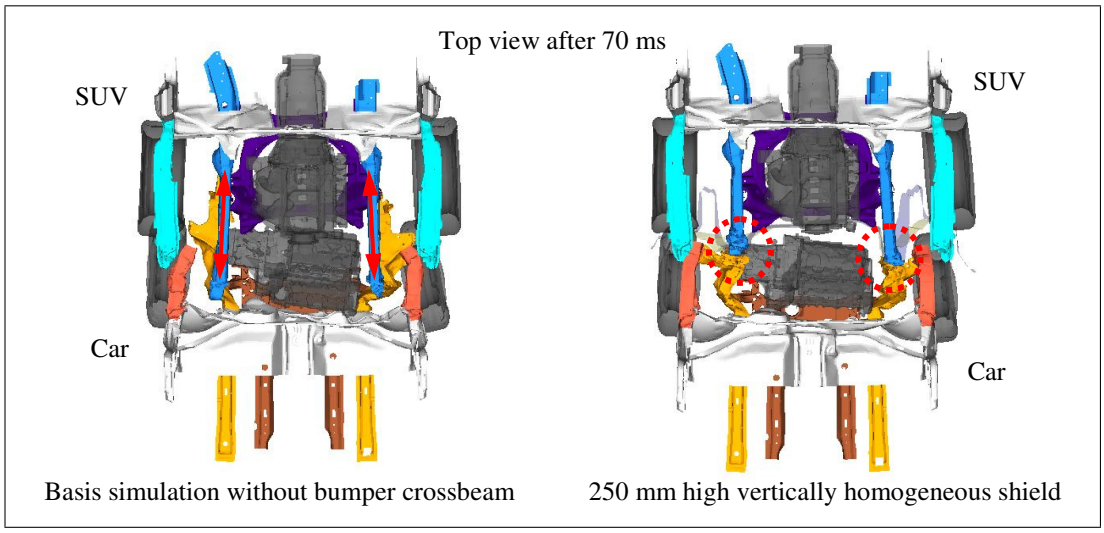

Figure 8.9: Vertical homogeneity in a 100% overlap collision simulation between a car and SUV with 125 mm raised driving height. The ideal homogeneous shields, main load paths, engine, wheels, and the compartment bulkhead are visible. The lack of interaction between the longitudinals is highlighted on the left, and the interaction between the primary load paths is highlighted on the right.

The 125 mm change in driving height does not eliminate the overlap between the car's shield and SUV's shield, and hence the transfer of forces between the two vehicles is able to occur as though the load paths were vertically aligned. As shown in Figure 8.9, this completely avoids the situation that arises in the basis simulation, where the SUV's longitudinals pass over the car's longitudinals. The general pattern of deformation is similar to the basis simulation with equal driving heights, although the dive angle of the car is slightly less in the simulation

with the vertical shield, which results in a $E\Delta v$ of the car that is 0.2 km/h lower. In comparison to the simulation with the vertically homogeneous shields at the normal driving height, the simulation at the raised driving height leads to an increased dive angle and $E\Delta v$ of the car. It is likely that this difference arises due to rotational moments generated between the higher centre of gravity of the SUV and the lower centre of gravity of the car.

The result generated with ideal shields in this simulation cannot be practically realised, but it demonstrates the importance and benefit of vertical alignment between primary load paths.[83] In Section 8.4.2, it is shown that the improvement of interaction between primary and secondary load paths only produces limited benefit when the primary load paths are not vertically aligned. It is therefore concluded that the vertical alignment of primary load paths is critical for a compatible collision.

8.5.3 Alternative height of homogeneous region

The optimum height of a vertically homogeneous region is investigated by comparing a 250 mm high shield with a 500 mm high shield in the 50% overlap configuration, the 100% overlap configuration, and the 100% overlap configuration with the 125 mm raised driving height that is also used in Section 8.5.2.

In comparison to the simulations with 250 mm high shields, the simulations with 500 mm high shields all lead to an increase in the mean mortality rate, but still represent an improvement over the basis simulations. Regardless of the collision configuration, the increase in height has a common outcome: the larger vertically homogeneous shields increase the loading on the upper longitudinals of the car and hence increase the deformation of the upper A-pillar and instrument panel. All other effects are insignificant.

In the previous two sections, it is shown that the benefit of a vertically ho-

[83] It may be possible to construct a shield-like structure, but it would invariably also transfer rotational moments across the collision interface. The ideal shields transfer these moments directly to the vehicles' centres of gravity and hence the deformation of the vehicles' front-ends is largely unaffected.

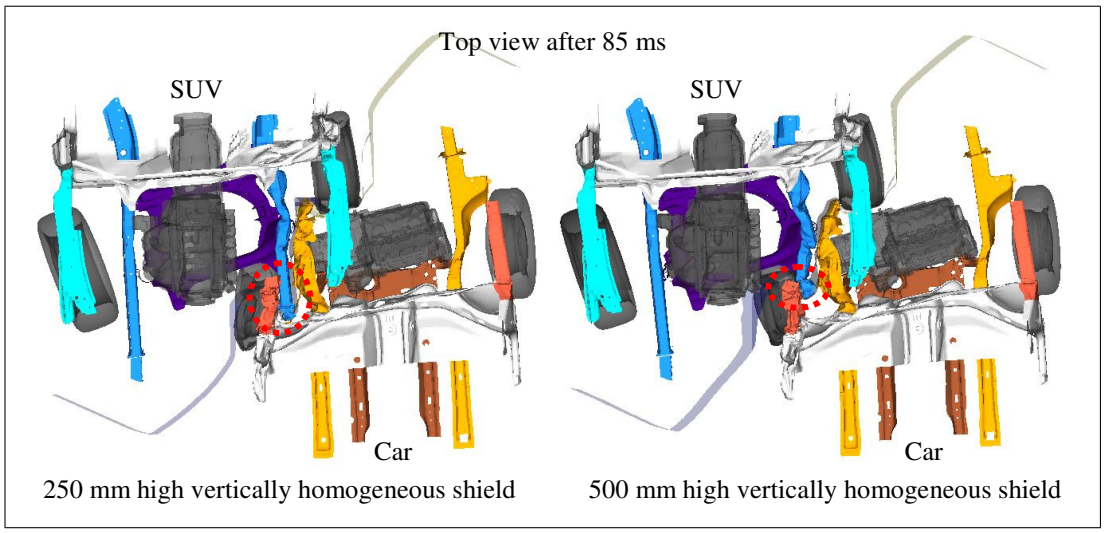

Figure 8.10: Vertical homogeneity in a 50% overlap collision simulation between a car and SUV. The ideal homogeneous shields, main load paths, engine, wheels, and the compartment bulkhead are visible. The different interaction between car's upper longitudinal and SUV's main longitudinal is highlighted.

mogeneous structure comes from an alignment between the primary load paths and the minimisation of vertical forces that lead to underride/override. As shown in Figure 8.10, by increasing the height of the vertically homogeneous region, the car's upper longitudinal interacts with the SUV's main longitudinal and is deformed to a greater extent. In order to minimise the compartment deformations, these simulations indicate that it is more effective to focus the forces on the primary load paths than to also overload the secondary load paths. It is therefore concluded that an increase in the vertically homogeneous region from 250 mm height to 500 mm height is counter-productive for compatibility.

Chapter summary

Front-to-front collision simulations are performed with variants of a mid-sized passenger car and a large SUV at an approach speed of 112 km/h. The compatibility measurement procedure from Chapter 7 is applied and used to assess whether the collisions are compatible according to the definition from Chapter 6. Ideal vertical homogeneity leads to a compatible result in the 100% overlap config-

uration, but neither vertical nor horizontal homogeneity are alone able to produce a compatible result in the 50% overlap configuration. The combination of vertical and horizontal homogeneity is not investigated.

In Section 8.4, it is shown that a horizontally homogeneous structure is effective when the primary load paths of the vehicles are in lateral alignment or when they have a lateral offset. However, the effectiveness of a horizontally homogeneous structure is limited when the primary load paths of the vehicles are not in vertical alignment.

In Section 8.5, it is shown that a vertically homogeneous structure is effective even when the primary load paths are in geometrical alignment. It is also concluded that the vertical alignment of the primary load paths is critical for achieving a compatible collision.

Horizontal and vertical homogeneity are compared using homogeneous regions 250 mm and 500 mm in height, and it is shown that the 250 mm high region results in more compatible collisions. Further alternatives are not analysed, and hence the true optimum may be greater or less than 250 mm in height. The width of the horizontally homogeneous region is also analysed, and it is shown that a wider region is more compatible.

In general, vertical homogeneity is effective in all front-to-front collisions, but horizontal homogeneity is not effective in 100% overlap collisions and only marginally better than vertical homogeneity in partial overlap collisions. In low overlap collisions, the results for vertical homogeneity are inconclusive, but the results for horizontal homogeneity show that a wide region is necessary. The results therefore indicate that the most effective changes to the basis models would be a 250 mm high, vertically homogeneous region encompassing the longitudinals and the addition of a horizontally homogeneous region outside of the longitudinals. Although this conclusion is limited by the features of the underlying vehicle models, which are not inhomogeneous and have certainly influenced the outcome, it may be generalised to other vehicles because the features of the models that

influence the results are typical for modern vehicle designs.

The results of this chapter indicate the robustness of the compatibility measurement procedure developed in Chapter 7, since benefits and disbenefits in the two vehicles are objectively balanced, as are benefits and disbenefits at different measurement points within each vehicle.

Chapter 9

Front-to-Side Collision Simulations

The effects of horizontal and vertical homogeneity are investigated in front-to-front collisions in Chapter 8, and in this chapter, the effects of these changes are analysed in front-to-side collisions. Furthermore, the potential for complementary increases in the B-pillar stiffness and door crossbeam stiffness are investigated. The comparison is again performed using the compatibility measurement procedure described in Chapter 7, with the aim of identifying any beneficial or detrimental combinations of structural attributes in the front-end and side of the vehicle.

As is the case with front-to-front compatibility research, simulation is also an established tool for research on compatibility in front-to-side collisions (see for example Barbat et al. 2007, Takizawa et al. 2007, Thompson et al. 2007).

The methods used to perform the modelling and simulations are described in Section 9.1, and the results according to the measurement procedure from Chapter 7 are given in Section 9.2. The effects of front-end horizontal and vertical homogeneity are discussed in Sections 9.3 and 9.4, respectively, and the effects of stiffened struck-vehicle door crossbeams and B-pillars are discussed in Sections 9.5 and 9.6, respectively. Sections 9.5 and 9.6 also include discussions of the effects of combining front-end homogeneity with stiffened side structures.

As is the case with the front-to-front simulations, the simulations in this chapter use the mid-sized passenger car and the large SUV that are introduced in Chapter 7.

9.1 Methods

The test and assessment method used for the simulations is described in Chapter 7 and is based on perpendicular front-to-simulations simulations with a large SUV as the striking vehicle with a velocity of 48 km/h and a mid-sized passenger car as the struck vehicle with a velocity of 24 km/h. The front-end homogeneity of the SUV is varied between the simulations using the methods described in the previous chapter and the stiffness car side structure is also varied. The two sections below describe the test matrix and the method used to modify the car side structure.

9.1.1 Test matrix

The matrix in Table 9.1 describes the simulations and includes cross-references to the relevant sections of the discussion. As is the case with the front-to-front collisions described in Table 8.1, Table 9.1 demonstrates the primary findings of the front-to-side simulations and hence several combinations of model variants are omitted in order to focus on the most relevant outcomes.

Four 'standard' simulations, which form the core of the test matrix, are highlighted in yellow in Table 9.1. In the first two of these simulations, a vertical and a horizontal homogeneous region 250 mm in height and covering the entire width of the SUV are analysed in collisions with an unmodified model of the car. In the second pair of simulations, the door crossbeams and the B-pillar of the car are stiffened and analysed in collisions with the 'basis' SUV model.

Additional changes to the SUV model are simulated to determine the effect

Table 9.1: Front-to-side collision simulations: Test matrix including cross references to the discussion.

SUV shield homogeneity:	**Horizontal**		**Vertical**		**Basis model**
SUV shield width:	**Wide**	**Narrow**	**Entire vehicle width**		**SUV without crossbeam**
SUV shield height:	**250 mm**	**250 mm**	**250 mm**	**500 mm**	
Basis car side structure	Section 9.3 Section 9.5.1 Section 9.6.1 Figure 9.3 Figure 9.7	Section 9.3.1 Figure 9.3	Section 9.4 Section 9.5.2 Section 9.6.2 Figure 9.4 Figure 9.8	Section 9.4.1 Figure 9.4	Section 9.3 Section 9.4 Section 9.5 Section 9.6 Figure 9.5 Figure 9.6
Car side structure with stiffened door crossbeams	Section 9.5.1	–	Section 9.5.2	–	Section 9.5 Figure 9.5
Car side structure with stiffened B-pillar	Section 9.6.1 Figure 9.7	–	Section 9.6.2 Figure 9.8	–	Section 9.6 Figure 9.6

of a 500 mm high vertically homogeneous region and a 'narrow' horizontally homogeneous region that only extends between the SUV's longitudinals. The combined effects of the homogeneous SUV front-ends and the stiffened car side are also investigated.

9.1.2 Modelling of side structural changes

The side structures of the passenger car are modified using more conventional measures than those applied to the front-end in Chapter 8. Rather than modelling perfectly homogeneous shields in the side of the passenger car structure, simple modifications are made to the stiffness of load bearing structures in the region deformed by the colliding SUV. The construction of an additional homogeneous shield in the side of the car is unnecessary, since the presence of a shield in the front-end of the SUV already ensures a homogeneous collision interface. An additional shield would only increase the area of the homogeneous region, which is already highly hypothetical. As highlighted in Figure 9.1, the structures selected for modification are the door crossbeams and the B-pillar, both of which are commonly optimised for collision performance in the normal vehicle design process (Seiffert & Wech 2003).

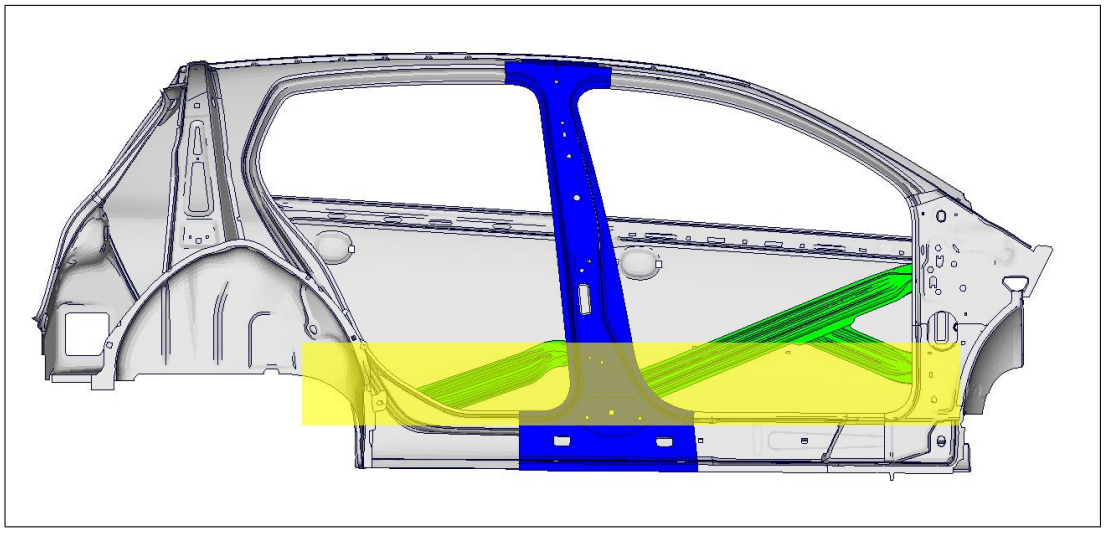

Figure 9.1: Stiffened side crossbeams (green) and stiffened B-pillar (blue) as used in front-to-side collision simulations. The alignment of the 250 mm high, wide shield at the initial point of contact is highlighted in yellow.

Other structures, including the A-pillar, C-pillar, window sill crossbeams, sill, and floor structure, are also relevant for an analysis of occupant protection in side collisions (Kersten 2004). However, these structures are excluded from the scope because they are unlikely to produce complementary effects with the horizontally and vertically homogeneous shields at the alignment shown in Figure 9.1.

To achieve the increases in component stiffness, the thicknesses of the components are increased by a factor of two.[84] In addition to the model variant with stiffened crossbeams and the model variant with a stiffened B-pillar, an unmodified basis model of the passenger car is also used in the front-to-side simulations.

In Sections 9.3 to 9.6, figures showing the main load paths, floor, and side frame of the car and the ideal homogeneous shields, main load paths, engine, wheels, and bulkhead of the SUV are used to highlight the interaction between the two vehicles. In Figure 9.2, the location and pre-collision geometry of these components is shown within the total vehicle structure.

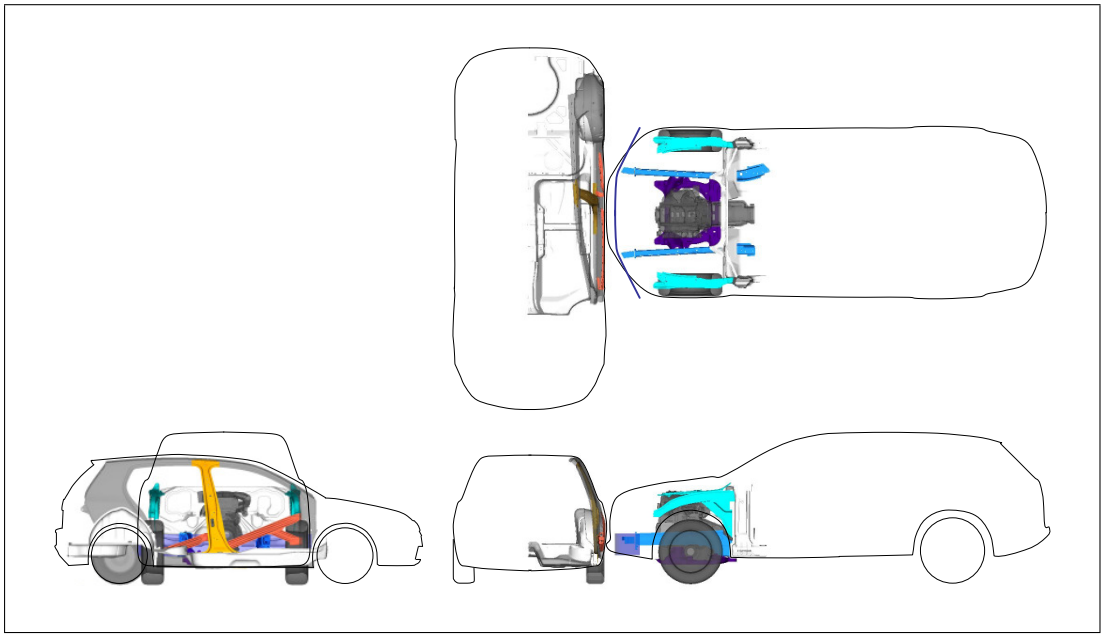

Figure 9.2: Geometry of the large SUV and the mid-sized passenger car prior to the front-to-side collision simulation. The ideal homogeneous shields, main load paths, engine, wheels, floor, bulkhead, and side frame are visible within the outlines of the vehicles.

[84] Changes to material strengths and the moduli of elasticity were also investigated, but the results were considered to be unsatisfactory because there was neither a substantial effect on the MMR nor an observable change in structural interaction.

9.2 Simulation results

The results of the front-to-side simulations are summarised in Table 9.2 and are discussed further in Sections 9.3 to 9.6.

Table 9.2: Results of front-to-side collision simulations between various variants of a large SUV and a mid-sized passenger car. The SUV has an initial velocity of 48 km/h and collides frontally with the side of the passenger car, which has an initial forwards velocity of 24 km/h. The shields represent the maximum theoretical performance for vertically homogeneous or horizontally homogeneous vehicle front-end structures.

SUV shield properties			**Car** $E\Delta v$ **(km/h)**	**SUV** $E\Delta v$ **(km/h)**	**Collision MMR**
Homogeneity	**Height**	**Width**			
Basis model car with:					
Basis SUV[a]	–	–	33.8	17.5	6.60‰
Horizontal	250 mm	Wide	28.9	19.4	2.68‰
Horizontal	250 mm	Narrow	36.3	15.8	9.86‰
Vertical	250 mm	Wide	29.7	16.3	3.13‰
Vertical	500 mm	Wide	29.3	17.3	2.86‰
Car with stiffened side crossbeams with:					
Basis SUV	–	–	30.6	16.9	3.71‰
Horizontal	250 mm	Wide	26.9	16.0	1.74‰
Vertical	250 mm	Wide	29.2	16.0	2.84‰
Car with stiffened B-pillar with:					
Basis SUV	–	–	31.8	19.6	4.64‰
Horizontal	250 mm	Wide	26.8	15.4	1.71‰
Vertical	250 mm	Wide	26.5	18.0	1.60‰

[a] Basis model SUV without homogeneous shield and without bumper crossbeam.

The maximum compartment deformation measured in the SUV is 3.5 mm, and the maximum mortality rate calculated for the SUV occupants is 0.001‰. These results show that the $E\Delta v$ measured in the SUV has effectively no influence on the collision Mean Mortality Rate (MMR), and hence the discussion in the following sections is focussed on the results in the passenger car.

9.3 Discussion: Front-end horizontal homogeneity

Horizontal homogeneity is analysed using a 250 mm high shield covering the entire width of the SUV's front-end. In comparison to the basis simulation, a substantial reduction in the mortality rate is measured, but the result remains higher than the nominal mortality rate for the collision.

In the basis simulation, the left longitudinal of the SUV interacts with the crossbeam in the front door of the car, but the right longitudinal and rear door crossbeam do not interact. As a consequence, high levels of local deformation occur in the rear door, which are also reflected in the rear passenger measurement points. The absence of the bumper crossbeam in the SUV results in reduced loading of the lower B-pillar, but the height of the SUV in comparison to the car results in higher levels of deformation at the window sill level.

At the initial point of contact, the horizontally homogeneous shield spreads the collision forces from just behind the A-pillar to the rear wheel of the car, although the loading of the A-pillar reduces as the car continues its forwards motion. This means that the deformation of the car structure is spread between the door crossbeams and the A-pillar, B-pillar, and C-pillar, and due to the additional deformation energy dissipated by the A-pillar and C-pillar, the deformation in the proximity of the occupants is reduced significantly. Only the deformation at the middle B-pillar point remains practically unchanged, since the reduction in loading caused by the distribution of forces to the A-pillar and C-pillar is balanced by the increase in loading caused by the horizontal homogeneity between the SUV's longitudinals. In sum though, the distribution of the deformation achieved by the horizontally homogeneous shield leads to a substantial reduction in the car's $_{E}\Delta v$.

9.3.1 Alternative width of homogeneous region

The use of a horizontally homogeneous shield covering the entire width of the SUV means that forces are distributed to the A-pillar and C-pillar of the car and

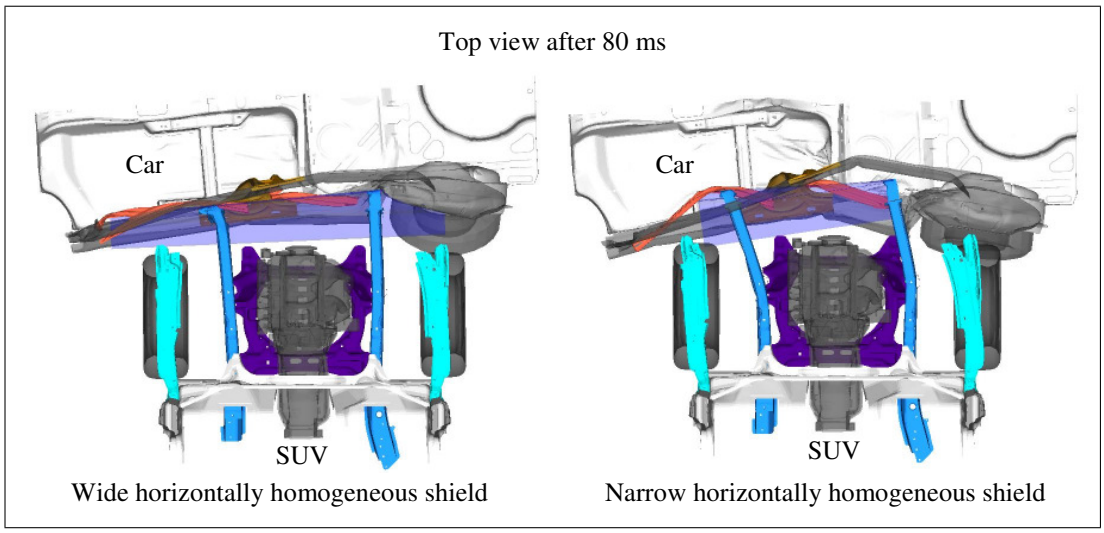

Figure 9.3: Horizontal homogeneity in a front-to-side collision simulation between a car and SUV. The ideal homogeneous shields, main load paths, engine, wheels, floor, bulkhead, and side frame are visible. The narrow shield results in more deformation in the passenger compartment than the wide shield.

away from the occupants. Although this is beneficial, in some cases an increase in horizontal homogeneity may only affect the space between the A- and C-pillars. To test this case, a 250 mm high shield covering only the space between the longitudinals of the SUV is also simulated. In comparison to both the simulation with the wide shield and the basis simulation, the simulation with the narrow shield leads to a substantial increase in the MMR.

As shown in Figure 9.3, with the limited width of the horizontally homogeneous shield, the additional loading of the A- and C-pillars of the car no longer arises, and the deformation is limited to the B-pillar and doors. In comparison to the wide shield, the narrow shield produces higher levels of deformation in the proximity of the occupants and a corresponding increase in the car's $_E\Delta v$. In comparison to the basis simulation, the narrow shield produces less deformation of the rear door but increased deformation of the front door and the B-pillar. The increase in deformation in the proximity of the driver is similar to the decrease in deformation in the proximity of the rear passenger, but the calculation of the $_E\Delta v$ is intentionally biased towards the front seat occupant, and hence this is assessed negatively.

Therefore, although horizontal homogeneity is beneficial when it leads to the distribution of loading to the A- and C-pillars, it is detrimental when the deformation is only focussed on the B-pillar. The simulations show that a vehicle without a bumper crossbeam would be particularly aggressive in a front-to-side collision if its longitudinals were to be aligned with the occupants of the collision partner. On the other hand, they also suggest that a vehicle with a front-end that is horizontally homogeneous over a narrow region would be aggressive in a broader range of front-to-side collisions since the narrow homogeneous region would more frequently align with the B-pillar.

Definitive conclusions regarding the width of the horizontally homogeneous region are limited by two factors. Firstly, the deformation points used for the assessment are biased with regards to B-pillar deformation, and the negative result calculated here may not relate to an increase in occupant injury risk in real accidents. Further research is therefore recommended to more precisely define the deformation points for use in the compatibility measurement procedure. Secondly, the result may reflect a need to synchronise increases in both horizontal homogeneity and B-pillar stiffness to avoid overloading the B-pillar. This is addressed in more detail in Section 9.6.

9.4 Discussion: Front-end vertical homogeneity

Vertical homogeneity is also analysed using a 250 mm high shield covering the entire width of the SUV's front-end. In comparison to the basis simulation, a substantial reduction in the mortality rate is measured, but the result again remains higher than the nominal mortality rate for the collision.

In the basis simulation, no interaction occurs between the SUV's longitudinals and the sill of the car. With the addition of the vertically homogeneous shield, only a slight degree of interaction occurs before the shield is pushed over the sill by the force of the SUV's longitudinals. As a result of the shield, interaction occurs between the right longitudinal and the structure below the rear

passenger seat, which is effectively a raised section of the vehicle floor. The deformation of the floor structure leads to a reduction in the load transferred to the B-pillar and rear door and hence a reduction in the car's $E\Delta v$.

9.4.1 Alternative height of homogeneous region

The benefit of the 250 mm high shield arises because it enables the transfer of loads to the car floor structure. However, due to a lack of overlap between the shield and the sill, the maximum potential of a vertically homogeneous structure is not realised. Therefore, a 500 mm high shield is also simulated, which lowers the bottom edge of the homogeneous region from 330 mm to 205 mm of ground clearance. The prohibitive effect that this would have on the off-road functionality of the SUV is ignored for the purposes of this analysis. In comparison to the simulation with the 250 mm high shield, the simulation with the 500 mm high shield leads to a slight decrease in the MMR, which still remains higher than the nominal MMR for the collision.

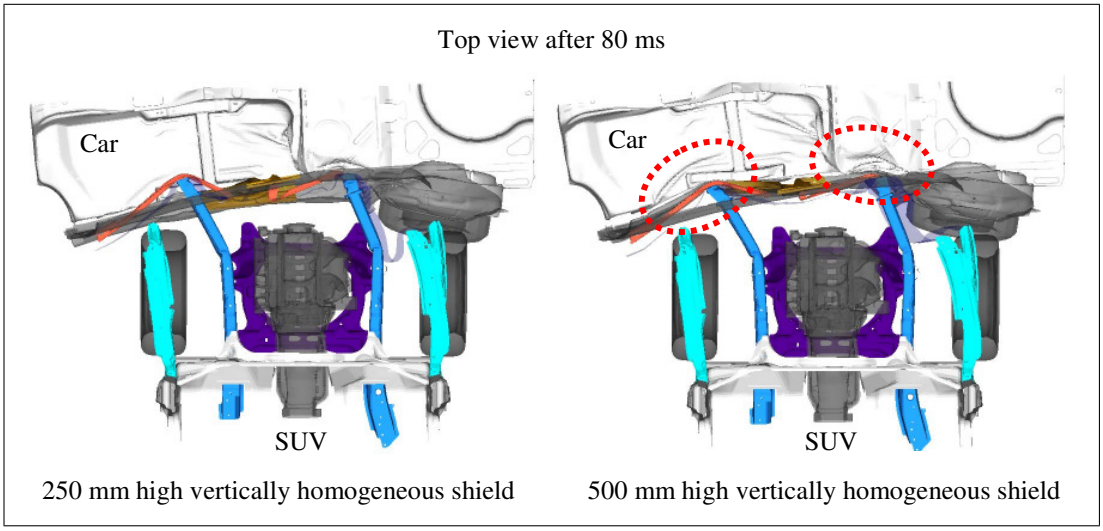

Figure 9.4: Vertical homogeneity in a front-to-side collision simulation between a car and SUV. The ideal homogeneous shields, main load paths, engine, wheels, floor, bulkhead, and side frame are visible. The 500 mm high shield interacts with the sill and induces more deformation in the floor structure.

The additional 125 mm of depth has the desired effect and both the left and right longitudinals of the SUV interact with the car's door sills. This leads to an

increase in the deformation of the car floor and a reduction in the deformation of the doors and B-pillar. In comparison to the 250 mm high shield, reduced deformation is measured at all but two of the measurement points: the lower B-pillar and the driver door middle. The increase in deformation measured at the lower B-pillar does not relate to an increase in loading at that point, but rather as a result of the increased loading of the sill on either side of the B-pillar. Rather than the loading coming externally from the SUV, the lower B-pillar is essentially pulled in towards the occupants by the deformation of the sill.

In comparison to the basis simulation, both the 250 mm high and 500 mm high vertically homogeneous shields induce increased levels of deformation at the lower measurement points. Although the overall result is positive for the car's occupants, these results indicate that increased attention may need to be directed towards the protection of the pelvis region in side collisions if the vertical homogeneity of front-end structures is increased.

The general conclusion that can be drawn from these simulations, and that reflects the results of previous research on front-to-side collisions (for example Wykes et al. 1998, Thompson et al. 2007), is that increased loading of the sill and floor is beneficial in a front-to-side collision. However, according to the compatibility measurement procedure described in Chapter 7, the difference between the results with the 250 mm shield and the 500 mm shield are equivalent to a change in Δv of less than 0.5 km/h. Hence, specifically with regards to the negative effect that the reduced ground clearance would have on the functionality of off-road vehicles, the additional height of the 500 mm shield may not be justified.

9.5 Discussion: Stiffened door crossbeams

The effect of stiffened door crossbeams is investigated using the basis SUV model without a bumper crossbeam. Compared to the basis simulation with the unmod-

ified car model, the stiffened door crossbeams lead to a reduction in the mean mortality rate.

No significant change in the vehicles' interaction can be observed, but, as shown in Figure 9.5, the stiffening of the car's crossbeams results in reduced deformation of the door crossbeams and also the B-pillar.

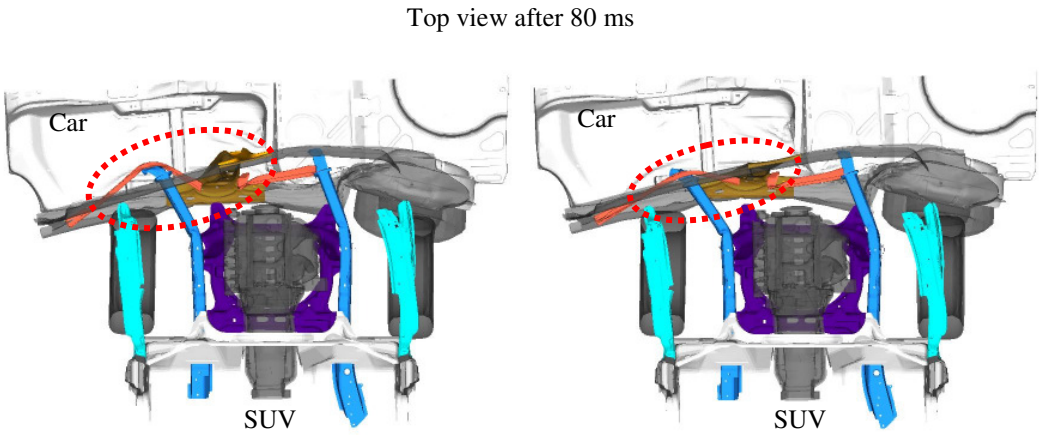

Figure 9.5: Effect of stiffened door crossbeams in a front-to-side collision simulation between a car and SUV. The main load paths, engine, wheels, floor, bulkhead, and side frame are visible. The difference in the deformations observed at the driver's door crossbeam and at the B-pillar are shown.

9.5.1 Effect of horizontally homogeneous front-end

The effect of stiffened door crossbeams in combination with a horizontally homogeneous front-end is investigated using the SUV model with the 250 mm high shield covering the entire width of the SUV's front-end. This combination of vehicle modifications leads to a lower MMR than either of the modifications achieve alone. Since the MMR in this simulation is less than the nominal rate of 2.0‰, it satisfies the definition of a compatible collision from Chapter 6.

The stiffened crossbeams reduce the overall deformation of the car side in comparison to the simulation with just the horizontally homogeneous front-end and hence slightly reduce the degree to which the SUV overrides the sill of the car.

The combination of a horizontally homogeneous front-end with stiffened door crossbeams is not complementary. This observation is based on a comparison of the car's $_E\Delta v$ and the MMR in the basis simulation, the simulation with stiffened door crossbeams, the simulation with a horizontally homogeneous front-end, and the simulation with both the stiffened door crossbeams and the horizontally homogeneous front-end. The addition of the stiffened crossbeams leads to a 9% reduction in the car's $_E\Delta v$ compared to the basis simulation, but the addition of the stiffened crossbeams to the simulation with the horizontally homogeneous front-end only leads to a 7% reduction. Similarly, the addition of the horizontally homogeneous front-end leads to a 14% reduction in the car's $_E\Delta v$ compared to the basis simulation, but the addition of the horizontally homogeneous front-end to the simulation with the stiffened crossbeams only leads to a 12% reduction.

9.5.2 Effect of vertically homogeneous front-end

The effect of stiffened door crossbeams in combination with a vertically homogeneous front-end is also investigated using the SUV model with the 250 mm high shield covering the entire width of the SUV's front-end. This combination of vehicle modifications leads to a lower MMR than either of the modifications achieve alone. The result is also almost identical to the simulation with the unmodified crossbeams and the 500 mm high vertically homogeneous shield.

In combination with the vertically homogeneous shield, the stiffened crossbeams increase the forces that are transferred to the lower B-pillar and upper A-pillar, which are where the front door crossbeam is attached. This results in reduced loading of the middle and upper parts of the B-pillar and a corresponding decrease in the car's $_E\Delta v$.

Using the approach described in the previous section, it can be determined that the effects of the stiffened door crossbeams with the vertically homogeneous shield are not complementary.

9.6 Discussion: Stiffened B-pillar

The effect of a stiffened B-pillar is investigated using the basis SUV model without a bumper crossbeam. Compared to the basis simulation with the unmodified car model, the stiffened B-pillar leads to a reduction in the mean mortality rate.

During the first half of the collision, the increased stiffness of the B-pillar results in an overall reduction of the car's deformation. However, approximately 50 ms after the initial point of contact between the vehicles, the force being transferred through the B-pillar and into the roof and floor begins to overload these load paths. Hence, as shown in Figure 9.6, the final deformations observed at the sill and roof are greater than those in the baseline simulation. However, the high stiffness of the B-pillar enables it to maintain its outwardly bowed profile, which results in generally lowered deformation measures and hence a lower $E\Delta v$.

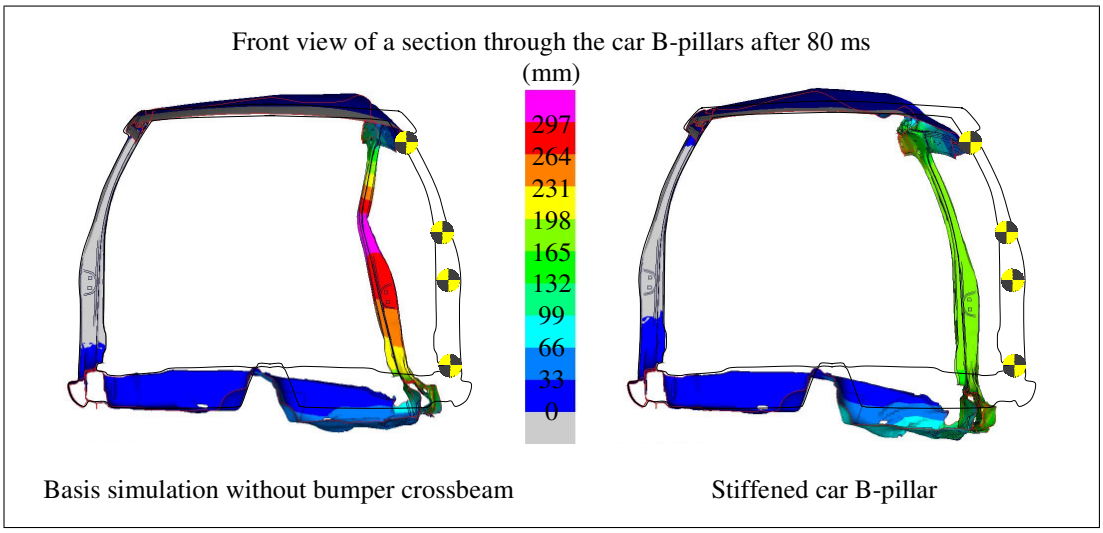

Figure 9.6: Effect of stiffened B-pillar in a front-to-side collision simulation between a car and SUV. A section through the B-pillars of the car is shown, with the original profile of the structure being shown as an outline. The B-pillar measurement points, as defined in Figure 7.2b, are also shown in their original positions. The colours indicate the deformation of the structure in the y-axis (sidewards) direction.

9.6.1 Effect of horizontally homogeneous front-end

The effect of a stiffened B-Pillar in combination with a horizontally homogeneous front-end is investigated using the SUV model with the 250 mm high shield covering the entire width of the SUV's front-end. This combination of vehicle modifications leads to a lower MMR than either of the modifications achieve alone. Since the MMR in this simulation is less than the nominal rate of 2.0‰, it satisfies the definition of a compatible collision from Chapter 6.

The benefit of horizontal homogeneity is identified in Section 9.3 as the ability to transfer loads to the A- and C-pillars away from the car occupants. With the stiffened B-pillar, the horizontally homogeneous shield deforms all three pillars to a lesser degree, and hence a benefit is measured for both the front and rear seat occupants. The reduction in B-pillar deformations occurs both with and without the horizontally homogeneous shield, but the introduction of the shield also results in a complementary reduction in the deformations measured in the proximity of the rear passenger, as shown in Figure 9.7.

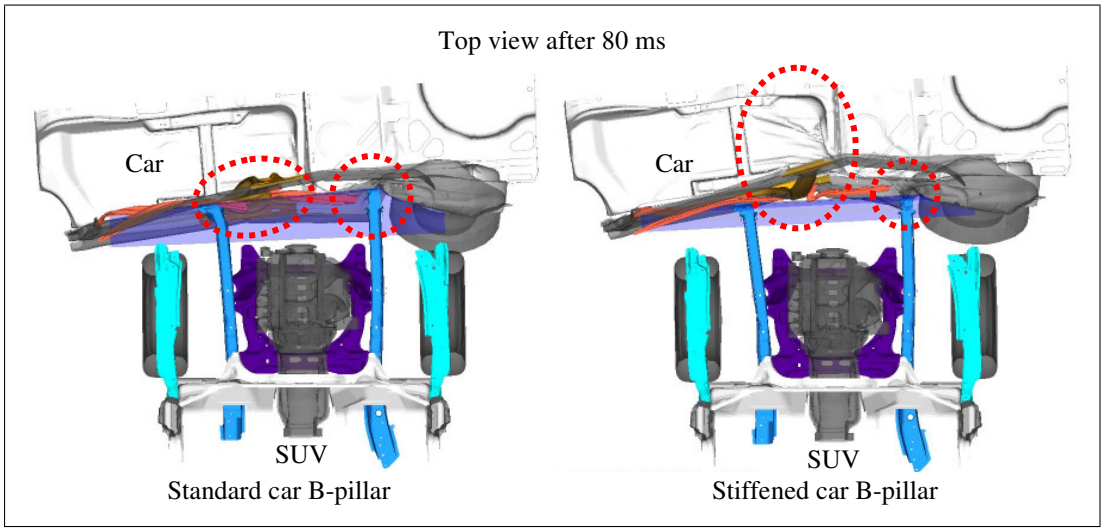

Figure 9.7: Effect of stiffened B-pillar in combination with horizontal homogeneity in a front-to-side collision simulation between a car and SUV. The ideal homogeneous shields, main load paths, engine, wheels, floor, bulkhead, and side frame are visible. The changed deformation pattern of the B-pillar and increased deformation of the sill and floor are highlighted. The corresponding reduction in deformation in alignment with the rear seat occupant is also highlighted.

The combination of the stiffened B-pillar with the horizontally homogeneous shield is complementary according the approach described in Section 9.5.1. The addition of the stiffened B-pillar to the simulation with the horizontally homogeneous front-end leads to a greater reduction in the car's $_E\Delta v$ than its addition to the basis simulation. Similarly, the addition of the horizontally homogeneous front-end to the simulation with the stiffened B-pillar leads to a greater reduction in the car's $_E\Delta v$ than its addition to the basis simulation.

9.6.2 Effect of vertically homogeneous front-end

The effect of a stiffened B-pillar in combination with a vertically homogeneous front-end is also investigated using the SUV model with the 250 mm high shield covering the entire width of the SUV's front-end. This combination of vehicle modifications leads to the lowest MMR observed in any of the simulations.

In Figure 9.1, it can be seen that the stiffened component in the B-pillar also extends into the sill. In the simulation involving the vertically homogeneous front-end, the stiffening of the sill results in it being deformed over a broader area. Hence, the benefit of vertical homogeneity, which is identified in Section 9.4

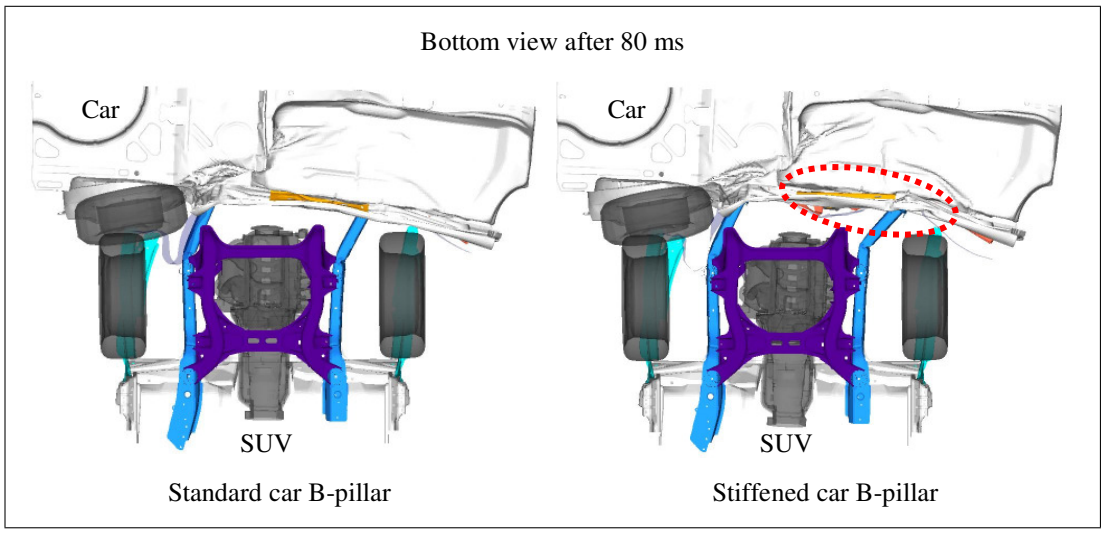

Figure 9.8: Effect of stiffened B-pillar in combination with vertical homogeneity in a front-to-side collision simulation between a car and SUV. The ideal homogeneous shields, main load paths, engine, wheels, floor, bulkhead, and side frame are visible. The increased deformation of the floor and the sill is highlighted.

as the ability to transfer loads to the sill and floor of the car, is increased.

Although the result described in this section does not directly address the effect of combining vertical homogeneity with a stiffer B-pillar, this combination is not addressed in any further detail. The increased stiffness could be limited to the B-pillar above the sill, but this would not reflect the function of the B-pillar, which is to transfer loads to the sill and roof. Further alternatives to model increased B-pillar stiffness without increased sill stiffness are not addressed.

The combination of the stiffened sill with the vertically homogeneous shield is complementary according to the approach described in Section 9.5.1.

Chapter summary

Front-to-side collision simulations are analysed using variants of a mid-sized passenger car and a large SUV, and the compatibility measurement procedure from Chapter 7 is used to assess whether the collisions are compatible according to the definition from Chapter 6. Compatible results are observed with the combination of ideal horizontal homogeneity and either a stiffened B-pillar or stiffened door crossbeams, and the lowest MMR is measured for the combination of vertical homogeneity with a stiffened sill.

In Section 9.3, it is shown that a horizontally homogeneous front-end is effective when loads are transferred to the A- and C-pillars, but may be detrimental when the loads are only focussed on the (unmodified) B-pillar. In Section 9.4, it is shown that the benefit of a vertically homogeneous front-end is derived from the transfer of collision forces to the sill and floor.

In Section 9.5, it is shown that stiffened door crossbeams have the positive effect of reducing the deformation of the vehicle side. However, the effects are not complementary with either the horizontally or the vertically homogeneous shields.

Finally, in Section 9.6, it is shown that a stiffened B-pillar is also effective at reducing the deformation of the vehicle side. The combination of a horizontally

homogeneous front-end and a stiffened B-pillar has a complementary effect on reducing the collision MMR. This suggests that design changes to increase both front-end horizontal homogeneity and B-pillar stiffness should be synchronised for maximum benefit. In the simulation involving the vertically homogeneous front-end, the principal effect of the stiffened B-pillar arises due to the stiffening of the car sill. The combination of the stiffened sill with the vertically homogeneous front-end has a complementary effect on reducing the collision MMR and also produces the lowest MMR of all simulations in this chapter.

In Chapter 5, it is shown that the mean risk of injury in front-to-side collisions is dependent on the mass ratio of the colliding vehicles, and it is hence concluded that collisions between vehicles with unequal masses are incompatible. In this chapter, simulations are performed with vehicles with a mass ratio of 1:1.9, and it is shown that changes to the front-end structure of the striking vehicle in combination with changes to the side structure of the struck vehicle can lead to a compatible result.

The robustness of the compatibility measurement procedure is not as strenuously tested in the front-to-side collision configuration, since the severity of the collision configuration results in the measurements from the SUV being practically irrelevant. However, the results do indicate the robustness of the method with regards to the objective assessment of benefits and disbenefits at different measurement points within the car: For example, the balance between deformation at upper and lower measurement points and between deformation affecting the front and rear seat occupants. However, there is some doubt whether the deformation pattern observed in Section 9.3.1 correlates with the real injury risk, and hence further research is recommended to more precisely define the deformation points for use in the compatibility measurement procedure.

Chapter 10

Assessment of Vehicle Compatibility

Regulation and consumer crash tests provide a method for assessing vehicle structures and either ensuring a minimum level of safety, in the case of regulatory tests, or encouraging higher levels of safety, in the case of consumer tests. Due to the complexity of the accident environment, many different tests and assessment procedures are performed to reproduce different collision types and conditions and to rate performance according to various criteria. Additional tests represent additional cost and provide diminishing returns. Therefore, the minimum number of tests are sought that are representative of the accident environment.

The objective of this chapter is to discuss the requirements for front and side test procedures based on the results from the preceding chapters, to assess existing test procedures and proposals, and to propose alternatives. In essence, the aim of this chapter is the application of the knowledge gained to improve vehicle safety.

10.1 Frontal assessment requirements

The results in this thesis identify several properties of frontal passenger vehicle collisions that are relevant for vehicle assessment. The configuration and severity

of frontal collisions are investigated in Chapters 4 and 5, the concepts underlying the nature of compatibility are discussed in Chapter 6, and the behaviour of homogeneous structures is analysed in Chapters 8 and 9. In this section, the main findings are summarised regarding the requirements for a frontal test procedure for the assessment of self and partner-protection.

10.1.1 Test configuration

The statistical analysis in Chapter 4 shows that collisions with other passenger vehicles are responsible for approximately 50% of MAIS 2+ injuries to belted passenger vehicle occupants in frontal collisions. But it also shows that approximately 20% are injured in frontal collisions with poles, posts, and trees, 10% in collisions with walls and barriers, and 10% in collisions with commercial vehicles. In front-to-front collisions between two passenger vehicles, the most frequent collision configurations are the full overlap configuration and the driver's side offset configuration with 33% to 66% overlap. In Chapter 5, it is shown that the most frequent front-to-side collision configuration involves full overlap of the vehicle front-end.

10.1.2 Test severity

The analysis of collision velocity in Chapter 4 shows that a Δv of 64 km/h, which corresponds to a test velocity of 56 km/h, results in a 20‰ mortality rate amongst belted passenger vehicle occupants, but it also shows that 75% of MAIS 3 injuries, which are associated with a 42‰ mortality rate, occur at Δv values less than 60 km/h. The results in Chapter 5 indicate that the velocities relevant to the analysis of partner-protection in front-to-side collisions are lower than the velocities found to be relevant for self-protection in front-to-front collisions. Selecting a test velocity is therefore a compromise between the lower speeds at which the frequency of injuries is greater and the higher speeds at which the probability of injury is greater.

10.1.3 Force-deformation compatibility

In Chapter 6, it is concluded that the force-deformation relationships of all vehicles should result in an equivalent level of occupant protection in any single vehicle collision. For vehicle-to-vehicle collisions, the force-deformation relationships of all vehicles should be optimised so that the mean risk of injury in any collision is independent of the type, size, and weight of either vehicle. Therefore, front-end deformation forces may differ between vehicle designs, but all vehicles should have a passenger compartment strength that is sufficient to deform the front-ends of all other passenger vehicles. This is in essence the 'bulkhead principle' (Zobel 1998).

It is often noted that the forces measured in vehicle-to-barrier tests are directly proportional to the test vehicles' masses (see for example Thomson & Edwards 2005, Mizuno et al. 2001). Since vehicle mass is readily available in accident statistics, its analysis is useful as an indicator of force-deformation compatibility. The analysis of mass ratio in Chapter 4 shows that the mean risk of injury in front-to-front collisions is independent of mass, and recent research by Chauvel et al. (2009) found that the risk of injury in single vehicle frontal collisions is also independent of mass. A clear need to address the issue of force-deformation compatibility, beyond that which is already achieved with the current requirements, is therefore not apparent.

10.1.4 Homogeneity

In Chapters 8 and 9, it is shown that horizontal homogeneity is beneficial in both front-to-front and front-to-side collisions and that it is also more effective when distributed over a wider region of the vehicle's front-end. The analysis of vertical homogeneity shows that all vehicles should be designed to achieve a common vertical alignment of primary structures, but that increasing the range of an interaction zone has only marginal additional benefit if interaction between the primary load paths is already achieved.

10.2 Fixed frontal barrier assessment approach

In this section, proposals are put forward for the assessment of frontal structures using fixed barriers. In the first three subsections, alternatives are proposed for the assessment of front-end structures, and in the fourth subsection, a proposal is put forward for the assessment of compartment strength. The combination of the compartment strength assessment with one of the front-end alternatives represents a complete assessment of a vehicle's frontal compatibility performance.

The test procedures described in this section apply the same approach to the assessment of front-end forces and deformations as ECE-R94, FMVSS 208, and other similar regulations and NCAP tests: For a given test severity, the front-end must dissipate the vehicle's kinetic energy and the restraint system must manage the compartment accelerations and deformations. Since the accelerations experienced by the ATDs in the compartment are proportional to the forces required to deform the front-end, an indirect limit is placed on the deformation forces by the performance of the restraint system. A direct limit on front-end forces, such as the $K_{W_{400}}$ work stiffness metric (Patel et al. 2007) or the PDB aggressiveness limit (Delannoy et al. 2000), does not take into account the relationship between force, acceleration, and restraint system performance. This type of limit is inappropriate because it regulates a vehicle design characteristic rather than a performance capability (UN-ECE 1998, §4.1.2.2).

10.2.1 Deformable barrier approach

Deformable honeycomb barriers have been used in regulatory test procedures for over 15 years and have been considered for the assessment of compatibility for almost as long. The barrier proposed in Figure 10.1 is based on the FWDB developed by the IHRA Compatibility and Frontal Impact Working Group but uses an adaptation of the progressive barrier stiffness characteristic that is also used in the PDB, AE-MDB, and ECE-R95 barrier.

Like the IHRA FWDB, the proposed barrier has a constant stiffness in the

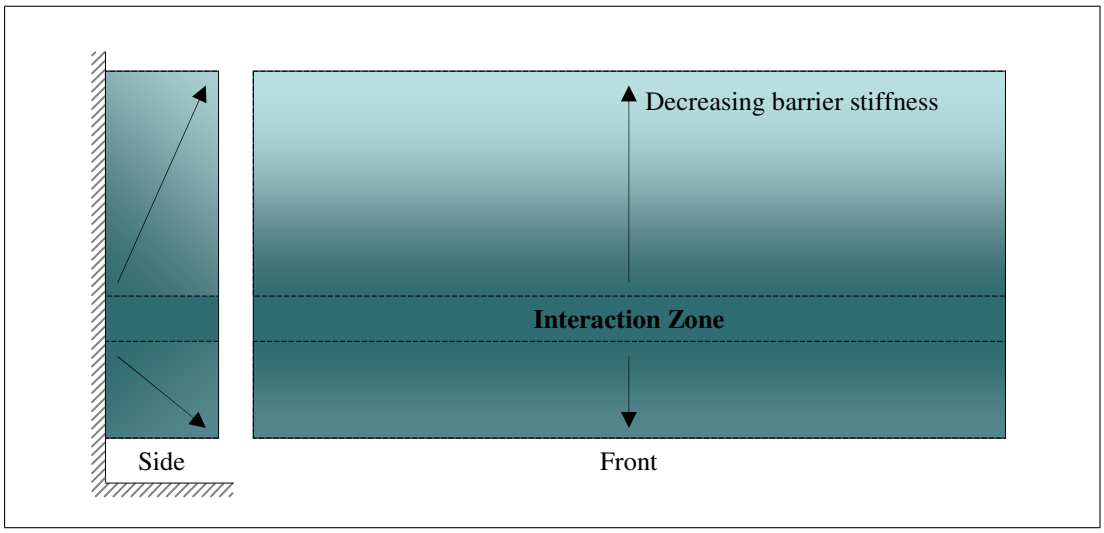

Figure 10.1: Adaptation of the FWDB developed by the IHRA Compatibility and Frontal Impact Working Group with variable stiffness properties in both depth and height to encourage both horizontal homogeneity and vertical alignment of structures.

horizontal direction that applies forces equally across the width of the vehicle. Unlike a rigid barrier, which homogeneously reacts all forces, the proposed barrier therefore encourages horizontally homogeneous vehicle structures that are able to transfer the distributed loading from the barrier back to the primary load paths.

A unique feature of the proposal is a vertical progression in the stiffness of the barrier to encourage the vertical alignment of structures. Contemporary barriers, which have an equal stiffness distribution in the vertical direction, encourage vertical homogeneity but do not influence vertical alignment. The proposed barrier is designed to induce increased deformation in a tested vehicle if its primary load paths are not aligned with the interaction zone, which is the stiffest part of the barrier.

The proposed barrier has two fundamental flaws, which are endemic to all fixed deformable barriers. Firstly, the additional deformation length afforded by a deformable element creates a distinction between the force-deformation characteristics of the front-end and the acceleration pulse that is experienced in the vehicle compartment (Schram 2008). For example, it has been shown that a deep barrier such as the PDB may produce compartment accelerations that are highly

misrepresentative of the front-end structure (VDA 2009). Secondly, a deformable element is capable of dissipating kinetic energy, which reduces the effective severity of the test. For example, it is claimed that the ECE-R94 barrier dissipates about 45 kJ of kinetic energy, which leads to a significant mass dependency in the test procedure (France 2007). In a more extreme case, it has been shown that a 1450 kg vehicle with a very stiff structure can be tested according to the PDB test procedure without dissipating any of its own energy (Lorenz 2008).

To limit the effect of these flaws, it is necessary to limit the depth of the deformable element and ensure that the vehicle contacts the rigid backing plate. However, this also limits the degree to which the proposed barrier can encourage a horizontally homogeneous, vertically aligned structure. It is therefore appropriate to supplement the barrier properties with direct measurements of the vehicle structure.

It is impossible to measure the way a vehicle reacts force using a flat, rigid barrier, and hence the assessment must be based on the force distribution that the vehicle applies to load cells mounted behind the deformable element. This approach has been applied for many alternative metrics for the assessment of homogeneity and vehicle geometry (Summers et al. 2001, Edwards et al. 2003*b*, O'Reilly 2005, Edwards et al. 2007*a*). However, as stated in the literature review, the currently proposed metrics suffer from a multitude of problems.

In order to assess the horizontal homogeneity of a vehicle's force distribution, a development of the *HSI* metric proposed by Edwards et al. (2007*a*), which resolves some of the robustness issues cited by Edwards (2009), is described in Appendix E, and a comparison to the robustness of the *HSI* metric is shown in Figure 10.2. For the three tests with the mid-sized passenger car described in Edwards (2009), the new Homogeneity Criteria (*HC*) determines the horizontal homogeneity of the vehicle to be between 60.2% and 67.6%. Although this still represents a considerable variation, it is a substantial improvement over the *HSI* metrics and comparable to the repeatability of the ATD injury measures in the tests (Edwards 2009, Figure 18).

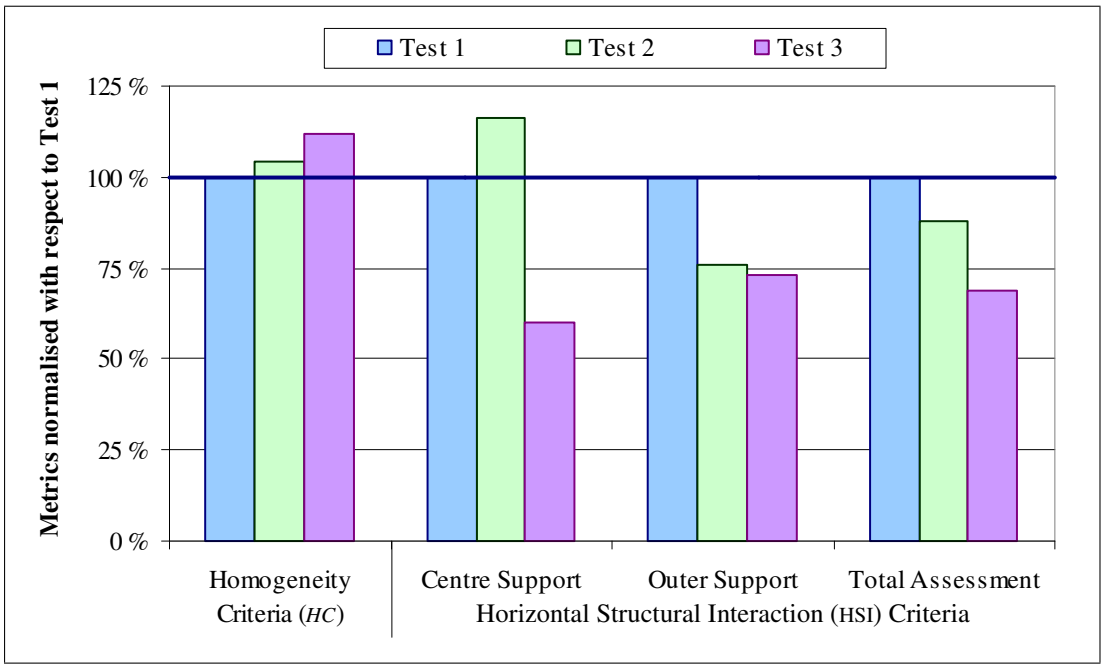

Figure 10.2: Comparison of the repeatability of two horizontal homogeneity metrics using test data from the APROSYS project (Edwards 2009).

The full overlap configuration is used for the proposed barrier, since this ensures the maximum loading on the restraint system for the assessment of the force-deformation relationship. The full overlap configuration also allows for the assessment of horizontal homogeneity over the complete width of the vehicle and without the interference of vehicle rotation.

10.2.2 Hydraulic barrier approach

The inherent problems of both rigid and deformable barriers can be overcome by constructing a barrier that deforms without dissipating energy. The hydraulic barrier concept in Figure 10.3 is capable of achieving this goal.

The barrier face with which the vehicle collides consists of many separate contact plates that are able to move forwards and backwards when loaded. Each contact plate is mounted on a hydraulic cylinder, which is filled with incompressible fluid and connected to all of the other cylinders so that they all share a common pressure. Therefore, if one of the plates is pushed backwards, all of the other plates move slightly forwards.

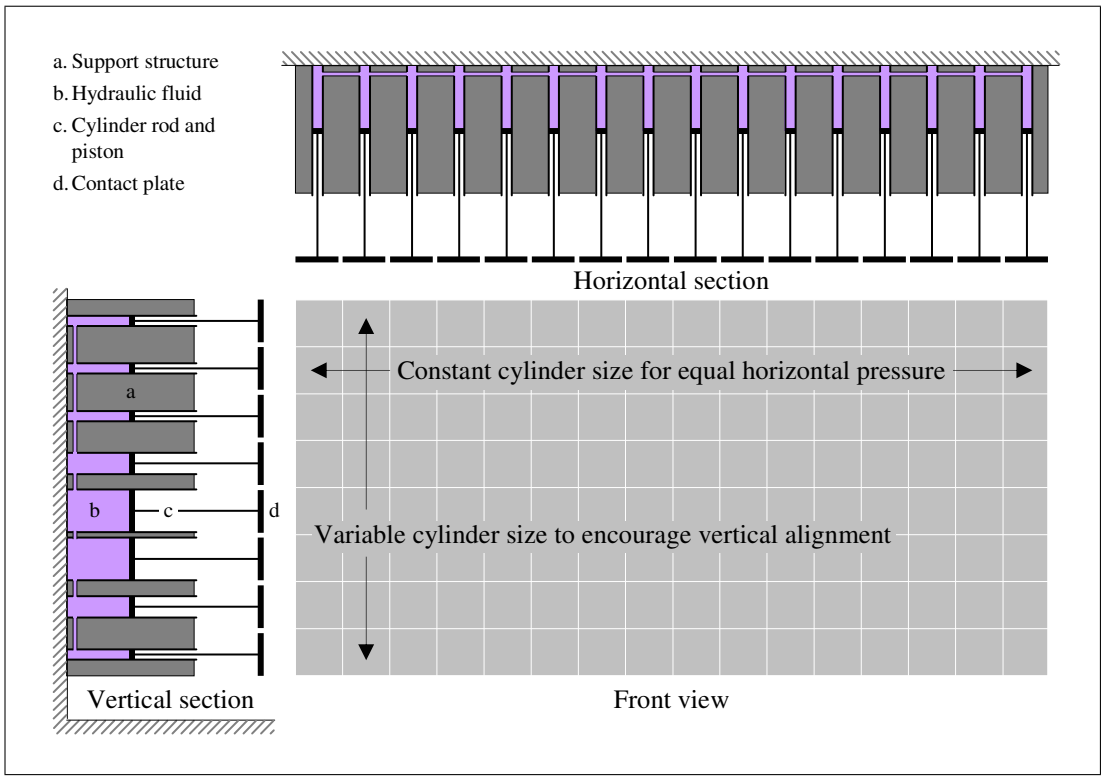

Figure 10.3: Barrier composed of movable plates supported by interconnected hydraulic cylinders of various sizes. Equal pressure present throughout the system results in differing displacement of the movable plates according to the forces applied and the size of the respective cylinder. Incompressible hydraulic fluid ensures that the barrier dissipates minimal energy and the severity is independent of vehicle mass.

The force applied by a hydraulic piston is a product of the pressure in the fluid and the area of the cylinder head. Therefore, by varying the cylinder sizes, a stiffness distribution can be achieved that encourages the vertical alignment of primary structures. By maintaining a constant cylinder size in the horizontal direction, the forces applied to a vehicle structure are equal across its width, and hence horizontal homogeneity would be encouraged. The encouragement of vertical alignment and horizontal homogeneity can be achieved without a direct assessment of the barrier forces and deformations, since an inhomogeneous vehicle design induces an inhomogeneous reaction from the barrier's cylinders. This acts aggressively towards the test vehicle and hence increases the ATD injury measures. Therefore, a hydraulic barrier enables the assessment of self-protection, vertical alignment, horizontal homogeneity, and, as described in Section 10.2, the test

vehicle's force-deformation characteristics simply by measuring the ATD injury values.

Schwarz (2002) proposed a similar hydraulic barrier concept that used independently defined force-deformation characteristics for each cylinder to create a stiffness distribution similar to a passenger vehicle front-end. However, the concept proposed by Schwarz is similar to a deformable barrier in that the displacement of the contact plates results in the dissipation of energy. With the concept described in Figure 10.3, the hydraulic fluid can only be transferred between cylinders, and hence the dissipation of energy is minimal.[85]

The barrier design in Figure 10.3 is only a concept and hence excludes details such as cylinder diameters and stroke. These and various other technical and practical issues need to be investigated before the construction of even a prototype barrier can be considered. The cost, maintenance, and performance of a hydraulic barrier also needs to be compared to those of conventional deformable barriers to determine the suitability of the concept for widespread application.

10.2.3 Intrinsic homogeneity assessments

Although the deformable barrier and hydraulic barrier approaches represent an improvement over current proposals, they do not achieve the full potential identified with the perfect shields in Chapters 8 and 9. Neither approach can ensure that vehicle structures are horizontally homogeneous and do not simply have an equal horizontal stiffness distribution. Hence, the interaction with the longitudinal beyond the collision overlap, which is observed in the 33% overlap collision in Figure 8.6, and the interaction with the A-pillar, B-pillar, and C-pillar in the front-to-side collision in Figure 9.3 cannot be guaranteed. Also, neither approach can ensure that the vertically aligned structures actually interact without override or underride, and hence the complete benefit observed in the front-to-front

[85] Energy is dissipated by friction and the work required to displace the masses of the contact plates, cylinder rods, and hydraulic fluid.

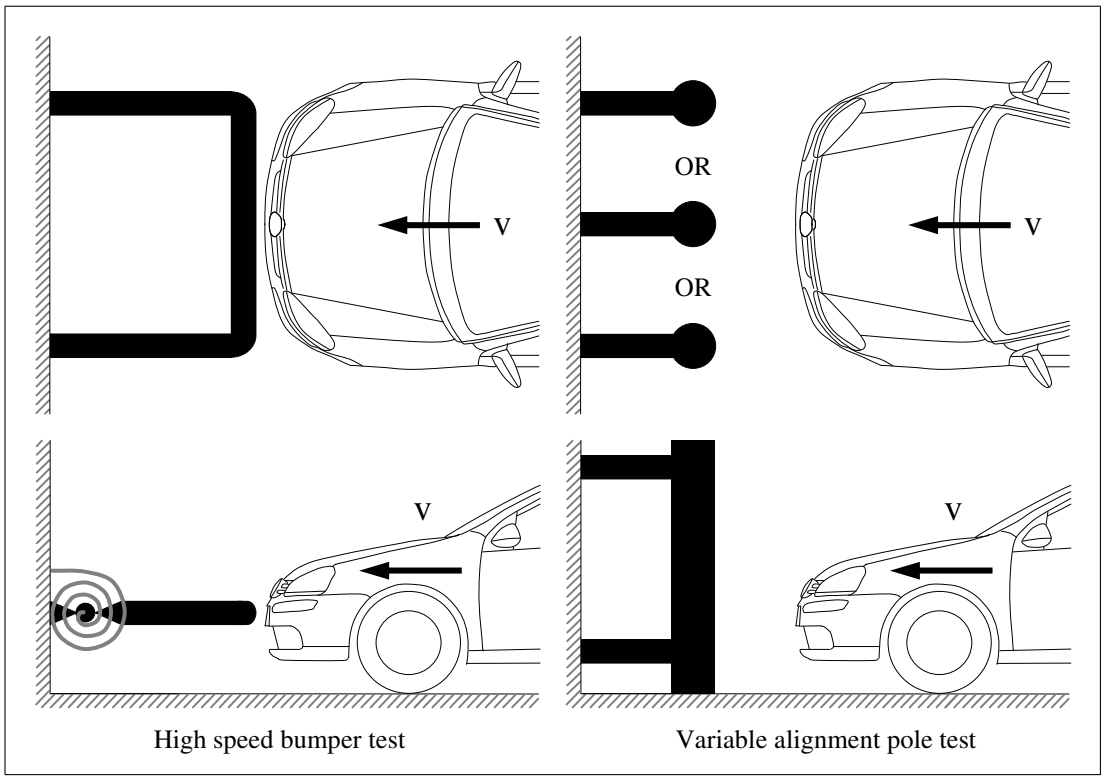

Figure 10.4: High speed bumper test with vertical instability to encourage vertical alignment of vehicle structures (left). Pole test with multiple alignments to ensure horizontal homogeneity of vehicle structures (right).

collision in Figure 8.7 also cannot be guaranteed. The testing approach shown in Figure 10.4 is therefore proposed as an alternative to the deformable barrier and hydraulic barrier approaches. Like the hydraulic barrier approach, the intrinsic assessment of homogeneity is achieved by measuring ATD responses: the test conditions are designed such that the ATD injury limits can only be achieved by a vehicle with a homogeneous structure.

A pole test is designed to represent a collision with a pole, post, or tree,[86] but is also representative of a collision with a horizontally inhomogeneous collision partner.[87] Therefore, a pole test can be used to ensure that vehicles are designed to transfer forces from the point of contact with the pole back to the longitudi-

[86]Research by the IIHS found that the injuries observed in real collisions with poles and trees do not correlate with the ATD injury measures observed in pole tests, but this is not considered to be critical for the application discussed in this thesis.

[87]A pole test is at least partially representative of an offset collision with another passenger vehicle where the primary load paths are not horizontally aligned, as observed in the 33% overlap and 66% overlap collisions that are shown in Chapter 8.

nals. A flaw with this approach is that a single test is insufficient to assess the vehicle's homogeneity, since a single pole test could be satisfied by realigning the primary load paths to match the test configuration. To test both the homogeneity and the restraint system performance, pole tests need to be performed over the entire width of the vehicle, including both alignment and non-alignment with the primary load paths. However, this represents a substantial increase in both testing and development costs.

Similar to the effect that a pole test has on horizontal homogeneity, a higher speed bumper test can be used to improve the vertical alignment and interaction between vehicle structures. In this case though, a single test is desirable in order to encourage alignment of the structures with the test bumper. A rigid test barrier can ensure alignment and interaction, but it also supports the transfer of the vertical forces that are responsible for override/underride. To assess or avoid these, the proposal in Figure 10.4 is spring mounted so that the test bumper rotates upwards or downwards when subjected to vertical loading.[88] An additional function of the bumper test is to assess the restraint system under conditions where the entire width of the vehicle is loaded and hence all of the load paths used in the pole tests are simultaneously activated.

The combination of pole and bumper tests could achieve an improvement in collision performance, but it also represents a dramatic increase in testing and development costs. It is also not clear whether it is practically feasible to construct the ideally homogeneous behaviour that is simulated in Chapters 8 and 9 and necessary to perform well in the pole tests.

10.2.4 Heavy vehicle force barrier

In Section 10.1.3, it is concluded that the current vehicle design requirements are adequate for the assessment of force-deformation compatibility. However, the relationship between force and deformation in heavy and light passenger vehicles

[88]The spring in Figure 10.4 also needs to be designed to avoid any instability in the system when it is subjected to purely horizontal loading.

is a topic that continues to be discussed in many research projects and working groups, and hence the following concept is presented as a possible approach to address this issue directly in a manner consistent with the findings of Chapter 6.

Ideally, a vehicle compartment should support high force levels without a substantial increase in deformation. Such a property is difficult to assess, since conventional test methods require the dissipation of kinetic energy by the vehicle structure, and even at high force levels, the dissipation of energy is minimal unless there is a substantial increase in deformation. Destruction tests have therefore been considered for the assessment of compartment strength (Edwards et al. 2002, Mizuno et al. 2003), but these can only be used to assess forces, since the vehicle is destroyed during the test and an assessment of deformation is either inaccurate or irrelevant.

The heavy vehicle force barrier concept, which is shown in Figure 10.5, is designed to allow vehicles to be tested at a high force level without the need to dissipate kinetic energy. In a collision with this barrier, the test vehicle collides with the contact plate and completely deforms its front-end as though it were colliding with a rigid barrier. The force levels then increase at the collision interface

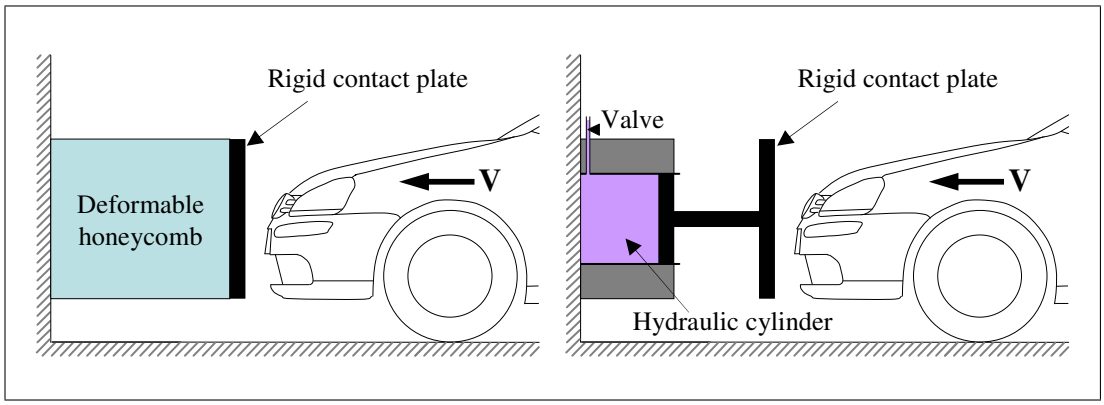

Figure 10.5: Alternative test procedures for the assessment of compartment strength using barriers capable of dissipating an effectively unlimited quantity of energy at a force level equivalent to the front-end of a heavy passenger vehicle. Equivalent behaviour may be achieved using either a rigid plate mounted forward of a stiff deformable honeycomb element (left) or a rigid plate mounted on one or more hydraulic cylinders with regulated maximum pressure (right).

and the compartment is loaded. Finally, the designated heavy vehicle force is reached and the contact plate begins to displace and and dissipate the remaining kinetic energy.

The test needs to be performed with a high initial velocity to ensure that the front-end of the vehicle is deformed and the target force level is reached. The use of ATDs to assess injury risk is therefore inappropriate, since the initial velocity lacks relevance in the accident environment.[89] An assessment of compartment deformation may be an appropriate measure of occupant protection.

Two alternative technical solutions for the heavy vehicle force barrier are shown in Figure 10.5: a conventional deformable honeycomb and a hydraulic system. In both cases, the contact plate needs to be rigid and limited to rearward displacement. The purposes of the honeycomb and the hydraulic cylinder are identical: to dissipate energy at a particular force level. The hydraulic system in Figure 10.5 differs from that in Figure 10.3 in that the regulated release of hydraulic fluid is allowed and hence work is performed. There are no apparent technical advantages of either the honeycomb or the hydraulic system, and hence the most repeatable and economic solution should be used.

An offset collision configuration is proposed for the heavy vehicle force barrier since this leads to more severe loading of the vehicle compartment. It also complements the full width configurations of the deformable barrier, hydraulic barrier, and bumper test proposed in the preceding sections.

10.3 Mobile frontal barrier assessment approach

A fixed barrier test is representative of a collision with a fixed object or a collision with another vehicle of equivalent mass. Fixed barrier tests are therefore equally representative of vehicle-to-object collision severity for all vehicle masses, but they under-represent the average severity of vehicle-to-vehicle collisions for light vehicles and over-represent it for heavy vehicles. In contrast, a mobile barrier is

[89] It is assumed that relevant collision velocities are addressed in the front-end test(s).

equally representative of vehicle-to-vehicle collision severity for all vehicle masses, but under or over-representative of the severity of vehicle-to-object collisions.

To ensure that the current levels of self-protection are not reduced for either heavy vehicles or light vehicles, a mobile barrier should only be considered as an additional test procedure to complement the current fixed barrier test regime. To ensure that the test procedure is relevant to the broadest possible range of collisions, the mobile barrier shown in Figure 10.6 should be representative of the median characteristics of the passenger vehicle fleet.

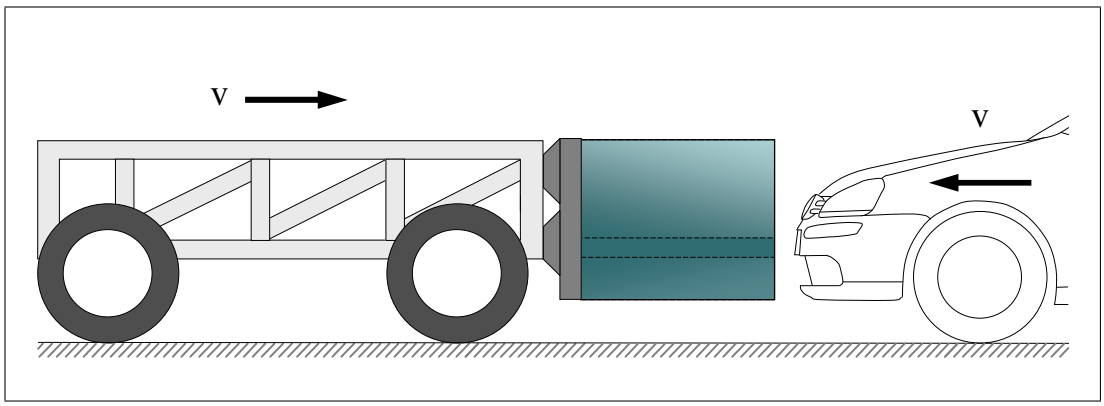

Figure 10.6: Mobile barrier for the assessment of compatibility in a front-to-front collision with another passenger vehicle. The deformable barrier concept is similar to that in Figure 10.1, but with the force and deformation characteristics of a representative vehicle.

The assessment of a compatible collision with a mobile barrier is more complex than the assessment of self-protection in a fixed barrier collision because, according to the definition of a compatible collision from Chapter 6, the test requirement must be based on the combined risk observed in both the vehicle and the barrier.[90] Hence, in addition to the established methods used to calculate injury risk with ATDs, methods also need to be developed to estimate an injury risk for the hypothetical occupants of the mobile barrier.

The assessment of injury risk for the mobile barrier can be based on its

[90]This assessment approach is contra to those in the literature, which tend to apply the 'observation of the vehicle' definition of compatibility. For example, Mackay et al. (1992) proposed an 'Aggressiveness Index' based on dummy readings measured in a standardised small car that was to perform a similar role to the mobile barrier in Figure 10.6. Similarly, Klanner et al. (1998) proposed a 'Compatibility rating procedure' based on the worst mark scored according to an assessment of ATD injury measures and an assessment of barrier deformation.

deformation and/or deceleration pulse. For example, the latter approach was used by Schram et al. (2006) to assess truck under-run protection. In that case, the accelerations measured by a MPDB were related to the expected cost of injury in the collision.[91] Although a direct relationship with the risk of injury was not calculated, the approach used by Schram et al. (2006) demonstrated that this would be feasible.

The current regulatory approach of using fixed ATD injury limits, such as the Head Injury Criterion $(HIC)_{36\text{ ms}} < 1000$ limit used in ECE-R94, are inappropriate for an assessment of a compatible collision. Instead, a combined risk of injury must be calculated using an approach similar to that proposed for future adoption in the United States New Car Assessment Program (US-NCAP) (NHTSA 2009), and that must be combined with the risk assessment from the mobile barrier. A regulatory limit should only be applied to the final assessment of the entire collision. A consequence of this approach is that one vehicle can satisfy the requirements with a $HIC_{36\text{ ms}} > 1000$ because it causes little damage to the barrier, but another vehicle can fail the requirements with a $HIC_{36\text{ ms}} < 1000$ because it is too aggressive towards the barrier.

Unlike a collision with a fixed barrier, with a mobile barrier the deformable element does not invalidate the connection between the forces required to deform the front-end and the relationship between acceleration and displacement in the passenger compartment. This is because the forwards motion of the barrier compensates for its deformation. The problem of vehicle designs misusing the kinetic energy dissipation potential of the barrier is also circumvented because excess deformation is negatively assessed by the rating of risk in the mobile barrier and must hence be actively avoided in the vehicle design process. In addition, the force-deformation relationships of tested vehicles are indirectly regulated by the requirement to optimise between occupant and barrier loading. Hence, as with the

[91] Note that the cost of injury was defined by Schram et al. (2006) according to the medical treatment of different levels of injury and that it did not include the full socio-economic cost of an injury. This resulted in lower costs being applied to AIS 6 injuries, which are associated with a high mortality rate.

fixed barrier approach, there is no need to measure and regulate this directly. To maximise the assessment capability of the mobile barrier, it is therefore proposed to use a deep deformation depth. This also enables the full potential of the variable stiffness characteristics of the deformable barrier described in Figure 10.1 to be realised and hence encourages both horizontal homogeneity and vertical alignment.

The analyses performed in this thesis do not indicate a clear preference for either an offset or a full overlap configuration for the mobile barrier test procedure. A full overlap collision tends to induce more severe accelerations and an offset configuration tends to induce more severe deformations. Further statistical analyses should be performed to identify which configuration provides the most benefit.

10.4 Side assessment requirements

As with Section 10.1, this section summarises the main findings of this thesis with regards to the requirements of a side test procedure for the assessment of self-protection. A need to address the partner-protection offered by the vehicle side is neither observed in the accident statistics nor is it discussed in the literature.

10.4.1 Test configuration

The statistical analysis in Chapter 5 shows that collisions with other passenger vehicles are responsible for approximately 45% of MAIS 2+ injuries to belted passenger vehicle occupants in side collisions, but that approximately 20% are injured in collisions with poles, posts, and trees, and 15% are injured in collisions with commercial vehicles. It is predicted that the proportion of lateral collisions with poles, posts, and trees will decrease as the proportion of vehicles fitted with ESC increases (Rieger et al. 2005), and hence the assessment of occupant protection in vehicle-to-vehicle collisions is the clear priority. In collisions between

two passenger vehicles, the most frequent front-to-side collision configurations are those involving deformation to the vehicle compartment, and, of these, a higher proportion involve additional deformation forward of the A-pillar than additional deformation rearward of the C-pillar. Approximately 60% of front-to-side collisions have a collision direction between 15° and 45° forward of the perpendicular.

10.4.2 Test severity

The analysis of collision velocity in Chapter 5 is limited by the quantity of data available, but it is shown that the mean velocity at which MAIS 2 injuries occur in front-to-side collisions is $\Delta v = 34$ km/h. With an enlarged dataset including older vehicles but limited to near side occupants, it is shown that MAIS 2 injuries occur at a median Δv of 30 km/h and MAIS 3 injuries occur at a median Δv of 40 km/h.

The statistical analysis in Chapter 5 shows that the mean risk of injury in a front-to-side collision is dependent on the mass ratio of the colliding vehicles. Further analysis of these data shows that the median mass of the striking vehicles is 1406 kg, but the median mass of those involved in collisions that cause MAIS 2+ injuries is 1627 kg.[92]

10.4.3 Force-deformation compatibility

Unlike the design of frontal structures, no compromise in the stiffness of side structures is necessary to optimise between self-protection and partner-protection. The test procedure therefore has no special requirements beyond the assessment of the side structure using loading conditions that are representative of the accident environment.

[92]Note that these median masses are based on collisions between vehicles with dates of manufacture between 1996 and 2005. For the datasets used in Figure 5.5b, the median mass of all striking vehicles is 1200 kg and the median mass of those involved in collisions that cause MAIS 2+ injuries is 1285 kg.

10.4.4 Homogeneity

The homogeneity of the side structure is also only relevant for self-protection. Again, a test procedure that produces loading conditions that are representative of the accident environment is therefore relevant. The test barrier itself should not be homogeneous, even though the objective defined in Section 10.1.4 is to increase the horizontal homogeneity of frontal structures. A homogeneous barrier reduces the requirement for homogeneity to be engineered into the vehicle side and hence results in less robust vehicle designs. However, the stiffness distribution of the barrier should reflect the loading expected from homogeneous front-end structures. For example, the increased loading on the B-pillar that is observed in Figure 9.3 may be reproduced by a stiffer portion of the barrier.[93]

10.5 Mobile side barrier assessment approach

Two different mobile barrier test configurations are currently used in regulations. As shown in Table 2.1, the perpendicular configuration is used in the ECE-R95 test procedure and also by the IIHS. The crabbed configuration, which combines a velocity vector that is angled with a barrier that is perpendicular to the vehicle, is used in FMVSS 214. Although the accident statistics show a significantly higher proportion of collisions with angled velocity vectors, this does not necessarily mean that the velocity vector of the ideal test procedure should also be angled. The purpose of a test procedure is to encourage good vehicle design, which may be better achieved using an alternative configuration.

The perpendicular configuration results in an even application of loading across the side of the vehicle, whereas the crabbed configuration causes the barrier to rotate and increase the loading where the rearward corner of the barrier contacts the vehicle. The perpendicular configuration therefore provides a more

[93] Note that the 'homogeneity' discussed in this section refers to the way forces are reacted by the barrier. An 'inhomogeneous' barrier may therefore have a constant stiffness distribution. See also Section 8.1.

robust procedure for applying loads to the occupant compartment. The perpendicular configuration applies axial loading to the honeycomb elements used for most MDBs, whereas the crabbed configuration applies shear forces to the barrier face that may lead to unpredictable failure modes (Seyer et al. 2000). Hence, although the perpendicular configuration is less representative of the collision angles observed in the accident statistics, it provides a more robust and controllable test procedure and, as shown in Figure 10.7, it is therefore the preferred configuration for this proposal.

The side structure of a vehicle is effectively devoid of a crumple zone, and it hence fulfils a similar role to that which the bulkhead performs in a frontal collision. Ideally, a vehicle side structure has force-deformation characteristics that minimise compartment deformation. A stiffer side structure has two principal advantages. Firstly, in a collision with a deformable object like a vehicle front-end, it is able to deform that object to a greater degree and hence gain additional distance over which the occupant can be decelerated. Secondly, in a collision with a rigid object, it is more effective at developing a velocity differential between the occupant and the restraint system, which can then apply forces to begin the occupant's deceleration.

The force-deformation characteristics of the side structures only affect self-protection, and hence an assessment using ATDs is appropriate. If a mobile barrier is used that has stiffness properties that are representative of frontal structures in the vehicle fleet, the design of the side structure and the restraint system must be optimised to provide occupant protection. Differences between the force-deformation relationships of different vehicles may then arise, but the performance criteria defined in the test procedure ensures that these differences are compensated for by the restraint system.

In Sections 10.2.1 and 10.3, the potential misuse of a deformable barrier to dissipate a large portion of the kinetic energy in a frontal test is criticised. In contrast, the design of vehicles that utilise the deformation potential of the

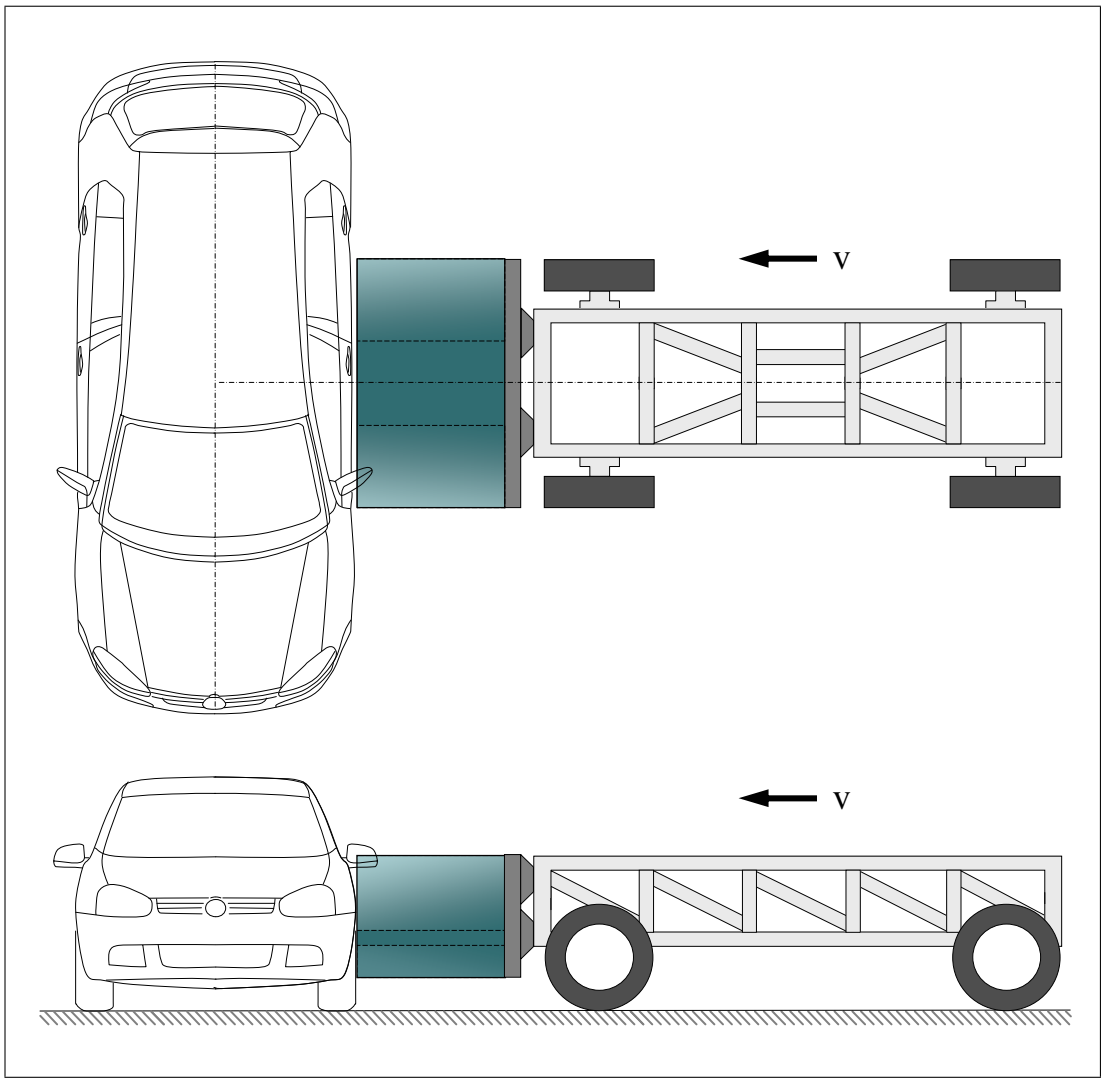

Figure 10.7: Mobile barrier for the assessment of compatibility in a front-to-side collision with another passenger vehicle. The vertical stiffness distribution of the deformable barrier is similar to that in Figure 10.1, but with the force and deformation characteristics of a representative vehicle. The horizontal stiffness distribution applies additional loading to the vehicle's B-pillar.

mobile barrier rather than the structural deformation of the vehicle side does not represent an increased risk for real world collisions. This deformation behaviour should be reproducible in real vehicle-to-vehicle collisions without increasing the risk of injury to the occupants.

Regardless of the approach used for the assessment of frontal structures, a common goal from Section 10.2 is the vertical alignment of the primary load paths. This alignment should therefore also be reflected in the barrier used for side collisions, and a variable stiffness distribution similar to that proposed in

Figure 10.1 is appropriate for this objective. Even though the perpendicular test configuration does not perfectly represent the accident statistics, the vertical alignment of the front-end structures is not affected by the collision alignment and angle. Hence, concentrated loading of the side structure within the interaction zone can still encourage robust vehicle designs that are relevant for a broad range of collision configurations.

The horizontal stiffness distribution of the barrier is more critical since the loading of the doors and pillars is dependent on both the collision angle and alignment. For example, various approaches to the horizontal distribution of barrier stiffness are proposed for the design of the AE-MDB. These include the AE-MDB v3.1, which has higher stiffness in the outer parts of the barrier to represent the colliding vehicle's longitudinals, and the AE-MDB v3.9, which has higher stiffness in the middle to increase loading on the B-pillar (Versmissen et al. 2007). In contrast, the IIHS barrier and FMVSS 214 barrier both have constant stiffness distributions in the horizontal direction.

The most positive results in Chapter 9 are achieved in simulations with stiffened B-pillars. It is therefore concluded that a stiffness distribution that more heavily loads the B-pillar would lead to the greatest improvements in compatibility.

Chapter summary

The results of the preceding chapters are summarised with respect to the requirements for the assessment of front and side structures. These include consideration of the test configuration, test severity, relationship between force and deformation, and the homogeneity of the structures. For frontal structures, aspects of both self-protection and partner-protection are considered, but, for side structures, the focus is directed towards self-protection.

In Section 10.2, several proposals for the assessment of frontal structures using fixed barriers are discussed. A deformable barrier is proposed that utilises

proven technology but has potential weaknesses due to the energy dissipation inherent to deformable honeycomb barriers. A hydraulic barrier is proposed that avoids the problem of energy dissipation in the barrier but uses technology that is untested in a crash test barrier application. The combination of a high speed bumper test and multiple pole tests is also proposed as a more stringent approach that better meets the technical requirements but may not be economically feasible. The common purpose of these three approaches is the assessment of the front-end, and an additional procedure is hence proposed for the assessment of compartment strength.

In Section 10.3, a proposal for the assessment of frontal structures using a mobile barrier is discussed. The proposal combines the assessment of both self-protection and partner-protection in accordance with the definition of a compatible collision from Chapter 6. It hence requires the combination of injury assessments in the test vehicle with deformation and/or acceleration assessments from the barrier to determine a mean injury risk for the collision. To avoid the risk of reduced self-protection in single vehicle collisions, the mobile barrier approach is proposed as an addition to existing fixed barrier tests.

Finally, in Section 10.5, approaches to the assessment of side structures are discussed. It is concluded that a mobile barrier with an inhomogeneous deformable element is appropriate for encouraging homogeneous structures. It is also concluded that the stiffness distribution of the deformable element should reflect the loading applied by vehicle front-ends to side structures. The vertical stiffness distribution therefore corresponds to the vertical alignment of front-end structures, and the horizontal stiffness distribution applies increased loading to the B-pillar.

Chapter 11

Conclusions

The objective of improving traffic safety is to minimise the number of injuries and fatalities that occur in the traffic accident environment. The value of every human life is equal, and hence a comparison of traffic safety policies should be performed without bias towards any particular group of road users.

In its broadest sense, compatibility is the optimisation of vehicle design to minimise the total number of injuries and fatalities that occur in all collisions in the accident environment. It is distinguished from traditional perceptions of occupant protection in that it requires vehicle designs to be optimised to protect other road users in addition to the vehicle's own occupants. The term compatibility does not describe the overall level of investment in vehicle safety features: Compatibility describes the optimum allocation of resources towards self-protection and partner-protection.

A broad definition of compatibility is useful for evaluating the overall impact of safety policies, but it is impractical for the analysis of individual collisions and hence a separate, subordinate definition of a compatible collision is also necessary. Injury risk is affected by collision characteristics including the collision configuration and the involved vehicles' initial velocities. Given a fleet of vehicles that is capable of providing some level of protection with respect to these collision characteristics, the collisions involving that fleet of vehicles are compatible if the combined risk of injury for all occupants involved in any particular collision is

independent of the vehicle, or vehicles, involved. Hence, if a passenger car collides with a tree, the risk of injury to the driver should be independent of the type, size, weight, or any other characteristic of the vehicle being driven. Similarly, if two vehicles collide, the combined risk of injury to both involved drivers should be independent of the type, size, weight, or any other characteristic of either vehicle. This does not mean that the individual risks of injury to both drivers should be the same. Instead, it means that the sum of all injuries sustained by both drivers should not be higher as a result of the particular vehicles that are involved. It should also be noted that compatible collisions may still occur when the vehicle fleet is composed of designs that use different combinations and implementations of safety systems. The objective of a compatible collision is an outcome that is independent of the vehicles' designs, and this requires that the safety systems in each vehicle are tailored to its type, size, weight, and other characteristics.

Accident statistics show that front-to-front and front-to-side collisions between passenger vehicles result in a high proportion of injuries and fatalities, and it is therefore relevant to analyse compatibility in these configurations. However, a high proportion of injuries and fatalities also occurs in collisions with other obstacles, and hence the priority of a compatible vehicle design must be directed towards self-protection.

Although vehicle mass is a convenient variable for the analysis of broad tendencies in the vehicle fleet, it is not a perfect indicator of the risk of injury in an individual collision, and the safety of an individual vehicle is influenced by many aspects of its design. From a fleet-wide perspective, the driver of a lighter vehicle typically experiences a higher risk of injury than the driver of a heavier vehicle when a collision occurs between two passenger vehicles with unequal masses. In a front-to-side collision, the mean risk of injury to the two involved drivers is also typically higher in collisions between vehicles with different masses. However, when a front-to-front collision between two passenger vehicles is analysed as a single event, the mean risk of injury for the two involved drivers is

independent of the collision mass ratio. From a societal perspective, the severity of the injuries caused by front-to-front collisions is therefore independent of the involved vehicles' masses.

The analysis of individual collisions is complicated by micro-effects that may or may not translate into changes in risk in the broader traffic accident environment. If a vehicle is tested outside of its design envelope, as may be the case in a severe vehicle-to-vehicle collision, the propensity for such micro-effects to occur increases. For research purposes, it is therefore inappropriate to use Anthropomorphic Test Devices (ATDs). The measurement of deformations, velocities, and accelerations presents a more robust approach, and the literature provides evidence of direct relationships between these measurements and the risk of occupant injury. However, the generalisation of such relationships is inexpedient, since proper consideration must be made of the synergies between the vehicle structure and the restraint system. To achieve valid results, a separate analysis of the deformations, velocities, and accelerations that occur in individual vehicle models is therefore necessary.

Vertical homogeneity and horizontal homogeneity are properties of a vehicle's design that describe its ability to react the forces that are applied during a collision. In front-to-front collisions, vertical homogeneity further improves the interaction between structures under dynamic loading even when initial, static alignment of the structures is provided. The principal benefit of vertical homogeneity is achieved by encouraging interaction between the primary load paths, and a taller homogeneous region that also encompasses secondary load paths may be counter-productive. Horizontal homogeneity has little influence on full overlap front-to-front collisions and is only marginally more effective than vertical homogeneity in partial overlap collisions. The ability to react forces that are applied outboard of a vehicle's longitudinals represents the greatest potential for a horizontally homogeneous design.

In front-to-side collisions, horizontal homogeneity is effective if forces can

be transferred to the A-pillar and C-pillar of the struck vehicle, and it is also complementary with increases in the stiffness of the B-pillar. Vertical homogeneity derives its benefit from the application of loads to the struck vehicle's sill, and it is hence also complementary with stiffened sills. In general, changes to the front-end of the striking vehicle complement changes to the side of the struck vehicle if the directions of the homogeneous characteristics intersect.

Changes in structural homogeneity may be achieved by the careful design of regulatory test conditions. Concepts for these tests include deformable honeycomb barriers, hydraulic barriers, and procedures that intrinsically encourage homogeneity. It is essential that the design of any new test precludes misuse and provides test conditions that are representative of the traffic accident environment.

For the assessment of a vehicle's side structure, partner-protection is insignificant and hence the test procedure may focus on the self-protection aspects of the design. In contrast, for the assessment of compatibility in front-to-front collisions, the vehicle should be assessed according to the definition of a compatible collision, which requires the calculation of a mean risk of injury. For the example of a Mobile Deformable Barrier (MDB), the assessment protocol should place a single limit on the combined performance of both the MDB and the test vehicle. Individual limits on either the vehicle or the MDB would lead to suboptimal compatibility in the vehicle fleet. The same approach is also appropriate for any fixed barrier assessment of a vehicle's front-end.

The principal contributions of this thesis to the general body of knowledge are the definition of a compatible collision within the general concept of compatibility and the independent analysis of horizontal and vertical structural homogeneity. New insight is also gained from the accident analysis, compatibility measurement procedure, and the discussion of vehicle test procedures.

11.1 Recommendations for future research

The research questions defined in Chapter 1 are all answered within the thesis, but several areas of research still warrant further investigation.

The finding that the mean risk of injury in a front-to-front collision is independent of the involved vehicles' mass ratio has broad ranging implications for policy-making and future research priorities. It should therefore be confirmed for other jurisdictions and with alternative data sources. The finding that the mean risk of injury in a front-to-side collision is dependent on the involved vehicles' mass ratio indicates that the front-to-side configuration should be the priority for future analyses. Current compatibility research programs in Europe, Japan, and the USA are not directly addressing the issue of front-to-side compatibility. Generally, the analyses of vehicle mass ratios show that compatibility should be investigated at the accident level rather than the vehicle level. The analysis of accidents as complete events is therefore recommended over the separate analysis of each involved vehicle.

The measurement procedure defined in Chapter 7 is effective for the simulations that are described in this thesis, but the assessment of injury risk in side collisions requires further validation. In particular, the assumptions described at the beginning of Section 7.2 should be reviewed for plausibility with respect to the accident data. If necessary, the assessment method may be supplemented with measurements of, for example, door intrusion velocity.

Research should be directed towards the development of constructive measures to improve structural homogeneity. For vertical homogeneity, this implies improved dynamic interaction between primary load paths in front-to-front collisions and improved interaction with struck vehicles' sills in front-to-side collisions. For horizontal homogeneity, attention needs to be directed towards the regions outboard of the vehicle's longitudinals.

The use of collision simulations in this thesis enables the analysis of a broad range of idealised structural behaviours, but simulation models do not provide

perfect representations of vehicles' structures, and hence the results must be interpreted with a degree of caution. Before making final judgements about the benefit to be derived from any of the vehicle structural modifications that are discussed above, full scale crash tests should be performed to investigate the limits of realistic structural behaviour and to confirm the simulation results.

Further research is needed to define appropriate test and assessment procedures for vehicle compatibility. The concepts described in Chapter 10 have merit and appear to represent an improvement over the procedures discussed in the literature. These concepts should be developed into completed test protocols, which can then be judged more objectively. Before being adopted as a design criterion, any test protocol should be evaluated with regards to costs, benefits, and the risks associated with future changes in the accident environment.

References

Abdel-Aty, M. & Abdelwahab, H. (2004), 'Analysis and prediction of traffic fatalities resulting from angle collisions including the effect of vehicles' configuration and compatibility', *Accident Analysis & Prevention* **36**(3), pp. 457–469.

Abe, A., Sunakawa, T., Fujii, S., Fukuschima, M. & Ogawa, S. (2005), Aggressivity-reducing structure of large vehicles in side vehicle-to-vehicle crash, *in* 'SAE 2005 World Congress', Society of Automotive Engineers, Detroit. Paper Number 2005-01-1355.

Ablaßmeier, W., Slaba, T., Walner, S., Hartlieb, M., Böning, S., Wrobel, B., Kamm, M., O'Brien, S., Schwarz, T., Zobel, R. & Ebner, H.-T. (2007), Opportunities for a worldwide compatibility evaluation - German manufacturer's position paper on crash compatibility, *in* '20th International Technical Conference on the Enhanced Safety of Vehicles', Lyon.

Acierno, S., Kaufman, R., Rivara, F. P., Grossman, D. C. & Mock, C. (2004), 'Vehicle mismatch: injury patterns and severity', *Accident Analysis & Prevention* **36**(5), 761–772.

Adler, M. D. & Posner, E. A. (2000), 'Implementing cost-benefit analysis when preferences are distorted', *The Journal of Legal Studies* **29**(2), pp. 1105–1147.

American College of Surgeons (2008), *National Trauma Data Standard, Data Dictionary, Version 1.2.1*, National Trauma Data Bank.

Appel, H. (1973), Aggressivität von Fahrzeugen als Teilproblem der passiven Sicherheit, *in* 'Jahrestagung Fahrzeugtechnik', Stuttgart.

Appel, H., Krammer, F., Glatz, W., Lutter, G., Baumann, J. & Weller, M. (1991), *Quantifizierung der passiven Sicherheit für Pkw-Insassen*, Report, Research project FP 8517/2, Bundesanstalt für Straßenwesen, Bergisch-Gladbach.

Arai, Y., Yamazaki, K., Mizuno, K. & Kubota, H. (2007), Full-width tests to evaluate structural interaction, *in* '20th International Technical Conference on the Enhanced Safety of Vehicles', Lyon.

Arbelaez, R., Dakin, G., Nolan, J., Dalmotas, D. & Tylko, S. (2002), IIHS side impact barrier: Development and crash test experience, *in* 'IMechE Conference Transactions: International Conference on Vehicle Safety 2002', London, pp. 73–88.

Augenstein, J., Perdeck, E., Mostafa, K., Digges, K., Bahouth, G. & Morgan, R. (2005), The role of intrusion in injury causation in frontal crashes, *in* 'SAE 2005 World Congress', Society of Automotive Engineers, Detroit. Paper Number 2005-01-1376.

Austin, R. (2005), Vehicle aggressiveness in real world crashes, *in* '19th International Technical Conference on the Enhanced Safety of Vehicles', Washington DC. Paper Number 05-0248.

Baker, B. C., Nolan, J. M., O'Neill, B. & Genetos, A. P. (2008), 'Crash compatibility between cars and light trucks: Benefits of lowering front-end energy-absorbing structure in suvs and pickups', *Accident Analysis & Prevention* **40**(1), pp. 116–125.

Baker, S. P., O'Neill, B. B., Haddon, William, J. & Long, W. B. (1974), 'The injury severity score: A method for describing patients with multiple injuries and evaluating emergency care', *Journal of Trauma* **14**(3), pp. 187–196.

Barbat, S. (2005), Status of enhanced front-to-front vehicle compatibility technical working group research and commitments, *in* '19th International Technical Conference on the Enhanced Safety of Vehicles', Washington DC. Paper Number 05-0463.

Barbat, S., Li, X. & Prasad, P. (2007), Vehicle-to-vehicle front-to-side crash analysis using a CAE-based methodology, *in* '20th International Technical Conference on the Enhanced Safety of Vehicles', Lyon.

Brieter, K. (2008), 'David gegen goliath', *ADAC Motorwelt* **8/2008**, pp. 22–23.

Broughton, J. (2008), 'Car driver casualty rates in great britain by type of car', *Accident Analysis & Prevention* **40**(4), pp. 1543–1552.

Bylow, L. F. & Savage, I. (1991), 'The effect of airline deregulation on automobile fatalities', *Accident Analysis & Prevention* **23**(5), pp. 443–451.

Cameron, M., Newstead, S. & Le, C. M. (1999), 'Rating the aggressivity of australian passenger vehicles towards other vehicle occupants and unprotected road users', *Traffic Injury Prevention* **1**(2), pp. 129–141.

Castaing, P. (2009), *Minutes of 5th meeting of the Informal Group on Frontal Impact – 25th May 2009*, Document FI-05-10, Economic Commission for Europe – Inland Transport Committee – World Forum for Harmonization of Vehicle Regulations – Working Party on Passive Safety – Informal Group on Frontal Impact, Geneva. (`http://www.unece.org/trans/doc/2009/wp29grsp/FI-05-10e.pdf`, accessed 30th September 2009).

Chauvel, C., Cuny, S. & Faverjon, G. (2009), Work progress regarding self-protection and partner-protection, *in* 'Minutes of 4th meeting of the Informal Group on Frontal Impact – 10th March 2009', Document FI-04-02, Economic Commission for Europe – Inland Transport Committee – World Forum for Harmonization of Vehicle Regulations – Working Party on Passive Safety – Informal Group on Frontal Impact, Paris.

Coimbra, R., Conroy, C., Hoyt, D. B., Pacyna, S., May, M., Erwin, S., Tominaga, G., Kennedy, F., Sise, M. & Velky, T. (2008), 'The influence of damage distribution on serious brain injury in occupants in frontal motor vehicle crashes', *Accident Analysis & Prevention* **40**(4), pp. 1569–1575.

Connelly, L. B. & Supangan, R. (2006), 'The economic costs of road traffic crashes: Australia, states and territories', *Accident Analysis & Prevention* **38**(6), pp. 1087–1093.

Conroy, C., Tominaga, G. T., Erwin, S., Pacyna, S., Velky, T., Kennedy, F., Sise, M. & Coimbra, R. (2008), 'The influence of vehicle damage on injury severity of drivers in head-on motor vehicle crashes', *Accident Analysis & Prevention* **40**(4), pp. 1589–1594.

CORDIS (2009), *Frontal impact and compatibility assessment research (FIMCAR)*, Office for Official Publications of the European Communities, Luxembourg. (`http://cordis.europa.eu/fetch?CALLER=FP7_PROJ_EN&ACTION=D&DOC=20&CAT=PROJ&QUERY=01241a269364:5717:5236f1a8&RCN=91919`, accessed 3rd October 2009).

Cuerden, R., Massie, P., O'Brien, S., Davies, H. & Edwards, M. (2007), *Accident Analysis for Specification of Advanced European Full Width (AE-FW) Test, Deliverable D1.2.3A*, APROSYS Project Consortium.

Dakin, G. J., Arbelaez, R. A., Nolan, J., Zuby, D. S. & Lund, A. K. (2003), Insurance institute for highway safety side impact crashworthiness evaluation program: impact configuration and rationale, *in* '18th International Technical Conference on the Enhanced Safety of Vehicles', Nagoya. Paper Number 03-0172.

Damm, R. (2006), *Test reports of a Supermini vehicle, Addendum Deliverable 29*, VC-Compat Consortium.

Danner, M., Appel, H. & Schimkat, H. (1980), Entwicklung kompatibler fahrzeuge, Technical report, HUK-Verband, TU-Berlin, Volkswagenwerk AG, Wolfsburg.

Davies, H., Edwards, M., Martin, T., Delannoy, P., Damm, R., van der Zweep, C. & Barberis, D. (2006), *Crash test results and analyses performed for initial validation of proposed compatibility test procedures, Deliverable 27*, VC-Compat Consortium.

Davies, H., Martin, T., Damm, R., Jenefeldt, F. & van der Zweep, C. (2005), *Crash test results and analyses for tests completed to month 18, Deliverable 17*, VC-Compat Consortium.

De Coo, P. A., Roberts, A., Seeck, A. & Cesari, D. (1998), Test methods for evaluating and comparing the performance of side impact barrier faces, *in* '16th International Technical Conference on the Enhanced Safety of Vehicles', Windsor. Paper Number 98-S8-O-02.

Delannoy, P. & Diboine, A. (2001), Structural front unit global approach, *in* '17th International Technical Conference on the Enhanced Safety of Vehicles', Amsterdam. Paper Number 01-0199.

Delannoy, P., Granjus, G. & Diboine, A. (2000), EUCAR summary, *in* 'Minutes of 15th meeting of the EEVC Working Group 15: Improvement of Crash Compatibility between Cars – 5-6 December 2000', EEVC WG15 Document 111, European Enhanced Vehicle-safety Committee, Crowthorne.

Delannoy, P., Martin, T. & Castaing, P. (2005), Comparative evaluation of frontal offset tests to control self and partner protection, *in* '19th International Technical Conference on the Enhanced Safety of Vehicles', Washington DC. Paper Number 05-0010.

Delannoy, P., Martin, T., Meyerson, S., Summers, L. & Wiacek, C. (2007), PDB

barrier face evaluation by DSCR and NHTSA's joint research program, *in* '20th International Technical Conference on the Enhanced Safety of Vehicles', Lyon.

Directive 2003/20/EC of the European Parliament and of the Council of 8 April 2003 amending Council Directive 91/671/EEC on the approximation of the laws of the Member States relating to compulsory use of safety belts in vehicles of less than 3,5 tonnes (2003), *Official Journal of the European Union L 115* pp. 0063–0067.

Dreyer, W., Richter, B. & Zobel, R. (1981), Handling, braking, and crash compatibility aspects of small, front-wheel drive vehicles, *in* 'SAE Passenger Car Meeting', Society of Automotive Engineers, Dearborn, Michigan. Paper Number 810792.

Edwards, M., Fails, A., Davies, H., Lowne, R. & Hobbs, A. (2001*a*), Review of the European frontal and side impact directives, *in* '17th International Technical Conference on the Enhanced Safety of Vehicles', Amsterdam. Paper Number 01-0437.

Edwards, M., Happian-Smith, J., Davies, H., Byard, N. & Hobbs, A. (2001*b*), The essential requirements for compatible cars in frontal collisions, *in* '17th International Technical Conference on the Enhanced Safety of Vehicles', Amsterdam. Paper Number 01-0158.

Edwards, M., Benedetto, A., Castaing, P., Davies, H., Faerber, E., Fails, A., Martin, T., Schaefer, R. & Thompson, A. (2002), A study to improve the crash compatibility between cars in frontal impact, Technical Report Contract Reference: E3-3 B2702/SI2.318663/2001 TRL, European Commission Directorate-General for Energy and Transport, Brussels.

Edwards, M., Davies, H. & Hobbs, A. (2003*a*), Development of test procedures and performance criteria to improve compatibility in car frontal collisions, *in*

'18th International Technical Conference on the Enhanced Safety of Vehicles', Nagoya. Paper Number 03-0086.

Edwards, M. J., Davies, H., Thompson, A. & Hobbs, A. (2003*b*), 'Development of test procedures and performance criteria to improve compatibility in car frontal collisions', *Proceedings of the Institution of Mechanical Engineers* **217**(4), pp. 233–245.

Edwards, M., Cuerden, R. & Davies, H. (2007*a*), Current status of the full width deformable barrier test, *in* '20th International Technical Conference on the Enhanced Safety of Vehicles', Lyon.

Edwards, M., de Coo, P., van der Zweep, C., Thomson, R., Damm, R., Martin, T., Delannoy, P., Davies, H., Wrige, A., Malczyk, A., Jongerius, C., Stubenböck, H., Knight, I., Sjöberg, M., Ait-Salem Duque, O. & Hashemi, R. (2007*b*), *Improvement of Vehicle Crash Compatibility through the Development of Crash Test Procedures (VC-Compat), Final Technical Report*, VC-Compat Consortium.

Edwards, M. (2009), Development of a high deceleration full width frontal impact test for Europe, *in* '21st International Technical Conference on the Enhanced Safety of Vehicles', Stuttgart.

EEVC WG6 (1982), Structures: Improved side impact in europe, *in* '9th International Technical Conference on the Enhanced Safety of Vehicles', Kyoto.

Eigen, A. M. & Glassbrenner, D. (2003), The relationship between occupant compartment deformation and occupant injury, Technical Report DOT HS 809 676, National Center for Statistics and Analysis, Washington DC.

Ellway, J. (2005), The development of an Advanced European Mobile Deformable Barrier face (AE-MDB), *in* '19th International Technical Conference on the Enhanced Safety of Vehicles', Washington DC. Paper Number 05-0239.

Ellway, J., Donaldson, W., Edwards, M., Versmissen, T. & Bosch-Rekveldt, M. (2006), *Development and Evaluation of the Advanced European Mobile Deformable Barrier (AEMDB) Test Procedure, Deliverable D1.1.1B*, APROSYS Project Consortium.

Elvik, R. (1999), 'Can injury prevention efforts go too far?: Reflections on some possible implications of vision zero for road accident fatalities', *Accident Analysis & Prevention* **31**(3), pp. 265–286.

Elvik, R. (2003), 'How would setting policy priorities according to cost-benefit analyses affect the provision of road safety?', *Accident Analysis & Prevention* **35**(4), pp. 557–570.

Elvik, R. & Vaa, T. (2004), *The handbook of road safety measures*, Elsevier, Oxford, UK.

ESI Group (2008), *Virtual Performance Solutions 2008: Explicit Solver Notes Manual*, ESI Group, Paris.

Euro NCAP (2003), *European New Car Assessment Programme (Euro NCAP) Frontal Impact Testing Protocol Version 4.0*, Euro NCAP, Brussels.

Evans, L. & Frick, M. C. (1993), 'Mass ratio and relative driver fatality risk in two-vehicle crashes', *Accident Analysis & Prevention* **25**(2), 213–224.

Evans, A. W. (2003), 'Estimating transport fatality risk from past accident data', *Accident Analysis & Prevention* **35**(4), pp. 459–472.

EVC (2003), *Enhancing Vehicle-to-Vehicle Crash Compatibility, Commitment for Continued Progress by Leading Automakers*, Alliance of Automobile Manufacturers and the Association International Automobile Manufacturers, Washington. Docket Number: NHTSA-2003-14623-0013.

EVC (2006), *Enhancing Vehicle-to-Vehicle Crash Compatibility, Commitment for Continued Progress by Leading Automakers, 2005 Update*, Alliance of Automo-

bile Manufacturers, Insurance Institute for Highway Safety, and the Association International Automobile Manufacturers, Washington. Docket Number: NHTSA-2003-14623-0035-0001.

EVC (2009), *Final Report: Voluntary Industry Effort to Further Enhance Front-to-Front Vehicle Crash Compatibility*, Alliance of Automobile Manufacturers, The Insurance Institute for Highway Safety and the Association International Automobile Manufacturers, Washington. Docket Number: NHTSA-2003-14623-0100.2.

Faerber, E., Cesari, D., Hobbs, A. C., Huibers, J., van Kampen, B., Paez, J. & Wykes, N. J. (1998), Improvement of crash compatibility between cars, *in* '16th International Technical Conference on the Enhanced Safety of Vehicles', Windsor. Paper Number 98-S3-O-02.

Faerber, E. (2007), EEVC approach to develop test procedure(s) for the improvement of crash compatibility between passenger cars, *in* '20th International Technical Conference on the Enhanced Safety of Vehicles', Lyon.

Faerber, E., Martin, T., Edwards, M., Thomson, R., Della Valle, G., Schram, R. & Huguet, J. (2007), *EEVC Working Group 15 Final Report to Steering Committee*, European Enhanced Vehicle-safety Committee.

Fallon, I. & O'Neill, D. (2005), 'The world's first automobile fatality', *Accident Analysis & Prevention* **37**(4), pp. 601–603.

Farmer, C. M. (2003), 'Reliability of police-reported information for determining crash and injury severity', *Traffic Injury Prevention* **4**(1), pp. 38–44.

Farmer, C. M., Braver, E. R. & Mitter, E. L. (1997), 'Two-vehicle side impact crashes: The relationship of vehicle and crash characteristics to injury severity', *Accident Analysis & Prevention* **29**(3), pp. 399–406.

Ferguson, S. A. (2007), 'The effectiveness of electronic stability control in reducing real-world crashes: A literature review', *Traffic Injury Prevention* **8**(4), pp. 329–338.

Fildes, B. N., Digges, K., Les, M. & Tingvall, C. (2000), Benefits of a 64km/h offset crash test in Australia, Technical Report 173, Monash University Accident Research Centre, Clayton.

Fildes, B. N., Lee, S. J. & Lane, J. C. (1993), Vehicle mass, size and safety, Technical Report CR 133, Federal Office of Road Safety, Canberra.

Frampton, R., Welsh, R., Thomas, P. & Fay, P. (2000), 'The importance of non-struck side occupants in side collisions', *Traffic Injury Prevention* **2**(2), pp. 151–163.

France (2007), *Regulation No. 94 (Frontal collision): Proposal for draft amendments*, Working Document ECE/TRANS/WP.29/GRSP/2007/17, Economic Commission for Europe – Inland Transport Committee – World Forum for Harmonization of Vehicle Regulations – Working Party on Passive Safety, Geneva. (`http://www.unece.org/trans/doc/2007/wp29grsp/ECE-TRANS-WP29-GRSP-2007-17e.pdf`, accessed 30th September 2009).

Fredette, M., Mambu, L. S., Chouinard, A. & Bellavance, F. (2008), 'Safety impacts due to the incompatibility of suvs, minivans, and pickup trucks in two-vehicle collisions', *Accident Analysis & Prevention* **40**(6), pp. 1987–1995.

Fujii, S., Fukushima, M., Abe, A., Ogawa, S., Fujita, H., Sunakawa, T. & Tanaka, Y. (2003), Vehicle front structure in consideration of compatibility, *in* '18th International Technical Conference on the Enhanced Safety of Vehicles', Nagoya. Paper Number 03-0518.

Fujiwara, T. & Murayama, H. (2007), Research into new side impact test based on accidents in Europe and Japan, *in* '20th International Technical Conference on the Enhanced Safety of Vehicles', Lyon.

Fujiwara, T. & Shigeta, K. (2009), Development of moving deformable barrier reproducing struck car deformation in real-world car-to-car side impact accidents in Europe and Japan., *in* '21st International Technical Conference on the Enhanced Safety of Vehicles', Stuttgart.

Gabler, H. C. & Hollowell, W. T. (2000), 'The crash compatibility of cars and light trucks', *Traffic Injury Prevention* **2**(1), pp. 19–31.

Gennarelli, T. A., ed. (1998), *Abbreviated Injury Scale 1990: Update 1998*, Association for the Advancement of Automotive Medicine (AAAM), Barrington.

Gennarelli, T. A. & Wodzin, E., eds (2005), *Abbreviated Injury Scale 2005*, Association for the Advancement of Automotive Medicine (AAAM), Barrington.

GIDAS Codebook (2007), unpublished version from 29.08.2007.

Glaz, J. & Sison, C. P. (1999), 'Simultaneous confidence intervals for multinomial proportions', *Journal of Statistical Planning and Inference* **82**(1), pp. 251–262.

Haddon, William, J. (1980), 'Advances in the epidemiology of injuries as a basis for public policy', *Public Health Reports* **95**(5), pp. 411–421.

Hartung, J., Elpelt, B. & Klösener, K.-H. (2005), *Statistik*, 13 edn, Oldenbourg Verlag, Munich.

Hauer, E. (2006), 'The frequency-severity indeterminacy', *Accident Analysis & Prevention* **38**(1), pp. 78–83.

Hautzinger, H. (1985), *Stichproben- und Hochrechnungsverfahren für Verkehrssicherheitsuntersuchungen*, Bundesanstat für Straßenwesen, Bergisch Gladbach.

Hautzinger, H., Pfeiffer, M. & Schmidt, J. (2004), Expansion of GlDAS sample data to the regional level: Statistical methodology and practical experiences, *in* '1st International Conference on ESAR "Expert Symposium on Accident Research"', Bundesanstat für Straßenwesen, Hanover.

Hill, J., Thomas, P., Smith, M., Byard, N. & Rillie, I. (2001), The methodology of on the spot accident investigations in the UK, *in* '17th International Technical Conference on the Enhanced Safety of Vehicles', Amsterdam. Paper Number 01-0165.

Hirayama, S., Watanabe, T., Obayashi, K. & Okabe, T. (2007), Second report of research on stiffness matching between vehicles for frontal impact compatibility, *in* '20th International Technical Conference on the Enhanced Safety of Vehicles', Lyon.

Hollowell, W. T. & Gabler, H. C. (1996), NHTSA's vehicle aggressivity and compatibility research program, *in* '15th International Technical Conference on the Enhanced Safety of Vehicles', Melbourne. Paper Number 96-S4-O-01.

Huang, M. (2002), *Vehicle Crash Mechanics*, CRC Press, Dearborn, Michigan, USA.

IIHS (2009), 'Car size, weight and safety', *Insurance Institute for Highway Safety: Status Report* **44**(4), pp. 1–7.

Javouhey, E., Guérin, A.-C. & Chiron, M. (2006), 'Incidence and risk factors of severe traumatic brain injury resulting from road accidents: A population-based study', *Accident Analysis & Prevention* **38**(2), pp. 225–233.

Jenefeldt, F. (2008), 'Investigating the effects of strengthening the crossbeam in frontal car-to-car impacts', *International Journal of Crashworthiness* **13**(1), pp. 1–8.

Juckett, D. A. & Rosenberg, B. (1993), 'Comparison of the gompertz and weibull functions as descriptors for human mortality distributions and their intersections', *Mechanisms of Ageing and Development* **69**(1-2), pp. 1–31.

Keall, M. D. & Newstead, S. (2008), 'Are suvs dangerous vehicles?', *Accident Analysis & Prevention* **40**(3), pp. 954–963.

Kersten, R. (2004), Methodik zur Entwicklung von crashkompatiblen Gesamtfahrzeugkonzepten, Doctoral thesis, Technische Universität Carolo-Wilhelmina zu Braunschweig.

Klanner, W., Felsch, B. & West, F. v. (1998), Evaluation of occupant protection and compatibility out of frontal crash tests against the deformable barrier, *in* '16th International Technical Conference on the Enhanced Safety of Vehicles', Windsor. Paper Number 98-S3-O-06.

Kockelman, K. M. & Kweon, Y.-J. (2002), 'Driver injury severity: an application of ordered probit models', *Accident Analysis & Prevention* **34**(3), pp. 313–321.

Kullgren, A. (1999), 'Crash-pulse recorders in real-life accidents: Influence of change of velocity and mean and peak acceleration on injury risk in frontal impacts', *Traffic Injury Prevention* **1**(2), pp. 113–120.

Levin, B. (1981), 'A representation for multinomial cumulative distribution functions', *The Annals of Statistics* **9**(5), pp. 1123–1126.

Liao, X., Li, Q., Yang, X., Li, W. & Zhang, W. (2008), 'A two-stage multi-objective optimisation of vehicle crashworthiness under frontal impact', *International Journal of Crashworthiness* **13**(3), pp. 279–288.

Lomanaco, C. (1998), International harmonized research activities (IHRA) status report of the advanced offset frontal crash protection working group, *in* '16th International Technical Conference on the Enhanced Safety of Vehicles', Windsor.

Lomonaco, C. & Gianotti, E. (2001), 5-years status report of the advanced offset frontal crash protection, *in* '17th International Technical Conference on the Enhanced Safety of Vehicles', Amsterdam. Paper Number 01-0491.

Loo, M., Stinton, T., Priddle, B., Seyer, K. & Wong, H. L. (2003), Combining the finite element models of the Ford Falcon and Subaru Legacy to improve vehicle

compatibility, *in* '18th International Technical Conference on the Enhanced Safety of Vehicles', Nagoya. Paper Number 03-0117.

Lorenz, B. (2008), Mobile progressive deformable barrier and mobile rigid barrier tests – MPDB and MRB, *in* 'Minutes of 3rd meeting of the Informal Group on Frontal Impact – 9th December 2008', Document FI-03-10, Economic Commission for Europe – Inland Transport Committee – World Forum for Harmonization of Vehicle Regulations – Working Party on Passive Safety – Informal Group on Frontal Impact, Paris.

Lowne, R. (2001), Research progress on improved side impact protection EEVC WG13 progress report, *in* '17th International Technical Conference on the Enhanced Safety of Vehicles', Amsterdam. Paper Number 01-0047.

Lowne, R. W. (1994), EEVC working group 11 report on the development of a front impact test procedure, *in* '14th International Technical Conference on the Enhanced Safety of Vehicles', Munich.

Mackay, G. M., Cheng, L., Smith, M. & Parkin, S. (1992), 'Restrained front seat car occupant fatalities–the nature and circumstances of their injuries', *Accident Analysis & Prevention* **24**(3), pp. 307–315.

MacKenzie, E. J., Rivara, F. P., Jurkovich, G. J., Nathens, A. B., Frey, K. P., Egleston, B. L., Salkever, D. S. & Scharfstein, D. O. (2006), 'A national evaluation of the effect of trauma-center care on mortality', *The New England Journal of Medicine* **354**(4), pp. 366–378.

Margaritis, D., Hoogvelt, B., de Vries, Y., Klootwijk, C. & Mooi, H. (2005), An analysis of sport utility vehicles involved in road accidents, *in* '19th International Technical Conference on the Enhanced Safety of Vehicles', Washington DC. Paper Number 05-0370.

Martin, J.-L. & Lenguerrand, E. (2008), 'A population based estimation of the

driver protection provided by passenger cars: France 1996-2005', *Accident Analysis & Prevention* **40**(6), pp. 1811–1821.

Matsui, Y., Hosokawa, N., Takagi, S., Yonezawa, H., Mizuno, K. & Kubota, H. (2007), Investigation for new side impact test procedures in Japan - effect of various moving deformable barriers and male/female dummies on injury criteria in side impact test, *in* '20th International Technical Conference on the Enhanced Safety of Vehicles', Lyon.

McNeill, A., Haberl, J., Holzner, M., Schoeneburg, R., Strutz, T. & Tautenhahn, U. (2005), Current worldwide side impact activities - divergence versus harmonisation and the possible effect on future car design, *in* '19th International Technical Conference on the Enhanced Safety of Vehicles', Washington DC. Paper Number 05-0077.

Meyerson, S. L. & Nolan, J. M. (2001), Effects of geometry and stiffness on the frontal compatibility of utility vehicles, *in* '17th International Technical Conference on the Enhanced Safety of Vehicles', Amsterdam. Paper Number 01-0091.

Meyerson, S., Wiacek, C., Delannoy, P. & Robert, G. (2009), Evaluation of advanced compatibility frontal structures using the progressive deformable barrier (PDB), *in* '21st International Technical Conference on the Enhanced Safety of Vehicles', Stuttgart.

Mizuno, K. & Kajzer, J. (1998), 'Compatibility analysis of mini cars in frontal collisions using madymo', *International Journal of Crashworthiness* **3**(2), pp. 123–134.

Mizuno, K. & Kajzer, J. (1999), 'Compatibility problems in frontal, side, single car collisions and car-to-pedestrian accidents in japan', *Accident Analysis & Prevention* **31**(4), pp. 381–391.

Mizuno, K., Tateishi, K. & Ezaka, Y. (2001), Test procedures to evaluate vehicle compatibility, *in* '17th International Technical Conference on the Enhanced Safety of Vehicles', Amsterdam. Paper Number 01-0127.

Mizuno, K., Tateishi, K., Arai, Y. & Nishimoto, T. (2003), Research on vehicle compatibility in Japan, *in* '18th International Technical Conference on the Enhanced Safety of Vehicles', Nagoya. Paper Number 03-0113.

Mizuno, K., Arai, Y. & Newland, C. A. (2004), 'Compartment strength and its evaluation in car crashes', *International Journal of Crashworthiness* **9**(5), pp. 547–557.

Mizuno, K., Arai, Y. & Notsu, M. (2005*a*), Full-width test and overload test to evaluate compatibility, *in* 'SAE 2005 World Congress', Society of Automotive Engineers, Detroit. Paper Number 2005-01-1373.

Mizuno, K., Arai, Y., Yamazaki, K., Yonezawa, H. & Notsu, M. (2005*b*), 'Test procedures for vehicle compatibility evaluation', *International Journal of Crashworthiness* **10**(5), pp. 473–481.

Mizuno, K., Arai, Y., Yamazaki, K., Kubota, H., Yonezawa, H. & Hosokawa, N. (2008), 'Effectiveness and evaluation of seas of suv in frontal impact', *International Journal of Crashworthiness* **13**(5), pp. 533–541.

Mostafa, K., Digges, K., Bahouth, G. & Morgan, R. (2005), Vehicle frontal stiffness in a front to front crash, *in* 'SAE 2005 World Congress', Society of Automotive Engineers, Detroit. Paper Number 2005-01-1375.

Newgard, C. D., Lewis, R. J., Kraus, J. F. & McConnell, K. J. (2005), 'Seat position and the risk of serious thoracoabdominal injury in lateral motor vehicle crashes', *Accident Analysis & Prevention* **37**(4), pp. 668–674.

Newstead, S. & Cameron, M. (1999), Updated correlation of results from the Australian New Car Assessment Program with real crash data from 1987 to 1996, Technical Report 152, Monash University Accident Research Centre, Clayton.

Newstead, S., Watson, L. & Cameron, M. (2008), Vehicle safety ratings estimated from police reported crash data: 2008 update. Australian and New Zealand crashes during 1987-2006, Technical Report 280, Monash University Accident Research Centre, Clayton.

NHTSA (2009), 'Consumer information; new car assessment program', *Federal Register* **73**(134), 40016–40015. Docket Number: NHTSA-2006-26555-0114.

Nilsson, G. (2004), Traffic Safety Dimensions and the Power Model to Describe the Effect of Speed on Safety, Doctoral thesis, Lund Institute of Technology and Society.

Nolan, J. M. & Lund, A. K. (2001), Frontal offset deformable barrier crash testing and its effect on vehicle stiffness, *in* '17th International Technical Conference on the Enhanced Safety of Vehicles', Amsterdam. Paper Number 01-0487.

Nolan, J. M., Powell, M. R., Preuss, C. A. & Lund, A. K. (1999), Factors contributing to front-side compatibility: A comparison of crash test results, *in* '43th Stapp Car Crash Conference', The Stapp Association, San Diago. Paper Number 99SC02.

Nusholtz, G., Xu, L., Velez, E. L., Hsu, T. & Kochekseraii, S. B. (2009), Reproducibility of AHOF400 and KW400, *in* '21st International Technical Conference on the Enhanced Safety of Vehicles', Stuttgart.

O'Brien, S., Zobel, R. & Schwarz, T. (2007), Assessment of compatibility for both self- and partner-protection, *in* 'VDI Fahrzeug- und Verkehrstechnik Tagung Innovativer Kfz-Insassen und Partnerschutz', Berlin.

O'Brien, S. (2008), Risks and opportunities: The assessment of self-protection and partner-protection in the USA, *in* 'SAE Government/Industry Meeting', Washington, DC.

O'Reilly, P. (2001), Status report of IHRA vehicle compatibility working group, *in*

'17th International Technical Conference on the Enhanced Safety of Vehicles', Amsterdam. Paper Number 01-0337.

O'Reilly, P. (2003), Status report of IHRA compatibility and frontal impact working group, *in* '18th International Technical Conference on the Enhanced Safety of Vehicles', Nagoya. Paper Number 03-0402.

O'Reilly, P. (2005), Status report of IHRA compatibility and frontal impact working group, *in* '19th International Technical Conference on the Enhanced Safety of Vehicles', Washington DC. Paper Number 05-0365.

Otte, D., Krettek, C., Brunner, H. & Zwipp, H. (2003), Scientific approach and methodology of a new in-depth-investigation study in Germany so called GIDAS, *in* '18th International Technical Conference on the Enhanced Safety of Vehicles', Nagoya. Paper Number 03-0161.

Otte, D. & Nehmzow, J. (2002), 'Codierungs-Katalog zur Dokumentation von Verkehrsunfällen: In Rahmen der Erhebungen am Unfallort, Hannover und Dresden'.

Park, C.-K., Thomson, R., Krusper, A. & Kan, C.-D. S. (2009), The influence of sub-frame geometry on a vehicle's frontal crash response, *in* '21st International Technical Conference on the Enhanced Safety of Vehicles', Stuttgart.

Patel, S., Prasad, A. & Mohan, P. (2009), NHTSA's recent test program on vehicle compatibility, *in* '21st International Technical Conference on the Enhanced Safety of Vehicles', Stuttgart.

Patel, S., Smith, D., Prasad, A. & Mohan, P. (2007), NHTSA's recent vehicle crash test program on compatibility in front-to-front impacts, *in* '20th International Technical Conference on the Enhanced Safety of Vehicles', Lyon.

Ragland, C. L. (1998), Offset test procedure development and comparison, *in* '16th International Technical Conference on the Enhanced Safety of Vehicles', Windsor. Paper Number 98-S1-O-03.

Rieger, G., Scheef, J., Becker, H., Stanzel, M. & Zobel, R. (2005), Active safety systems change accident environment of vehicles significantly – a challenge for vehicle design, *in* '19th International Technical Conference on the Enhanced Safety of Vehicles', Washington DC. Paper Number 05-0074.

Roberts, A. K. & van Ratingen, M. R. (2003), Progress on the development of the Advanced European Mobile Deformable Barrier face (AE-MDB), *in* '18th International Technical Conference on the Enhanced Safety of Vehicles', Nagoya. Paper Number 03-0126.

Rodgers, K. (1998), International harmonized research activities (IHRA) status report of the vehicle compatibility working group, *in* '16th International Technical Conference on the Enhanced Safety of Vehicles', Windsor.

Roussarie, M.-L., Zeitouni, R. & Adalian, C. (2007), Enhancement of side impact protection using an improved test procedure, *in* '20th International Technical Conference on the Enhanced Safety of Vehicles', Lyon.

Samaha, R. R. & Elliott, D. S. (2003), NHTSA side impact research: motivation for updated test procedures, *in* '18th International Technical Conference on the Enhanced Safety of Vehicles', Nagoya. Paper Number 03-0492.

Samaha, R. R., Molino, L. N. & Maltese, M. R. (1998), Comparative performance testing of passenger cars relative to FMVSS 214 and the EU 96/EC/27 side impact regulations: Phase 1, *in* '16th International Technical Conference on the Enhanced Safety of Vehicles', Windsor. Paper Number 98-S8-O-08.

Saunders, James W., I. & Prasad, A. (2005), NHTSA's frontal offset research program, *in* '19th International Technical Conference on the Enhanced Safety of Vehicles', Washington DC. Paper Number 05-0206.

Scarboro, M., Rudd, R. & Sochor, M. (2007), Nearside occupants in low delta-v side impact crashes: Analysis of injury and vehicle damage patterns, *in* '20th International Technical Conference on the Enhanced Safety of Vehicles', Lyon.

Schiff, M. A., Tencer, A. F. & Mack, C. D. (2008), 'Risk factors for pelvic fractures in lateral impact motor vehicle crashes', *Accident Analysis & Prevention* **40**(1), pp. 387–391.

Schram, R. (2008), Additional research of the NL, *in* 'Minutes of 3rd meeting of the Informal Group on Frontal Impact – 9th December 2008', Document FI-03-07, Economic Commission for Europe – Inland Transport Committee – World Forum for Harmonization of Vehicle Regulations – Working Party on Passive Safety – Informal Group on Frontal Impact, Paris.

Schram, R., Leneman, F. J. W., van der Zweep, C. D., Wismans, J. S. H. M. & Witteman, W. J. (2006), 'Assessment criteria for assessing energy-absorbing front underrun protection on trucks', *International Journal of Crashworthiness* **11**(6), pp. 597–604.

Schram, R. & Versmissen, T. (2007), The development of a mobile deformable barrier test procedure, *in* '20th International Technical Conference on the Enhanced Safety of Vehicles', Lyon.

Schwarz, T. (2002), *Selbst- und Partnerschutz bei frontalen Pkw-Pkw-Kollisionen (Kompatibilität)*, Fortschritt Berichte VDI, Reihe 12, Nr. 502, Berlin.

Seiffert, U., Hamilton, J. & Boersch, F. (1974), Compatibility of traffic participants, *in* 'Third International Conference on Automotive Safety', Vol. 1, San Francisco.

Seiffert, U. & Wech, L. (2003), *Automotive Safety Handbook*, SAE International, Warrendale, Pa., USA.

Seiffert, U. & Wech, L. (2007), *Automotive Safety Handbook*, 2 edn, SAE International, Warrendale.

Severy, D. M., Brink, H. M. & Blaisdell, D. M. (1971), Smaller vehicle versus larger vehicle collisions, *in* S. H. Backaitis, ed., 'Vehicle Compatibility in Automotive Crashes', Society of Automotive Engineers, Warrendale, pp. 285–335.

Seyer, K. (2001), International harmonised research activities side impact working group status report, *in* '17th International Technical Conference on the Enhanced Safety of Vehicles', Amsterdam. Paper Number 01-0151.

Seyer, K. (2003), International harmonised research activities side impact working group status report, *in* '18th International Technical Conference on the Enhanced Safety of Vehicles', Nagoya. Paper Number 03-0579.

Seyer, K. A., Newland, C. A. & Terrell, M. B. (2003*a*), 'Australian research to develop a vehicle compatibility test', *International Journal of Crashworthiness* **8**(2), pp. 143–150.

Seyer, K. A., Newland, C. A. & Terrell, M. B. (2003*b*), Australian research to support the IHRA vehicle compatibility working group, *in* '18th International Technical Conference on the Enhanced Safety of Vehicles', Nagoya. Paper Number 03-0274.

Seyer, K., Newland, C. & Terrell, M. (2000), The effect of mass, stiffness and geometry on injury outcome in side impacts – a parametric study, *in* '44th Stapp Car Crash Conference', The Stapp Association, San Diago. Paper Number 2000-01-SC01.

Seyer, K., Terrell, M., Fildes, B., Dyte, D. & Digges, K. (1998), Development and benefits of a harmonised dynamic side impact standard, *in* '16th International Technical Conference on the Enhanced Safety of Vehicles', Windsor. Paper Number 98-S8-O-02.

Sison, C. P. & Glaz, J. (1995), 'Simultaneous confidence intervals and sample size determination for multinomial proportions', *Journal of the American Statistical Association* **90**(429), pp. 366–369.

Stanzel, M. & Page, Y. (2006), *APROSYS Accident Analysis on Car Accidents with Respect to Advanced Front Impact and Compatibility, Deliverable D8.3.2*, APROSYS Project Consortium.

StBA (2006), *Verkehr: Verkehrsunfälle 2005*, Fachserie 8 Reihe 7, Statistisches Bundesamt, Wiesbaden.

Subramaniam, K., Verma, M., Nagappala, R., Tedesco, R. & Carlin, L. (2007), Evaluation of stiffness matching concepts for vehicle safety improvement, *in* '20th International Technical Conference on the Enhanced Safety of Vehicles', Lyon.

Summers, S. M., Hollowell, W. T. & Prasad, A. (2003), NHTSA's research program for vehicle compatibility, *in* '18th International Technical Conference on the Enhanced Safety of Vehicles', Nagoya. Paper Number 03-0307.

Summers, S. M., Prasad, A. & Hollowell, W. T. (1999), NHTSA's vehicle compatibility research program, *in* 'International Congress & Exposition', Society of Automotive Engineers, Detroit. SAE Paper 1999-01-0071.

Summers, S. M., Prasad, A. & Hollowell, W. T. (2001), NHTSA's research program for vehicle aggressivity and fleet compatibility, *in* '17th International Technical Conference on the Enhanced Safety of Vehicles', Amsterdam. Paper Number 01-0249.

Summers, S. & Prasad, A. (2005), NHTSA's recent compatibility test program, *in* '19th International Technical Conference on the Enhanced Safety of Vehicles', Washington DC. Paper Number 05-0278.

Swanson, J., Rockwell, T., Beuse, N., Summers, L., Summers, S. & Park, B. (2003), Evaluation of stiffness measurements from the U.S. new car assessment program, *in* '18th International Technical Conference on the Enhanced Safety of Vehicles', Nagoya. Paper Number 03-0527.

Takizawa, S., Higuchi, E., Iwabe, T., Emura, M., Kisai, T. & Suzuki, T. (2007), Investigation of structural factors influencing compatibilty in vehicle-to-vehicle side impacts, *in* '20th International Technical Conference on the Enhanced Safety of Vehicles', Lyon.

Takizawa, S., Higuchi, E., Iwabe, T., Kisai, T. & Suzuki, T. (2005), Study of load cell MDB crash tests for evaluation of frontal impact compatibility, *in* '19th International Technical Conference on the Enhanced Safety of Vehicles', Washington DC. Paper Number 05-0235.

Taschenmacher, R. (2009), *Verkehrsunfallaufnahme*, 3 edn, Verlag Deutsche Polizeiliteratur GmbH, Hilden.

Tencer, A. F., Kaufman, R., Huber, P. & Mock, C. (2005), 'The role of door orientation on occupant injury in a nearside impact: A ciren, madymo modeling and experimental study', *Traffic Injury Prevention* **6**(4), pp. 372–378.

Thomas, G. (2006), Compatibility and structural interaction in passenger vehicle collisions, Doctoral thesis, RMIT University.

Thompson, A., Puppini, R., Ferichola, G., Guerra, L. J., García, A. & Edwards, M. (2007), *Main Influencing Factors in Side Impact Compatibility and Concepts for a Side Impact Compatibility Test, Deliverable D1.1.5B*, APROSYS Project Consortium.

Thomson, R. & Edwards, M. (2005), Passenger vehicle crash test procedure developments in the VC-Compat project, *in* '19th International Technical Conference on the Enhanced Safety of Vehicles', Washington DC. Paper Number 05-0008.

Thomson, R., Edwards, M., Martin, T., van der Zweep, C., Damm, R. & della Valle, G. (2007), 'Car-car crash compatibility: development of crash test procedures in the vc-compat project', *International Journal of Crashworthiness* **12**(2), pp. 137–151.

Tingvall, C., Krafft, M., Lie, A. & Kullgren, A. (2003), The role of impact velocity and change of velocity in side impacts, *in* '18th International Technical Conference on the Enhanced Safety of Vehicles', Nagoya. Paper Number 03-0219.

Ueno, M., Hatano, K., Fukushima, N. & Tsuburai, Y. (2007), Development of new generation mobile deformable barrier, *in* '20th International Technical Conference on the Enhanced Safety of Vehicles', Lyon.

UN-ECE (1998), *Agreement concerning the establishing of Global Technical Regulations for wheeled vehicles, equipment and parts which can be fitted and/or used on wheeled vehicles*, United Nations Economic Commission for Europe, Geneva.

Uwai, H., Toyosaki, S., Sagawa, K. & Takahashi, N. (2007), A study on AHOF400 which is possible car-to-SUV compatibility evaluation method, *in* '20th International Technical Conference on the Enhanced Safety of Vehicles', Lyon.

van de Wiel, M. A., Di Bucchianico, A. & van der Laan, P. (1999), 'Symbolic computation and exact distributions of nonparametric test statistics', *The Statistician* **48**(4), pp. 507–516.

van der Sluis, J. (2000), Vehicle compatibility in car-to-car collisions: Literature review in the framework of the european research project "improvement of crash compatibility between cars", workpackage 1, Technical report, SWOV Institute for Road Safety Research, Leidschendam.

van Schijndel-de Nooij, M. & Wismans, J. (2008), 'APROSYS: advances in secondary safety research', *International Journal of Crashworthiness* **13**(6), pp. 591–598.

VDA (2009), Detailed discussion of the VDA position on the proposal for draft amendments to UN-ECE R94, *in* 'Minutes of 4th meeting of the Informal Group on Frontal Impact – 10th March 2009', Document FI-03-09, Economic Commission for Europe – Inland Transport Committee – World Forum for Harmonization of Vehicle Regulations – Working Party on Passive Safety – Informal Group on Frontal Impact, Paris.

Verma, M. K. (2007), Enhanced vehicle collision compatibility – progress report of US technical workgroup for front-to-front compatibility, *in* '20th International Technical Conference on the Enhanced Safety of Vehicles', Lyon. Paper Number 07-0291.

Verma, M. K., Nagappala, R., Murugan, M. & Tung, Y. J. (2004), 'Evaluation of structural parameters for vehicle crash compatibility', *International Journal of Crashworthiness* **9**(6), pp. 577–586.

Versmissen, T., van Schijndel, M., Edwards, M. & Langner, T. (2007), Development and evaluation of the side impact test procedure proposed by IHRA, *in* '20th International Technical Conference on the Enhanced Safety of Vehicles', Lyon.

WHO (2008), *The Global Burden of Disease: 2004 Update*, World Healt Organisation, Geneva. (`http://www.who.int/healthinfo/global_burden_disease/GBD_report_2004update_full.pdf`, accessed 1st September 2009).

Wood, D. P. (1997), 'Safety and the car size effect: A fundamental explanation', *Accident Analysis & Prevention* **29**(2), pp. 139–151.

Wood, D. P., Veyrat, N., Simms, C. & Glynn, C. (2007), 'Limits for survivability in frontal collisions: Theory and real-life data combined', *Accident Analysis & Prevention* **39**(4), pp. 679–687.

Wood, D. & Walsh, D. (2002), 'Car to car interaction in frontal collisions: A model for the behaviour of the car population and options for improved crashworthiness', *International Journal of Crashworthiness* **7**(1), pp. 79–96.

Wykes, N. J., Edwards, M. J. & Hobbs, C. A. (1998), Compatibility requirements for cars in frontal and side impact, *in* '16th International Technical Conference on the Enhanced Safety of Vehicles', Windsor. Paper Number 98-S3-O-04.

Yamamoto, T., Hashiji, J. & Shankar, V. N. (2008), 'Underreporting in traffic

accident data, bias in parameters and the structure of injury severity models', *Accident Analysis & Prevention* **40**(4), pp. 1320–1329.

Yonezawa, H., Harigae, T. & Ezaka, Y. (2001), Japanese research activity on future side impact test procedures, *in* '17th International Technical Conference on the Enhanced Safety of Vehicles', Amsterdam. Paper Number 01-0267.

Yonezawa, H., Minda, H., Harigae, T., Sakurai, M. & Nishimoto, T. (2003), Investigation of new side impact test procedures in Japan, *in* '18th International Technical Conference on the Enhanced Safety of Vehicles', Nagoya. Paper Number 03-0328.

Yonezawa, H., Hosokawa, N., Minda, H. & Notsu, M. (2005), Investigation of new side impact test procedures in Japan, *in* '19th International Technical Conference on the Enhanced Safety of Vehicles', Washington DC. Paper Number 05-0188.

Yonezawa, H., Mizuno, K., Hirasawa, T., Kanoshima, H., Ichikawa, H., Yamada, S., Koga, H., Yamaguchi, A., Arai, Y. & Kikuchi, A. (2009*a*), Summary of activities of the compatibility working group in Japan, *in* '21st International Technical Conference on the Enhanced Safety of Vehicles', Stuttgart.

Yonezawa, H., Hosokawa, N., Tanaka, Y., Matsui, Y., Takagi, S., Hirasawa, T., Kanoshima, H. & Mizuno, K. (2009*b*), Investigation for new side impact test procedures in Japan, *in* '21st International Technical Conference on the Enhanced Safety of Vehicles', Stuttgart.

Zeidler, F. & Knöchelmann, F. (1998), 'The influence of frontal crash test speeds on the compatibility of passenger cars in real world accidents', *International Journal of Crashworthiness* **3**(1), pp. 7–16.

Zobel, R. (1998), Demands for compatibility of passenger vehicles, *in* '16th International Technical Conference on the Enhanced Safety of Vehicles', Windsor. Paper Number 98-S3-O-10.

Zobel, R. & Schwarz, T. (2001), Development of criteria and standards for vehicle compatibility, *in* '17th International Technical Conference on the Enhanced Safety of Vehicles', Amsterdam. Paper Number 01-0140.

Appendix A

Database and variables used in the accident analysis

The German In-Depth Accident Survey (GIDAS) database includes data from accident surveys conducted in the regions of Hanover, Lower Saxony, and Dresden, Saxony, as shown in Figure A.1. The Hanover project began in 1973 and has been carried out according to a systematic sampling plan since mid 1984 (Hautzinger 1985). The Dresden project was added in 1999 and has used Hautzinger's sampling plan since its inception (Hautzinger et al. 2004). Data are collected in two six-hour shifts per day, which alternate on a two-weekly basis. During each shift, the first reported accident with personal injury is analysed and recorded in the database. However, because only one team is active per shift, analysis of concurrent accidents is impossible. Hence, after completing the analysis of the first case, the next most recent accident is selected for the subsequent analysis, and intermediate accidents are ignored.

Because of the sampling methods used, the data collected since 1985 are considered representative of the German national accident statistics (Hautzinger et al. 2004). The only significant limitation of the GIDAS data is that accidents are only considered where at least one person is injured. This makes it impossible to use GIDAS to accurately predict changes in the numbers of uninjured passengers,[94]

[94]For example, an older generation vehicle may be involved in a collision, and its occupants

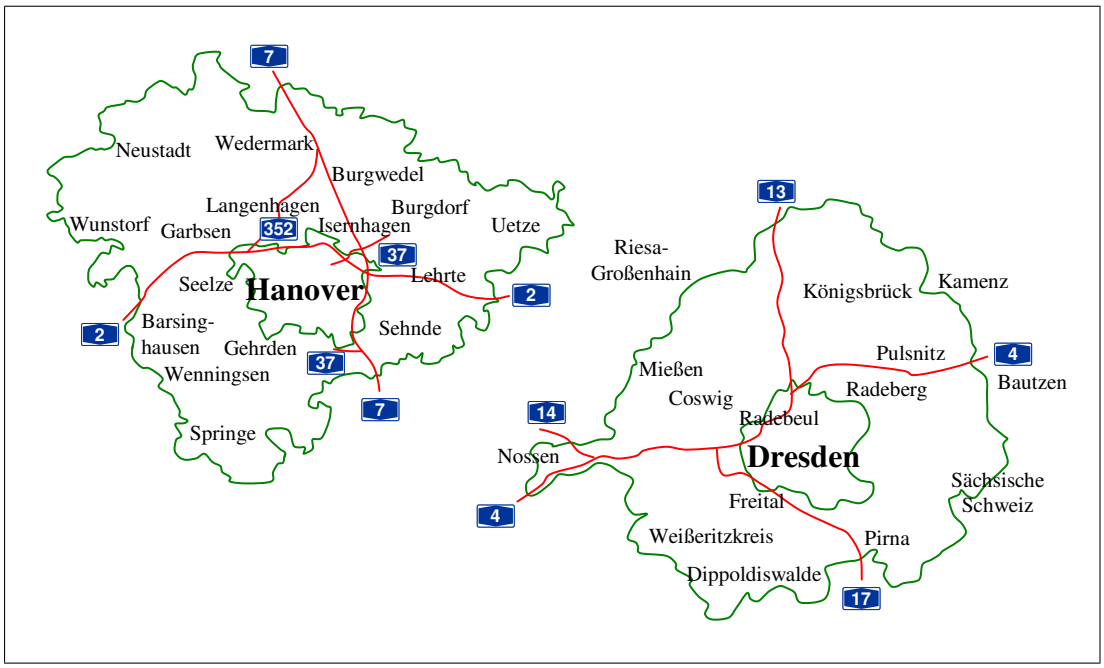

Figure A.1: Regions of Hanover and Dresden in which GIDAS data are collected.

however, for the purposes of this thesis, this limitation is not considered to be significant.

Figure A.2 shows the distribution of accident years and vehicle manufacturing date for the database extract used in the accident analysis. Although the extract is from February 2008, very few reconstructions are included from 2006 and 2007, and hence these years are excluded from the analysis. Figure A.2b shows the distribution of manufacturing dates in the sample, and it can be seen that the most modern vehicles are under-represented due to their relatively short-term exposure in the accident environment. Within the subset of vehicles with dates of manufacture between 1996 and 2005, the median manufacturing date is in 1998, and the 75$^{\text{th}}$ percentile is in 2000.

may be injured. A newer generation vehicle may be involved in an identical collision, but due to improvements in occupant protection its occupants may remain uninjured. This change is not reflected in GIDAS because there are no injuries in the second collision and hence it would not be recorded in the database.

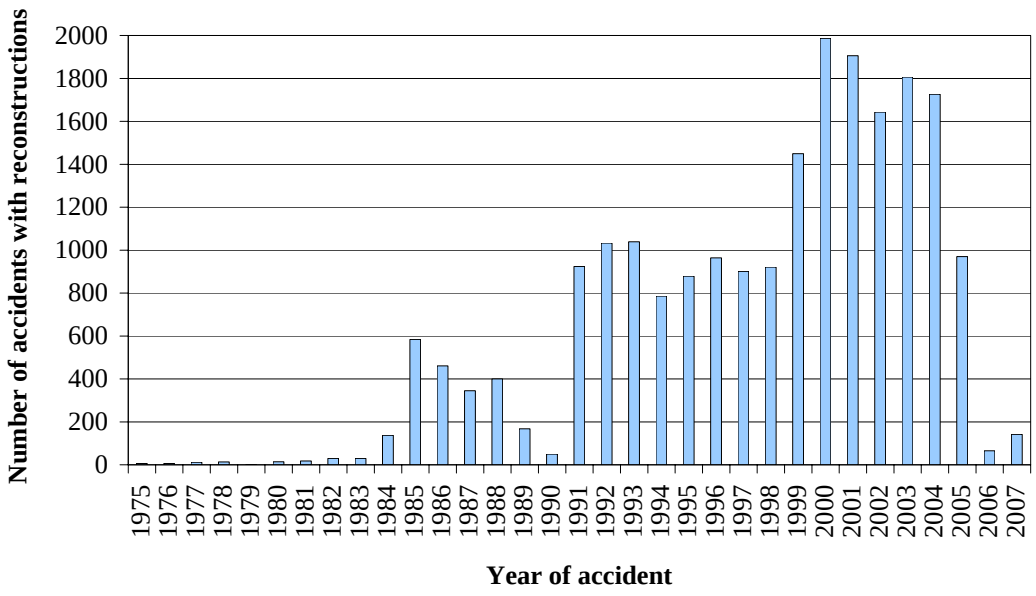

(a) Accidents per year with full reconstructions.

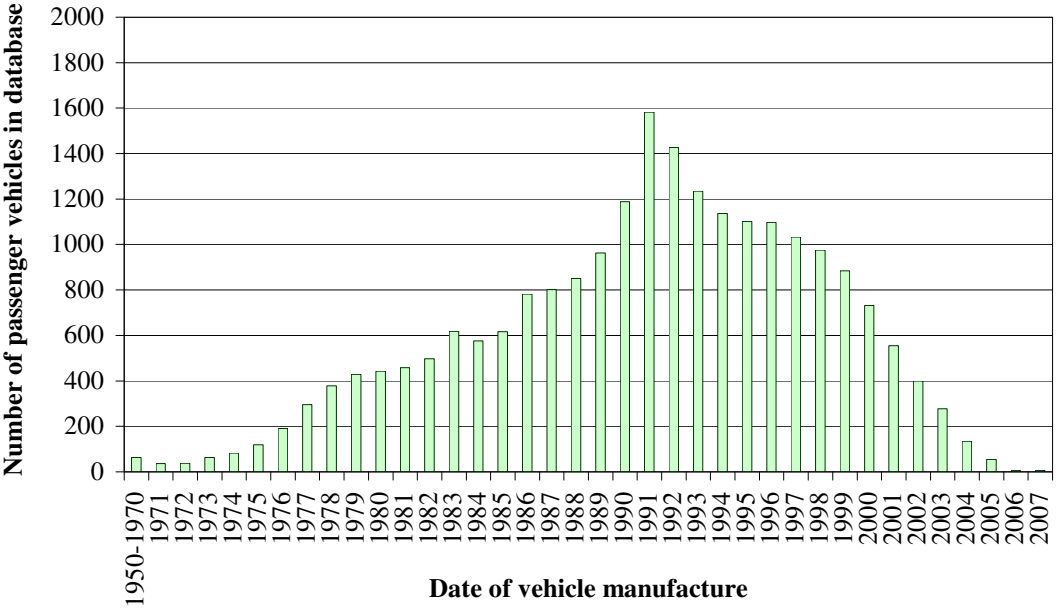

(b) Number of passenger vehicles with respect to the date of manufacture.

Figure A.2: Properties of the GIDAS database extract used for the accident analysis. The database extract is from February 2008.

A.1 Vehicle Deformation Indices

The Vehicle Deformation Index (VDI) variables describe various aspects of a vehicle's deformation and correspond to the Collision Deformation Code (CDC) variables used in other accident databases and defined in the Society of Automotive Engineers (SAE) Standard J224a Collision Deformation Classification. The descriptions below are adapted from the *GIDAS Codebook* (2007), which is not identical to the SAE Standard. However, the descriptions from the GIDAS codebook reflect the manner in which the data are actually collected and are hence a more relevant reference.

Direction of force (VDI 1) describes the principal direction of the force that damaged the vehicle. The angle is calculated based on a vector analysis of the collision impulse and reported with ±15°accuracy. As shown in Figure A.3, the value is recorded in terms of 'hours' from an analogue clock, with 12 o'clock being a force applied from directly forward of the vehicle.

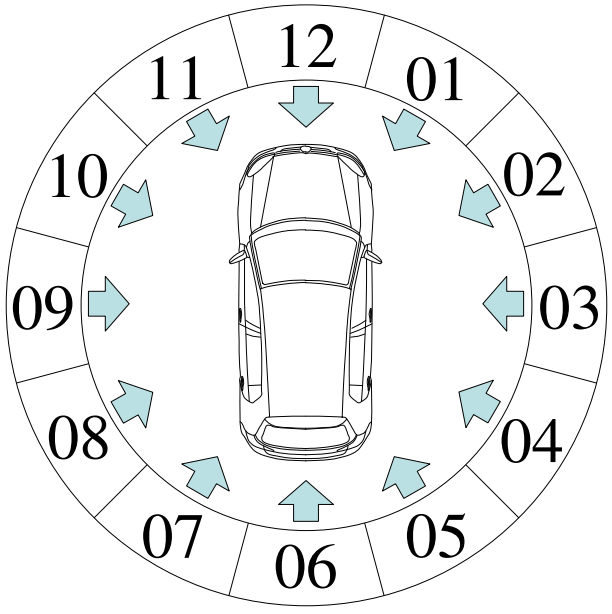

VDI1	Description
00	not applicable
01	1 o'clock
02	2 o'clock
03	3 o'clock
04	4 o'clock
05	5 o'clock
06	6 o'clock
07	7 o'clock
08	8 o'clock
09	9 o'clock
10	10 o'clock
11	11 o'clock
12	12 o'clock
99	unknown

Figure A.3: Direction of force as defined by VDI 1. The database values and their corresponding descriptions are shown on the right.

Location of damage (VDI 2) describes the location of the vehicle component that sustains the principal damage in a collision as shown in Figure A.4.

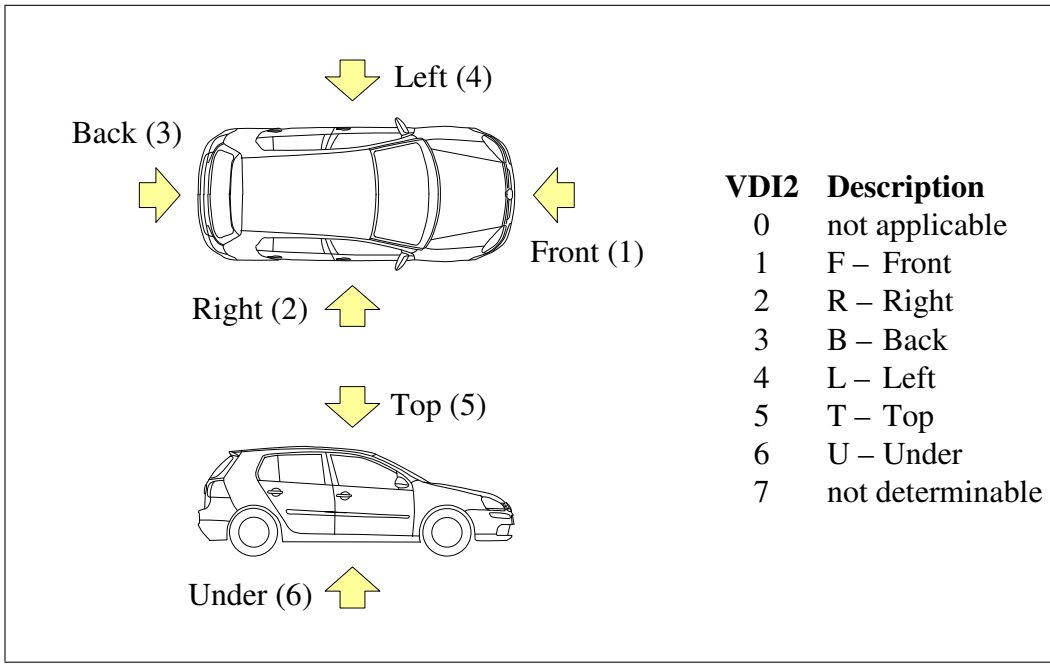

Figure A.4: Location of damage as defined by VDI 2. The database values and their corresponding descriptions are shown on the right.

Horizontal description of damage (VDI 3) describes the specific horizontal location of damage to the vehicle front, rear, or side as shown in Figure A.5.

Vertical description of damage (VDI 4) describes the specific vertical location of damage to the vehicle front, rear, or side as shown in Figure A.6.

Degree of deformation (VDI 6) is described in terms of the number of zones between the point at which the primary damage to the vehicle begins and the point at which it ends. The zones are described in Figure A.7. For example, a frontal collision with a tree could begin with deformation in zone 1 and end with deformation in zone 5, and hence VDI 6 = 5 would be coded. Alternatively, an underrun collision could begin with deformation in zone 3 and end with deformation in zone 6, and hence it would be coded with VDI 6 = 4.

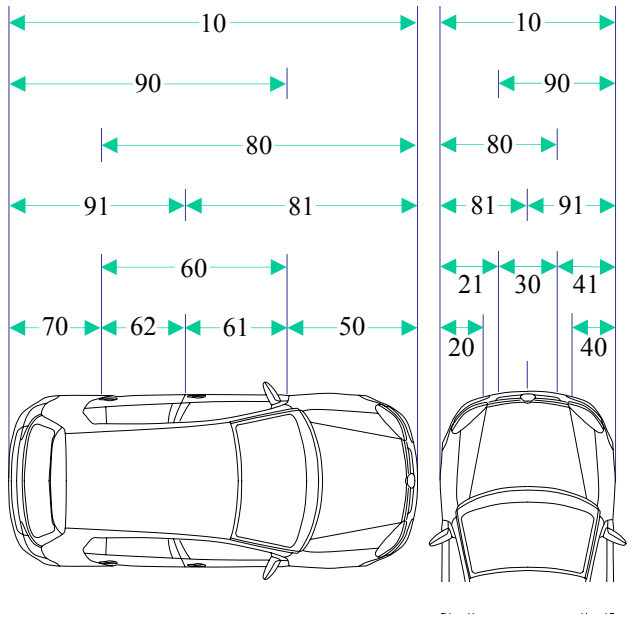

VDI3	Description
00	not applicable
10	D0 – entire front/side/rear (>⅔)
20	L0 – ¼ from left side
21	L1 – ⅓ from left side
30	C0 – middle ⅓
40	R0 – ¼ from right side
41	R1 – ⅓ from right side
50	F0 – forward of A-pillar
60	P0 – between A- and C-pillars
61	P1 – between A- and B-pillars
62	P2 – between B- and C-pillars
70	B0 – behind C-pillar
80	Y0 – ⅔ from left side/front
81	Y1 – ½ from left side/front
90	Z0 – ⅔ from right side/back
91	Z1 – ½ from right side/back

Figure A.5: Horizontal description of damage as defined by VDI 3. The regions shown for the right and front of the vehicle are equally applicable to the left and rear of the vehicle. The database values and their corresponding descriptions are shown on the right.

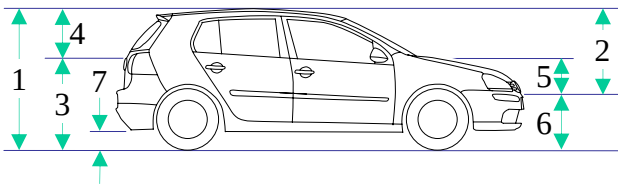

VDI4	Description
0	not applicable
1	A – all
2	H – above bumper
3	E – below belt-line
4	G – above belt-line
5	M – between bumper and belt-line
6	L – bumper and lower
7	W – wheels only
9	X – not determinable

Figure A.6: Vertical description of damage as defined by VDI 4. The database values and their corresponding descriptions are shown on the right.

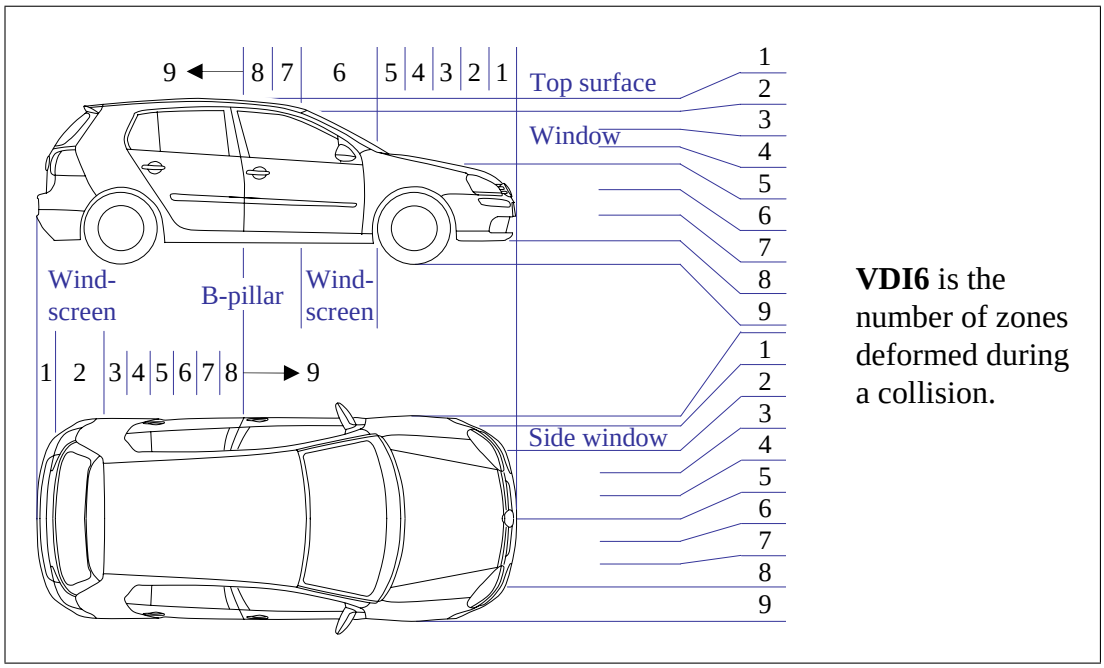

Figure A.7: Degree of deformation as defined by VDI 6. For descriptions of the vehicle regions for wagon and van type vehicles see *GIDAS Codebook* (2007).

A.1.1 Categories derived from the GIDAS variables

In several cases, the detail in the GIDAS database is too specific for the analysis, and hence it is simplified into fewer categories. In other cases, the detail is not specific enough, and hence multiple variables are combined in order to obtain the necessary information.

Mode of transport is simplified using the categories described in Table A.1. These categories are applied in Figure 3.2, and the definition of a passenger vehicle occupant is also used in the subsequent analyses in Chapters 3, 4, and 5.

Type of object struck is described using the categories from Table A.1 if the collision partner is another vehicle. For all other objects, the categories described in in Table A.2 are used.

Collision direction is determined using a combination of the VDI 1 and VDI 2 variables so that both the direction of force and the location of damage are taken into account. Furthermore, accidents that involve a rollover, which may or

Table A.1: Definition of transport modes as used in Figure 3.2. Note that this table includes two columns of 'vehicle types' per row.

Mode	Code	Vehicle Type	Code	Vehicle Type
Non Vehicle Occupant	-	Pedestrian	39	Bicycle
	35	Motorcycle > 125cc	40	Light motorcycle
	36	Small motorcycle < 50cc	41	Light powered bicycle
	37	Moped	42	Trike
	38	Powered bicycle	43	Motorcycle < 125cc
Passenger Vehicle Occupant	0	Car, no further details	16	Hardtop coupé
	1	Car, 2 doors	17	Sportscar
	2	Car, 2 doors plastic	18	Off-road vehicle
	3	Car, 2 doors, fastback	19	Car-like off-road vehicle
	4	Car, 4 doors	20	Convertible w/o rollbar
	5	Car, 4 doors, fastback	21	Convertible w. rollbar(s)
	6	Car, 3-door wagon	22	Convertible w. roof sect.
	7	Car, 5-door wagon	23	Convertible w. roof sect.
	8	Car, pick-up		and rollbar(s)
	9	Car, more than 5 seats	24	Other type of car
	10	Very small car	25	Minibus
	11	Car, 3 wheels	26	Transporter
	12	Coupé	56	Camper (transporter)
	13	Coupé, plastic	60	Van small
	14	Wagon-coupé	61	Van mid-sized
	15	Hardtop limousine	62	Van large
Commercial Vehicle Occupant	27	Small truck	34	Other commercial vehicle
	28	Truck < 7.5t	50	Road tanker < 7.5t
	29	Truck > 7.5t	51	Road tanker > 7.5t
	30	Road train	52	Articulated road tanker
	31	Bus	53	Tank truck
	32	Articulated lorry < 7.5t	57	Camper (bus)
	33	Articulated lorry > 7.5t		
Other, Unknown	44	Wheel chair	96	Train
	45	Quad	97	Tram
	55	Agricultural vehicle	98	Several
	58	Horse	99	Unknown

Table A.2: Definition of struck objects as implemented in Chapters 3, 4, and 5. Note that this table includes two columns of struck objects per row.

Object	**Code**	**Description**	**Code**	**Description**
Ground, Ditch	121	Road surface	171	Ditch - driven over
	122	Sidewalk/bicycle lane	172	Ditch - driven through
	123	Other paved road	173	Downward slope
	124	Sand, gravel	174	Earth wall
	125	Grass, lawn	177	Kerbstone
	126	Field	178	Railway track
	170	Road side ditch		
Wall, Barrier	150	Guard rail	181	Bridge pier (wide)
	151	Distance guard rail	182	Wire-mesh fence
	152	Double guard rail	183	Wooden fence
	153	Guard rail pillar	184	Fence, partbricked
	154	Sigma-pillar	185	Wall
	175	Noise barrier	186	House wall
	176	Bridge balustrade		
Pole, Post, Tree	155	Pillar	163	Power pole (wood)
	156	Pole of traffic sign	164	Power pole (metal)
	158	Sign bridge	166	Tree (fell over)
	159	Traffic light	167	Tree (stable)
	161	Street light	180	Bridge pier (narrow)
	162	Street light $>$ 1 lamp		
Other, Unknown	110	Animal	120	Object on road
	111	Bird	157	Arm of traffic sign
	112	Cat, rabbit	160	Switchbox
	113	Dog	165	Bush/shrubbery
	114	Pig, wild boar	179	Other traffic guide
	115	Deer	189	Stationary obstacle
	116	Sheep, goat	190	Water
	117	Horse, donkey	191	Own trailer
	118	Cattle	998	Others
	119	Other animal	999	Unknown

may not be coded as the most severe event, are filtered out. Even as a secondary collision, a rollover may have a significant influence on the injury outcome of the vehicle occupants and could lead to scatter in the statistics. The types of collisions are described in Table A.3.

Table A.3: Definition of collision direction as implemented in Chapters 3, 4, and 5. For clarity, the 'rollover' and 'other, unknown' categories are omitted from the table.

Collision direction	**Location of damage (VDI 2)**	**Direction of force (VDI 1)**
Front	Front	{11, 12, 1}
Side	Right	{2, 3, 4}
	Left	{8, 9, 10}
Rear	Back	{5, 6, 7}
Oblique	Front	{2, 3, 4, 5} {7, 8, 9, 10}
	Right	{5, 6, 7, 8} {10, 11, 12, 1}
	Left	{4, 5, 6, 7} {11, 12, 1, 2}
	Back	{1, 2, 3, 4} {8, 9, 10, 11}

Appendix B

Raw data used in the accident analysis

This appendix contains the raw data from selected figures from the accident analysis. In particular, it contains the data used to create each of the stacked pie charts in Chapters 3, 4, and 5.

Table B.1: Accident data used in Figure 3.1.

AIS/ MAIS	AIS			MAIS		
	Survived	**Deceased**	**95% CI**[a]	**Survived**	**Deceased**	**95% CI**
1	6533	13	[0.1%, 0.3%]	13326	20	[0.1%, 0.2%]
2	492	3	[0.1%, 1.8%]	3201	12	[0.2%, 0.7%]
3	238	4	[0.5%, 4.2%]	791	35	[3.0%, 5.8%]
4	11	2	[1.9%, 45%]	191	34	[11%, 20%]
5	8	5	[14%, 68%]	66	91	[50%, 66%]
6	0	27	[87%, 100%]	0	119	[97%, 100%]

[a] Confidence Interval (CI).

Table B.2: Accident data used in Figure 3.2a.

Mode of transport	MAIS				95% Confidence intervals		
	0-1	2	3	4-6	MAIS 2+	MAIS 3+	MAIS 4+
Passenger Vehicle	22708	1566	351	425	[9.0%, 10%]	[2.9%, 3.3%]	[1.5%, 1.9%]
Commercial Veh.	1787	62	33	21	[5.1%, 7.3%]	[2.1%, 3.7%]	[0.7%, 1.7%]
Non Vehicle Occ.	4958	1676	530	319	[33%, 35%]	[11%, 12%]	[3.8%, 4.7%]
Other, Unknown	587	9	2	1	[1.0%, 3.5%]	[0.1%, 1.5%]	[0.0%, 0.9%]

Table B.3: Accident data used in Figure 3.3a.

Object struck	MAIS				95% Confidence intervals		
	0-1	2	3	4-6	MAIS 2+	MAIS 3+	MAIS 4+
Passenger Vehicle	3772	196	22	18	[5.2%, 6.7%]	[0.7%, 1.4%]	[0.3%, 0.7%]
Commercial Veh.	279	28	11	10	[11%, 19%]	[4.0%, 10%]	[1.5%, 5.5%]
Non Vehicle Occ.	2117	1	0	0	[0.0%, 0.3%]	[0.0%, 0.2%]	[0.0%, 0.2%]
Other Vehicle	39	7	2	0	[8.9%, 33%]	[0.5%, 14%]	[0.0%, 7.4%]
Pole, Post, Tree	212	69	14	17	[27%, 38%]	[6.9%, 14%]	[3.2%, 8.6%]
Wall, Barrier	231	31	6	7	[12%, 21%]	[2.5%, 7.9%]	[1.0%, 5.2%]
Ground, Ditch	160	35	3	7	[16%, 28%]	[2.4%, 8.8%]	[1.4%, 6.9%]
Other, Unknown	101	5	0	2	[2.6%, 13%]	[0.2%, 6.5%]	[0.2%, 6.5%]

Table B.4: Accident data used in Figure 3.4a.

Collision direction	MAIS				95% Confidence intervals		
	0-1	2	3	4-6	MAIS 2+	MAIS 3+	MAIS 4+
Front	3363	153	32	21	[5.0%, 6.6%]	[1.1%, 1.9%]	[0.4%, 0.9%]
Side	1252	84	17	19	[7.3%, 10%]	[1.8%, 3.6%]	[0.8%, 2.2%]
Rear	920	21	0	2	[1.6%, 3.6%]	[0.0%, 0.8%]	[0.0%, 0.8%]
Oblique	1022	46	3	1	[3.5%, 6.1%]	[0.1%, 1.0%]	[0.0%, 0.5%]
Rollover	257	64	6	17	[21%, 30%]	[4.3%, 10%]	[2.9%, 7.8%]
Other, Unknown	97	4	0	1	[1.6%, 11%]	[0.0%, 5.3%]	[0.0%, 5.3%]

Table B.5: Accident data used in Figure 4.1a.

Object struck	MAIS				95% Confidence intervals		
	0-1	2	3	4-6	MAIS 2+	MAIS 3+	MAIS 4+
Passenger Vehicle	1974	98	15	8	[4.8%, 6.9%]	[0.7%, 1.6%]	[0.2%, 0.8%]
Commercial Veh.	90	14	6	5	[15%, 30%]	[4.9%, 16%]	[1.4%, 10%]
Non Vehicle Occ.	1042	0	0	0	[0.0%, 0.4%]	[0.0%, 0.4%]	[0.0%, 0.4%]
Other Vehicle	11	0	0	0	[0.0%, 28%]	[0.0%, 28%]	[0.0%, 28%]
Pole, Post, Tree	101	31	8	6	[23%, 39%]	[5.3%, 16%]	[1.5%, 8.7%]
Wall, Barrier	110	16	5	5	[13%, 27%]	[3.6%, 13%]	[1.2%, 8.4%]
Ground, Ditch	62	14	0	1	[11%, 30%]	[0.0%, 7.0%]	[0.0%, 7.0%]
Other, Unknown	38	1	0	0	[0.1%, 13%]	[0.0%, 9.0%]	[0.0%, 9.0%]

Table B.6: Accident data used in Figure 4.2a.

Collision direction	MAIS				95% Confidence intervals		
	0-1	2	3	4-6	MAIS 2+	MAIS 3+	MAIS 4+
Front	205	24	3	1	[8.1%, 17%]	[0.5%, 4.3%]	[0.0%, 2.4%]
Side	206	10	1	0	[2.6%, 8.9%]	[0.0%, 2.5%]	[0.0%, 1.7%]
Rear	374	10	2	0	[1.6%, 5.4%]	[0.1%, 1.9%]	[0.0%, 1.0%]
Oblique	60	3	1	0	[1.7%, 15%]	[0.0%, 8.4%]	[0.0%, 5.6%]
Rollover	19	1	1	0	[1.2%, 30%]	[0.1%, 24%]	[0.0%, 16%]
Other, Unknown	4	0	0	0	[0.0%, 60%]	[0.0%, 60%]	[0.0%, 60%]

Table B.7: Accident data used in Figure 4.3a

Direction of force	MAIS				95% Confidence intervals		
	0-1	2	3	4-6	MAIS 2+	MAIS 3+	MAIS 4+
Collision partner							
VDI 1 = 11	61	7	1	1	[6.1%, 23%]	[0.3%, 10%]	[0.0%, 7.7%]
VDI 1 = 12	93	11	2	0	[6.7%, 20%]	[0.2%, 6.6%]	[0.0%, 3.4%]
VDI 1 = 1	51	6	0	0	[4.0%, 22%]	[0.0%, 6.3%]	[0.0%, 6.3%]
Occupant's vehicle							
VDI 1 = 11	65	7	1	1	[5.7%, 22%]	[0.3%, 9.4%]	[0.0%, 7.3%]
VDI 1 = 12	96	9	1	0	[4.6%, 17%]	[0.0%, 5.1%]	[0.0%, 3.4%]
VDI 1 = 1	44	8	1	0	[8.1%, 30%]	[0.0%, 10%]	[0.0%, 6.7%]

Table B.8: Accident data used in Figure 4.3b.

Location of damage	MAIS				95% Confidence intervals		
	0-1	2	3	4-6	MAIS 2+	MAIS 3+	MAIS 4+
Collision partner							
Left < 33%	45	1	0	0	[0.1%, 12%]	[0.0%, 7.7%]	[0.0%, 7.7%]
Left 33% - 66%	37	9	3	1	[15%, 40%]	[2.2%, 19%]	[0.1%, 11%]
All, Centre	69	9	0	0	[5.4%, 21%]	[0.0%, 4.6%]	[0.0%, 4.6%]
Right 33% - 66%	29	3	0	0	[2.0%, 25%]	[0.0%, 11%]	[0.0%, 11%]
Right < 33%	14	2	0	0	[1.6%, 38%]	[0.0%, 21%]	[0.0%, 21%]
Occupant's vehicle							
Left < 33%	48	0	0	0	[0.0%, 7.4%]	[0.0%, 7.4%]	[0.0%, 7.4%]
Left 33% - 66%	48	11	2	0	[12%, 34%]	[0.4%, 11%]	[0.0%, 5.9%]
All, Centre	58	8	0	1	[6.3%, 24%]	[0.0%, 8.0%]	[0.0%, 8.0%]
Right 33% - 66%	28	4	1	0	[5.1%, 32%]	[0.1%, 16%]	[0.0%, 11%]
Right < 33%	12	1	0	0	[0.2%, 36%]	[0.0%, 25%]	[0.0%, 25%]

Table B.9: Accident data used in Figure 5.1a.

Object struck	MAIS				95% Confidence intervals		
	0-1	2	3	4-6	MAIS 2+	MAIS 3+	MAIS 4+
Passenger Vehicle	633	52	7	8	[7.5%, 12%]	[1.2%, 3.5%]	[0.5%, 2.2%]
Commercial Veh.	83	11	5	4	[12%, 28%]	[4.1%, 16%]	[1.1%, 10%]
Non Vehicle Occ.	445	1	0	0	[0.0%, 1.2%]	[0.0%, 0.8%]	[0.0%, 0.8%]
Other Vehicle	14	3	2	0	[9.1%, 51%]	[1.3%, 33%]	[0.0%, 18%]
Pole, Post, Tree	68	21	3	8	[23%, 42%]	[5.6%, 19%]	[3.5%, 15%]
Wall, Barrier	43	8	0	1	[8.2%, 30%]	[0.0%, 10%]	[0.0%, 10%]
Ground, Ditch	38	10	0	1	[12%, 37%]	[0.1%, 11%]	[0.1%, 11%]
Other, Unknown	23	1	0	2	[2.4%, 30%]	[0.9%, 25%]	[0.9%, 25%]

Table B.10: Accident data used in Figure 5.2a.

Collision direction	MAIS				95% Confidence intervals		
	0-1	2	3	4-6	MAIS 2+	MAIS 3+	MAIS 4+
Front	160	18	2	2	[7.7%, 18%]	[0.6%, 5.5%]	[0.1%, 3.9%]
Side	30	1	0	0	[0.1%, 17%]	[0.0%, 11%]	[0.0%, 11%]
Rear	5	0	0	0	[0.0%, 52%]	[0.0%, 52%]	[0.0%, 52%]
Oblique	64	6	0	0	[3.2%, 18%]	[0.0%, 5.1%]	[0.0%, 5.1%]
Rollover	3	1	0	0	[0.6%, 81%]	[0.0%, 60%]	[0.0%, 60%]
Other, Unknown	5	0	0	0	[0.0%, 52%]	[0.0%, 52%]	[0.0%, 52%]

Table B.11: Accident data used in Figure 5.3a.

Direction of force	MAIS				95% Confidence intervals		
	0-1	2	3	4-6	MAIS 2+	MAIS 3+	MAIS 4+
Collision partner							
VDI 1 = 11	48	4	0	0	[2.1%, 19%]	[0.0%, 6.8%]	[0.0%, 6.8%]
VDI 1 = 12	55	9	2	2	[11%, 30%]	[1.6%, 14%]	[0.4%, 10%]
VDI 1 = 1	57	5	0	0	[2.7%, 18%]	[0.0%, 5.8%]	[0.0%, 5.8%]
Occupant's vehicle							
VDI 1 ∈ {2, 10}	103	9	1	1	[4.9%, 17%]	[0.2%, 6.2%]	[0.0%, 4.8%]
VDI 1 ∈ {3, 9}	35	7	1	0	[8.4%, 33%]	[0.1%, 12%]	[0.0%, 8.2%]
VDI 1 ∈ {4, 8}	22	2	0	1	[2.5%, 31%]	[0.1%, 20%]	[0.1%, 20%]

Table B.12: Accident data used in Figure 5.3b.

Location of damage	MAIS				95% Confidence intervals		
	0-1	2	3	4-6	MAIS 2+	MAIS 3+	MAIS 4+
Collision partner							
Left < 33%	23	0	0	0	[0.0%, 15%]	[0.0%, 15%]	[0.0%, 15%]
Left 33% - 66%	24	3	0	0	[2,4%, 29%]	[0.0%, 13%]	[0.0%, 13%]
All, Centre	60	8	2	1	[8.0%, 26%]	[0,9%, 12%]	[0.0%, 7,6%]
Right 33% - 66%	22	4	0	1	[6,3%, 38%]	[0,1%, 19%]	[0,1%, 19%]
Right < 33%	30	3	0	0	[1,9%, 24%]	[0.0%, 11%]	[0.0%, 11%]
Occupant's vehicle							
Front	41	6	0	0	[4,8%, 26%]	[0.0%, 7,5%]	[0.0%, 7,5%]
Front incl. Comp.	40	5	1	0	[4,9%, 26%]	[0,1%, 12%]	[0.0%, 7,7%]
Compartment	49	3	0	0	[1,2%, 16%]	[0.0%, 6,8%]	[0.0%, 6,8%]
Entire side	3	2	1	1	[18%, 90%]	[3,7%, 71%]	[0,4%, 58%]
Rear incl. Comp.	14	2	0	0	[1,6%, 38%]	[0.0%, 21%]	[0.0%, 21%]
Rear	9	0	0	1	[0,3%, 45%]	[0,3%, 45%]	[0,3%, 45%]

Appendix C

Calculation of confidence intervals

This section discusses the methods used to calculate the binomial and multinomial confidence intervals, which are applied in the statistical analysis. Although no binomial data are actually analysed in this thesis, the injury levels are treated as such because the number of injuries at a particular injury level is of little interest, whereas the number of injuries above or below a particular level is of great interest. For example, confidence intervals are calculated for the p(MAIS 3+) level, i.e. the probability of sustaining either a MAIS 3, MAIS 4, MAIS 5 or MAIS 6 injury. Since an injury is either MAIS 3+ or MAIS 2-, i.e. a MAIS 0, MAIS 1 or MAIS 2 injury level, these two categories form a binomial.

C.1 Binomial confidence intervals for small sample sizes

In a statistical analysis based on a limited data set, a confidence interval is used to provide a range of values over which an observation may be valid with regards to the total population. When the available data set is large enough, a normal distribution can be assumed and the calculation of confidence intervals is relatively simple. Most literature on confidence intervals deals with this case. However, when the dataset is small, the assumption that the data are normally distributed

becomes invalid and alternative methods must be used. The method used in this thesis is taken from Hartung et al. (2005) and is based on a Pearson-Clopper interval.

> The random variable X, which describes the frequency of an event A, is binomially distributed. Hence:
>
> $$P(X = m) = \binom{n}{m} p^m (1-p)^{n-m}$$
>
> and
>
> $$P(X \geqq m) = \sum_{k=m}^{n} \binom{n}{k} p^k (1-p)^{n-k}$$
>
> where n is the sample size, m is the number of the event occurred in the sample, and p is the point estimate of the probability.
>
> We now need to find an interval that includes, with the probability of $1-\alpha$, the real probability p that the event will occur. Hence we must determine the boundaries of the interval, p_1 and p_2:
>
> $$P(X \geqq m) = \sum_{k=m}^{n} \binom{n}{k} p_1^k (1-p_1)^{n-k} = \frac{\alpha}{2}$$
>
> $$P(X \leqq m) = \sum_{k=0}^{m} \binom{n}{k} p_2^k (1-p_2)^{n-k} = \frac{\alpha}{2}$$
>
> Now since:
>
> $$P(X < x) = 1 - P(F \leqq \frac{n-x}{x+1} \cdot \frac{p}{1-p}) \text{ with } F \sim F_{s(x+1),2(n-x)}$$
>
> use of the relevant quantiles in the F-distribution allow us to determine the the desired $1-\alpha$ confidence interval for p as $[p_1, p_2]$:
>
> $$p_1 = \frac{mF_{2m,2(n-m+1);\alpha/2}}{n-m+1+mF_{2m,2(n-m+1);\alpha/2}}$$
>
> $$p_2 = \frac{(m+1)F_{2(m+1),2(n-m);1-\alpha/2}}{n-m+(m+1)F_{2(m+1),2(n-m);1-\alpha/2}}$$
>
> Translation of Hartung et al. (2005, Section 3.1.1, pp. 203–204)

In the original text of the method described above, the reader is directed to the appendices in order to determine the relevant quantiles of the F-distribution. This may be avoided, however, if computer software such as Microsoft Excel is being used. In Excel, values from the F-distribution may be calculated directly with the 'FINV' formula. As such, the term $F_{2m,2(n-m+1);\alpha/2}$ is entered into Excel

as `FINV(A1/2,2*M1,2*(N1-M1+1))`, where `A1`, `M1` and `N1` are the cells containing the values for α, m, and n respectively. Note that the input sequence of the α, m, and n terms in the 'FINV' formula is different to the sequence used in the formulas from Hartung et al. (2005).

C.2 Multinomial confidence intervals

The calculation of multinomial confidence intervals follows the approach of Sison & Glaz (1995), which is based on the approximation for multinomial probabilities proposed by Levin (1981). This approach calculates a simultaneous parametric bootstrap confidence region for a multinomial proportion, utilising the Edgeworth expansion. This method of calculating multinomial confidence intervals is superior to the methods of Quesenberry & Hurst, Goodman, and Fitzpatrick & Scott (Sison & Glaz 1995).

For a multinomial distribution with k possible outcomes, let $X_1, \ldots, X_k$ be the number of occurrences observed for each of these outcomes in a sample of n observations. For example, when rolling a die $n = 30$ times, there are $k = 6$ possible outcomes, which would be measured as $X_1, \ldots, X_6$.

Let the probability of each outcome in the distribution be $p_1, \ldots, p_k$, where $p_i \geq 0$ and $\sum_{i=1}^{k} p_i = 1$. Note that this is different from the observed sample distribution, which is described by $\hat{p}_1, \ldots, \hat{p}_k$, where $\hat{p}_1 = X_1/n, \ldots, \hat{p}_k = X_k/n$. Hence in the dice example above, the probability of each outcome p_i should be $1/6$, but the observations based on $n = 30$ rolls of a die may provide different values of $\hat{p}_1, \ldots, \hat{p}_k$.

The purpose of the confidence intervals is to describe the real distribution of p_i, based on the observed distribution of $\hat{p}_i$. Sison & Glaz (1995) propose the interval:

$$\left(\hat{p}_i - \frac{c}{n} \leq p_i \leq \hat{p}_i + \frac{c + 2\rho}{n}; 1 \leq i \leq k\right) \tag{C.1}$$

where c is a positive integer and ρ is a factor to compensate for the skewed

nature of the multinomial distribution. These values are described in more detail below. The confidence intervals for the distribution $p_1, \ldots, p_k$ may be expressed as $[\hat{p}_1 - c/n; \hat{p}_1 + (c + 2\rho)/n], \ldots, [\hat{p}_k - c/n; \hat{p}_k + (c + 2\rho)/n]$.

A $(1 - \alpha)$ confidence interval describes a range, which is based on the observed value $\hat{p}_i$, for which there is a $(1 - \alpha)$ probability that the range includes the value p_i. This range is calculated by finding the value of the integer c that solves the equation:

$$Pr\left(\hat{p}_i - \frac{c}{n} \leq p_i \leq \hat{p}_i + \frac{c}{n}; 1 \leq i \leq k\right) = 1 - \alpha \tag{C.2}$$

which is mathematically equivalent to:

$$Pr\left(np_i - c \leq X_i \leq np_i + c; 1 \leq i \leq k\right) = 1 - \alpha \tag{C.3}$$

Note that, although the equations described above represent many events for $1 \leq i \leq k$, the final probability is a real number, not a matrix.

Because $p_1, \ldots, p_k$ are unknown, the value of c in Equation C.3 can be approximated by considering a random multinomial distribution $X_1^\star, \ldots, X_k^\star$, which has n observations from a population with probabilities equal to $\hat{p}_1, \ldots, \hat{p}_k$. The actual probability of an event in this new distribution, $\hat{p}_i$, is therefore chosen to be the same as the observed values of X_i/n. Note that the distribution $X_1^\star, \ldots, X_k^\star$ does not represent any measured data, but is simply a mathematical tool to enable the calculation.

According to Sison & Glaz (1995), as $n \to \infty$, the distributions of $(X_1 - np_1)/\sqrt{n}, \ldots, (X_k - np_k)/\sqrt{n}$ and $(X_1^\star - n\hat{p}_1)/\sqrt{n}, \ldots, (X_k^\star - n\hat{p}_k)/\sqrt{n}$ converge to the same multivariate normal distribution. Hence, the value of c in Equation C.3 can be approximated by solving:

$$\upsilon(c) = Pr\left(n\hat{p}_i - c \leq X_i^\star \leq n\hat{p}_i + c; 1 \leq i \leq k\right) = 1 - \alpha \tag{C.4}$$

which, since $\hat{p}_i = X_i/n$, simplifies to:

$$\upsilon(c) = Pr\left(X_i - c \leq X_i^\star \leq X_i + c; 1 \leq i \leq k\right) = 1 - \alpha \tag{C.5}$$

This equation asks the question, for what value of c is the probability that the unknown values $X_i^\star$ are in the ranges $X_i - c$ to $X_i + c$ equal to $1 - \alpha$, given the values of X_i and n observations from a multinomial distribution with probabilities $\hat{p}_i$. Because c, X_i, and $X_i^\star$ are integers, there is generally no value of c that can exactly solve the above equation. Hence, a value is sought such that $\upsilon(c) < 1 - \alpha < \upsilon(c+1)$.

In order to calculate $\upsilon(c)$, the approach of Levin (1981) is adapted for a doubly truncated interval, given here in the same form as Equation C.5 above:

$$\begin{aligned}\upsilon(c) &= Pr\left(X_i - c \leq X_i^\star \leq X_i + c; 1 \leq i \leq k\right) \\ &\approx \frac{n!}{n^n e^{-n}} \left\{\prod_{i=1}^{k} Pr\left(X_i - c \leq V_i \leq X_i + c\right)\right\} \left\{Pr\left(\sum_{i=1}^{k} Y_i = n\right)\right\}\end{aligned} \tag{C.6}$$

where V_i are independent observations from a Poisson distribution with a mean $\lambda_i = n\hat{p}_i = X_i$, and Y_i are independent observations from a truncated Poisson distribution with the parameter $\lambda_i = n\hat{p}_i = X_i$ and truncated to the range $[X_i - c, X_i + c]$.

The first factor in Equation C.6 may be difficult to calculate as n becomes large and hence $n!$ becomes extremely large. Levin (1981) therefore proposes the use of the Stirling approximation of $n!$ such that the first factor simplifies to $\sqrt{2\pi n}$.

The second factor in Equation C.6 is calculated using the cumulative distribution function of the Poisson distribution, which takes the form:

$$\sum_{j=0}^{\kappa} \frac{e^{-\lambda}\lambda^j}{j!} \tag{C.7}$$

where κ is the discrete number of occurrences of an event, and λ is the mean

(and variance) of the distribution. Hence, the second factor in Equation C.6 is calculated by taking the product of:

$$Pr\left(X_i - c \leq V_i \leq X_i + c\right) = \sum_{j=0}^{X_i+c} \frac{e^{-X_i} X_i^j}{j!} - \sum_{j=0}^{X_i-c-1} \frac{e^{-X_i} X_i^j}{j!} \tag{C.8}$$

over the range $1 \leq i \leq k$.

The final factor in Equation C.6 is calculated using the Edgeworth expansion for the doubly truncated Poisson distribution Y_i, which is (Sison & Glaz 1995):

$$Pr\left(\sum_{i=1}^{k} Y_i = n\right) = f\left(\frac{n - \sum_{i=1}^{k} \mu_i}{\sqrt{\sum_{i=1}^{k} \sigma_i^2}}\right) \frac{1}{\sqrt{\sum_{i=1}^{k} \sigma_i^2}} \tag{C.9}$$

where:

$$f(x) = \left(\frac{1}{\sqrt{2\pi}} e^{-x^2/2}\right) \times \left(1 + \frac{\gamma_1}{6}(x^3 - 3x) + \frac{\gamma_2}{24}(x^4 - 6x^2 + 3) + \frac{\gamma_1^2}{72}(x^6 - 15x^4 + 45x^2 - 15)\right) \tag{C.10}$$

and (Glaz & Sison 1999):

$$\gamma_1 = \frac{\sum_{i=1}^{k} \mu_{3,i}}{\left(\sum_{i=1}^{k} \sigma_i^2\right)^{3/2}} \tag{C.11}$$

$$\gamma_2 = \frac{\sum_{i=1}^{k} \left(\mu_{4,i} - 3\sigma_i^4\right)}{\left(\sum_{i=1}^{k} \sigma_i^2\right)^{2}} \tag{C.12}$$

In order to complete the above calculations, the factorial and central moments of Y_i must be determined. The r^{th} factorial moments of a Poisson distribution truncated to the range $[b, a]$ are calculated using the formula (Sison & Glaz 1995):

$$\mu_{(r)} = \lambda^r \left(1 + \left[\frac{\sum_{j=b-r}^{b-1} e^{-\lambda} \lambda^j / j! - \sum_{j=a-r+1}^{a} e^{-\lambda} \lambda^j / j!}{\sum_{j=b}^{a} e^{-\lambda} \lambda^j / j!}\right]\right) \tag{C.13}$$

Hence, for $i = 1, \ldots, k$, $\lambda = X_i$ and truncation to the range $[X_i - c, X_i + c]$, the

above formula becomes:

$$\mu_{(r),i} = X_i^r \left(1 + \left[\frac{\sum_{j=X_i-c-r}^{X_i-c-1} e^{-X_i} X_i^j/j! - \sum_{j=X_i+c-r+1}^{X_i+c} e^{-X_i} X_i^j/j!}{\sum_{j=X_i-c}^{X_i+c} e^{-X_i} X_i^j/j!} \right] \right) \quad \text{(C.14)}$$

Note that the mean of the truncated Poisson distribution, μ_i, is equivalent to the first central moment, $\mu_{(1),i}$. Having calculated the first to fourth factorial moments of the distribution, the central moments can finally be obtained using the usual formulae (Levin 1981):

$$\mu_{2,i} = \mu_{(2),i} + (\mu - \mu^2) \quad \text{(C.15)}$$

$$\mu_{3,i} = \mu_{(3),i} + \mu_{(2),i}(3 - 3\mu) + (\mu - 3\mu^2 + 2\mu^3) \quad \text{(C.16)}$$

$$\mu_{4,i} = \mu_{(4),i} + \mu_{(3),i}(6 - 4\mu) + \mu_{(2),i}(7 - 12\mu + 6\mu^2) + (\mu - 4\mu^2 + 6\mu^3 - 3\mu^4) \quad \text{(C.17)}$$

Note here that the second central moment, $\mu_{2,i}$, is equal to the variance, σ_i^2.

C.2.1 Summary of the calculation method

In order to calculate a $1 - \alpha$ confidence interval for a given sample of n observations, $X_1, \ldots, X_k$ are known, and hence $\hat{p}_1, \ldots, \hat{p}_k$ are easily calculated. A series of iterations using Equation C.6 is then required to calculate a value of c such that $v(c) < 1 - \alpha < v(c+1)$.

Equation C.6 is solved using Equation C.8 to determine its second factor and Equation C.9 to determine its third factor. In order to solve Equation C.9, the first, second, third and fourth factorial moments of the truncated Poisson distribution should be calculated using Equation C.14. This needs to be repeated for each value of $1 \leq i \leq k$. The factorial moments can then be used to calculate the central moments using Equation C.15. Equation C.9 can finally be solved with the assistance of Equations C.10 and C.11.

Finally, once the correct value of c is determined, the confidence intervals for each value of $1 \leq i \leq k$ can be calculated using Equation C.1.

Appendix D

Statistical test theorem

The following statistical test is an adaptation of the methods described by van de Wiel et al. (1999) for the calculation of the Mann-Whitney U-Test and the Jonckheere-Terpstra Test.

Consider groups of samples of size $\{m_1, \ldots, m_k\}$ and $\{n_1, \ldots, n_k\}$ that both have k populations. X_{ij} is the j^{th} observation from the i^{th} population in the group $\{m_1, \ldots, m_k\}$, and Y_{ij} is the j^{th} observation from the i^{th} population in the group $\{n_1, \ldots, n_k\}$. Let μ_{X_i} and μ_{Y_i} be the mean values of X_{ij} and Y_{ij} in the groups $\{m_1, \ldots, m_k\}$ and $\{n_1, \ldots, n_k\}$, respectively.
The null hypothesis is:

$$H_0 : \mu_{X_i} = \mu_{Y_i} \quad \text{for all} \quad i = 1 \ldots k \tag{D.1}$$

The test hypothesis is:

$$H_1 : \mu_{X_i} \geq \mu_{Y_i} \quad \text{for all} \quad i = 1 \ldots k \tag{D.2}$$

Let φ_i be the number of observations Y_{ij} from the sample n_i that are less than the values of X_{ij} in the sample m_i:

$$\Rightarrow \varphi_i = \sum_{j=1}^{m_i} \#\left(Y_{ij} < X_{ij}\right)$$

Let S be the statistic that is the sum of φ_i for all populations:

$$\Rightarrow S = \sum_{i=1}^{k} \varphi_i$$

Let M be the maximum value possible for S:

$$\Rightarrow M = \sum_{i=1}^{k} m_i n_i$$

The probability generating function for the above statistic is:

$$\sum_{l=0}^{M} \Pr\left(S = l\right) x^l = \prod_{i=1}^{k} \frac{1}{\begin{pmatrix} m_i + n_i \\ m_i \end{pmatrix}} \frac{\prod_{l=n_i+1}^{m_i+n_i} \left(1 - x^l\right)}{\prod_{l=1}^{m_i} \left(1 - x^l\right)} \tag{D.3}$$

Both sides of the probability generating function can be expanded to create two polynomial functions of the order M. The probability that S would take on the value calculated above can therefore be determined from the corresponding coefficient on the right hand side of the equation, i.e. $\Pr(S = l)$ is equal to the coefficient of x^l from the right of the equation. Finally, the p-value is calculated as $1 - p = \Pr(S \leq l)$, which is equal to the sum of the coefficients of x^l up to $l = S$.

Appendix E

Horizontal homogeneity criteria

Consider a load cell wall with $i = 1..8$ rows and $j = 1..16$ columns of 125 mm $\times$ 125 mm load cells. Taking the approach of Edwards et al. (2007*a*), let f_{ij} be the peak force measured in each load cell during the first 40 ms of the collision. Then define the target cell force (TC_i) for each load cell in a particular row as:

$$TC_i = \frac{\sum_{j=1}^{16} f_{ij}}{\text{vehicle width}/125 \text{ mm}} \tag{E.1}$$

This definition is similar to that defined by Edwards et al. (2007*a*) and determines the average force per load cell over the width of the vehicle. However, in contrast to Edwards et al. (2007*a*), this definition does not include a limit on the target cell load, as this can be a source of error between tests with different vertical alignments. The justification for a capped target is also weak because, although it is designed to avoid targets that are impossible to achieve, increasing the stiffness of the barrier would achieve this goal without the need for a cap.

Similar to the *HSI* criteria, the target cell force is then used to determine the number of cells in each row that are compliant (RC_i). For load cells that are below the threshold, partial credit is given.

$$RC_i = \sum_{j=1}^{16} \text{if}\left(f_{ij} \geq TC_i, 1, \frac{f_{ij}}{TC_i}\right) \tag{E.2}$$

The entire width of the load cell wall is assessed even for narrow vehicles, as this improves the repeatability of the metric especially where the horizontal alignment of the vehicles differs between tests. The metric remains independent of vehicle width though, since this is included in the definition of TC_i. Unlike the 'centre support' and 'outer support' components of the *HSI* metric, RC_i does not distinguish between homogeneity outside or between the longitudinals. This also improves repeatability where the horizontal alignment of the vehicles differs between tests.

Finally, the homogeneity criteria HC is calculated by dividing RC_i by the number of load cells actually covered by the width of the vehicle. Assuming that the third and fourth rows of the load cell wall correspond to the desired interaction zone,[95] the average value is calculated for these two rows:

$$HC = \frac{1}{2}\sum_{i=3}^{4}\frac{RC_i}{\text{vehicle width}/125\text{ mm}} \tag{E.3}$$

Unlike the proposal defined by Edwards et al. (2007*a*), a broader assessment area including the second to fifth rows is not specified since the results of the simulations in Chapters 8 and 9 only support the assessment of a 250 mm high horizontally homogeneous region.

[95] See Ablaßmeier et al. (2007, p2) for a definition of a "Common Zone for Structural Interaction" and Faerber et al. (2007, p12) for a description of the load cell wall alignment and corresponding "Common interaction zone."